

Towards personalized medicine in kidney transplantation: Unravelling the results of a large multi-centre clinical study

DISSERTATION

zur Erlangung des akademischen Grades

Doctor rerum naturalium
(Dr. rer. nat.)

eingereicht an der
Lebenswissenschaftlichen Fakultät der Humboldt-Universität zu Berlin

von
Ldo. Arturo Blázquez Navarro

Präsidentin
der Humboldt-Universität zu Berlin

Prof. Dr.-Ing. Dr. Sabine Kunst

Dekan der Lebenswissenschaftlichen Fakultät
der Humboldt-Universität zu Berlin

Prof. Dr. Bernhard Grimm

Gutachter/innen

1. Prof. Dr. Dr. h. c. Edda Klipp
2. Prof. Dr. Hans-Dieter Volk
3. Prof. Dr. Klemens Budde

Tag der mündlichen Prüfung:

10.02.2020

1. Table of contents

1.	Table of contents	3
2.	Summary	9
3.	Zusammenfassung	10
4.	Acknowledgements / Danksagung / Agradecimientos	11
5.	Introduction	13
5.1	Personalized medicine: Promise and challenges	13
5.2	Personalized approaches to renal transplantation	13
5.3	Basic concepts of data management	16
5.3.1	The stages of data management	16
5.3.2	Defining and achieving quality data	17
5.3.3	Data pre-processing for data analysis	18
5.4	Data analysis methods for systems medicine	18
5.4.1	Statistical analysis of clinical studies	19
5.4.2	Machine learning approaches for disease biomarker discovery	21
5.4.3	Mathematical modelling as a tool for mechanistic understanding	23
5.5	Scope and structure of this dissertation	27
6.	Data management in the e:KID study	29
6.1	Background: e:KID, a systems medicine study for kidney transplantation	29
6.1.1	Design of the e:KID study: Patient cohort and selected markers	29
6.1.2	Organizational aspects of the consortium	30
6.2	Database design and integration for the e:KID study	31
6.2.1	Structure of the original Harmony database	32
6.2.2	Design of the e:KID database	34
6.2.3	Data integration in the e:KID study	35
6.3	Data cleaning in the e:KID study	36
6.3.1	Improving conformance of the database	36
6.3.2	Management of missing data	37
6.3.3	Evaluating the plausibility of data with biostatistical methods	39
6.4	Data pre-processing in the e:KID study	42
6.4.1	Generation of new variables for data analysis	42
6.4.2	Statistical transformation and normalization of variables	43
6.4.3	Dealing with strong centre effects: The case of GFR	43
6.4.4	Working with variables with missing values	44

6.5	Lessons learned from data management at the e:KID study	45
7.	BKV, CMV, and EBV interactions and their effect on graft function one year post-renal transplantation: Results from a large multi-centre study	47
7.1	Main text	48
7.2	Supplementary materials	57
7.2.1	Figure S1	57
7.2.2	Figure S2	57
7.2.3	Figure S3	58
8.	Sex-associated differences in cytomegalovirus prevention: Prophylactic strategy is associated with a strong kidney function impairment in female renal transplant patients.....	59
8.1	Main text	60
8.2	Supplementary materials	88
8.2.1	Table S1.....	88
8.2.2	Table S2.....	88
8.2.3	Table S3.....	93
8.2.4	Figure S4	100
8.2.5	Figure S5	100
9.	A novel approach reveals that HLA class 1 single antigen bead-signatures provide a means of high-accuracy pre-transplant risk assessment of acute cellular rejection.....	103
9.1	Main text	104
9.2	Supplementary materials	114
9.2.1	Figure S1	114
9.2.2	Figure S2	114
9.2.3	Figure S3	114
9.2.4	Table S1.....	115
9.2.5	Table S2.....	115
9.2.6	Table S3.....	116
9.2.7	Table S4.....	117
9.2.8	Table S5.....	119
10.	Differential T cell response against BK virus regulatory and structural antigens: A viral dynamics modelling approach.....	121
10.1	Main text	122
10.2	Supplementary materials	142
10.2.1	Figure S1	142
10.2.2	Figure S2	142
10.2.3	Figure S3	146

10.2.4	Table S1	149
10.2.5	Table S2	150
10.2.6	Table S3	152
10.2.7	Table S4	153
11.	Summary of the manuscripts in the context of personalized medicine	155
11.1	Studying the prevalence, risk factors and consequences of combined viral reactivations: A thorough exploratory statistical analysis.....	155
11.2	Improving prevention of cytomegalovirus complications: A hypothesis-based assessment of sex-treatment interactions on transplantation outcomes by means of multivariate statistics	156
11.3	Predicting acute cellular rejection employing pre-transplant antibody profiles: Identification of markers for risk assessment using a machine learning tool.....	157
11.4	Inferring mechanisms of T cell response against BK virus: A mathematical model of viral dynamics.....	158
12.	Outlook: Personalized medicine and big data	161
13.	References	163
14.	Selbstständigkeitserklärung.....	181

*A Jeff, por más siglos de doctorado juntos /
An Jeff, für weitere Promotionsjahrhunderte zusammen*

2. Summary

In this doctoral thesis, I present my work on personalized medicine for renal transplantation, with a focus on opportunistic viral infections. This work comprises insights on the demographic, clinical and therapeutic factors leading to a positive transplantation outcome, a risk assessment tool for cellular rejection, a common clinical complication, and a model of the antiviral immune response.

In spite of the surgical and pharmacological developments in the last decades, long-term graft survival rates in kidney transplantation are still poor. Personalization of treatment is expected to lead to a drastic improvement in long-term outcomes. With this goal, a cohort of 587 patients was characterized for a wide range of markers during the first post-transplantation year to assess their long-term prognosis. Here, I describe along four manuscripts and two chapters the processes of management and analysis of the cohort data, and their use for hypothesis generation and hypothesis testing.

In detail, we have studied the clinical evolution of patients after renal transplantation with emphasis on two most relevant complications: viral reactivations – particularly those of BK virus and cytomegalovirus – and acute rejection. We have analysed in depth these phenomena by (i) exhaustively analysing the associations between different viral reactivations and their influence on transplantation outcome, (ii) evaluating the effects of antiviral treatment strategies on viral reactivation and other transplantation outcomes with emphasis on sex-associated differences, (iii) developing a tool for the pre-transplantation risk assessment of acute cellular rejection, and (iv) creating a mathematical model for the personalized characterization of the immune response against the BK virus under immunosuppression. Diverse analysis methods were applied to achieve these goals, both in exploratory and hypothesis-guided approaches, ranging from uni-, bi- and multivariate biostatistics to ordinary differential equation modelling and machine learning methods. Critical to the success of these analyses was a careful management of the large number of heterogeneous data collected in the study, especially in data cleaning, database integration, management of missing data and data pre-processing.

Taken together, these four studies have the potential of improving patient care, optimizing monitoring of viral reactivations, stratifying antiviral prevention strategies, tailoring immunosuppression and monitoring to the individual risk of acute rejection, and contributing to personalization of immunotherapy. They demonstrate how the large volume of data obtained within a clinical study can be employed to further the development of personalized medicine, employing effective data management, analysis and interpretation strategies. We expect these results to eventually inform clinical practice, thereby improving long-term survival and quality of life after kidney transplantation.

3. Zusammenfassung

Die vorliegende Dissertation hat die Entwicklung personalisierter medizinischer Lösungen bei Nierentransplantationen, mit Schwerpunkt auf opportunistischen Virusinfektionen, zum Gegenstand. Sie umfasst (i) Einblicke in die demografischen, klinischen und therapeutischen Faktoren, die zu einem positiven Transplantationsergebnis führen, (ii) ein Tool zur Risikobewertung der zellulären Abstoßung, einer häufigen klinischen Komplikation, und (iii) ein Modell der antiviralen Immunantwort.

Trotz der chirurgischen und pharmakologischen Fortschritte der letzten Dekaden ist das Langzeitüberleben von Nierentransplantaten noch unzureichend. Es wird erwartet, dass eine Personalisierung der Behandlung zu einer erheblichen Verbesserung der Langzeitergebnisse führt. Vor diesem Hintergrund wurde eine Kohorte von 587 Patienten im ersten Jahr nach der Transplantation untersucht um ein breites Spektrum von Markern für die langfristige Prognose etabliert. In dieser Dissertation werden in vier Manuskripten und zwei Kapiteln die Prozesse des Managements und der Analyse der Daten der Kohorte, sowie deren Verwendung für die Formulierung und Überprüfung von Hypothesen beschrieben.

Der klinische Verlauf von Patienten nach Nierentransplantation wurde untersucht. Zwei der wichtigsten Komplikationen standen hierbei im Vordergrund: Virusreaktivierungen – insbesondere der BK- und Cytomegalieviren – und akute Abstoßung. Diese Phänomene wurden unter Nutzung verschiedener Ansätze eingehend analysiert: (i) Systematische Analyse der Assoziationen zwischen verschiedenen Virusreaktivierungen und deren Einfluss auf das Transplantationsergebnis; (ii) Bewertung der Auswirkungen antiviraler Behandlungsstrategien auf die Reaktivierung von Viren und andere Transplantationsergebnisse; (iii) Entwicklung eines Tools zur Prätransplantation-Risikoeinschätzung der akuten zellulären Abstoßung und (iv) Erstellung eines mathematischen Modelles für die personalisierte Charakterisierung der Immunantwort gegen das BK-Virus unter Immunsuppression. In diesem Zusammenhang wurden verschiedene Analysemethoden angewendet, sowohl explorativ wie auch hypothesengeleitet, von uni-, bi- und multivariater Biostatistik bis hin zu gewöhnlichen Differentialgleichungsmodellen und Methoden des maschinellen Lernens. Kritisch für den Erfolg dieser Analysen war ein sorgfältiges Management der Vielzahl der in der Studie gesammelten heterogenen Daten, insbesondere bei der Datenbereinigung, Datenbankintegration, Verwaltung fehlender Daten und Datenvorverarbeitung.

Zusammengenommen haben diese vier Studien das Potenzial, (i) die Patientenversorgung zu verbessern, (ii) die Überwachung von Virusreaktivierungen zu optimieren, (iii) Präventionsstrategien gegen virale Reaktivierungen zu stratifizieren, (iv) die Immunsuppression und das Monitoring der Patienten auf das individuelle Risiko akuter Abstoßung anzupassen, und (v) zur Personalisierung der Immuntherapie beizutragen. Die Studien zeigen, wie das große Datenvolumen einer klinischen Studie zur Weiterentwicklung der personalisierten Medizin unter Einsatz effektiver Strategien für Datenmanagement, Analyse und Interpretation genutzt werden kann. Es ist zu erwarten, dass diese Ergebnisse die klinische Praxis beeinflussen und so das langfristige Überleben und die Lebensqualität der Patienten verbessern.

4. Acknowledgements / Danksagung / Agradecimientos

Eine Promotion ist eine Reise mit bekanntem Anfang und ungewissem Ende. Sie kann über Umwege in neue, unerwartete Bereiche führen. Solch eine Herausforderung ist daher nur mit den richtigen Reisebegleitern zu bewältigen. Ihnen allen gebührt mein Dank. Und damit diese Dankbarkeit wirklich vom Herzen kommt, habe ich diese wenigen Worte in denjenigen Sprachen verfasst, die mich mit jedem einzelnen verbunden haben.

Ich möchte zu allererst meiner Doktormutter Edda Klipp danken, für ihr Vertrauen und ihre Hilfe schon lange bevor ich mit der Promotion beginnen durfte: Ohne dich hätte ich diesen Weg überhaupt nicht beschreiten können.

Avidan Neumann, you gave me the first opportunity to embark in this project, an opportunity that would change my life, and you introduced me to the fascinating world of viral dynamics models. Thanks a lot for this!

Nina Babel hat mich aufgenommen und unterstützt in einer Zeit hoher Ungewissheit, als der Weg dieser Promotion zu scheitern drohte. Dafür allein müsste ich schon zutiefst dankbar sein. Aber zudem bist du mir eine unschlagbare Vorgesetzte gewesen und die Referenz schlechthin für alle komplizierten klinischen Fragen: Ich freue mich schon auf die zukünftige, gemeinsame Arbeit.

Besonderer Dank gilt Michal Or-Guil. Diese Dissertation ist das Ergebnis von unseren langen Diskussionen, von deiner analytischen Schärfe, deiner breiten Expertise, deiner Ermutigung, immer weiter in die Tiefe zu gehen, und nicht zuletzt deiner Großzügigkeit. Dafür möchte ich dir von ganzem Herzen danken!

Diese Arbeit wäre ohne das e:KID-Konsortium nicht möglich gewesen, das die Proben gesammelt, charakterisiert und analysiert hat und durch das meine Arbeit finanziert wurde. Da möchte ich insbesondere Birgit Sawitzki und Christian Hugo danken, sowie Oliver Thomusch von der Harmony-Studie, für Ihre sehr hilfreichen klinischen und immunologischen Input in der Diskussion meiner Ergebnisse.

Ich möchte mich auch bei den vielen Kollegen bedanken, die mir in dieser Zeit geholfen haben. Insbesondere danke ich Nicole Wittenbrink: für deine Hilfsbereitschaft, deinen kritischen Sinn und für alles, was ich von dir gelernt habe. Ich bedanke mich auch bei Karsten Jürchott, vor allem für seine Hilfe bei meinem R-Einstieg, bei Ulrik Stervbo für seine unverzichtbare Unterstützung bei meiner ersten Veröffentlichung, Chris Bauer, für sein fachliches Wissen insbesondere in maschinellem Lernen, und bei Chantip Dang-Heine und Patrizia Wehler, ohne die ich aus Datenmangel (fast) keine der Datenanalysen dieser Dissertation hätte machen können. Ich darf nicht vergessen, mich bei allen anderen in der AG Babel zu bedanken, auch wenn das Ergebnis unserer Zusammenarbeit noch nicht in dieser Dissertation zu lesen ist (aber in der nahen Zukunft!). Insbesondere bedanke ich mich bei Toralf Roch, Constantin Thieme, Sharon Bajda und Tina Kornprobst: Ich habe mich bei euch von Anfang angenommen und willkommen gefühlt!

Ich möchte auch der Berlin-Brandenburg Schule für Regenerative Therapien (BSRT) und dem Bundesministerium für Bildung und Forschung (BMBF) für die Finanzierung meiner Arbeit danken. Für die Hilfe mit allen bürokratischen Hürden möchte ich mich auch bei Sabine

Bartosch (BSRT), Delia Maier, Heike Kristens und Angela Hahn (Charité Universitätsmedizin) und Jana Lahmer (Humboldt-Universität zu Berlin) bedanken.

Den vielen Freunden, die ich in Berlin kennengelernt habe und mich in dieser Zeit ertragen durften, möchte ich danken. Insbesondere danke ich Vasilis, Fabio, Andreas, Omid, Steffi und Alex, y también a Roser y Marina. También quiero dar las gracias a todos mis amigos que me han apoyado desde la distancia, como Damián, Jorge, Ovidio, Antonio, Fran, Bea o Elena. Gracias por preguntarme cuando voy para allá, y por hacerme sentir que nunca me fui cuando estoy allí.

Para mi familia, mis abuelos y mis hermanos Ricardo y Rodrigo (Rodrigo, mira la página 38) solo puedo tener palabras de un cariño que no ha perdido brillo solo porque haya(mos) crecido y ahora nos veamos en veranos y navidades. Y mis padres... habéis sido para mí norte por el que guiarme, un puerto seguro ante cualquier contratiempo, amor a prueba de toda frustración: Soy porque sois.

Ich muss unbedingt Alexandra hier erwähnen: danke, dass du mich mit so liebevoll in deine Familie aufgenommen hast. Danke, dass du dich immer um alles sorgst, danke für die schönen Opernabende. Du bist die beste Schwiegermutter, die man sich vorstellen kann!

Und Jeff. Wir haben uns an demjenigen Tag kennengelernt, an dem ich meine Zusage für das Projekt bekam, was der Anfang meiner Promotion werden sollte. Du hast mir mehr Freude, mehr Liebe, mehr Frieden, mehr Stärke und mehr Tiefe in dieser Zeit gegeben, als es in diesen kleinen, armen Worten passen könnte: Bleibe unausgesprochen, was kaum ausgesprochen werden kann.

Ich möchte letztlich allen anderen, unerwähnten Menschen danken, die mir in dieser Zeit geholfen haben. Wenn ich dich vergessen habe, sehe bitte von meinem Fehler ab: Es war nur mein schlechtes Gedächtnis.

5. Introduction

5.1 Personalized medicine: Promise and challenges

The medicine of the future is envisaged as personalized, predictive, preventive and participatory.^{1–3} The development of techniques to tailor medical decisions based on individual patient needs is the main goal of research in personalized medicine.^{4–6} In this framework, also known as precision or P4 medicine, patients are stratified based on their disease subtype, genotype, treatment response, etc. so that medical decisions are based on individual patient characteristics rather than on general population characteristics.^{4–7} Personalized approaches are thus expected to lead to better disease prevention and optimized treatment, thereby extending and improving the life of patients.^{1,5,8}

Tailoring medical decisions to the patient has been a goal of medicine ever since antiquity, and a certain degree of personalization based on single variables has long been standard, e.g. adjusting of dose for body mass or adjusting therapy according to clinical history.^{3,7} However, high-throughput omics have made it possible to obtain an unprecedented amount of complex and heterogeneous data on each individual patient, opening new possibilities for the development of personalized medicine.^{7,9,10} Systems medicine approaches aim to take advantage of these multi-dimensional data, integrating it with information from other sources e.g. clinical and lifestyle data, with the goal of better grasp the complexity of disease, as the result of multiple biological interactions.^{7,9,11} A systems understanding could therefore be especially adequate for the prevention, diagnosis and therapy design of complex illnesses – such as complications of renal transplantation.^{2,4,12,13}

However, major challenges in personalized systems medicine remain to be addressed.^{5,8,14,15} While generation of quality data has become increasingly fast and cheap, current bottlenecks pertain mainly data management and analysis – including but not limited to data storage and management issues, concerns in analysis of heterogeneous data, interpretation of complex results and performance of prediction models.^{4,5,7} Consequently, more effective data management and analysis strategies are paramount.

5.2 Personalized approaches to renal transplantation

Transplantation is the best available treatment for kidney failure.^{16–18} In the last thirty years, the development of new immunosuppressive protocols has led to a clear improvement of short term patient and graft survival.^{19,20} However, this progress has not resulted in similar improvements in the long-term: median graft survival time still remains at around ten years.^{19–21} Moreover, in spite of functioning grafts, complications associated with immunosuppression – e.g. viral reactivation, cardiovascular disease, cancer, diabetes, etc. – result often in a decrease of quality of life and premature death of the patient.^{13,19–24} Under-immunosuppression, on the other hand, can lead to acute rejection, causing graft dysfunction and eventually graft loss.^{16,25–27} Therefore, in a context of increasing incidence of kidney failure and difficulties in decreasing the waiting time for an organ donation, personalized approaches to immunosuppressive treatments could improve transplantation outcomes.^{13,16,19,25,28–30}

Current approaches in personalized medicine for renal transplantation include, among others: (i) improvement of organ allocation, better defining HLA mismatches critical to the development of complications; (ii) describing the immunological characteristics leading to graft tolerance in absence of immunosuppression and improving techniques to induce this state; (iii) investigating the efficacy and safety of drug protocols in stratified cohorts; (iv)

developing non-invasive markers for the early detection of complications; and (v) developing tools to predict the risk of individual patients to suffer certain complications, especially acute rejection.^{16,31–35} In Table 1, a non-exhaustive selection of studies comprising these five directions is shown.* Interestingly, several study approaches are based on multi-omics or multicomponent data, i.e. medium to large volumes of heterogeneous data. These studies attempt to model transplant complications or outcomes based not on mono-factorial analyses, but by capturing systemic patterns and interactions.

Name	Reference No.	Type of study	Expected outcome	Analysed data in addition to clinical information	Patient No.	Current state
Eplets Matching[†]	NCT03818698	Observational	Assessment of association of HLA mismatching and rejection	HLA typing	1000	Ongoing
HLA-DQ[‡]	NCT03896919	Observational	Assessment of association of HLA-DQ mismatching and rejection	HLA-DQ typing	30	Ongoing
ARTIST	NCT01516177	Observational	Assessment of frequency of known operational tolerance signatures	B cell receptor sequence	250	Completed
TEACH	NCT03504241	Interventional	Induction of operational tolerance		6	Ongoing
VIPP	NCT00372229	Interventional	Validation of antiviral prevention strategies for intermediate risk constellation		300	Completed
nEverOld	NCT01631058	Interventional	Evaluation of immunosuppressive therapy for elderly population		90	Ongoing
Harmony	NCT00724022	Interventional	Validation of immunosuppressive therapy for low risk constellation		600	Completed
TAC3A5	NCT03020589	Interventional	Validation of immunosuppressive regime based on genotype	Genotype	260	Ongoing
S&L	NCT03672110	Interventional	Validation of low-dose immunosuppressive therapy for normal risk constellation		400	Ongoing
CTOT-04	NCT00337220	Observational	Evaluation of non-invasive rejection markers	Urine mRNA signature	500	Completed

* See Table S5 in 9.2.8 for an exhaustive selection and comparison of studies on the early prediction of acute rejection in kidney transplantation.

[†] The official name of the study is “Study of Eplets Matching in Kidney Transplantation”; no official acronym was found.

[‡] The official name of the study is “HLA-DQ in Acute Kidney Transplantation Rejection”; no official acronym was found.

KTD-innov	NCT03582436	Observational	Development of non-invasive rejection markers	Multi-omics	750	Ongoing
ROCKET	-	Observational	Early diagnosis and prediction of complications	Multi-omics	>2000	Ongoing
iBOX	NCT03474003	Observational	Risk assessment tool of long-term graft survival		8000	Ongoing
TOGETHER	NCT03873623	Observational	Validated risk assessment tool of acute rejection	Blood RNA signature	250	Ongoing
EU-TRAIN	NCT03652402	Observational	Risk assessment tool of long-term graft survival	Multi-component	500	Ongoing
BIOMARGIN	NCT02832661	Observational	Validation of biomarkers for graft lesions	Multi-omics	500	Ongoing
e:KID		Observational	Risk assessment tool of long-term graft survival	Multi-component	600	Ongoing

Table 1. A non-exhaustive selection of studies in kidney transplantation relevant for personalized medicine. Source of information is the registry ClinicalTrials.gov, except for the ROCKET and the e:KID studies; for the former the source is era-learn.eu, for the latter sys-med.de. The patient cohort of the e:KID study corresponds to that of the Harmony study. The category multi-component refers to studies incorporating data from heterogeneous sources (DNA, RNA, proteins, metabolites, etc.) but not necessarily multi-omics, as in Lee *et al.*³⁶

In this dissertation, the results of work performed as part of the e:KID study is presented.* The main goal of this study is to optimize the treatment of patients starting at the first weeks after transplantation. The e:KID approach regards the immune system as a whole, considering the interplay of its components at molecular, cellular and physiological levels. For this, a wide range of immune system and complication markers were measured in patients including e.g. cell type populations, gene expression and concentration of cytokines and metabolites. e:KID does not employ an unsupervised high throughput multi-omics approach with the goal of generating a large amount of data.^{11,12,37} Rather, unlike many systems medicine studies, the choice of markers was based on the expertise of the consortium partners. For example, the expression of tolerance associated genes were measured, as they might be markers for the effectivity of immunosuppression; metabolomics profiling of urine was performed based on previous knowledge of their diagnostic capacity for acute rejection.^{26,38,39}

Combining the measured markers with data on the clinical course of the patients, the e:KID approach is expected to achieve a deeper understanding of the processes leading to a good transplantation outcome, and how these outcomes could be improved. A wide range of analytic methods – encompassing biostatistics, machine learning and mathematical modelling – were envisaged. Therein, predictive models on the outcomes and main transplantation complications are to be developed; main interest areas comprise renal function, acute rejection and viral reactivations. Further, exploratory and hypothesis-guided studies were planned to assess the contribution of demographic factors, therapeutic strategy and complications on transplantation outcome. The results of the e:KID study as a whole are then to be integrated and validated in a upcoming second phase of the study. As a final result, an

* For more detail on the study design, see section 6.1.

exhaustive systems medicine-based model is envisioned, with the goal of allowing clinicians to optimize the treatment based on individual criteria.

5.3 Basic concepts of data management

The final goal of data management is achieving high-quality data, and submitting them on time to those responsible for data analysis.^{40,41} According to the US Institute of Medicine, high quality data are those data “strong enough to support conclusions and interpretations equivalent to those derived from error-free data”.⁴² Data management can be defined as the development, execution and supervision of practices to control, protect, deliver and enhance the value of data.⁴³ Data management is a multidisciplinary endeavour, with no “one-size-fits-all” solutions, and requires the expertise of specialized data scientists.^{40,44,45} Data management strategies are critical for data analysis, and therefore reporting on the followed strategies is a recommended practice.⁴⁶

5.3.1 The stages of data management

Data management is a complex procedure, including database design, data entry, data integration, data cleaning, management of missing data, database locking and data pre-processing.^{40,41,47}

The design of the database has to meet the needs of the study, especially taking into account the process of data entry.^{40,48} A well-designed database is vital for the subsequent integration of the data from different, heterogeneous experiments. Database design should not be performed blindly, but be the result of a requirement analysis, considering the nature of study and the key research questions to be answered, as well as the background of the researchers who are to make use of the database.⁴⁸ Data entry within a clinical trial is usually performed employing an electronic case report form (eCRF).^{40,49} Similar to the database, eCRFs are specially tailored for the needs of a specific study, containing questions on the results of each clinical examination, adverse events, medication change etc.^{40,49} A careful design of the eCRF can partially prevent the introduction of errors, e.g. allowing the selection of categorical variables to avoid typewriting mistakes and defining hard cut-offs for numeric values.⁴⁹

In a systems medicine study, the clinical data entered through the eCRF have to be integrated with further, experimental data of heterogeneous characteristics.^{4,7} The goal of data integration is to allow users to fetch data from the different sources, combining, manipulating and employing them for the analysis.^{50–52} But the integration of heterogeneous data from different sources is not a trivial task where data can be just blindly juxtaposed within a database; it depends on the biological and statistical problem at hand and the heterogeneity and origin of the data.^{50–52} Furthermore, for certain data types, e.g. genomic data, pre-processing of the data is necessary for their integration due to their high degree of noise.⁵² Therefore, data integration is a duty that requires input from both data scientists and the experimentalists responsible for the data, employing agreed standards.^{50–52}

The resulting integrated database of a clinical study is then in a *semper reformanda* state, i.e. it is in need of corrections within a continuous process of cleaning. Data cleaning should not be understood as a mere intermediate step before data integration into the database, but rather as an iterative process, in which the goal is to ideally achieve high quality data.^{40,41,47} For more details on how high quality data are defined, and on the handling of errors, see section 5.3.2. However, to prevent that the data cleaning process eternizes and arbitrary changes are performed in the database, the database has to be closed for edition at some

point so that it cannot be altered in any way.⁴⁰ This process is known as database locking; database locking is performed after the data integration and cleaning are considered to be complete and it is the end of data management activities.⁴⁰

5.3.2 Defining and achieving quality data

There are several theoretical frameworks on data quality for clinical studies; a useful framework employed in this work regards quality as the sum of three dimensions: conformance, completeness and plausibility.^{53,54} Conformance of data is defined as its compliance with the pre-specified standards, which can be variable- or study-specific.^{53,54} Data completeness evaluates the presence or absence of data and whether these agree with the expectations in the study, independently of the value of these data.^{53,54} Lastly, plausibility describes whether the data values are believable, based on expert knowledge on the variable at hand and the techniques employed for its measurement.^{53,54}

Conformance encompasses three sub-categories: value conformance, relation conformance and computational conformance.^{53,54} Value conformance describes whether the value of a data point is in the allowable range and the right format, relational conformance describes whether data points agree with the information of other data points, while computational conformance corresponds to whether values were calculated correctly. For the detection of non-conformances in data, the implementation of hard cut-offs for the allowable range, as well as the merging of databases can be of use.⁴⁶

Missing data can be due to several causes, including the patients skipping a study visit, loss of samples, errors in data entry, interruptions in data flow, as well as decisions taken by experimentalists.⁴⁶ Missing data are classified in three categories:

1. Missing completely at random: Data with no systematic differences between missing and observed values, e.g. missing measurement because of a technical problem.⁵⁵⁻⁵⁷
2. Missing at random: Data with systematic differences between missing and observed values that can be explained with available data, e.g. an increased number of missing measurements among older patients of an age-dependent variable.⁵⁵⁻⁵⁷
3. Missing not at random: Data with systematic differences between missing and observed values that can only be explained by the missing data themselves, e.g. an increased number of missing measurements in patients with a pathological value of the variable.⁵⁵⁻⁵⁷

Missing data can have profound consequences on the data analysis: They reduce the statistical power of the study, thereby reducing the ability to detect differences between groups.^{55,57,58} More importantly – in the case of missing data at random and missing data not at random – missing data introduce a bias into the results of data analysis.^{55,57,58} When missing data are unexpectedly encountered, the data flow has to be investigated, as in some cases measured data are lost due to breaks in data flow.⁴⁶ In case the data were never measured, several pre-processing methods can be employed to handle the missing data points (for more details, see sub-section 5.3.3).^{55,57,58}

Implausibility of data is also a multi-factorial phenomenon. It can be caused by e.g. errors in the experiment, data entry and data integration, leading to implausible values or implausible distributions of data.^{46,59} These can be detected using graphical exploration of their statistical distribution: Typing errors in the data collection can lead to extreme outliers; differing units in the data can be a cause of a multimodal distribution of a variable.^{46,47} Expert knowledge on

the data is necessary for investigation of implausibility, leading to the need of assistance in data cleaning.⁴⁶

5.3.3 Data pre-processing for data analysis

Data in a cleaned and locked database might not necessarily be in the form needed for analysis – data pre-processing is necessary under several circumstances. This is particularly the case for datasets with missing data points. There is a number of pre-processing techniques that can be employed in this case, including the use of only complete cases (which can introduce a bias in the results), replacing missing values by the last measured value (for variables with small changes in time) as well as imputation methods.^{55,57,58} Imputation methods attempt to estimate the values of the missing data by using the available data, based on the assumption that they are missing at random: single imputation methods provide an estimated value for each missing value; multiple imputation generates several imputed data sets to take into account the uncertainty of imputation.^{55,57,58}

A further reason for data pre-processing can be the requirements of the analytical techniques.^{60–62} For example, parametric tests such as the t-test require a normal distribution of the variable at hand; logistic regression techniques requires a binary dependent variable.^{63,64} Moreover, while a certain data structure might not be a strong requirement, some analytical techniques lead to better results when employing certain normalization techniques e.g. in neural networks.⁶⁰ There are several techniques that can be employed to transform the data into a certain structure, including log transformation, z-score normalization, rank transformation or binarization; detailed knowledge of the underlying assumptions of the employed analytical techniques as well as of the structure of the employed data is paramount.^{60,65,66}

Another factor that should be considered when pre-processing the variables in any multi-centre study are centre effects.⁶⁷ Centre effects are differences in the results of the study caused by differences between the participating centres.⁶⁷ Possible causes include differences in the demographic composition of each centre sub-cohort, in the treatment of the patients and in the sample analysis.⁶⁷ Only the third cause of centre effects can be avoided relatively easily by implementing a central measurement of all samples. A possible approach for the pre-processing of variables with strong centre effects is the normalization of the data.⁶⁵ In such approaches, the results obtained from each study centre are scaled and centred, so that e.g. the mean value and the standard deviation of the data is the same for all transplantation centres.⁶⁵ However, such approaches assume that the mean value and standard deviation *should* be the same for all transplantation centres, i.e. there are no differences in demographic composition and outcomes. Therefore, such approaches cannot be applied without knowledge of the expected centre effects for the variable.

5.4 **Data analysis methods for systems medicine**

Data analysis has to take into account the intrinsic high degree of complexity of the data, which makes the unaided interpretation impossible.^{4,5} A large plethora of methods, including machine learning, ordinary differential equation mathematical modelling, biostatistics, network analysis and time series analysis, are currently employed in systems medicine studies.^{4,5,10,12,68} These methods can be applied for four different categories of analytics: (i) descriptive analysis, to describe the patient outcomes; (ii) diagnostic analysis, to explain the patient outcomes; (iii) predictive analysis, to anticipate future patient outcomes; and (iv) prescriptive analysis, which attempts to change patient outcomes.⁶⁹ However, the application

of these methods for data analysis is not trivial, and it is important that the data scientist understands the medical problem at hand, the method in-depth and the goal of the analysis.^{4,69} Different methods are adequate for the acquisition of different insights, e.g. machine learning techniques are excellent for the detection of complex predictive patterns, but can hardly provide a diagnostic understanding of the patterns – a mathematical model might be thus more adequate for this problem.^{5,69,70}

In the next sections, basic concepts of the methods employed in this thesis are provided, with special emphasis on how they can be employed to achieve descriptive, diagnostic and predictive insights for personalized medicine.

5.4.1 Statistical analysis of clinical studies

5.4.1.1 *Clinical statistics: Basic concepts and methods*

The classical approach for the analysis of a clinical study is based on the concept of end-point.^{71,72} An end-point is a clinical variable that informs of the success of an intervention, e.g. the mortality rate or the rate of response to a therapy.⁷¹ Clinical studies usually have one primary end-point and may have one or more secondary end-points; the primary end-point is the most relevant for the research question, while secondary end-points can be used to better interpret the primary end-point.⁷¹ In interventional trials, the differences in the end-points are assessed for two or more groups receiving different treatments; in observational studies the influence of other variables such as demographic characteristics on the end-point is assessed.^{73,74} However, the wealth of data generated within a clinical study allows for far more than end-point assessment in pre-defined groups: Exploratory analyses can be undertaken to gain further understanding of the physiological and pathological processes taking place during the study.⁷⁵

Common methodologies employed for the statistical analysis of clinical studies include uni-, bi- and multivariate approaches.^{76,77} Univariate analysis provides a description of the data distribution, i.e. central tendency and dispersion; visualisation techniques to provide an intuitive understanding of the distribution are also recommendable.^{77,78} Bivariate analysis can be employed to compare end-points between patient groups in interventional and observational studies.⁷² The differences in a categorical end-point between two or more groups can be compared through the chi-square test (Fisher's exact test for a small number of patients); for continuous end-points, the Mann-Whitney U test (t test if normally distributed) is employed for two groups, while for three or more groups ANOVA is recommended.^{77,78} Pearson's and Spearman correlation tests are useful to compare two continuous variables.⁷⁸ Multivariate techniques, ranging from regression to machine learning, can be employed to model more complex relationships between variables, e.g. determining the demographic characteristics predictive for a certain outcome.^{76,79}

5.4.1.2 *The interpretation of multiple tests and non-randomized studies*

Importantly, the interpretation of the results of bio-statistical tests depends highly on the study design. A clear and detailed definition and pre-specification of the groups and end-points, a small number of hypotheses and outcomes, as well as prior strong biological evidence are necessary to consider results as confirmatory, both for observational and interventional studies.^{75,80} On the other hand, a large number of groups, hypotheses and outcomes lead to the performance of multiple statistical tests.⁸¹ Multiple testing inflates the type I error (i.e. falsely detected associations) to unacceptable limits, with 99.4% probability of at least one

false positive test out of 100 and 23% for only five tests for the conventional alpha value of 0.05.^{81,82} Several statistical methods can be employed to minimise the type I error for multiple independent tests, such as the Bonferroni adjustment; but these methods increase the risk of type II errors (non-detected associations).^{80–82} Because of this, multiple testing correction is essential for confirmatory analyses, even for a relatively low number of tests. But for exploratory analyses – since the goal is to generate hypotheses for further study – multiple testing correction might be even counterproductive.^{80–82} Non-adjusted results of multiple tests should therefore be clearly reported as exploratory.^{81,82}

Among interventional studies, randomised controlled trials are the gold standard design for assessing the effect of different treatments on the pre-defined end-points.^{83,84} The randomisation process, if properly implemented, makes the treatment group(s) and the control group comparable with respect to known and unknown factors affecting the outcome.^{73,83} Therefore, it can be assumed that any significant differences in outcome between the groups is caused by the different treatments.^{85–87} On the other hand, differences between groups in a non-randomized trial can be potentially caused by a confounder.^{74,83,88,89} Confounders are factors associated with both the treatment groups and the end-points; they can mask the effect of a treatment or lead to spurious associations between treatment and end-point.^{88–91} Confounders might be demographic factors, e.g. age and sex, or be study-specific, such as protocol differences between centres.^{83,90} Therefore, to avoid bias in the interpretation of data from non-randomized trials, it is essential to control for confounders.^{83,90,91} There are several techniques for controlling for confounders, including the comparison of baseline characteristics between groups, stratification or matching of patients for suspected confounders and multiple regression.^{83,91}

Multiple regression – linear regression for continuous and logistic regression for categorical end-points – is considered the most powerful tool for dealing with confounders.^{83,91} Then again, the choice of potential confounders to be included in a regression model is not trivial: While some authors highlight the importance of background knowledge to guide confounder selection, this is not possible in all cases, so that data-driven approaches are necessary.^{83,92,93} A popular strategy selects the variables based on their bivariate association with end-point and/or treatment groups, but this excludes confounders that can only be detected in multivariate analysis, e.g. two variables negatively associated with each other but with a positive effect on the end-point.^{83,92–94} On the other hand, controlling for all relevant variables in a full regression model can lead to overfitting and multicollinearity, especially for studies with a low number of patients and high number of variables.^{83,95,96} Variable selection methods can prevent the problems associated with full models without resorting to bivariate analysis and are thus the most adequate approach to control for confounders – backward elimination is a standard and recommended approach for that.^{93,96} Conventional backward elimination starts with a full model and removes variables sequentially based on the P value, until all variables have a P value below a set threshold.⁹² Nevertheless, this selection can be arbitrary and inflate the significance of the rest of the factors.^{93,96} The use of a selection criterion based on information theory, such as Akaike's information criterion, has been suggested to overcome these problems.^{93,96}

However, in spite of the approaches for controlling for confounders, non-randomized interventional studies are considered to lead to exploratory results, rather than confirmatory.^{74,83,91} The reason for that, among others, is that no method can control for confounders that have not been measured.^{83,89,91} On the other hand, the results of such

studies can be very valuable, as they might suggest previously unknown relationships between the treatment and outcome, leading to a larger output and higher efficiency in the analyses of a large clinical trial.^{73,75,83}

5.4.2 Machine learning approaches for disease biomarker discovery

5.4.2.1 *Introduction to machine learning*

A complex phenomenon cannot be captured based solely on one significant difference in one end-point between two sub-groups.^{97,98} The confirmatory study approach, described above, disregards individual differences to achieve (sub-)population-wide insights – other analytical approaches are more appropriate to create personalized solutions.^{97,98} With the increase in high-throughput data and computation capacity, machine learning approaches have become nearly ubiquitous for the analysis of complex phenomena.^{5,99,100}

Machine learning algorithms basically teach computers how to learn from the data. In contrast to regression, they are not based on the application of a set of mathematical rules, but learn directly and automatically from the data, making no assumption on the relationship between input data (so called features in the machine learning jargon) and the clinical outcome of interest.^{100–102} Machine learning methods can be classified into two broad categories: unsupervised learning algorithms, which require only the input features and attempt to unveil structures within the data; and supervised learning algorithms, which employ labelled data and attempt to predict the value of the labels based on the features.^{100,102} For example, while an unsupervised approach can classify patients in n clusters based on their transcriptomic profile, supervised approaches can be used to predict their age based on the same data.^{100,102} Machine learning models are built based on a training data set; for supervised learning it is possible to estimate the prediction performance in terms of specificity and sensitivity.^{100,102} Yet, this measure might not be representative of the performance in the general population as the model might overfit the training set, i.e. the model fits the data in an arbitrary way only due to a high number of features.^{100,102} Therefore, it is recommendable to split the available data in three sets, where the first is employed for training, the second for model selection and the third for model performance assessment.^{100,102} For smaller data sets that cannot be split, alternative techniques can be employed to assess the performance.^{102,103} These include internal cross-validation and permutation tests or label shuffling.^{102,103} Furthermore, feature selection algorithms can be beneficial to increase the efficiency and accuracy of the learning process, reducing the complexity of the data and prioritising features potentially informative or important for prediction.^{104–106}

Support vector machines (SVM) are a popular supervised machine learning methodology in biological and clinical research.^{79,107–109} It is usually employed for binary classification, but there are SVM implementations for multiclass classification and regression problems.^{107,110,111} SVM regard data as points in a high-dimensional space.^{107,112} For example, a data set consisting of the expression of three genes from forty patients, half of them with a positive disease progression, is regarded as forty labelled points in a three-dimensional feature space (see Figure 1). The algorithm attempts to determine the label disease progression for each patient based on their position in this three-dimensional space; this is performed dividing the space with a plane that splits the space in half and separates the patients based on their progression, so that the plane has the maximum possible distance to the points.¹¹² In real implementations of SVM with a higher number of features, this three-dimensional plane becomes one or more hyperplanes.^{107,112} As a linear separation of the data still might not be feasible, a kernel

function can be applied to generate non-linear hyperplanes.^{107,112} There is a large diversity in the implementation of the core idea of SVM, ranging from the use of different kernel functions to alternative methods based on SVM.^{62,107,111–113} One of these alternative methods is the potential support vector machine (P-SVM).⁶² In contrast to classical SVM, P-SVM performs feature selection as well as the estimation of the prediction performance; furthermore it works satisfactorily for small patient cohorts and the experience has shown it to be especially appropriate for the search of biomarkers in certain contexts, such as antibody binding profiles.⁶²

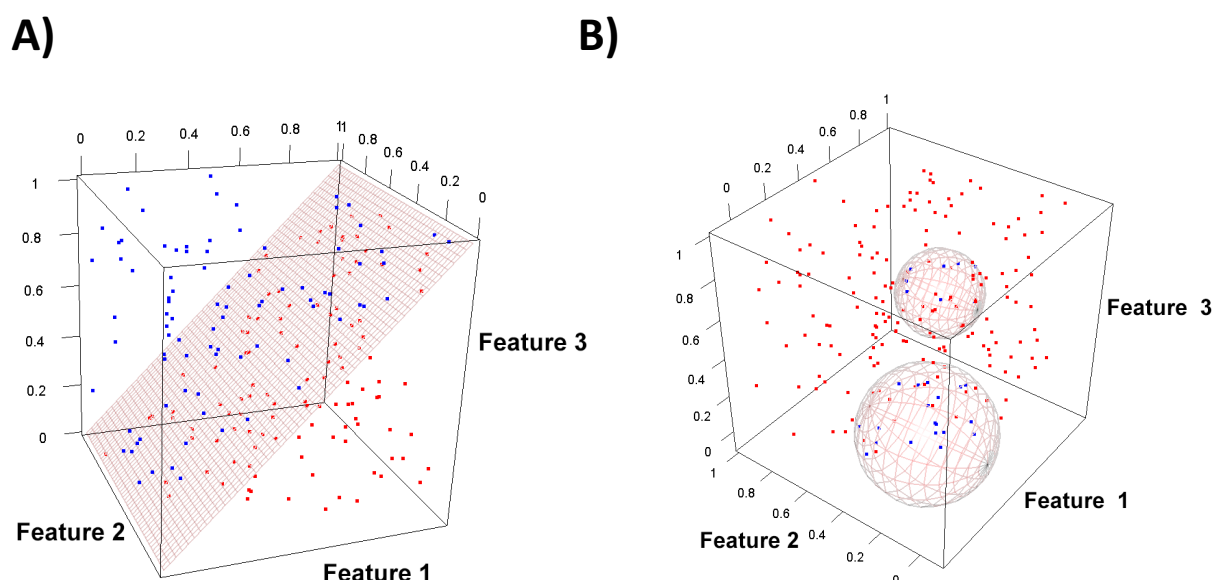


Figure 1. Two illustrative examples of classification employing SVM. (A) The algorithm separates two classes (represented as blue and red points) employing a linear three-dimensional plane. A combination of features 1 and 3 are employed for the classification. (B) The algorithm separates two classes employing a non-linear kernel, based on all three features.

Other examples of machine learning methodologies include hierarchical, k-means and spectral clustering and sparse coding for unsupervised problems, and random forests and decision trees for supervised problems; artificial neural networks can be employed both for supervised and unsupervised problems.^{100,102,114} The latter are considered especially promising, as complex (multi-layer) neural networks are the basis of most deep learning methods.^{115–118} Deep learning methods aim to extract abstract features from the raw input data, in a way roughly comparable to the way human brains process information, potentially improving the analysis of heterogeneous and complex data sets.^{115–118}

5.4.2.2 Machine learning in clinical research: Opportunities and challenges

Machine learning methods are applied extensively in a wide range of biological and clinical studies, including the analysis of imaging technology output, processing of text annotations in literature, prediction of three-dimensional protein structure or the analysis of biological interactions in high-throughput experiments.^{118–120} Their capacity to detect patterns in large, heterogeneous datasets makes them essential for the development of personalized systems medicine, especially in the search for predictive disease biomarkers.^{5,68} In fact, machine learning is being employed in the search of biomarkers for virtually every complex clinical process, including cardiovascular disease, cancer, diabetes, Alzheimer, HIV, osteoporosis, Huntington's disease, and even ageing.^{121–127} In kidney transplantation, the goals in biomarker discovery comprise the non-invasive, cost-effective monitoring of graft function, early

diagnosis of complications (especially rejection), evaluation of the effective immunosuppression and graft tolerance and prediction of long-term outcomes.^{12,13} While such a biomarker panel has not been clinically validated yet, there are several promising results.¹² These include, but are not limited to: A non-invasive urinary marker for acute cellular rejection, several early risk assessment models for acute cellular rejection (see Table S5 in 9.2.8 for an exhaustive comparison of predictors in the literature), a 595-gene expression signature of graft operational tolerance or validated genetic risk scores for the development of post-transplantation diabetes.^{12,35,128–131}

However, although machine learning approaches hold big promise for biomarker discovery, the prediction performance is often not sufficient to justify their validation and application in the clinic.^{5,99} Machine learning algorithms, as sophisticated as they might be, depend on the quality and quantity of the data and, importantly, on their adequacy for the research question – no algorithm can squeeze information out of data that hold no information.^{5,99,132} Moreover, the training of machine learning algorithms usually requires high quantities of data of a large number of patients, but many omics high-throughput data have high technical measurement errors.^{5,99} This is challenging, as there are no satisfactory methods to discriminate between signal and noise.^{5,99} Likewise, a careful choice of the training cohort is central to the performance of the algorithm in the general population, as machine learning procedures are highly sensitive to selection biases in the patient cohort.^{5,99,133} This has led in the past to *racist* and *sexist* algorithms, due to under- or over-representation of some ethnicities in the training set.^{5,134}

All the problems highlighted above will be improved with the development of cheaper, more precise high-throughput techniques, allowing the performance of measurements in large, representative patient cohorts. But there are deeper issues pertaining the core of machine learning that hinder their use in clinic: They can be very difficult to interpret.^{5,133,135} Machine learning methods do not detect causal relationships between biomarker and outcome, but capture a highly complex biomarker signal and employ it for an outcome prediction, i.e. they do not necessarily provide a mechanistic understanding of the problem at hand.^{101,135,136} Because of this, machine learning approaches cannot replace classical hypothesis-based research yet, but rather complement and enrich it.⁵ Moreover, most algorithms are “black boxes”: They work, but we do not understand why or how, as the used patterns cannot be intuitively understood.^{5,135,137} The issue of interpretability will likely become more acute with the development of deep learning algorithms.^{5,115,135} This is highly problematic, as trust in the algorithm by clinicians and patients is essential for their application in real life medicine.^{5,133} Therefore, there are now increasing efforts to develop software to better interpret the results of machine learning models.^{115,133,135,137–139} Understanding why the machine gives a diagnosis or predicts an outcome will thus be key to the application of these algorithms in day-to-day clinical practice, therefore improving patient care and quality of life.

5.4.3 Mathematical modelling as a tool for mechanistic understanding

5.4.3.1 *Introduction to mathematical modelling in clinical research*

The classical research approach in biology – in contrast to the newer, data-driven machine learning approach – is based in the generation and verification of hypotheses.^{5,136,140,141} A hypothesis is a qualitative model of a biological mechanism (if A then B) with implications that can be tested through experimental procedures; the results of the experiment determine whether the model has to be modified.¹³⁶ Mathematical modelling is an extension of the same

concept, as they are a quantitative, objective, abstract description of a set of hypotheses.^{136,142,143} In contrast to traditional hypotheses, mathematical models are “working” hypothesis, whose behaviour can be directly studied.^{142,143} As such, they can be employed for the testing of hypotheses, and have to be revised in light of experimental results.^{136,142–144} Mathematical models compile the existing knowledge on a biological question in a rigorous way, highlighting gaps in knowledge.^{143,144} A validated model can be employed to simulate different conditions and perturbations, which would be very costly to perform in an experiment.^{143–146}

Mathematical modelling is an essential tool in many scientific areas – including physics, chemistry, meteorology, seismology – and are widely employed in engineering, where they have accelerated and improved development.^{142,146,147} Although mathematical models are not as widely used for clinical questions as for engineering problems – probably due to the inherent complexity of biological processes – there are considerable efforts in areas as diverse as cancer, degenerative disease, vaccines, immunology and pharmacokinetics.^{144,146–154}

The process of model development in biology is not trivial, as the same process can be described in more than one way, employing different mathematical formalisms.^{143,146,155} Moreover, different approaches for studying the same problem may provide different insights.^{143,155} To decide the type of modelling approach, it is essential to clearly formulate the research question to be addressed.^{143,155} With a research question, the available experimental data and information from the literature including existing models can be employed to determine the general type of the model.^{143,155} There are several possibilities for model architectures, including Boolean networks (determinist models with binary variables), partial differential equation models (determinist models with continuous variables considering time and space differences) or stochastic models (models taking into account random effects).^{9,155} Among all modelling frameworks, ordinary differential equations (ODE) are the simplest modelling deterministic framework with quantitative variables.^{155,156} ODE models describe the variations of a set of variables over time, disregarding spatial differences for the variables.^{9,155} Because of this, ODE models are by far the most common framework for various kinds of biological problems, including modelling of metabolic pathways, ecological or immune dynamics.^{155–157}

Based on the structural decisions, a first version of the model can be built.^{143,155} This first version contains parameters that have an essential influence on the behaviour of the model.¹⁴³ While some parameters might have been determined in previous studies, often many parameters are not generally determined, as they depend on e.g. experimental conditions, patients and even the time of the measurement – in fact, many biological parameters are not even determinable.^{147,155} The value of these parameters for the given research question has to be estimated by fitting the model to the experimental data.¹⁵⁵ Fitting is performed by optimising the model so that the predicted results approximate as much as possible the experimental data.^{155,158} The deviation of the predicted data from the experimental data is quantified by the objective function.¹⁵⁵ During fitting, the possible combinations of parameter values are scanned; the parameter set leading to the lowest value of the objective function is selected.^{155,158} Although several functions can be employed, the sum of squared residuals is a common objective function, which can be employed for model selection.¹⁵⁵

After the parameters have been tentatively fitted, the quality of the model – including both the structure and the values of the parameters – can be assessed based on its capacity to

reproduce the training experimental data set, as well as other validation data sets.¹⁵⁵ In practice, modelling often involves several cycles of model generation, fitting and testing.¹⁵⁵

5.4.3.2 Application of mathematical models for viral dynamics

Modelling has a considerable history of applications in the area of viral infections and the immune response against them: After pioneer work on HIV, there are models describing (parts of) the dynamics of influenza virus, Hepatitis B and C, West Nile virus, Epstein-Barr virus, cytomegalovirus or BK virus, among others.^{70,154,166–171,156,159–165} These modelling efforts have greatly increased our knowledge of infection dynamics, with insights spanning from basic biology to clinical decisions.^{156,172} A paradigmatic case is HIV, which was thought to be a slowly-replicating virus (similarly to other lentiviruses): Two mathematical models suggested for the first time in 1995 that the virus was replicating and being cleared very fast, leading to an apparent steady state.^{156,173,174} These rapid dynamics have deep consequences in the treatment, as fast viral replication is associated with the apparition of drug resistances.^{156,173}

More recently, mathematical modelling of HIV has suggested the presence of latent infected cells that occasionally reactivate; modelling is also employed to interpret the viral kinetics during and after antiviral therapy and to predict the success (or failure) of different tentative therapies.^{175–177} In the case of influenza, mathematical modelling has been among others successfully used to predict the viral load kinetics of infection, the efficiency of antiviral immune responses, the efficacy of vaccines and mechanisms of co-infection with other pathogens.^{178–182} The latter case is especially interesting, as it was a mathematical model that first suggested an effect of influenza in reducing *Streptococcus pneumoniae* clearance –this effect has been experimentally validated.^{172,178,183–186} In fact, the experimentally observed decrease in anti-streptococcus immune response corresponds with the estimated value of the parameter in the model.^{172,178,183,184,186} Importantly, the fact that there were various inaccuracies in the model did not hinder its capacity to make accurate predictions on the virus-bacteria interactions.^{172,183,186}

For BK virus, although the number of existing models is reduced, mathematical modelling has been employed to demonstrate its fast replication and clearing dynamics and the cytopathic effects of the virus; likewise, the influence of immunosuppression on the BK virus proliferation and serum creatinine have been modelled.^{164,165,171}

Even though there are numerous mathematical approaches to model viral dynamics, the most commonly used model is the so-called basic or standard viral dynamics model (Figure 2).^{70,172,187–189} The basic viral dynamics model is an ODE model based in the ecological predator-prey model.^{70,145,172} It consists of one compartment and three variables (target cells, infected cells and virus), where virus infect target cells leading to infected cells, which produce more virus; target cells replicate and die at a constant rate, while infected cells die at a higher rate and virus is likewise constantly cleared.⁷⁰ Variations of the basic viral dynamics model have been used to model the infection of both acute and chronic infections, including HIV, influenza virus, hepatitis B, Dengue virus, yellow fever, cytomegalovirus and BK virus, among others.^{163,166,167,170,171,190,191} This is probably due to the fact that most viral infections have similar kinetics, with exponential increase in the beginning and a peak, after which a mono-bi- or tri-phasic decay leads to clearing or a steady state (depending on whether it is an acute or a chronic infection).¹⁷⁸

A)

$$\frac{dT}{dt} = \lambda - d \cdot T - k \cdot V \cdot T$$

$$\frac{dI}{dt} = k \cdot V \cdot T - \delta \cdot I$$

$$\frac{dV}{dt} = p \cdot I - c \cdot V$$

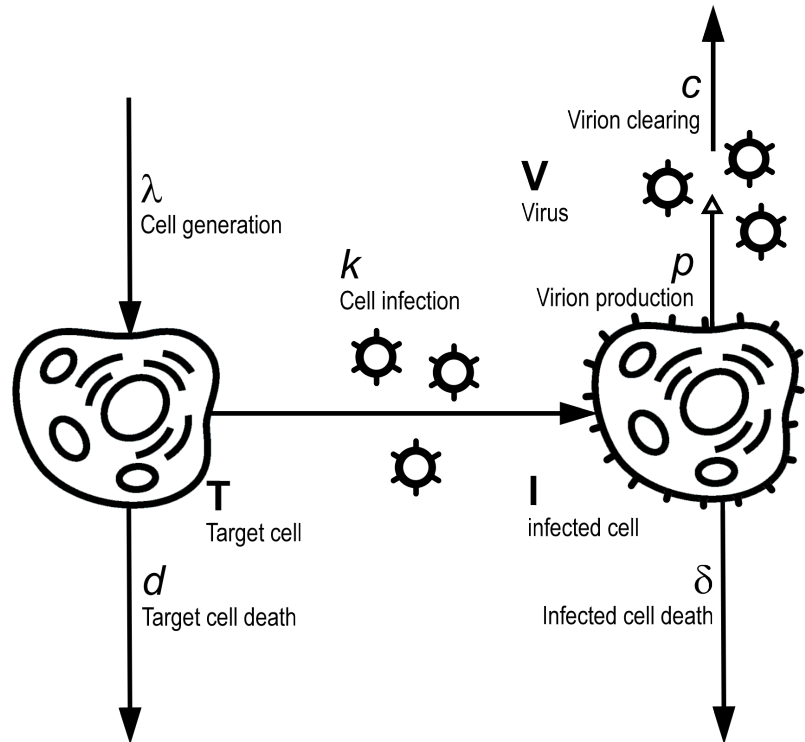
B)

Figure 2. The basic viral dynamics model.

The basic model of viral dynamics, as described by Perelson *et al.* 2002, is depicted as (A) a system of differential equations and (B) a graphical representation.⁷⁰

5.4.3.3 Interpretation of modelling results: Parameter identifiability and model selection

Parameter estimation attempts to approximate the real parameter set i.e. the parameters that determine the studied dynamics assuming that the model structure is an adequate approximation to the problem.¹⁵⁵ However, different parameter sets may lead to the same final value of the objective function, meaning that there is no unique solution to the parameter estimation.^{155,192–194} This situation is defined as non-identifiability, which can be of structural or of practical nature.^{155,192–194} Structural non-identifiability is caused by the very definition of the model, so that no possible experimental data could lead to identifiable parameters; on the other hand, practical non-identifiability is caused when the quantity or quality of the data is not sufficient to approximate the value of all parameters.^{155,192–194} Structural identifiability is a necessary condition for practical identifiability.^{192,195} Practical non-identifiability is especially likely if the model has too many parameters for the measured data, potentially leading to an overfitted model.^{155,192,194}

There are several techniques that can be employed to detect non-identifiability and how experimental data should be to lead to identifiable parameters.^{192–194} They can be applied at the design stage, before model fitting to the experimental data is performed, and even before the experimental data are collected.^{192–194} Procedures for assessing structural identifiability include the direct test and differential algebraic methods; for the practical identifiability Monte Carlo approaches or sensitivity analysis can be employed.^{192,196,197} Moreover, due to measuring error, even if a model is identifiable, the parameters can only be estimated within a certain confidence interval.¹⁹³ Confidence intervals can be calculated through bootstrapping and analytic techniques.^{193,198–200} A wide confidence interval denotes a variable whose value has not been determined precisely and might even be practically unidentifiable.^{193,195,201}

However, non-identifiability of parameters does not necessarily mean that the model is not useful or appropriate for the research question.^{172,194,198} Relevant quantitative conclusions about the parameter values can be gained from over-parameterized models.^{147,172} Moreover, the estimation of parameters is often not the final goal of a mathematical model.¹⁹⁴ The relevance of model identifiability depends thus on the objective of the modelling approach; it is central when the actual values of the parameters are part of the research question, or when the goal is to predict the dynamics of a variable (e.g. infected cells) that cannot be directly measured.¹⁹⁴ If these conditions do not apply, models with non-identifiable parameters can provide qualitative and quantitative information, especially in rejecting certain hypotheses over others.^{147,172,194}

Modelling different biological hypotheses to test and compare them is a method of achieving new insights on the data.¹⁷² In this approach, several models representing different hypotheses are fitted to the data set, where the degree of agreement of the data can be employed to prefer or reject certain hypotheses.¹⁷² It has been employed to gain biological insights, for example on the immune response after influenza or yellow fever vaccination.^{172,190,202} While hypothesis testing can be performed examining the model behaviour and comparing it with qualitative data, fitting the model to quantitative data opens the possibility for formal model selection.^{155,172,203}

In model selection, a better fit of the data is not sufficient evidence by itself to prefer a model over others.¹⁵⁵ This is because a model with a higher number of parameters might be able to overfit the data, leading to a lower value of the objective function.¹⁵⁵ To account for this effect, selection criteria based on information theory are employed: The most widely-used are Akaike's information criterion (AIC), the corrected Akaike's information criterion (AICc) and the Bayesian information criterion (BIC) – the main difference between the criteria is how much they penalize the number of free parameters, where BIC and AICc are preferred for small sample sizes.^{155,204} These selection criteria are based in the maximum likelihood function of the model.^{155,204} Assuming independent, normally distributed errors, the likelihood is considered to be equivalent to the sum of squared residuals.^{155,204} Selection criteria allow to rank models where those with a lower value have a higher degree of empirical support; while there is no notion of significance, a difference in the range [0,2] with the best performing model is considered to give the hypothesis substantial support.^{155,204} Other approaches for model selection include the likelihood ratio test for nested models, swarm optimization or the least squares approximation methods.^{155,157,205,206}

Importantly, employing several models to test hypotheses does not result in the confirmation of the best model according to a given criterion, i.e. it cannot confirm that the chosen model is the *real one*.¹⁴⁷ Like in statistical hypothesis testing, the real question is not whether a model is confirmed, but whether it is rejected or not, where a rejection means that the given model is not a reasonable explanation for the experimental data.¹⁴⁷ If there is no further information, the results of a non-rejected model – even the best performing model – are to be regarded as suggestions that have to be validated through model-driven experiments.¹⁴⁷

5.5 Scope and structure of this dissertation

In the subsequent chapters, I present my work on personalized medicine for renal transplantation patients, performed within the systems medicine research alliance e:KID, in which I participated as a data scientist. This doctoral thesis describes the results achieved within the consortium, framed as a perspective on the very broad methodological possibilities

for data analysis and interpretation in systems personalized medicine. The next chapters are structured as follows: (i) a chapter describing the data management strategies applied within the e:KID study in detail, as these strategies were critical for the presented results and are therefore an integral part of my doctorate; (ii) four chapters containing the publications of this thesis and their respective supporting information; (iii) a chapter summarising the results of the publications in the context of personalized medicine and, finally, (iv) an outlook on future analytical approaches that are already possible with current data and personal reflections on the future possibilities of systems personalized medicine.

6. Data management in the e:KID study

In this chapter, the data management strategies employed within the e:KID study are described in detail, as these strategies were critical for the presented results and are therefore an integral part of my doctorate. As explained in the introduction (section 5.3), effective data management strategies are essential for achieving high-quality data, adequate for data analysis and interpretation.^{40–42} Here, following the recommended best-practices on data management, I report on the processes of database design, data entry, database integration, data cleaning and data pre-processing in the e:KID study.⁴⁶ Additionally, background information on the e:KID study and consortium is provided in section 6.1, as a detailed understanding of the study is essential for the management of its data.

Even though my role in the e:KID consortium was primarily in data analysis and interpretation, because of these activities I worked intensively on the database. Therefore while I did not have the opportunity to participate at the design of the e:KID database, I have been able to participate in the processes of data cleaning and pre-processing. In this chapter, I report on the whole process of data management, highlighting my personal contribution.

6.1 Background: e:KID, a systems medicine study for kidney transplantation

6.1.1 Design of the e:KID study: Patient cohort and selected markers

e:KID was designed as an experimental sub-study of the large multi-centre Harmony clinical trial (NCT00724022), profiting from the measurements and samples collected during the trial. Harmony is an open-label, randomised controlled study that examined the impact of immunosuppressive therapies in transplantation outcomes one year after renal transplantation.³¹ The standard practice for immunosuppressive therapy, the so-called quadruple therapy comprising basiliximab induction therapy, corticosteroids maintenance therapy, mycophenolate mofetil (MMF) and tacrolimus was compared with two alternative triple therapies: (i) basiliximab, MMF and tacrolimus and (ii) rabbit antithymocyte globulin, MMF and tacrolimus.³¹

A total of 615 low immunological risk patients from 21 transplantation centres were recruited for the study; 587 patients underwent renal transplantation between 2008 and 2012.³¹ Blood and urine samples were collected in parallel from the participants of the study along eight visits during the first post-transplantation year.³¹ Over three thousand samples were analysed for clinical variables, including renal function, rejections, infections, diabetes markers and cardiovascular risk factors.³¹ The primary end-point was the incidence of acute transplant rejection; secondary end-points included patient and graft survival, graft function, viral reactivations and diabetes occurrence, among others.³¹

While no advantage of the triple maintenance therapies was found for the primary end-point, the study demonstrated that these therapies are comparable in regard to safety with the standard quadruple therapy: For low immunological risk patients, (i) antithymocyte globulin and basiliximab induction therapies can be employed equivalently and (ii) corticosteroids maintenance is not necessary.³¹ In summary, the Harmony study was a major step towards stratification of immunosuppressive therapies, providing novel evidence for new standard immunosuppressive strategies.

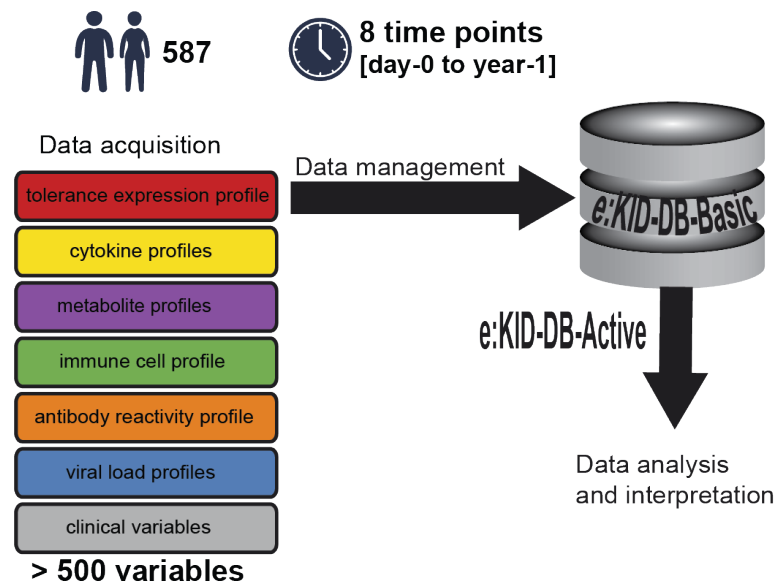


Figure 3. The e:KID approach. Figure adapted from previous work by Nicole Wittenbrink.

As explained in the Introduction, the main goal of e:KID is to optimize the treatment of patients, by creating a personalized profile that can be used to understand the key individual factors determining transplantation outcome. As a continuation of Harmony, e:KID employed its measurements and observations, as well as the large number of samples collected during the trial. In order to establish the personalized profile, these samples were further characterized for markers of the immune system and transplantation complications by the e:KID consortium (Figure 3); for the list of measured parameters see Table 2.

Sample type	Marker type	Marker	#Variables
Whole blood	Immune cell subtypes	T cells, CD4 ⁺ cells, CD8 ⁺ cells, T regulatory cells, follicular B helper T cells, natural killer cells, B cells and neutrophilic granulocytes	8
Whole blood	Gene expression of tolerance and rejection markers	CD79B, CD200, CD247, CD274, CXCL10, FCRL1, FCRL2, FOXP3, HMMR, HS3ST1, LAG3, MAN1A1, MS4A1, NAV3, PNOC, SH2D1B, SLC8A1, TCL1A, TLR5 and TMEM176B	20
Serum	Cytokine concentration	IL17, TNF α , IL6, IL19, IL-22, SCF, sST2, BD2, angiogenin and endostatin	11
Urine	Antibody reactivity profile	IP10	
Serum	Antibody reactivity profile	Anti-HLA-1 and anti-HLA-2	116
Whole blood	Viral load	BK virus	3
Serum		Cytomegalovirus and Epstein-Barr virus	
Urine	Nuclear magnetic resonance metabolomics spectrum		377

Table 2. Summary of the markers measured as part of the e:KID study.

6.1.2 Organizational aspects of the consortium

The e:KID approach would not be possible without the expertise of a multidisciplinary consortium. Therefore, an alliance of ten partners was created, encompassing hospitals, research centres and private companies (see Figure 4). The team was highly heterogeneous, and incorporated clinicians, data scientists and experimentalists specialized in the different markers measured within the study. Sample management, experimental data generation, database management, data cleaning, data analysis and data interpretation were undertaken as an iterative process, in which new markers are measured based on the obtained results.

This iterative character allows for an ever-improving quality of the analysis, taking advantage of the combined expertise of clinicians, experimentalists and data scientists.

Data scientists worked mainly within three e:KID partners, all with roles in data management, analysis and interpretation. While there was some degree of specialization – e.g. a dedicated partner for management – a network-centric structure was decided to take advantage of the different areas of expertise of the data scientists.²⁰⁷ Therein, most decisions on data cleaning and data pre-processing were taken by the whole data scientist team, in communication with the rest of the consortium. Analysis was likewise performed by the data scientist team, based on the research questions and expertise of the rest of the partners; interpretation of the results was discussed with clinicians and experimentalists.

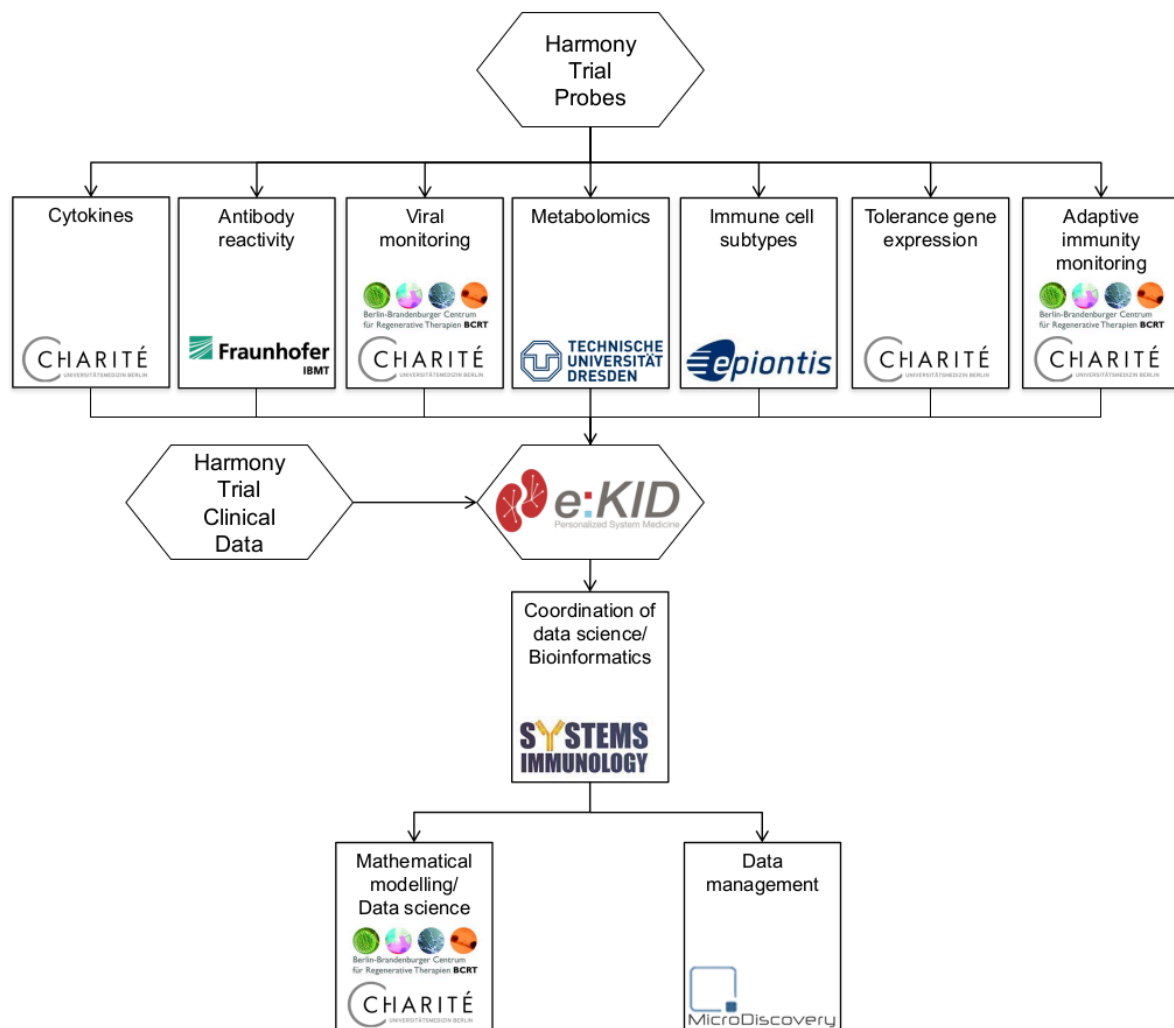


Figure 4. Structure and approach of the e:KID consortium. Organizational structure of the e:KID consortium, including the function of the different partners. Experimental partners are shown in the upper part of the figure; data science partners are shown in the lower part.

6.2 Database design and integration for the e:KID study

In this section, the processes of database design and integration in e:KID are reported, explaining the background and goals of the main structural decisions. Many of the structural decisions are motivated by the Harmony trial and structure of its database. Therefore, a short

overview on the Harmony database is provided first in sub-section 6.2.1, as it is necessary to understand the database design (6.2.2) and integration processes (6.2.3) in e:KID.

6.2.1 Structure of the original Harmony database

The Harmony database is composed by a total of 53 tables (see Table 3) in SAS format. It comprises e.g. data on the baseline characteristics of the patient cohort, their evolution and outcomes in the first year post-transplantation and the medication employed during the study. The large majority of the tables correspond to patient data; the rest contain metadata necessary for the understanding of the database.

Table Name	Visit	Nº Entries	Nº Variables	Patient Data?	1P-1R?
Chronic Kidney Disease	1	631	25	Yes	Yes
Demography	1	637	28	Yes	Yes
Osteodensitometry	2	592	31	Yes	Yes
Osteodensitometry	8	509	31	Yes	Yes
Exclusion	1	633	34	Yes	Yes
Inclusion	1	635	22	Yes	Yes
Laboratory Analysis	1	630	127	Yes	Yes
Laboratory Analysis	2	594	106	Yes	Yes
Laboratory Analysis	3	567	118	Yes	Yes
Laboratory Analysis	4	547	121	Yes	Yes
Laboratory Analysis	5	529	134	Yes	Yes
Laboratory Analysis	6	503	121	Yes	Yes
Laboratory Analysis	7	477	125	Yes	Yes
Laboratory Analysis	8	513	143	Yes	Yes
Medical History I	1	632	41	Yes	Yes
Medical History II	1	631	34	Yes	Yes
Physical Examination	1	631	61	Yes	Yes
Reminder	2	590	24	Yes	Yes
Reminder	3	565	24	Yes	Yes
Reminder	4	545	24	Yes	Yes
Reminder	5	528	24	Yes	Yes
Reminder	6	497	24	Yes	Yes
Reminder	7	471	24	Yes	Yes
Reminder	8	506	24	Yes	Yes
Transplantation	1	632	62	Yes	Yes
Virology	1	630	25	Yes	Yes
Vital Signs	2	604	25	Yes	Yes
Vital Signs	3	583	25	Yes	Yes
Vital Signs	4	555	25	Yes	Yes
Vital Signs	5	537	25	Yes	Yes
Vital Signs	6	514	25	Yes	Yes
Vital Signs	7	487	25	Yes	Yes
Vital Signs	8	524	25	Yes	Yes
Study Completion / Withdrawal		636	59	Yes	Yes
Study Population Definition		637	4	Yes	Yes
Study Medication		16424	22	Yes	No
Trough Levels		19473	18	Yes	No
Adverse Event		6619	31	Yes	No

Opportunistic Infections	412	29	Yes	No
Non Opportunistic Infections	511	28	Yes	No
Concomitant Medication	29142	28	Yes	No
Biopsy / Rejection	867	36	Yes	No
Days of Hospitalization	1887	19	Yes	No
Unplanned Laboratory Analysis	252	143	Yes	No
Unplanned Virology	418	25	Yes	No
Unplanned Osteodensitometry	6	31	Yes	No
Comments	966	16	Yes	No
Laboratory Definition	27	14	No	
Normal Range	1525	22	No	
Centres	31	13	No	
Visits Coding	23	9	No	
Option Sets Coding	140	6	No	
Option Sets Definition	670	7	No	

Table 3. Tables of the Harmony database. 1P-1R denotes those tables with only one row per patient.

Such data structures, with a high number of tables with thousands of elements each, are common in large clinical studies. The structure is determined by the method employed for the data collection, the electronic case report form (eCRF).^{40,49} At each visit of the Harmony study, the physician/study nurse had to fill a set number of eCRFs, including a reminder form interrogating on events between the visits and prompting the filling of other forms based on the responses. The data introduced in the eCRF (as well as the metadata of the responses) were cleaned by the Harmony consortium, becoming the Harmony database, which can be interpreted with help of a separate report detailing the contents of the eCRF. This database collects the whole bulk of information generated within the study – largely exceeding the goals of the clinical trial – making it an invaluable source of information for further studies on the cohort.

The data is organized according to the unique patient identifier (PID). It is an unambiguous identifier for each patient, used throughout the Harmony database. The PID also contains the reference of the transplantation centre, allowing for an easy classification of the patients.

The tables containing patient data are heterogeneous in their structure, as in some cases each patient is described in only one row (1P-1R), while other tables may contain more than one row per patient (1P-MR). The majority of the 1P-1R tables correspond to observations performed within the eight pre-programmed visits of the clinical study. The rest of the tables containing patient data correspond either to unplanned observations or to observations that can be potentially performed at any point in the study. The large majority of these are 1P-MR, with each row corresponding to a measurement performed at a different time point. Thus, to identify a row of a 1P-MR table unambiguously, one date variable is necessary, together with the PID identifier. Likewise, at least one date variable is included for most 1P-1R tables. As the date variables are defined independently for each table, differences between them are possible e.g. the Vital Sign and Laboratory Analysis tables may contain a different date for visit 3 of patient 4900101. This is necessary for the correct annotation of observations performed at different dates but corresponding to the same visit and was central in the considerations for data management and cleaning of the e:KID study.

6.2.2 Design of the e:KID database

For the database of the e:KID study, a radically different design was chosen, in order to accommodate the new data as well as the needs of the project. As explained in section 6.1, for the e:KID study a new longitudinal data set was generated using the samples collected during the eight visits of the Harmony study. These new data should be integrated with all the information from the Harmony database deemed relevant for achieving the goals of the e:KID study. The new data set had a substantially lower degree of complexity – it was largely quantitative and no variables were measured outside the pre-defined visits. These data were generated in an experimental setting, in contrast to the clinical setting of the Harmony database.

The iterative workflow of e:KID, as well as the high number of data scientists who would employ the data set for the analyses required an easy-to-handle database. It was therefore decided that the database was to take the form of a single file in a standard format in order to make the data transmission within the consortium easier. This implies a series of design decisions that fundamentally affect the work with data.

The first structural decision concerned the inclusion of study metadata, which explain the meaning of all measured variables. In this case, there were two main alternatives, either to create a detailed description in the form of a report, or to summarize the information as a secondary table in the main database file. The main advantage of the first option was the facilitation of the transmission of knowledge on the database, making it easier for an uninvolved data scientist to eventually analyse the results in the future, as was the case in the Harmony study and its eCRF report. However, the second option was preferred, as it fitted better the goals of our project: Achieving a flexible, simple transmission of the data in a context in which several versions of the database are to be created.

A)

PID	Visit	Variable 1	Variable 2
4900101	1		
4900101	2		
4900101	3		
4900102	1		

B)

ID	Variable 1 Visit 1	Variable 2 Visit 1	Variable 1 Visit 2
4900101			
4900102			
4900103			

Figure 5. Two possible structures for the e:KID database. (A) The long table structure incorporates more than one row per PID and a visit variable. (B) The wide table structure incorporates one row per PID and several columns per measured variable, accounting for the different visits.

A key question was the structure of the main database. Longitudinal data can be represented as a *long* table and a *wide* table (Figure 5).²⁰⁸ A *long* table contains each measured variable as one column, so that longitudinal measurements of the variable are shown as different rows; the *wide* table format represents each patient as one row, so that longitudinal measurements of each variable are shown as different columns of the table.²⁰⁸ Each structure has advantages and disadvantages. The *long* structure is much simpler to handle: It is easy to select the values of a variable for a concrete visit or the time course for one patient. On the other hand, non-longitudinal data, such as the demographic information of the Harmony database, would have to be included as a second additional table or, alternatively as an additional visit of the main table, greatly complicating the data structure. Moreover, not all Harmony study variables

were measured at the eight visits – for some variables (e.g. drug trough levels) there are even more available measurements. Lastly, the *wide* structure makes the iterative incorporation of new measurements in the database substantially easier, as the new measurements can just be added as additional columns at the end of the table. Because of all the referred reasons, a *wide* table format was elected as the basis for the e:KID database.

The third structural issue that had to be addressed for the creation of the e:KID table was the handling of multiple date values referring to distinct collected samples and clinical observations, but pertaining to the same visit and patient. As explained above, the date of the clinical observations and sample collection in the Harmony database is defined separately for each table (in some tables there is even more than one date variable), so that there can potentially be different measurement dates for the same visit and patient. This feature of the Harmony database was elected to allow for more flexibility and precision in the recording of sampling times and clinical observations, as it is potentially possible that two medical examinations pertaining the same visit were performed on different days. In the e:KID database it would have been possible to collapse these dates into only one consensus date, allocating a single date to each visit. This would make analyses simpler due to the lower number of variables but would also imply a loss of information. Therefore, it was decided to keep the different dates in the database.

Based among others on the outlined structural decisions, the database e:KID-DB-Basic was designed with the goal of optimizing data management. Simultaneously, scripts were developed for the adaptation of the e:KID-DB-Basic for use within the consortium. These scripts transform the large, difficult to handle *wide* table with multiple date variables into several smaller tables (e:KID-DB-Active). This working structure comprises one *long* table for each e:KID marker type (viral load, cytokine concentration, etc.) together with several *long* tables for events that are not associated with a visit (e.g. acute rejection events) and an additional table for the demographic characteristics of the cohort. The tables on the e:KID data were structured based on the visit number together with PID as the unique identifiers of each row; date variables were collapsed for the sake of simplicity as the median of all available dates of each visit. The scripts were designed in parallel to e:KID-DB-Basic using the data management and analysis software R, so that for every new version of e:KID-DB-Basic, a new version of e:KID-DB-Active would be generated.

6.2.3 Data integration in the e:KID study

In the e:KID consortium, data are integrated into the main database as an iterative process, so that analyses could be begun before all expected data have been measured and submitted. For the inclusion of new data, the experimentalists create a table in Excel or CSV format, ordering the data according to a sample number, PID, date of the measurement and visit. Data standards, such as the employed pre-processing methods and detection limits, are defined by the experimentalists according to their expertise and informing the data scientists. For example, in the case of the nuclear magnetic resonance spectra data, it was decided to include them after transformation through binning, in order to reduce the dimensionality of data; gene expression data were likewise normalized for three house-keeping genes.^{209,210} Experimentalists also provide the data needed for the interpretation of the variables, which are then included in the metadata secondary table. Afterwards, the data scientists clean the data (for more details see section 6.3), consulting with the experimentalists in case of discrepancies, and adding the new data as additional columns to the existing database. Likewise, the selection of Harmony data to include in the e:KID database is operated as an

iterative process, so that different variables were included or excluded based on the changing demands of the partners.

However, data integration is not seen as a task finished with the incorporation of newly generated data into the e:KID-DB-Basic; further data integration decisions can be taken based on the results of data analysis. Consequently, the same experimental data were in some cases incorporated in several different forms into e:KID-DB-Basic. For instance, viral load data were first included only as the raw measurements for each sample. But, as a result of the performed analyses on viral reactivations (see chapter 7), raw viral load data were transformed into categorical data classifying patients according to their peak viral load.²¹¹ These categorical data were incorporated as well to the database, as they are essential for the reproduction of the obtained results.²¹¹ Similarly, for antibody reactivity profiles, in the first versions of the database only mixed antigen bead results were included for the sake of simplicity. But as it became clear that raw single antigen bead reactivities can be employed for prediction of acute rejection (see chapter 9), it was decided to incorporate these data into e:KID-DB-Basic as well.¹³⁰

As a result of the above described database design and integration decisions, e:KID-DB-Basic was created as an R-Data object containing two tables: a main table containing 4651 variables in its current version and a description table with the description of these variables. There is as of July 2019 no final, locked version of the database; 16 versions of e:KID-DB-Basic have been generated and distributed to the e:KID consortium between November 2015 and March 2019. In parallel, scripts for the conversion of the data into the working e:KID-DB-Active were generated. These databases and the scripts are the basis for the work of the consortium, including this dissertation.

6.3 Data cleaning in the e:KID study

The data cleaning process of e:KID-DB-Basic is especially interesting from a theoretical point of view, as it combines data from the cleaned and locked Harmony database, which – as all large databases – still contains errors and discrepancies, and newly generated data. Therefore, all cleaning approaches should encompass an examination and correction of both new and old data. In this section, I describe the data cleaning process of e:KID-DB-Basic based on the criteria of conformance, completeness and plausibility and my contribution to this process, employing paradigmatic examples and highlighting the importance of these corrections in the analyses performed as part of the manuscripts of this thesis.

6.3.1 Improving conformance of the database

Errors in the database can be detected and corrected based on the criterion of conformance (see sub-section 5.3.2). Following this criterion, a transplantation date in the year 3012, a second study visit 378 days after transplantation or a value of cytomegalovirus viral load of 2.231234 copies·mL⁻¹ can be replaced by year 2012, 13 days after transplantation and a viral load below detection limit, respectively. On the other hand, there are cases in which it is not possible to make an educated guess on the real value e.g. a negative concentration, leaving as the only option the deletion of the data point.

In the case of e:KID-DB-Basic, the criterion of relational conformance was especially useful for data cleaning, due to its structural characteristics: As explained in sub-section 6.2.1, the data collected within Harmony at each one of the eight visits were recorded at several tables, each one containing at least one date variable. Therefore, for the same visit and patient, all date

variables should be the same or have a difference of a few days. Moreover, information on the date was also coded through the visit number as it implies a temporal frame (visit 1 is pre-transplantation, visit 2 two weeks afterwards, etc.). This abundance of time-related information shall be referred here as quasi-redundancies: In e:KID-DB-Basic, these quasi-redundancies were kept and further date variables were recorded for each newly measured marker.

These quasi-redundancies in the database can be employed for the cleaning of e:KID-DB-Basic, as they provide multiple observations of the real data. However, data cleaning based on the relational conformance of the data cannot be based solely on the criterion of majority, as an error in one annotation at one Harmony table can be propagated if this variable is used as a reference in e:KID markers, becoming the most common in e:KID-DB-Basic. Therefore, data flows between variables have to be considered, prioritising independent and older observations over newer or dependent observations, i.e. date variables directly imported from the Harmony tables will be more accurate observations of the correct date compared to those in e:KID-DB-Basic.^{46,212}

Based on the principle of conformance, I performed a manual cleaning of all the data concerning viral loads in e:KID-DB-Basic. In total, I cleaned the data for 3330 samples and 3 different variables, finding and resolving 360 inconsistencies regarding date and/or visit number of the measurement and detecting and removing 60 duplicated data entries from the database. These changes were incorporated into the 1.2. version of e:KID-DB-Basic, and were essential for the analyses of viral reactivations performed in two of the here presented manuscripts (chapters 7 and 8).^{211,213}

6.3.2 Management of missing data

There was no single patient in the e:KID study with available measurements for all markers and visits (Figure 6). This is not surprising, and a large part of the missing values can be easily explained and do not introduce a bias into the data: Some marker types (e.g. cytokines and tolerance gene expression) were only routinely measured at visits one, two and five for a sub-cohort (ACRS) of the study, in order to reduce the costs of the study. The ACRS sub-cohort was chosen to study the causes of acute cellular rejection and was composed by the patients who suffered rejection and a control group who had no serious adverse events. Therefore, the limitations were part of the study design and samples were measured using a uniform criterion, to ensure a high degree of completeness within the sub-cohort: These missing values do not imply a reduction of the statistical power for the sub-cohort, but rather a limitation in the observation of the marker time course.

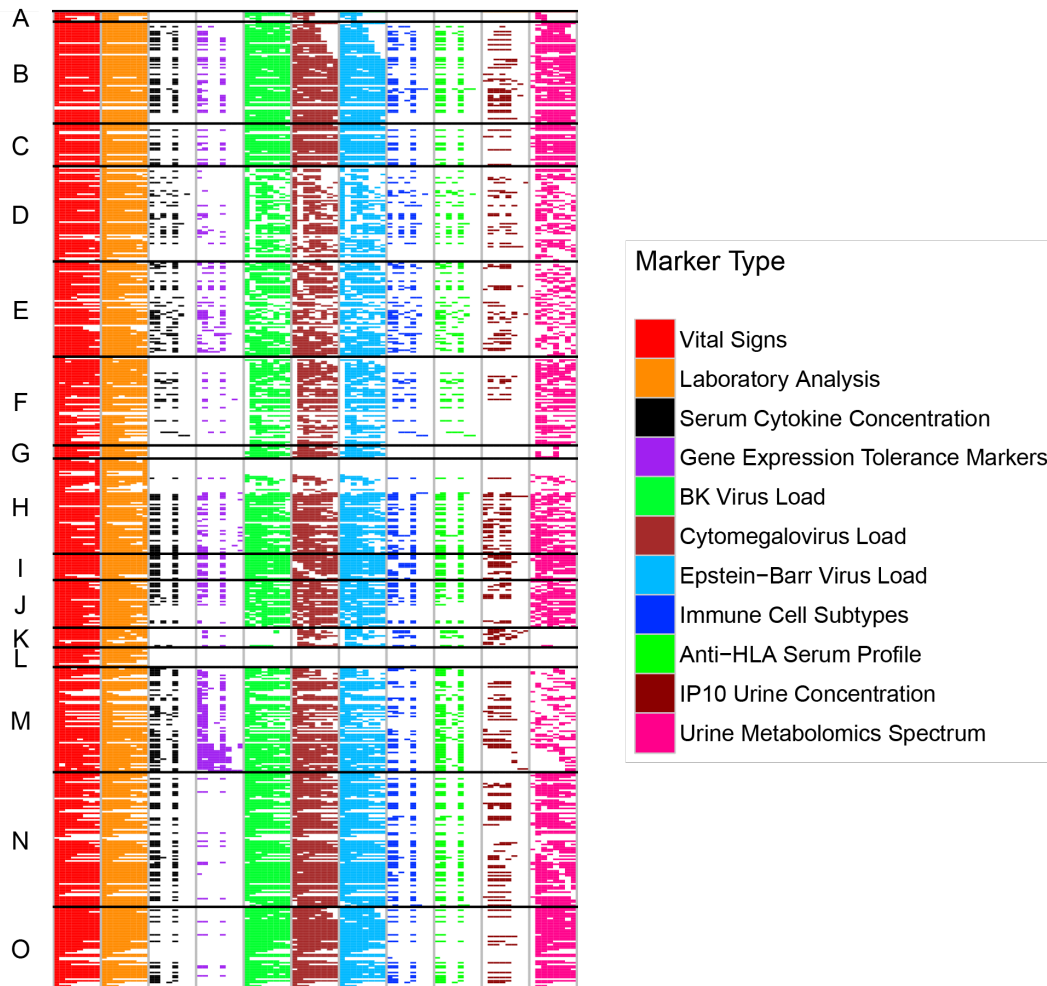


Figure 6. Representation of the data completeness in the e:KID study. Each row represents one patient of the study, ordered by PID, and each column a variable at a certain study visit. Missing values are represented as empty (white) cells; each measured marker type corresponds to a colour. The letters on the left side denote the (pseudonymized) study centres. Vertical grey lines delimit the marker types, while the black horizontal lines delimit the study centres. It should be noted that a coloured cell denotes only that at least one marker of the corresponding type was measured; for some marker types (e.g. cytokines or gene expression), not all markers were measured for all samples. Figure generated with Rodrigo Blázquez Navarro.

For some centres, such as G and L, a reduced number of markers were measured if at all, due to low sample availability. Such cases of missing values do not necessarily suppose a bias in the results, they are missing (completely) at random (see sub-section 5.3.2) – it is unlikely that there is a relationship between outcome and centre and even in this case, the variation could be explained with observed variables. However, there is a large number of missing values that – if not carefully considered – may introduce a bias into data analyses: Variables measured in urine (IP10 and metabolomics spectrum) could only rarely be measured at the first visit for medical reasons; many data are missing at the later visits even for the most frequently measured markers, which is likely a consequence of these patients being lost to follow-up.

As explained in the introduction (sub-section 5.3.2), when missing data are encountered that cannot be explained, the data flow has to be investigated, as in some cases the data have been in fact measured but have been lost during data collection or management and can be recovered.⁴⁶ An example of break in data flow is the pre-transplantation blood pressure values

of the patients, which were missing in e:KID-DB-Basic. After detecting that these data were systematically missing for visit 1, I revised the Harmony database, finding that these data were part of the Harmony table “Physical Examination”, while the corresponding measurements for the rest of the study visits were in the tables “Vital Signs”. This difference in naming led most likely to the break in data flow, which was corrected in e:KID-DB-Basic version 1.15.

Alternatively, in the cases a variable was never measured in a sample, the consortium was responsible for deciding whether these should be performed. For the cases in which they cannot or should not be measured, there are data pre-processing tools which can help increase the statistical power and reduce the bias of the analysis (see sub-section 5.3.3); the managing of missing data in the four manuscripts of this dissertation is described in sub-section 6.4.4.

6.3.3 Evaluating the plausibility of data with biostatistical methods

As explained in the introduction (sub-section 5.3.2), the plausibility of data points can be assessed employing a large array of methods, including frequency and distribution analysis.^{46,47}

An illustrative example of the use of frequency analysis within the e:KID study is the cleaning of the Epstein-Barr viral (EBV) load data. These EBV load data were included for the first time in the version 1.8. of e:KID-DB-Basic. But I observed that these data were not plausible: While for the other viruses over three thousand samples were measured, in the case of EBV there were values only for 309 samples. Moreover, there was a surprisingly high prevalence of viral load over the detection limit ($250 \text{ copies} \cdot \text{mL}^{-1}$) in the samples (63%), compared to BK virus (14%) and cytomegalovirus (5%), which are known to be similarly prevalent as EBV in the human population.^{214–216} I found the reason of these irregularities in conversation with the experimentalist who had generated the data: The coding employed for the calculation of the viral load generated an error message for loads below the detection limit, as it attempted to perform a division by zero; a value of zero was used to denote missing samples. This convention was not immediately evident: The error messages had been interpreted by the database manager as missing values and zero values as loads below detection limit. The data were therefore corrected in a new version of e:KID-DB-Basic. The new data on EBV showed that 3163 samples had been measured and a prevalence of viral load over detection limit of 5% had been found – very similarly to cytomegalovirus. These corrected data were employed in our analyses of EBV viral reactivations performed in two of the here presented manuscripts (chapters 7 and 8).^{211,213}

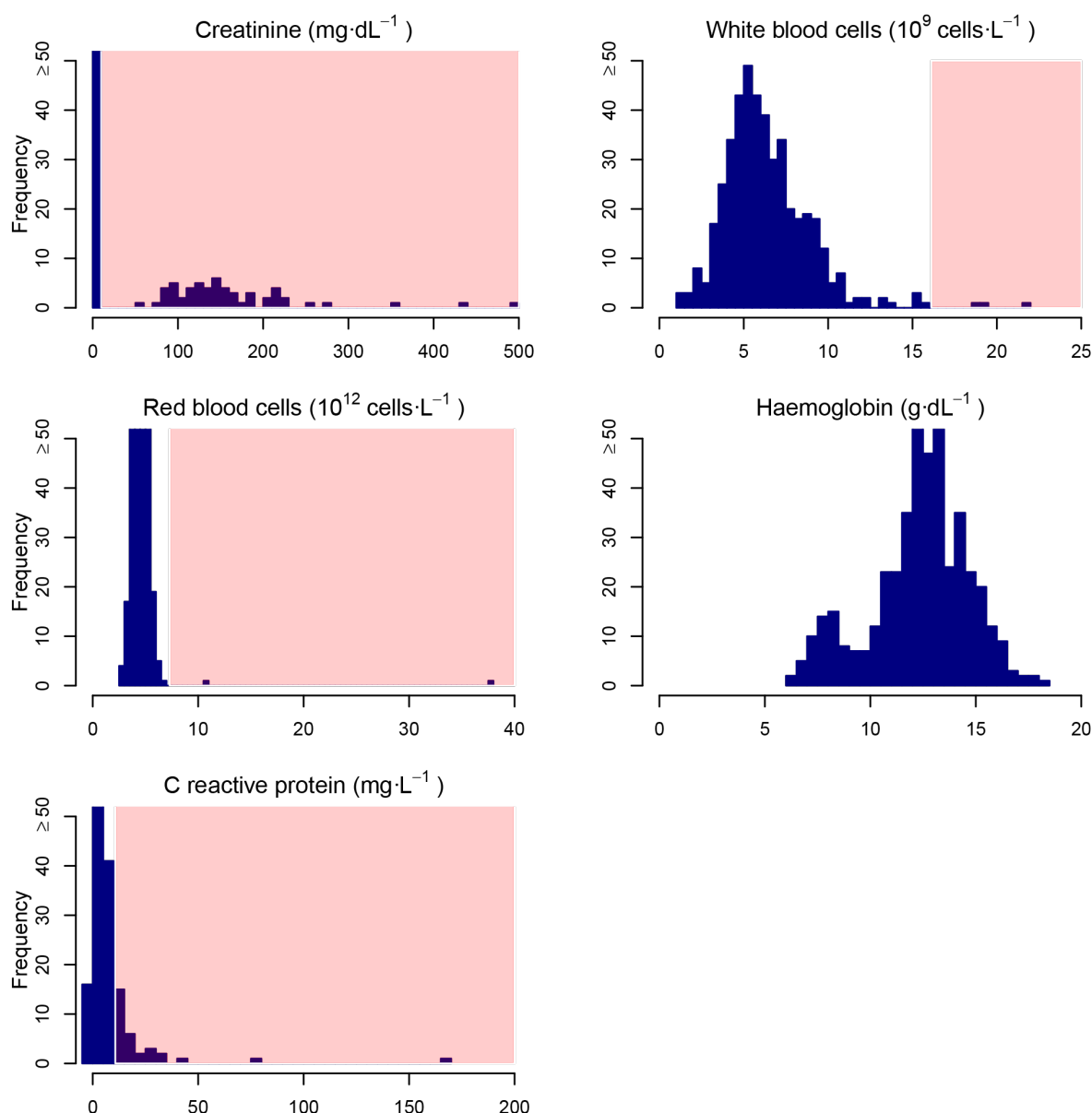


Figure 7. Histogram of the distribution of five clinical variables at visit 8 from the e:KID-DB-Basic before cleaning. These variables were collected in the Harmony database and imported into the version 1.2. of e:KID-DB-Basic and correspond to the final study visit, one year after transplantation. Shaded is the interval corresponding to extreme outliers, defined by Tukey's fences with $k=3$. Note that the y-axis is truncated at frequency 50 to make the outliers more easily identifiable.

Statistical distribution analysis variables was also employed for the identification of implausible values. In Figure 7, the distribution of some clinical variables one year after transplantation is shown, as recorded in e:KID-DB-Basic 1.2. These clinical variables were originally measured within the Harmony study, cleaned and recorded in the table "Laboratory Analysis (Visit 8)".

As it can be observed in the figure, there were extreme outliers for white, red blood cells and C reactive protein; these could potentially be caused by typing errors or different units. An examination of centre effects revealed that the patients with extreme outliers were not grouped into one centre, thereby discarding a systematic difference in the units employed. While such high white blood cell counts and C reactive protein concentrations can be found in the literature, my discussions with the clinical laboratory revealed that the outliers in red

blood cell count are not biologically possible and were most probably due to an experimental error.^{217–219} Therefore, I proposed the removal from the database of the outliers in the red blood cell count, while the outliers of white blood cells and C reactive protein were kept in the database.

The case of creatinine – a marker of kidney function – is especially interesting. There was a very large number of outliers and a bimodal distribution: The large majority of the patients (N=387, 87.4%) had a blood concentration below 10 mg·dL⁻¹, while for the rest of the patients (N=56, 12.6%), concentration was over 30 mg·dL⁻¹. Such a large difference strongly suggested that the data were in different units; the fact that 96.4% of the patients with creatinine over 30 were transplanted in one centre (centre B) further supports this suspicion. Moreover, creatinine levels of 30 mg·dL⁻¹ are not possible, as already a serum creatinine ≥ 4 mg·dL⁻¹ indicates the need of dialysis.²²⁰ My analyses showed that assuming these outlier concentrations were actually measured in $\mu\text{mol}\cdot\text{L}^{-1}$ (a widely used standard for creatinine levels) led to a normalization of the distribution (see Figure 8). The resulting distribution therefore supports the suspicion on the different units. These corrected creatinine data were essential for the analyses of renal function performed in two of the here presented manuscripts (chapters 7 and 8).^{211,213}

In the case of haemoglobin, a solution was not as evident, as in spite of the bimodality of the distribution, all individual values can be considered possible.^{221,222} However, there were strong centre effects, again for centre B: In this centre 100% (N=55) of the patients had haemoglobin levels ≤ 12 g·dL⁻¹ (considered diagnostic for anaemia)²²¹, while for the other centres the prevalence was of 37.2%. Therefore, I concluded that haemoglobin levels in centre B were measured in mmol·L⁻¹, another standard unit. The results of the conversion can be observed in Figure 5; as it can be seen, the patients from centre B now distribute similarly to the rest of the population. The newly calculated data for haemoglobin concentration were therefore incorporated into e:KID-DB-Basic.

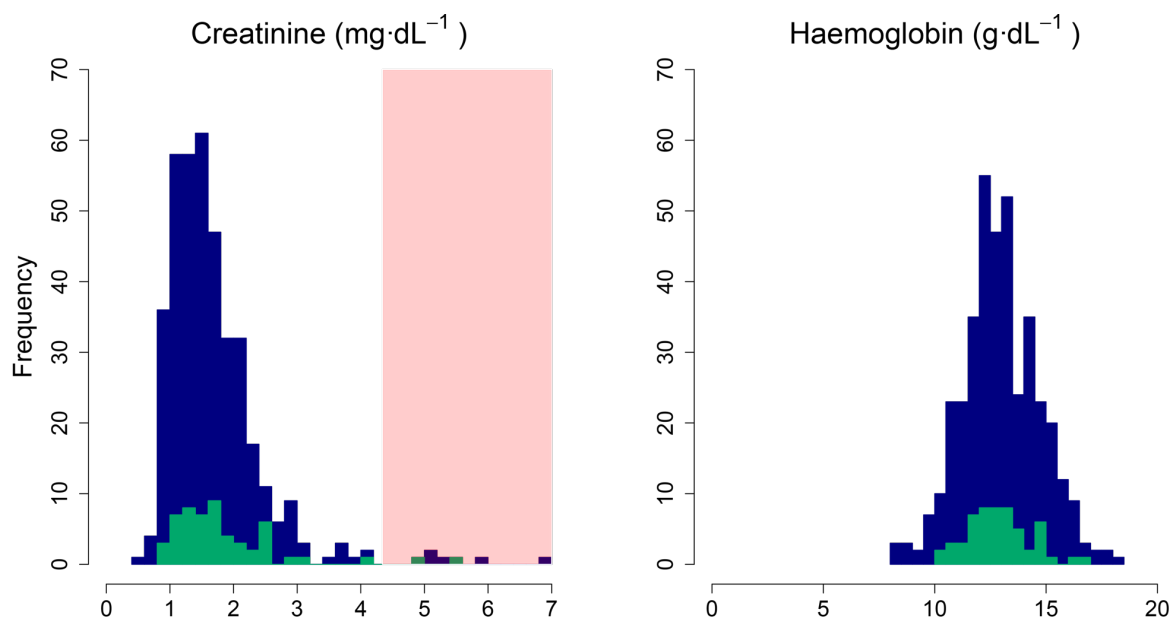


Figure 8. Histogram of the distribution of creatinine and haemoglobin concentrations at visit 8 after cleaning. In green is depicted the distributions in patients from centre B, in blue the distribution for the rest of the cohort. Shaded is the interval corresponding to extreme outliers, defined by Tukey's

fences with $k=3$. As it can be observed, the patients from centre B are now distributed similarly to the rest of the cohort.

These examples show the opportunities and limitations of the methods based on examination of statistical distributions. While they can be performed very fast and without special clinical knowledge, decisions cannot be taken solely based on the statistical distribution: The same phenomenon, i.e. extreme outliers, has a different interpretation for red blood cell counts as for C reactive protein or creatinine concentration. They also highlight how many mistakes in clinical databases are not typographic, but rather the result of employing different conventions (units, coding, etc.). In this case, for multi-centric studies it is useful to explore systematic centre-associated differences, even if all values are in the range of possible, as in the case of haemoglobin. In summary, these examples demonstrate that a basic understanding of the clinical values, their expected distribution, the different employed standards and their information flow is paramount to any data cleaning based on the examination of statistical distributions.

6.4 Data pre-processing in the e:KID study

Often data cannot be employed in the state in which they are contained in the e:KID-DB-Basic: Some raw variables are of difficult use and require pre-processing. This pre-processing is different from data cleaning, as it is context-dependent: It does not suppose the correction of errors, as the values are (supposedly) correct *per se*, but rather the adaption of the values for a concrete data analysis procedure. Therefore, the results from data pre-processing do not necessarily lead to the generation of a new version of e:KID-DB-Basic but result in changes in the database e:KID-DB-Active for data analysis. In this section, I will address some examples pre-processing of the e:KID data necessary employed in data analysis, including management of missing data.

6.4.1 Generation of new variables for data analysis

The requirement of pre-processing variables for their ulterior use in analysis can be due to different causes. One common case is that of variables not explicitly collected because they can be easily calculated using other data. This is the case for e.g. body mass index and EBV mismatch (a function of donor and recipient serostatus). These newly calculated variables should not be included in the main database e:KID-DB-Basic, as they would constitute a redundancy, unnecessarily increasing the size of the database and the probability of introducing new errors. Nevertheless, since they were needed for data analysis, they are automatically calculated in the scripts generating e:KID-DB-Active.

Often more than one measurement of the same variable for the same patient and time point can be found in the database. These are replicates, which can be used to monitor the precision of an experiment.²²³ In the e:KID-DB-Basic 1.7., for example, two replicates (measured at two different time points) for cytomegalovirus (CMV) viral load were included. A total of 728 measurements (23.4%) were replicated, for which the majority (96.7%) showed a small difference in the results of the replicates ($<500 \text{ copies} \cdot \text{mL}^{-1}$). As the precision of these measurements is comparable, the average was used for data analysis and was included as a new variable in e:KID-DB-Active. However, this did not seem an adequate solution for the few cases with very large differences (e.g. sample 805 had $19114 \text{ copies} \cdot \text{mL}^{-1}$ in the first replicate and no detectable viral load in the second). Therefore, in conversation with the experimentalist responsible for the measurements, it was decided to measure these discrepant values a third time: 32 samples – including both discrepant and non-discrepant

viral loads – were re-measured. The average of all three replicates is inappropriate for the analysis of discrepant data, as it takes into account values that differ extremely from the other two: Therefore, from that point on, the median was employed as the reference variable for data analysis of CMV reactivations (chapters 7 and 8).^{211,213}

6.4.2 Statistical transformation and normalization of variables

In the e:KID study, a mixed approach was taken for the statistical transformation of variables: Part of the data had to be transformed before their integration in e:KID-DB-Basic, e.g. metabolomics and gene expression data (see sub-section 6.2.3). However, most data are included in the raw state, leaving the possibility open for different transformations that are adequate for the use in the analysis approaches.

An example of the importance of variable transformation can be found in our manuscript on predictive antibody profiles for acute cellular rejection, which is part of this doctoral thesis (chapter 9).¹³⁰ Binding interactions of serum antibodies with HLA antigens were measured as a list of quantitative variables, which denote the intensity of binding for each antigen.¹³⁰ But conventional methods employed to predict acute rejection require a binary value (presence-absence of binding) of the binding interactions.^{224–230} However, it is controversial how the binarization of the data should be calculated – some authors favour a fixed threshold, while others prefer an individual threshold for each patient.^{130,231} Moreover, a binarization of the data necessarily leads to a loss of information on the strength of the interactions. Therefore, in this manuscript we investigated the influence of the data transformation method on the quality of prediction of acute rejection, comparing the performance of raw data, normalized quantitative data and binarized data.¹³⁰ Our results showed that quantitative, normalized data had the best performance employing the P-SVM machine learning algorithm.^{62,130} This demonstrates the central importance of data transformation for the obtaining of satisfactory results.

6.4.3 Dealing with strong centre effects: The case of GFR

A particularly relevant case of variable with a strong centre effect was the glomerular filtration rate (GFR). GFR is an estimation of renal function and is widely employed both in the clinic and in research.²³² It is calculated using the serum creatinine concentration and the demographic characteristics of the patient, employing different formulae.^{233–235} After examining the data distribution of GFR, I observed very strong differences between centres, with centre O having significantly higher GFR values. A large part of the variation stemmed from the fact that two different formulae were employed in Harmony: MDRD-IV and Cockcroft-Gault.^{234,235} The reason for this is that GFR is an important decision tool in the clinic – it is recommendable for a good patient outcome that physicians work with the standard they have experience on. To avoid confusions, the formula employed for each calculation was recorded in the Harmony database. However, the results of MDRD-IV and Cockcroft-Gault are not comparable: They employ different units and have a slightly different biological meaning (Cockcroft-Gault is considered rather an estimation of creatinine clearance).^{234–236} Furthermore, there were additional differences in the way in which each centre calculates the GFR, as some centres cap all values below or above a certain threshold, based on their clinical experience.

Because of all this, we decided to avoid centre effects in the GFR calculation by recalculating it centrally for all samples, based on the available data collected in the Harmony study. Additionally to MDRD-IV and Cockcroft-Gault, the newer CKD-EPI formula for the calculation was employed (see Figure 9) for a comparison of the results with the centre GFR values).

^{232,234,235} The GFR calculated through all three formulae was incorporated into e:KID-DB-Basic 1.14; we employed the CKD-EPI formula as the reference for data analysis in two of the manuscripts presented in this doctoral thesis (chapters 7 and 8), as it has been shown to be the most accurate formula.^{232,236}

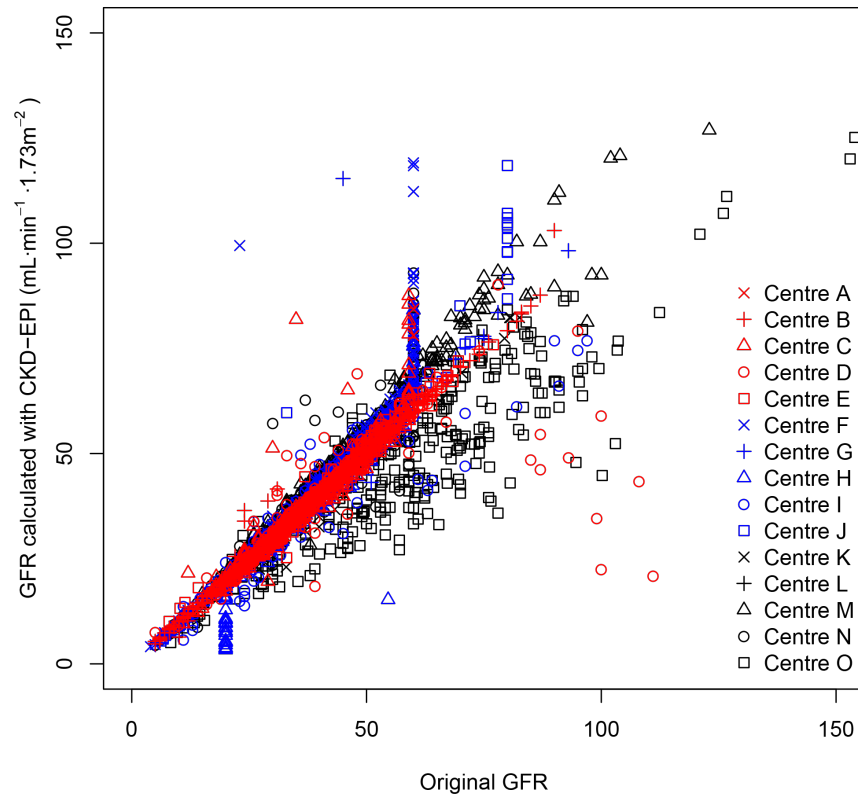


Figure 9. Comparison of the newly calculated GFR values with the values in the clinical for all samples. The colour and point type denote the (pseudonymized) centre where the sample was collected. No units are given for the original GFR, as it is a mixture of values calculated in $\text{mL}\cdot\text{min}^{-1}\cdot 1.73\text{m}^{-2}$ (MDRD-IV) and $\text{mL}\cdot\text{min}^{-1}$ (Cockcroft-Gault). As it can be observed, most values correlate linearly with the newly calculated GFR; the clearest exception was centre O, which was the only one employing exclusively Cockcroft-Gault. Note the capping of the GFR values in centres F (≥ 60), H (≤ 20) and J ($\text{GFR} \geq 80$).

However, it should not be assumed that the newly calculated GFR is free from centre effects: The variable still relies on the serum creatinine concentrations measured at each transplantation centre, so that protocol differences between centres may introduce a bias. Moreover, the variable can be influenced by differences in patient demographics and management between the centres. Because of this – especially for studies seeking to identify a causal relationship between a factor and GFR – the variation introduced by centre effects is to be taken into account into the study. This was the case in our manuscript on the differences in outcome between two different therapeutic strategies (see chapter 8).²¹³

6.4.4 Working with variables with missing values

While in other analyses performed within the e:KID study imputation was essential for the analyses, it was not needed in any of the four manuscripts of this doctoral thesis; missing values were handled depending on the data analysis methods, as well as on the study design.^{130,211,213,237} The reason for that was based on methodological considerations, as well

as on data completeness. Here, I will shortly describe how missing values were taken into account into the design of our work.

In our two manuscripts employing biostatistical methods (chapters 7 and 8), the effects of missing data had to be considered in the analysis.^{211,213} In these manuscripts, the glomerular filtration rate (GFR) was the main outcome variable, and its distribution for patients with different viral reactivation history or different therapeutic strategies was compared.^{211,213} As the loss of patients to follow-up increases the number of missing GFR values in the later visits of the study, the statistical power of the GFR comparison one year after transplantation was reduced.^{211,213} However, the statistical effect was high enough to observe significant effects for conditions associated with a 20% reduction of median GFR.^{211,213} Moreover, the risk of bias in the analyses introduced by missing values was reduced, as all analyses were run taking into account the entire GFR time course, from the second visit (in which missing values are very reduced).^{211,213}

While imputation of missing values is often performed in machine learning methods, it was not necessary in the case of our manuscript (chapter 9): Only half of the patients of the sub-cohort had available measurements, but these measurements had no missing values.¹³⁰ Lastly, missing values were not considered in our manuscript on mathematical modelling of the immune system (chapter 10) due to the analysis method.²³⁷ Each patient time course was modelled individually at different time points, therefore the modelling approach explicitly estimates all values between the available measurements.²³⁷ For this estimation it is indifferent whether there is an available measurement x days after transplantation for all patients, the critical factor is rather the frequency of the available measurements.

These examples from our work demonstrate that there is no “one-size-fits-all” strategy for the handling of missing data.^{55,57,58} We employed only available data for the analysis, and while imputation strategies were considered, they were not deemed adequate due to their intrinsic uncertainty. However, for further, future works (such as the search of predictive markers for viral reactivation) employing a large number of markers and patients, imputation might prove to be an adequate and useful strategy for the handling of missing values. In summary, the strategies have to take into account the goals and methods of the analysis, as well as the number of available measurements, the evidence of possible bias due to missing data not at random and the practical possibility of data imputation.

6.5 Lessons learned from data management at the e:KID study

Data management in the e:KID study has been and is a complex endeavour: Two different data sets are integrated into the study, including an older, cleaned and locked clinical database and newly generated, heterogeneous study data. These data are measured, integrated, cleaned and analysed in an iterative process; to this day, new data are still being generated, including the acquisition of long-term follow-up data of the patients. Likewise, the structure of the data science team, working at different partners but centrally organized, requires a high degree of communication and coordination that is not easily attainable. The size of the consortium, with ten different partners from the clinic, academia and industry, adds up to the complexity of the study, as these partners have patently different preferences and expertise: All these research focuses have to be harmonized and taken into account into the data management process.

While there are formal education programmes on data science and data management in particular, these programmes cannot cover the increasing demand for data scientists.^{44,238}

Because of this, many data scientists have no formal training and learning is based on the experience of peers and the personal, practical experience. This was also my case.

Here I present a summary of my personal experience working at e:KID in form of some practical advice on data management:

1. Design your data management for the study you wish. While generic solutions seem like an easy way out for database design, integration and cleaning, they can make the process more error-prone. A deep understanding of the study goals and the expected data is necessary to guide data management in a successful way.
2. A standard is useless if you are the only one who knows it. Data integration cannot be performed without standards that have been previously agreed with the experimentalists, in order to avoid confusions in how the results should be interpreted. Ideally, these standards should be established before experiments are performed.
3. When in doubt, go to the original source. All former versions of the data are to be kept, especially as submitted by the experimentalists. Tracking the data flow is essential for correcting mistakes occurring during data management.
4. Possible does not mean plausible. The definition of thresholds does not suffice for the detection of anomalous data, as errors can also manifest as inliers. The distribution of the data as a whole has to be considered: An analysis of the differences between centres can be of use.
5. An image is worth a thousand tests. Data visualization is essential for achieving a deep understanding of the data and to notice patterns that would stay unrecognized otherwise; it can help to detect implausible data distributions and outliers better than any statistical test.
6. Understand the experiments as if you had done them yourself. Data integration and cleaning cannot be performed without knowledge of the experimental procedures and the underlying physiology. It is not enough that the experimental and clinical partners have this knowledge: The data managers need broad, interdisciplinary knowledge to work on the data.
7. Always talk to the people. Even if the data managers have a broad knowledge of the physiological processes and the experiments, the clinicians and experimentalists know better and can help them make informed decisions on the data.

7. BKV, CMV, and EBV interactions and their effect on graft function one year post-renal transplantation: Results from a large multi-centre study

This chapter refers to the manuscript published as:

Blazquez-Navarro A, Dang-Heine C, Wittenbrink N, Bauer C, Wolk K, Sabat R, Westhoff TH, Sawitzki B, Reinke P, Thomusch O, Hugo C, Or-Guil M and Babel N (2018). BKV, CMV, and EBV Interactions and their Effect on Graft Function One Year Post-Renal Transplantation: Results from a Large Multi-Centre Study. *EBioMedicine*. 34:113-121. doi:10.1016/j.ebiom.2018.07.017



Contents lists available at ScienceDirect

EBioMedicine

journal homepage: www.ebiomedicine.com
EBioMedicine
 Published by THE LANCET

Research Paper

BKV, CMV, and EBV Interactions and their Effect on Graft Function One Year Post-Renal Transplantation: Results from a Large Multi-Centre Study



Arturo Blazquez-Navarro ^{a,b}, Chantip Dang-Heine ^a, Nicole Wittenbrink ^b, Chris Bauer ^c, Kerstin Wolk ^{a,d}, Robert Sabat ^{d,e}, Timm H. Westhoff ^f, Birgit Sawitzki ^{a,j}, Petra Reinke ^{a,g}, Oliver Thomusch ^h, Christian Hugo ⁱ, Michal Or-Guil ^{b,*,1}, Nina Babel ^{a,f,*,1}

^a Berlin-Brandenburg Center for Regenerative Therapies (BCRT), Charité-Universitätsmedizin Berlin, Augustenburger Platz 1, 13353 Berlin, Germany

^b Systems Immunology Lab, Department of Biology, Humboldt-Universität zu Berlin, Philippstr. 13, 10115 Berlin, Germany

^c MicroDiscovery GmbH, Marienburger Str. 1, 10405 Berlin, Germany

^d Psoriasis Research and Treatment Center, Institute of Medical Immunology, Department of Dermatology and Allergy, Charité-Universitätsmedizin Berlin, Charitéplatz 1, 10117 Berlin, Germany

^e Interdisciplinary Group of Molecular Immunopathology, Institute of Medical Immunology, Department of Dermatology and Allergy, Charité-Universitätsmedizin Berlin, Charitéplatz 1, 10117 Berlin, Germany

^f Medical Department 1, Universitätsklinikum der Ruhr-Universität Bochum, Ruhr-Universität Bochum, Hölkeskampring 40, 44625 Herne, Germany

^g Berlin Center for Advanced Therapies (BeCAT), Charité-Universitätsmedizin Berlin, Augustenburger Platz 1, 13353 Berlin, Germany

^h Klinik für Allgemein- und Viszeralchirurgie, Universitätsklinikum Freiburg, Hugstetter Straße 55, 79106 Freiburg, Germany

ⁱ Universitätsklinikum Carl Gustav Carus, Medizinische Klinik III - Bereich Nephrologie, Fetscherstraße 74, 01307 Dresden, Germany

^j Molecular Immune Modulation, Institute for Medical Immunology, Charité-Universitätsmedizin Berlin, Augustenburger Platz 1, 13353 Berlin, Germany

ARTICLE INFO

Article history:

Received 22 May 2018

Received in revised form 6 July 2018

Accepted 13 July 2018

Available online 30 July 2018

Keywords:

BK virus

Cytomegalovirus

Epstein-Barr virus

Kidney transplantation

Graft function

Combined reactivation

ABSTRACT

Background: BK virus (BKV), Cytomegalovirus (CMV) and Epstein-Barr virus (EBV) reactivations are common after kidney transplantation and associated with increased morbidity and mortality. Although CMV might be a risk factor for BKV and EBV, the effects of combined reactivations remain unknown. The purpose of this study is to ascertain the interaction and effects on graft function of these reactivations.

Methods: 3715 serum samples from 540 kidney transplant recipients were analysed for viral load by qPCR. Measurements were performed throughout eight visits during the first post-transplantation year. Clinical characteristics, including graft function (GFR), were collected in parallel.

Findings: BKV had the highest prevalence and viral loads. BKV or CMV viral loads over 10,000 copies·mL⁻¹ led to significant GFR impairment. 57 patients had BKV-CMV combined reactivation, both reactivations were significantly associated ($p = 0.005$). Combined reactivation was associated with a significant GFR reduction one year post-transplantation of $11.7 \text{ mL} \cdot \text{min}^{-1} \cdot 1.73 \text{ m}^{-2}$ ($p = 0.02$) at relatively low thresholds (BKV > 1000 and CMV > 4000 copies·mL⁻¹). For EBV, a significant association was found with CMV reactivation ($p = 0.02$), but no GFR reduction was found. Long cold ischaemia times were a further risk factor for high CMV load.

Interpretation: BKV-CMV combined reactivation has a deep impact on renal function one year post-transplantation and therefore most likely on long-term allograft function, even at low viral loads. Frequent viral monitoring and subsequent interventions for low BKV and/or CMV viraemia levels and/or long cold ischaemia time are recommended.

Fund: Investigator Initiated Trial; financial support by German Federal Ministry of Education and Research (BMBF).

© 2018 The Authors. Published by Elsevier B.V. This is an open access article under the CC BY-NC-ND license (<http://creativecommons.org/licenses/by-nc-nd/4.0/>).

* Correspondence to: Michal Or-Guil, Systems Immunology Lab, Department of Biology, Humboldt-Universität zu Berlin, Philippstr. 13, 10115 Berlin, Germany

** Correspondence to: Nina Babel, Medical Department 1, Universitätsklinikum der Ruhr-Universität Bochum, Ruhr-Universität Bochum, Hölkeskampring 40, 44625 Herne, Germany

E-mail addresses: m.oguill@biologie.hu-berlin.de (M. Or-Guil), nina.babel@charite.de (N. Babel).

¹ Corresponding authors contributed equally to this work.

Research in context

Evidence Before this Study

Viral reactivations of BK virus (BKV), cytomegalovirus (CMV), and Epstein-Barr virus (EBV) are common complications in recipients of renal transplantation. Combined reactivations of these viruses have been observed repeatedly in the past and interplay between BKV and CMV has been shown *in vitro*. Different interaction mechanisms have been proposed. However, it is currently unclear whether there are associations in viral reactivations *in vivo*. Moreover, it is not clear so far what is the cause of such combined reactivations and whether combined reactivations have more serious impact on graft function than the corresponding mono-reactivations. To obtain information on the state-of-art, we searched MEDLINE, PubMed, and Google Scholar for papers published after January 2003, using the terms "renal transplantation BKV", "renal transplantation CMV", "renal transplantation EBV", "coinfection BKV CMV", "coinfection BKV EBV", "coinfection CMV EBV". No language restrictions were employed. The quality of evidence was assessed prioritizing epidemiological studies over case reports and *in vitro* studies.

Added Value of this Study

This is the first large, prospective multi-centre study to systematically analyse the clinical course of BKV, CMV, and EBV reactivations at eight pre-defined time points during the first post-transplantation year. Almost ten thousand viral load measurements were performed. It is the first study to provide clinical evidence of the relevance of BKV-CMV combined reactivations, showing, already at moderate viral loads (BKV > 1000 and CMV > 4000 copies mL⁻¹), an impact on renal function one year post-transplantation with a median drop in renal function of 11.7 mL min⁻¹ 1.73 m⁻². This observation is reinforced by the fact that a significant association was found between BKV and CMV during the first post-transplantation year. Moreover, it is the first large study to find an association between cold ischaemia time and high level CMV viral load: High-level CMV (> 10,000 copies mL⁻¹) was associated with significantly longer cold ischaemia time for cadaveric graft (median difference: 284 min), compared to patients without CMV or CMV below the threshold. Furthermore, this study shows BKV as the most relevant viral adverse event in kidney transplantation, as it had the highest prevalence, the highest viral loads and lowest clearing rate. Our results have revealed a prevalence of presumptive BKV nephropathy of 10.9% (over the 1–10% prevalence in the literature), in spite of the patients belonging to an immunological low-risk cohort. In conclusion, it is a confirmation that BKV is an emergent pathogen that must be tackled in order to improve the efficacy of current transplantation protocols.

Implications of All the Available Evidence

We have provided the most systematic analysis so far of BKV, CMV, and EBV virus reactivations in renal transplantation, as part of a large, prospective multi-centre study. Their viral loads were analysed at eight time points during the first transplantation year. With our results, we showed a clinical impact of BKV-CMV combined reactivation, even at low viral load levels. In addition, we performed in-depth analyses of the impact of different modifiable and non-modifiable risk factors on virus reactivation. Therefore, we consider our work as crucial for the management of viral reactivations after kidney transplantation, leading to a better monitoring and treatment for kidney transplantation patients with BKV and/or CMV low viral loads, as well as patients with long cold ischaemia times and additional CMV risk factors.

1. Introduction

Viral reactivations are a major cause of morbidity and mortality for recipients of solid organ transplantation [1]. In kidney transplantation, BK virus (BKV), cytomegalovirus (CMV), and Epstein-Barr virus (EBV) are major pathogens. These viruses are very common in healthy population, with an approximate prevalence of 80%, 60%, and 90%, respectively [2–4]. Primary infection usually occurs during childhood, but the virus stays latent and asymptomatic under normal conditions [5,6]. Individuals with compromised immune systems, i.e. after a solid organ transplantation, are prone to both primary infection and reactivations with clinically relevant symptoms [7,8].

BKV is an emerging pathogen and the cause of BKV-associated nephropathy (BKVAN), a major complication in renal transplantation [6]. It is linked to kidney malfunction and rejection, leading to graft loss in up to 60% of affected patients [6,8,9]. The incidence of BKVAN is 1–10% in renal transplantation [10]. BKVAN is usually encountered in a context of over-immunosuppression, even though it is not associated with a specific immunosuppressive drug [9,11,12]. Early diagnosis is vital for a successful treatment, but BKVAN progression occurs without clinical signs except for increasing serum creatinine concentrations and diagnosis relies on renal biopsy [9,11]. However, BKV serum load over 10,000 copies mL⁻¹ is a generally accepted surrogate marker defining "presumptive BKVAN" [11].

CMV is a major viral pathogen after kidney transplantation, linked among others to retinitis, pneumonitis, colitis, encephalitis and importantly, allograft damage, allograft loss and death [5,8,13,14]. CMV proliferation may occur through reactivation of a latent infection, a new donor-transmitted infection or acquired from the general population due to the immunosuppression [13]. However, the highest risk is encountered by CMV seronegative patients receiving a transplant from a seropositive donor (D⁺R⁻) [13]. EBV in kidney transplantation is mainly associated with post-transplant lymphoproliferative disorders (PTLD) [5,7]. PTLD is a severe complication in solid organ transplantation, occurring in around 1% of patients mostly after the first post-transplant year [7,15,16]. It comprises a very broad spectrum of disorders, from spontaneously regressing to lethal B cell proliferations [4,7].

In this work, we assess the impact and relevance of BKV, CMV, and EBV reactivations in a large, prospective multi-centre study, analysing renal transplant in clinical follow-up during the first year after transplantation. Our work focuses on potential interactions between viruses and their combined impact on graft function, as well as the risk factors associated with each virus, including the role of immunosuppressive therapy.

2. Patients and Methods

2.1. Patient Population

We conducted a sub-study within the randomized, multi-centre, investigator-initiated Harmony trial (NCT 00724022) [17] to prospectively monitor viral load of BKV, CMV, and EBV at predetermined eight study visits and correlate it with clinical outcome parameters. Following the KDIGO clinical guideline, BKV viral load monitoring was performed in serum rather than urine, as the former has a higher BKVAN diagnostic value [18,19]. Viral monitoring was non-interventional and centrally performed. The study was carried out in compliance with the Declaration of Helsinki and Good Clinical Practice. A total of 540 patients undergoing kidney transplantation between 08/2008 and 11/2012 were analysed (Fig. 1).

2.2. Patient Medication

Patients were randomized to one of three therapeutic groups, as described before [17]. The immunosuppressive therapy included induction with either monoclonal IL-2R antibody basiliximab (arms A and B)

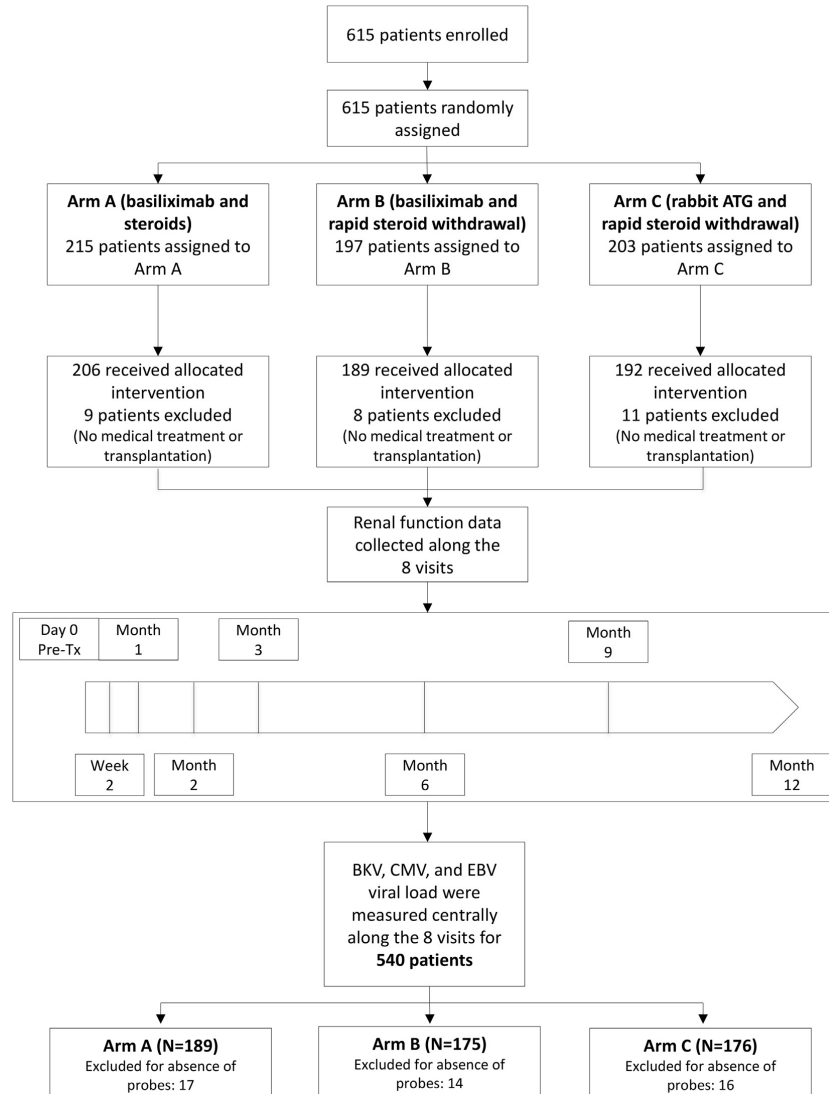


Fig. 1. Trial profile.

(Simulect®, Novartis) or rabbit ATG (arm C) (Thymoglobulin®, Sanofi). Maintenance immunosuppression consisted of tacrolimus (Advagraf®, Astellas) and mycophenolate mofetil (MMF) with (arm A) or without steroids (arms B and C). Patients with mismatch-based risk (seronegative recipient and seropositive donor) for CMV or EBV as well as patients from arm C received at least a 3 months prophylaxis with valganciclovir.

2.3. Patient Monitoring

Patients were monitored for creatinine along eight visits, scheduled at day 0 (pre-transplantation), 2nd week, 1st month, 2nd month, 3rd month, 6th month, 9th month, and 12th month. Glomerular filtration rate was calculated using the CKD-EPI formula; values are given in

$\text{mL} \cdot \text{min}^{-1} \cdot 1.73 \text{ m}^{-2}$ [20]. Tacrolimus blood trough levels were measured independently of the eight visits described above, according to the internal study centre standards. Suspected episodes of acute rejection had to be confirmed through biopsy; histologic characteristics were described according to the Banff criteria of 2005 [21]. Routine surveillance biopsies were allowed but not mandatory. Borderline rejections were disregarded in the analysis.

2.4. Screening of BKV, CMV, and EBV Viraemia

Peripheral blood samples from the eight visits were centrally monitored for BKV, CMV, and EBV by TaqMan quantitative polymerase chain reaction (qPCR), as described previously [19]. Briefly, DNA was isolated

from serum (BKV) or whole blood (CMV and EBV) using a QIAamp DNA Mini Kit (Qiagen Corp, Hilden, Germany) according to the manufacturer's instructions. PCR was based on the TaqMan platform and used the Prism 7700 Sequence Detector (ABI). In the case of BKV, PCR amplifications were set up in a reaction volume of 25 μ L using primer and probe at final concentrations of 900 nM and 5 μ M [19]. Primers and probe were designed to amplify the VP1 gene [19]. CMV and EBV were amplified using the same protocol; primers and probe sequences, as well as reagent concentrations are shown in Table 1. The detection level was the lowest viral load measured within the range of linearity.

2.5. Clinical Management of BKV, CMV, and EBV

BKV, CMV, and EBV reactivations and disease were monitored according to intern centre standards. qPCR (and/or pp65 CMV antigenemia tests) and symptom monitoring were performed. Viral loads over 10,000 copies·mL⁻¹ for BKV and over 1000 copies·mL⁻¹ for CMV and EBV were considered clinically relevant. Reactivations were treated based on centre internal standards. According to the study protocol, suggested treatment included a reduction of the total immunosuppression e.g. reduction of tacrolimus and MMF dose. For CMV, patients would receive additionally a (val)ganciclovir treatment for three weeks according to local standards, followed by (val)ganciclovir prophylaxis for, at least, four weeks. After reactivation, patients were regularly monitored for viral load, first weekly, than monthly and then three-monthly until the end of the study.

2.6. Viraemia-Based Patient Classification

Patients were classified based on their peak viral load values for BKV, CMV, and EBV during follow-up (Table 2). Patients with viral loads over detection level were classified as BKV⁺, CMV⁺, or EBV⁺. Patients of the former group with, at least, one measurement over 2000 copies·mL⁻¹ were classified as elevated viraemia (eBKV, eCMV, and eEBV); patients with viral load over 10,000 copies·mL⁻¹ were classified as high-level viraemia (hBKV, hCMV, and hEBV). Altogether, patients were classified into up to nine overlapping groups.

2.7. Statistical Analysis

Qualitative variables were described using counts and frequencies and compared using Pearson's chi-square test with continuity correction (unless otherwise stated), odds ratio (OR) and 95% confidence intervals (95%CI) are provided. Quantitative variables are described as median and interquartile range (IQR). The differences between continuous variables are analysed using the Mann-Whitney test. Three-dimensional contingency tables are reduced to two dimensions (flattened) for chi-square test analysis, iteratively controlling for each one of the three variables; average of the three obtained p values is given. A cut-off of 0.05 for the p value was used on all tests to discard

Table 1
CMV and EBV qPCR reagent characteristics.

Reagent	Sequence	Concentration
CMV Forward primer	5'-CTG CGT GAT ATG AAC GTG AAG G-3'	300 nM
CMV Reverse primer	5'-GCT GTT GGC GAA ATT AAA GAT GA-3'	900 nM
CMV Probe	5'-CGC CAG GAC GCT GCT ACT CAC GA-3'	5 μ M
EBV Forward primer	5'-TCC CGG GTA CAA GTC CCG-3'	900 nM
EBV Reverse primer	5'-TGA CCG AAG ACG GCA GAA AG-3'	900 nM
EBV Probe	5'-TGG TGA GGA CGG TGT CTG TGG TTG TCT T-3'	5 μ M

Table 2
Summary of viraemia-based patient classification sub-groups.

Abbreviation	Definition	Threshold
BKV ⁺	Detectable BKV viral load for at least one visit	>DL (250 copies·mL ⁻¹)
CMV ⁺	Detectable CMV viral load for at least one visit	>DL (250 copies·mL ⁻¹)
EBV ⁺	Detectable EBV viral load for at least one visit	>DL (250 copies·mL ⁻¹)
eBKV	Elevated BKV viral load for at least one visit	>2000 copies·mL ⁻¹
eCMV	Elevated CMV viral load for at least one visit	>2000 copies·mL ⁻¹
eEBV	Elevated EBV viral load for at least one visit	>2000 copies·mL ⁻¹
hBKV	High-level BKV viral load for at least one visit	>10,000 copies·mL ⁻¹
hCMV	High-level CMV viral load for at least one visit	>10,000 copies·mL ⁻¹
hEBV	High-level EBV viral load for at least one visit	>10,000 copies·mL ⁻¹

or confirm significant associations. Analyses were performed with R (Version 3.1.1).

2.8. Statistical Analysis of Immunosuppressant Usage

The relation between immunosuppressant usage (MMF daily dose and tacrolimus trough levels) and viral reactivations was analysed by comparing the usage between patients with reactivation (sample) and patients with no viral reactivation (control).

In detail, the analysis was performed as follows: The sample group was defined as the patients with viral load for the virus *v* over a threshold *th* at any visit, while the control group were all patients with no reactivation for virus *v*. Monitoring of drug usage was performed for the sample group at the first visit with reactivation over *th*, and for the control group for randomly selected visits so that the analysed visits have the same frequencies as in the sample group and that each patient is taken into account only once. For MMF daily drug dose, the dose at viral load monitoring was compared, for tacrolimus trough levels the last measurement before monitoring visit was considered. Only viral reactivations occurring after transplantation were considered.

Mann-Whitney test with 100 replicates was employed for the comparison, with the null hypothesis that drug usage in the sample group was not higher than in the control group. A difference was considered significant if the null hypothesis was rejected ($p < 0.05$) for at least 80% of the replicates. Statistics of drug usage are given as the median over all replicates of the median and IQR of the sample and control groups, as well as median p value.

2.9. Role of the Funding Source

The trial was designed and run by NB, who received financial support from the German Federal Ministry of Education and Research (BMBF). The funders had no role in data collection, data analysis, data interpretation, or writing of the manuscript. ABN, CH, MO, and NB had full access to all study data and had final responsibility for the decision to submit for publication.

3. Results

3.1. BKV Is the most Relevant Viral Reactivation in Renal Transplantation Recipients

A total of 3715 blood samples from 540 patients (18 centres) were analysed for BKV, CMV, and EBV. Detection limit (DL) was 250 copies·mL⁻¹. Demographic and clinical characteristics of the patients are shown in Table 3. Prevalence, viral load, temporal sequence and

Table 3

Patient demographic and clinical characteristics, treatment details and transplantation outcomes. Data are given in number (percentage) or median (interquartile range) and range.

Variable	Measurement	Total (N = 540)
Male sex		346 (64.1%)
Age (years)	Median (IQR)	56 (45–64)
	Range	[19, 75]
BMI (kg m ⁻²)	Median (IQR)	25.8
	Range	(23.2–29.0)
Living donor		66 (12.2%)
Second transplantation		22 (4.1%)
Cold ischaemia time: only cadaveric donors (min)	Median (IQR)	660 (488–880)
	Range	[35, 1712]
Average MMF daily dose (mg·day ⁻¹)	Median (IQR)	1505
	Range	(1058–1990)
		[0–3994]
Average tacrolimus trough level (ng·mL ⁻¹)	Median (IQR)	9.5 (8.5–10.5)
	Range	[5.5, 27.0]
Graft loss one year post-transplantation		22 (4.1%)
Death one year post-transplantation		16 (3.0%)
Graft survival one year post-transplantation		504 (93.3%)
GFR one year post-transplantation (mL·min ⁻¹ ·1.73 m ⁻²)	Median (IQR)	47.6
	Range	(35.0–60.8)
		[7.6, 126.9]

recurrence are presented in Table 4 and Fig. 2. Overall, BKV was the most relevant reactivation, with the highest prevalence, viral loads, incidence of prolonged reactivations and the lowest rate of clearing: 260 of the patients (48.1%) were BKV⁺ (see Viraemia-based patient classification section), 121 (22.4%) were eBKV and 59 (10.9%) were hBKV; 109 (20.2%) patients had prolonged viraemia; median viral load peak value was 1505 [779–8452] copies·mL⁻¹ and rate of clearing was 80.5%.

3.2. Elevated CMV Is Significantly Associated with Higher Cold Ischaemia Time

Demographic and clinical characteristics were analysed univariately for association with each one of the nine viraemia groups (Table 5). Following characteristics were analysed: sex, age, body mass index, donor type, number of previous transplants, EBV and CMV donor and recipient serostatus and mismatch-associated risk, and cold ischaemia time. CMV donor seropositivity was significantly associated with CMV reactivation for all three thresholds, as was CMV mismatch-associated risk. Interestingly, CMV mismatch-associated risk was similarly associated with eEBV. eEBV was also associated with CMV recipient seronegativity, CMV mismatch-associated risk and EBV mismatch-associated risk. Finally, we found a relation between CMV and cold ischaemia time for patients with cadaveric transplants: this difference was observed for both eCMV and hCMV, with increasing difference for higher viral loads. For

BKV, no significant differences were found for any of the three thresholds.

3.3. CMV Reactivation Is Significantly Associated with BKV and EBV

We examined the association between the reactivations, including pair-wise analyses (Fig. 3). 13 patients (2.41%) had viraemia over DL for all three viruses. The association was significant (average $p = 0.0021$); the number of triple-infected patients was 45% higher than expected for no association.

There was a highly significant association between BKV and CMV for all three thresholds: BKV⁺-CMV⁺ ($p = 0.0052$; OR = 1.97, 95%CI = 1.24–3.11), eBKV and eCMV ($p = 0.0216$; OR = 2.33, 95%CI = 1.18–4.60) and hBKV and hCMV (Fisher's exact test: $p = 0.0016$; OR = 5.75, 95%CI = 1.80–17.0). There was a significantly higher number of sera positive for both virus ($p = 0.0145$; OR = 1.72, 95%CI = 1.13–2.62). There was no clear temporal pattern: 45.6% had detectable BKV before CMV, and 33.3% had CMV before BKV.

CMV and EBV were also significantly associated for CMV⁺-EBV⁺ ($p = 0.0237$; OR = 1.85, 95%CI = 1.11–3.08) and for eCMV-eEBV (Fisher's exact test: $p = 0.0416$; OR = 2.76, 95%CI = 1.05–7.08) – there were no hCMV-hEBV patients. There was a significantly higher number of sera simultaneously positive for both virus ($p = 0.0193$; OR = 2.07, 95%CI = 1.17–3.69). EBV preceded CMV in 51.9% of cases and was observed after CMV in 29.6%.

There was no significant association between BKV and EBV.

3.4. CMV Serostatus Is the Only Demographic Characteristic Associated with Combined Reactivations

We analysed the differences of demographic and clinical characteristics for combined reactivations with respect to the rest of patient population. BKV⁺-CMV⁺ was associated with CMV seropositivity of donor ($p < 0.00001$; OR = 5.34, 95%CI = 2.37–12.0) and CMV mismatch-based risk ($p = 0.0001$; OR = 3.02, 95%CI = 1.72–5.30); eBKV-eCMV was associated with CMV mismatch-based risk ($p = 0.0278$; OR = 3.64, 95%CI = 1.24–10.7). CMV⁺-EBV⁺ was likewise associated with CMV seropositivity of donor ($p = 0.0127$; OR = 3.97, 95%CI = 1.35–11.6).

3.5. Therapy Arm Was Not Associated with Elevated or High-Level Viral Loads

EBV⁺ was significantly associated with immunosuppressive regimen ($p = 0.0303$): Arm C (ATG and rapid steroid withdrawal) had a higher EBV⁺ prevalence ($p = 0.0225$; OR = 1.69, 95%CI = 1.10–2.60). Interestingly, the lowest EBV⁺ prevalence was found in arm B (basiliximab and rapid steroid withdrawal) ($p = 0.0432$; OR = 0.59, 95%CI = 0.37–0.96). This effect was not found for higher viral load thresholds. There were no significant differences between therapeutic arms for BKV or CMV or their combinations.

Table 4

Viral reactivation statistics. Data are given in number (percentage) or median (interquartile range) and range. The percentages of the first four categories refer to the total number of patients (N = 540). For the clearing statistics, the percentage corresponds to the ratio of: number of patients with detectable viraemia (at least once between visits 1 and 7) and with no viral load in the eighth visit (cleared patients), and the total number of patients with detectable viraemia; patients who did not have viral load measurements at the last time point (visit 8) were excluded from the analysis.

	BKV	CMV	EBV
Patients with detectable viraemia (>DL)	260 (48.1%)	92 (17.0%)	109 (20.2%)
Patients with elevated viraemia (>2000 copies·mL ⁻¹)	121 (22.4%)	39 (7.22%)	37 (6.85%)
Patients with high-level viraemia (>10,000 copies·mL ⁻¹)	59 (10.9%)	18 (3.33%)	11 (2.04%)
Patients with prolonged viraemia (more than one positive measurement)	109 (20.2%)	35 (6.48%)	36 (6.67%)
Viraemia patients with no detectable viraemia one year post-transplantation (clearing)	128 (80.5%)	61 (95.3%)	48 (85.7%)
Time until first detectable viraemia (days)	Median (IQR)	61 (23–178)	66 (54–185)
	Range	[0, 380]	[0, 386]
Peak viraemia per patient (copies·mL ⁻¹)	Median (IQR)	1505 (779–8452)	1491 (710–5850)
	Range	[DL, 3849694]	[DL, 136722]
			[DL, 1369425]

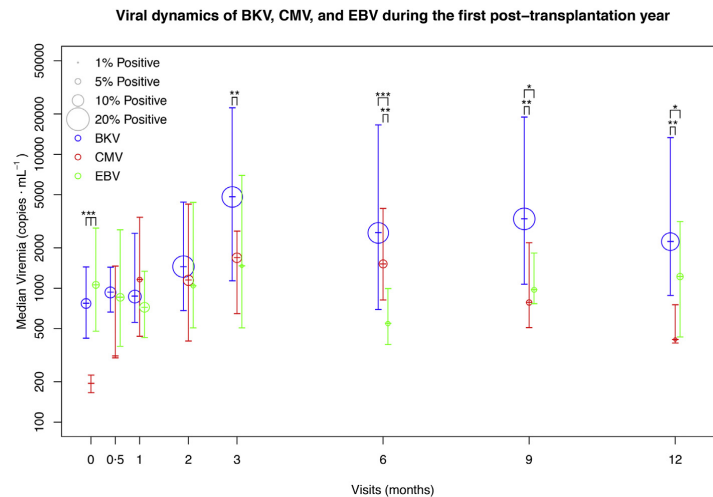


Fig. 2. Viral dynamics of BKV, CMV, and EBV during the first post-transplantation year. Prevalence and viral load levels for BKV (blue), CMV (red), and EBV (green) are plotted for the eight visits of the study. The size of the points is a function of the prevalence of positive measurements (viral load over detection level). The height of the points represents the median viral load (copies · mL⁻¹) of positive measurements; the bars indicate the interquartile range. Asterisks indicate a significant difference calculated with the Mann-Whitney test (* $p < 0.05$; ** $p < 0.01$; *** $p < 0.001$) in viral load (only samples with detectable viral load) for each virus.

3.6. High Tacrolimus Trough Levels Were Associated with Detectable CMV Reactivation

High tacrolimus trough levels were significantly associated with CMV⁺: With 100 replicates, we obtained a significant p value for 96% of replicates (median $p = 0.0142$). While the median of the last tacrolimus trough level measured before CMV reactivation was 9.1 [7.1–11.1] ng · mL⁻¹, the trough levels for the control group of patients without CMV reactivation were 8.2 [6.4–10.2] ng · mL⁻¹. On the other hand, we did not find any effect of MMF daily dose on viral reactivation, as there were no significant replicates for any combination of threshold and virus.

To discard the possibility that the lack of detection of an association of MMF daily doses with reactivation is caused by a poor choice of thresholds, the analysis was repeated for both drugs and all thresholds between DL and 20,000 copies · mL⁻¹, with steps of 1000 copies · mL⁻¹. However, the results demonstrated no effect of MMF daily dose levels on viral reactivation, as well as no effect of tacrolimus trough levels on BKV or EBV, with 0% of significant replicates.

3.7. High-Level CMV Viraemia Was Positively Associated with Acute Rejection

hCMV was significantly associated with acute rejection (Fisher's exact test: $p = 0.0393$; OR = 3.27, 95%CI = 1.08–9.41). Three patients (60.0%) had viral load over DL before acute rejection; only one of the patients had a CMV load >10,000 copies · mL⁻¹ before rejection. No significant association was found between acute rejection and BKV or EBV.

Patients who received an anti-rejection therapy did not have a significantly higher incidence of viral reactivation for any of the pre-defined thresholds. Furthermore, there was no significant association between the use of steroid or ATG anti-rejection therapies and viral reactivation.

3.8. Severe PTLD Was a Rare Event in Conjunction with High EBV Load

There were two cases of PTLD (0.37%) in the cohort, of which one was severe. Even though both PTLD cases affected patients in arm C, there was no significant association between therapy arm and PTLD

Table 5

Results of univariate analysis. Demographic and clinical characteristics were analysed for association with each one of the nine pre-defined viraemia sub-groups (Table 2), compared to the rest of population. The effect size is shown according to the employed test: OR (95%CI) for Chi-squared and Fisher's exact test and median of sub-group (IQR) vs. median of rest of cohort (IQR) for Mann-Whitney test. Only significant ($P < 0.05$) differences are shown.

Variable	Viraemia Group	P Value	Test	Effect size
CMV donor seropositivity	CMV ⁺	<0.00001	Chi-squared	3.75 (2.12–6.64)
	eCMV	0.0024	Chi-squared	3.89 (1.60–9.45)
	hCMV	0.0237	Chi-squared	5.45 (1.24–23.9)
CMV recipient seropositivity	eEBV	0.0154	Chi-squared	0.39 (0.19–0.81)
	CMV ⁺	0.0002	Chi-squared	2.46 (1.54–3.93)
CMV mismatch-based risk (D ⁺ R ⁻)	eCMV	0.0025	Chi-squared	2.87 (1.47–5.60)
	hCMV	0.0254	Fisher's exact	3.09 (1.17–8.16)
	eEBV	0.0053	Chi-squared	2.70 (1.37–5.31)
	eEBV	0.0236	Chi-squared	3.77 (1.31–10.9)
EBV mismatch-based risk (D ⁺ R ⁻)	eCMV	0.0199	Mann-Whitney	819 (539–1078) vs. 660 (484–855)
	hCMV	0.0140	Mann-Whitney	944 (702–1058) vs. 660 (484–859)

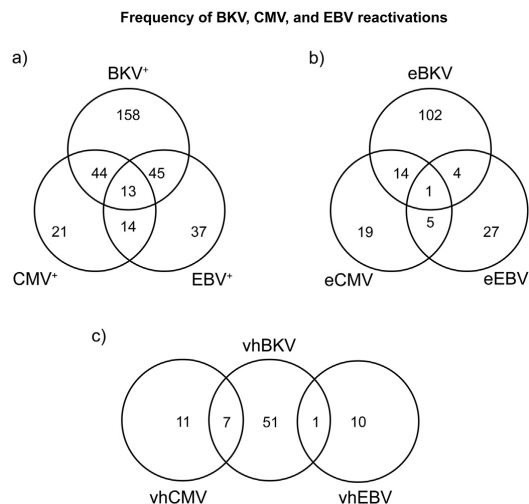


Fig. 3. Frequency of triple, combined and mono-reactivations of BKV, CMV, and EBV during the first post-transplantation year. Number of patients with reactivations and all their possible combinations are plotted as a Venn diagram. Fig. 3a depicts the combinations of BKV⁺, CMV⁺, and EBV⁺, i.e. viral load over detection level. Fig. 3b depicts the combinations of elevated viral load sub-groups (eBKV, eCMV, and eEBV, > 2000 copies·mL⁻¹). Fig. 3c depicts the combinations of high-level viral load sub-groups (vhBKV, hCMV, and hEBV, > 10,000 copies·mL⁻¹).

incidence (Fisher's exact test: $p = 0.21$). The patient with severe PTLTD had EBV viral load over DL for visits 4 and 5, with a peak viral load of 12,271 copies·mL⁻¹; the patient with mild PTLTD showed no EBV viral load. None of the patients showed viral load over DL for CMV or BKV.

3.9. High-Level BKV and CMV Were Associated with Lower Graft Function One Year Post-Transplantation

Patients with hBKV had a significantly lower GFR (42.3 [31.9–50.6] mL·min⁻¹·1.73 m⁻² – $p = 0.0096$) one year after transplantation compared to patients with no viraemia (BKV, CMV, and EBV below DL; 51.2 [35.4–63.6] mL·min⁻¹·1.73 m⁻²) (Fig. 4). Median reduction was 8.9 mL·min⁻¹·1.73 m⁻². Patients with hCMV had a significant GFR loss from the 6th month onwards, with a median difference of 13.9 mL·min⁻¹·1.73 m⁻² one year after transplantation ($p = 0.0021$ –37.3 [29.1–45.4] vs. 51.2 [35.4–63.6] mL·min⁻¹·1.73 m⁻²) (Fig. 4). The relationship of BKV and CMV with GFR loss was robust for a very wide range of thresholds (Figs. S1 and S2). No significant relationship was observed between EBV and GFR.

3.10. A Combination of BKV and CMV Viraemia Leads to Lower Graft Function Already at Moderate Viral Loads

To better capture the possible effect of combined viral reactivations on graft function, as well as the effect of the viral load threshold used to classify the patients into viraemia groups, a systematic exploration of viral load thresholds was performed (Fig. S3). Patients with combined BKV and CMV viraemia had lower GFR already for low viral load levels. For example, patients with BKV > 1000 copies·mL⁻¹ and CMV > 4000 copies·mL⁻¹ ($N = 16$) demonstrated a significant impairment of GFR from the ninth month onwards and a median loss of 11.7 mL·min⁻¹·1.73 m⁻² compared to non-reactivating patients at the first post-transplantation year ($p = 0.0172$; 39.5 [30.7–46.6] vs. 51.2 [35.4–63.6] mL·min⁻¹·1.73 m⁻²) (Fig. 4). Moreover, these patients had (non-significant) lower GFR than patients with mono-reactivation

($N = 166$; BKV > 1000 or CMV > 4000 copies·mL⁻¹) from the second week of the study onwards, with a median difference one year post-transplantation of 3.33 mL·min⁻¹·1.73 m⁻².

There was no bias in the use of antiviral treatment for combined reactivations (Fisher's exact test: $p = 0.70$): 68.8% of the patients with BKV > 1000 and CMV > 4000 copies·mL⁻¹ were treated with (val)ganciclovir, while for patients with BKV < 1000 and CMV > 4000 copies·mL⁻¹ the prevalence of treatment was 58.3%.

4. Discussion

In this work, the prevalence of BKV, CMV, and EBV and their impact on patients undergoing kidney transplantation have been analysed for the first time in a large multi-centre study. With the increasing efficacy of immunosuppressive therapies and the subsequent decrease of acute rejection, reactivations are expected to gain clinical importance in renal transplantation. The main findings of our study include:

- Superiority of BKV over CMV and EBV from the epidemiological point of view with the highest incidence and viral load;
- Significant association between CMV with BKV or EBV, but not between EBV and BKV;
- Combined BKV and CMV reactivation significantly associated with lower graft function one year post-transplantation, even at low viral load levels.

Our results show that BKV, with the highest incidence rate and median peak viral load and the lowest clearing rate, is the most relevant viral reactivation of the three from the epidemiological point of view for kidney recipients. Prevalence of presumptive BKV nephropathy (BKV > 10,000 copies·mL⁻¹) [11] was on the higher end of the common estimations for BKV nephropathy (1–10%) [11,22], although the patient cohort consisted of immunological low-risk patients. In contrast to BKV, CMV, and EBV were observed with a lower but still substantial prevalence in around one fifth of the patients. In both cases, viraemia had most frequently an episodic character, with viraemia clearance rates over 85%.

A key finding of our study is the impact of BKV-CMV combined reactivation on GFR one year post-transplantation – an important predictor of transplant survival [23] – even at relatively low viral load levels. Patients with no viral reactivation experienced an increase in the median GFR between the third and the twelfth post-transplantation month. Such positive GFR slopes in patients without transplant complications have been observed before in the literature, e.g. Guba et al. [24]. However, in patients with BKV or CMV viral load over 10,000 copies·mL⁻¹, no such increase was observed, leading to a significantly lower GFR. Remarkably, patients with moderate BKV-CMV combined reactivation (BKV > 1000 copies·mL⁻¹ and CMV > 4000 copies·mL⁻¹) also had a significantly lower GFR (median difference: 11.7 mL·min⁻¹·1.73 m⁻²). This finding is especially interesting since currently only much higher BKV levels are generally considered of clinical relevance so far [25]. Thus, our data provide evidence regarding BKV-CMV combined reactivation as a relevant complication of the post-transplantation period.

The impact of BKV-CMV combined reactivation on GFR is especially relevant due to the reciprocal effects between the viruses. BKV-CMV combined reactivations have been observed repeatedly in the past and interactions between both are plausible [9,14,26–29]. However, the existence of an epidemiological association is controversial: A previous large retrospective study from our group identified a significant association between CMV and BKV viraemia [9], but a large prospective study by Elfadawy et al. showed a negative association between antecedent CMV and BKV incidence [14]. Moreover, Elfadawy et al. did not find any effect of BKV, CMV or their combination on GFR and only symptomatic CMV was linked with graft survival. A reason for the first difference

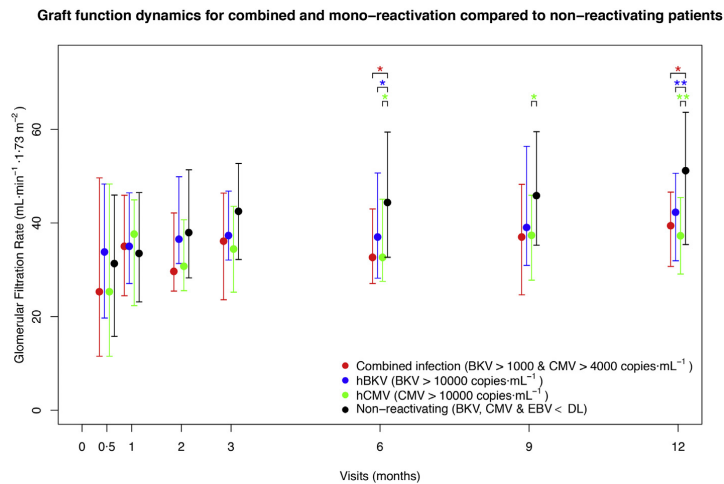


Fig. 4. Graft function dynamics of patients with BKV and CMV mono-reactivations and combined reactivations, in comparison to non-reactivating patients. Median GFR ($\text{mL} \cdot \text{min}^{-1} \cdot 1.73 \text{ m}^{-2}$) for patients with BKV-CMV combined reactivation (red; $N = 16$), hBKV (blue; $N = 59$), hCMV (green; $N = 18$) and non-reactivating (black; $N = 208$) for the last seven visits is plotted. Coloured groups are not mutually exclusive – a patient might belong to more than one sub-group. The bars indicate the interquartile range. Coloured asterisks indicate a significant difference calculated with the Mann-Whitney test (* $p < 0.05$; ** $p < 0.01$) in GFR of the corresponding group with respect to the non-reactivating group. Day 0 is not shown, as it is pre-transplantation.

lies probably on the fact that Elfadawy et al. was an interventional study [14]. As the authors suggest, interventions following CMV diagnosis are a plausible cause for the seemingly protective effect of CMV against BKV [14]. For the contradiction on GFR effects, the most likely cause is the different stratification strategies of viral reactivations: while in our study systematic viral load cut-offs were employed, Elfadawy et al. employed a symptom-based approach for CMV and no stratification strategy for BKV [14]. However, as shown in our results (e.g. Fig. S1–S3), the choice of viral load threshold is important for the identification of virus-associated renal function impairments. Our results show that stratification of reactivations according to viral load is key to identifying which patients might develop a lower GFR as a consequence of apparently asymptomatic reactivations.

Our study also showed a significant association between CMV and EBV. This is in agreement with a previous study showing an association of these viruses [30]. However, no clinical relevance of this association was found, possibly due to the low number of affected patients. Literature offers likewise an unclear picture on the clinical relevance of this combined reactivation: Even though a previous study showed a link between CMV-EBV combined reactivation and PTLN in liver transplantation recipients [31], we found no case of PTLN in patients with CMV-EBV combined infection. The only case of severe PTLN in the cohort suffered from high-level ($>10,000$ copies·mL⁻¹) EBV mono-reactivation. Nevertheless, our results cannot exclude a relationship between CMV-EBV combined reactivation and PTLN, as the majority of PTLN cases in adult renal transplantation occur after the first post-transplantation year [7,15,16]. There are to our knowledge no recent studies showing a clinical relevance for CMV-EBV combined reactivation in kidney recipients.

Acute rejection was significantly associated with high-level CMV viral loads ($>10,000$ copies/mL). A mutual relation of these two phenomena, where CMV boosts rejection and rejection boosts reactivations, seems likely. However, the number of cases was too low to offer an unambiguous cause-effect relation. No relationship with acute rejection was found for BKV or EBV. This is remarkable for BKV, as it is known from the literature to be associated with rejection [9]; the absence of association could be linked to the remarkably low rejection rate found in the patient cohort [17].

Regarding risk factors, therapy arm did not have any significant effect on BKV or CMV incidence. This highlights the safety of both rabbit ATG and steroid withdrawal therapies in renal transplantation with respect to BKV and CMV [17]. On the other hand, EBV reactivations were significantly associated with arm C (ATG and rapid steroid withdrawal). This finding is consistent with a previous study [32]. Likewise, the only two cases of PTLN in the cohort were encountered in arm C, but the association was not statistically significant. Interestingly, arm B (basiliximab and rapid steroid withdrawal) had a significantly lower EBV prevalence than the rest. However, it should be emphasized that there was no association between arm and elevated (>2000 copies·mL⁻¹), high-level EBV ($>10,000$ copies·mL⁻¹), or PTLN. Finally, no significant relationship was found between MMF daily dose and viraemia. In agreement with Elfadawy et al., we found that higher tacrolimus trough levels were however a risk factor for detectable CMV reactivation [14]. On the other hand, there was no evidence for an effect of tacrolimus on BKV or EBV reactivation. Other clinical risk factors showed no association with BKV. This highlights the current uncertainty on its risk factors, with the literature yielding inconsistent results [9,33–36]. CMV and EBV were, as expected, significantly associated with patient-donor serological mismatch. Interestingly, we have observed a significant association between high-level CMV viraemia ($>10,000$ copies·mL⁻¹) and longer cold ischaemia time for cadaveric organs, an association first observed in a very recent study with only eight patients [37]. Since such viral loads are associated with lower GFR, our data suggest reinforcing CMV-surveillance after transplantations with a long cold ischaemia time, especially for cases of high CMV mismatch-associated risk.

Our study has some limitations. First, the follow-up period – one year – is too short to observe long-term effects. Our analyses were explorative and are not corrected for multiple testing to maximize the obtained information, on the basis of the precautionary principle. Secondly, other factors affecting renal function (e.g. bacterial infections, use of nephrotoxic drugs) were not analysed. Moreover, transplantation outcomes were assessed on the basis of estimated GFR and not on a histological basis. Nevertheless, the fact that GFR is a recognised predictor for long-term transplantation outcomes supports the relevance of our conclusions [23]. However, these limitations are outweighed by the

fact that it is the first large multi-centre study that has examined BKV, CMV, and EBV in kidney transplantation in a systematic and parallel way, as well as the first to offer a detailed analysis of viral associations and their impact on transplantation outcomes. Almost ten thousand viral load measurements were performed along the eight pre-programmed visits – all measurements were performed in the same centre and following the same, standardised protocol, thereby ensuring the comparability of results.

In conclusion, our work offers an extensive outlook on the impact and relevance of BKV, CMV, and EBV and their interactions after kidney transplantation. In our study, BKV emerges as the most relevant viral complication from the epidemiological point of view, with the highest prevalence, highest viral load, and the lowest clearing rates. Long cold ischaemia time is confirmed to be significantly associated with elevated CMV viraemia. An association between CMV and EBV is shown, albeit without any evidence of enhancement of their clinical effects. Finally, we further demonstrate a highly significant association between BKV and CMV reactivations, shown for the first time to be of clinical interest, with an increase of damaging effects by both viruses already at moderate viral loads. The results of our study have the potential to change the BKV and CMV management, appealing for a stricter monitoring and intervention in kidney transplantation patients with BKV or CMV low viral loads as well as long cold ischaemia times.

Supplementary data to this article can be found online at <https://doi.org/10.1016/j.ebiom.2018.07.017>.

Funding Sources

This work was funded by the German Federal Ministry of Education and Research (BMBF)01ZX1312. The funder had no role in data collection, data analysis, data interpretation, writing of the manuscript, or manuscript submission.

Declaration of Interests

The authors declare no competing interests.

Author Contributions

NB, NW, CH, OT, CB, KW, RS, THW, BS, PR, and MO contributed to the study design, sample collection, and sample management. Data were generated by CDH, data interpretation by ABN, NB, and MO, and drafting of the manuscript by ABN, NB, and MO. All authors have contributed to the manuscript and approved the final version of the manuscript for submission.

Acknowledgements

This work was supported by the German Federal Ministry of Education and Research (BMBF) within the framework of the e:Med research and funding concept (01ZX1312).

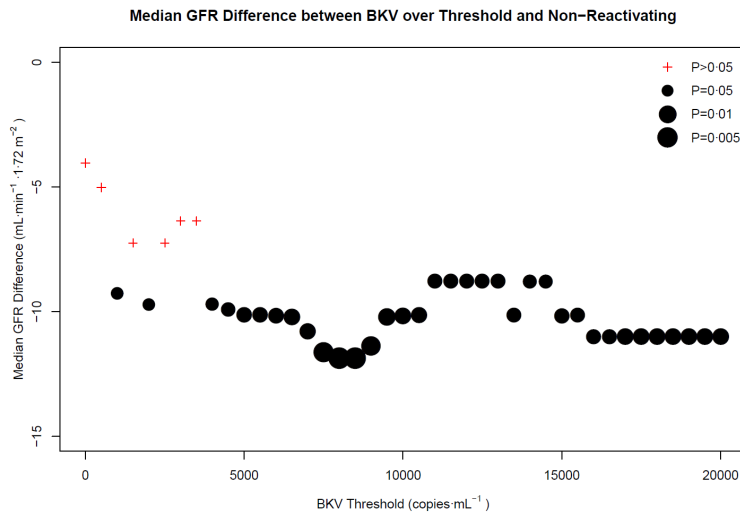
References

- [1] Alangaden, G.J., Rama, T., Gruber, S.A., et al., 2006]. Infectious complications after kidney transplantation: current epidemiology and associated risk factors. *Clin Transplant* 20, 401–409.
- [2] Egli, A., Infanti, L., Dumoulin, A., et al., 2009]. Prevalence of polyomavirus BK and JC infection and replication in 400 healthy blood donors. *J Infect Dis* 199, 837–846.
- [3] Griffiths, P., Baraniak, I., Reeves, M., 2015]. The pathogenesis of human cytomegalovirus. *J Pathol* 235, 288–297.
- [4] Ng, S.-B., Khoury, J.D., 2009]. Epstein-Barr virus in lymphoproliferative processes: an update for the diagnostic pathologist. *Adv Anat Pathol* 16, 40–55.
- [5] Le Page, A.K., Mackie, F.E., McTaggart, S.J., Kennedy, S.E., 2013]. Cytomegalovirus & Epstein-Barr virus serostatus as a predictor of the long-term outcome of kidney transplantation. *Nephrology (Carlton)* 18, 813–819.
- [6] Babel, N., Volk, H.-D., Reinke, P., 2011]. BK polyomavirus infection and nephropathy: the virus – immune system interplay. *Nat Rev Nephrol* 7, 399–406.
- [7] Petrara, M.R., Giunco, S., Serraino, D., Dolcetti, R., De Rossi, A., 2015]. Post-transplant lymphoproliferative disorders: from epidemiology to pathogenesis-driven treatment. *Cancer Lett* 369, 37–44.
- [8] Egli, A., Binggeli, S., Bodaghi, S., et al., 2007]. Cytomegalovirus and polyomavirus BK posttransplant. *Nephrol Dial Transplant* 22, viii72–viii82.
- [9] Schachtner, T., Babel, N., Reinke, P., 2015]. Different risk factor profiles distinguish early-onset from late-onset BKV-replication. *Transpl Int* 28, 1081–1091.
- [10] Hirsch, H.H., Steiger, J., Polyomavirus, B.K., 2003]. *Lancet Infect Dis* 3, 611–623.
- [11] Hirsch, H.H., Brennan, D.C., Drachenberg, C.B., et al., 2005]. Polyomavirus-associated nephropathy in renal transplantation: interdisciplinary analyses and recommendations. *Transplantation* 79, 1277–1286.
- [12] Blazquez-Navarro, A., Schachtner, T., Stervbo, U., et al., 2018]. Differential T cell response against BK virus regulatory and structural antigens: a viral dynamics modeling approach. *PLoS Comput Biol* 14, 1–20.
- [13] Fehr, T., Cippà, P.E., Mueller, N.J., 2015]. Cytomegalovirus post kidney transplantation: prophylaxis versus pre-emptive therapy? *Transpl Int* 28, 1351–1356.
- [14] Elfadawy, N., Flechner, S.M., Liu, X., et al., 2013]. CMV Viremia is associated with a decreased incidence of BKV reactivation after kidney and kidney-pancreas transplantation. *Transplantation* 96, 1097–1103.
- [15] Végo, G., Hajdu, M., Sebestyén, A., 2011]. Lymphoproliferative disorders after solid organ transplantation-classification, incidence, risk factors, early detection and treatment options. *Pathol Oncol Res* 17, 443–454.
- [16] Babel, N., Vergopoulos, A., Trappe, R.U., et al., 2007]. Evidence for genetic susceptibility towards development of posttransplant lymphoproliferative disorder in solid organ recipients. *Transplantation* 84, 387–391.
- [17] Thomsch, O., Wiesener, M., Opgenoorth, M., et al., 2016]. Rabbit-ATG or basiliximab induction for rapid steroid withdrawal after renal transplantation (harmony): an open-label, multicentre, randomised controlled trial. *Lancet* 388, 3006–3016.
- [18] Kasiske, B.L., Zeier, M.G., Chapman, J.R., et al., 2011]. KDIGO clinical practice guideline for the care of kidney. *Rev Nephrol Dial y Traspl* 31, 6–21.
- [19] Babel, N., Fendt, J., Karaivanov, S., et al., 2009]. Sustained BK viremia as an early marker for the development of BKV-associated nephropathy: analysis of 4128 urine and serum samples. *Transplantation* 88, 89–95.
- [20] Levey, A.S., Stevens, L.A., Schmid, C.H., et al., 2009]. A new equation to estimate glomerular filtration rate. *Ann Intern Med* 150, 604–612.
- [21] Solez, K., Colvin, R.B., Racusen, L.C., et al., 2007]. Banff '05 meeting report: differential diagnosis of chronic allograft injury and elimination of chronic allograft nephropathy ('CAN'). *Am J Transplant* 7, 518–526.
- [22] Trofe, J., Gordon, J., Roy-Chaudhury, P., et al., 2004]. Polyomavirus nephropathy in kidney transplantation. *Prog Transplant* 14, 130–140.
- [23] Kasiske, B.L., Israni, A.K., Snyder, J.J., Skeans, M.A., 2011]. The relationship between kidney function and long-term graft survival after kidney transplant. *Am J Kidney Dis* 57, 466–475.
- [24] Guba, M., Pratschke, J., Hugo, C., et al., 2010]. Renal function, efficacy, and safety of Sirolimus and mycophenolate Mofetil after short-term Calcineurin inhibitor-based quadruple therapy in De novo renal transplant patients: one-year analysis of a randomized multicenter trial. *Transplant J* 90, 175–183.
- [25] Sood, P., Senanayake, S., Sajeet, K., et al., 2012]. Management and outcome of BK viremia in renal transplant recipients: a prospective single-center study. *Transplantation* 94, 814–821.
- [26] Nada, R., Sachdeva, M.U.S., Sud, K., Jha, V., Joshi, K., 2005]. Co-infection by cytomegalovirus and BK polyoma virus in renal allograft, mimicking acute rejection. *Nephrol Dial Transplant* 20, 994–996.
- [27] Park, S.B., Kwak, J.H., Lee, K.T., et al., 2006]. Polyoma virus-associated nephropathy and concurrent cytomegalovirus infection in the kidney transplant recipients. *Transplant Proc* 38, 2059–2061.
- [28] Toyoda, M., Puliya, D.P., Amet, N., et al., 2005]. Co-infection of polyomavirus-BK and cytomegalovirus in renal transplant recipients. *Transplantation* 80, 198–205.
- [29] Kristoffersen, A.K., Inge, J., Morten, O., 1997]. The Human Polyomavirus Bk T Antigen Induces Gene Expression in Human Cytomegalovirus. 52 pp. 61–71.
- [30] Meyer, T., Scholz, D., Warnecke, G., et al., 1996]. Importance of simultaneous active cytomegalovirus and Epstein-Barr virus infection in renal transplantation. *Clin Diagn Virol* 6, 79–91.
- [31] Mañez, R., Breinig, M.C., Linden, P., et al., 1997]. Posttransplant lymphoproliferative disease in primary Epstein-Barr virus infection after liver transplantation: the role of cytomegalovirus disease. *J Infect Dis* 176, 1462–1467.
- [32] Bamoulid, J., Courivaud, C., Coaquette, A., et al., 2013]. Subclinical Epstein-Barr virus viremia among adult renal transplant recipients: incidence and consequences. *Am J Transplant* 13, 656–662.
- [33] Bormi-Duval, C., Caillard, S., Olagne, J., et al., 2013]. Risk factors for BK virus infection in the era of therapeutic drug monitoring. *Transplantation* 95, 1498–1505.
- [34] Pai, D., Mann, D.M., Malik, A., Hoover, D.R., Fyfe, B., Mann, R.A., 2015]. Risk factors for the development of BK virus nephropathy in renal transplant recipients. *Transplant Proc* 47, 2465–2469.
- [35] Hirsch, H.H., Vincenti, F., Friman, S., et al., 2013]. Polyomavirus BK replication in de novo kidney transplant patients receiving tacrolimus or cyclosporine: a prospective, randomized, multicenter study. *Am J Transplant* 13, 136–145.
- [36] Bonvoisin, C., Weekers, L., Khignesse, P., Grosch, S., Milicevic, M., Krzesinski, J.-M., 2008]. Polyomavirus in renal transplantation: a hot problem. *Transplantation* 85, 542–548.
- [37] Schlott, F., Steubl, D., Hoffmann, D., et al., 2017]. Primary cytomegalovirus infection in seronegative kidney transplant patients is associated with protracted cold ischemic time of seropositive donor organs. *PLoS One* 12, 1–10.

7.2 Supplementary materials

7.2.1 Figure S1

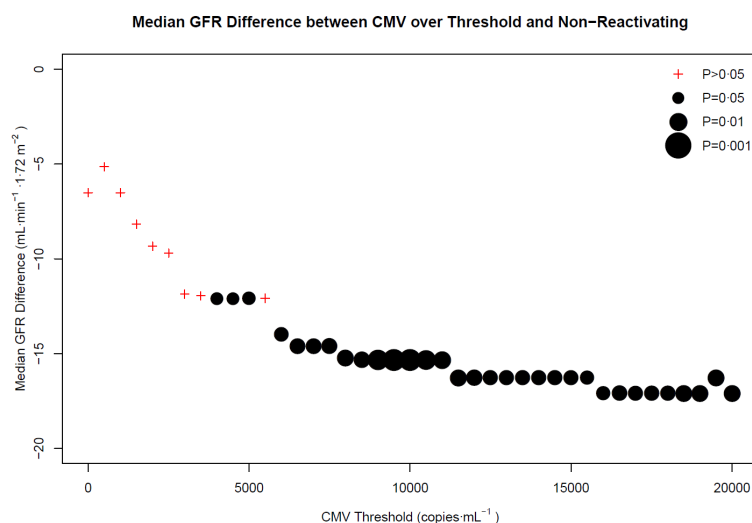
Influence of BKV threshold on median GFR loss one year post-transplantation



A systematic exploration of the influence of BKV viral load threshold choice on GFR one year post-transplantation was performed. Patients with BKV peak viral load over the threshold were compared with the patients with no viral reactivation (BKV, CMV and EBV below DL, N = 208). All thresholds between 0 and 20,000 $\text{copies} \cdot \text{mL}^{-1}$, with steps of 500 $\text{copies} \cdot \text{mL}^{-1}$, were evaluated. Significance was evaluated through the Mann-Whitney test. The height of the points indicates the median difference in GFR one year post-transplantation between the BKV sub-group and the non-reactivating sub-group. Non-significant differences were plotted as red crosses, significant differences ($p < 0.05$) as black points whose size indicate the p value. As it can be observed, for all thresholds there was a negative effect of BKV on GFR one year post-transplantation, which was significant for all thresholds between 4000 and 20,000 $\text{copies} \cdot \text{mL}^{-1}$.

7.2.2 Figure S2

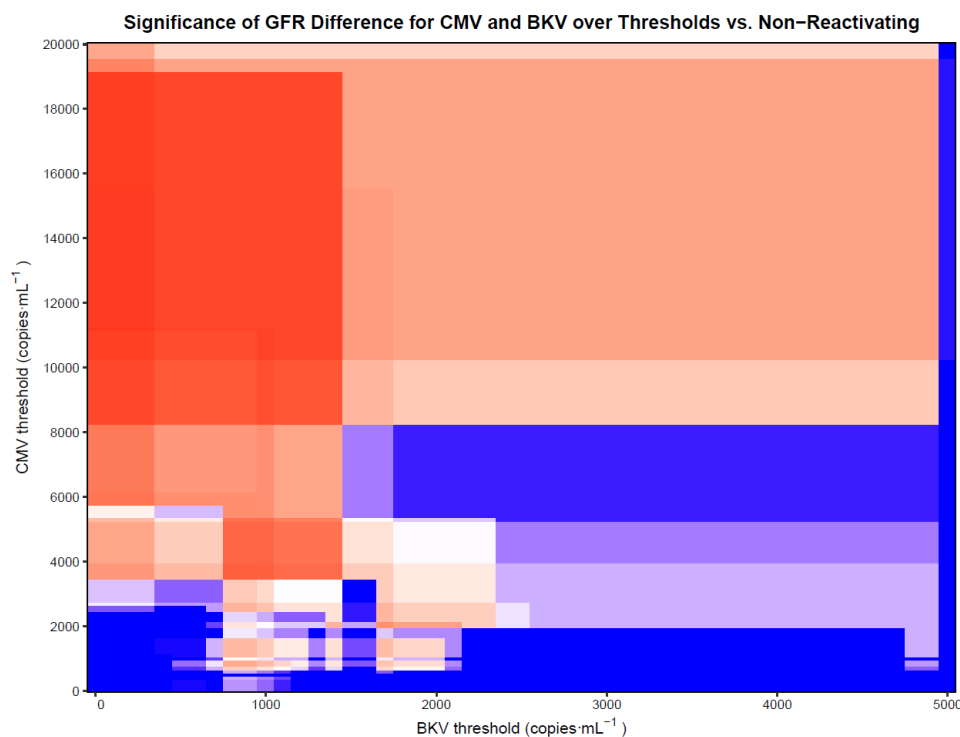
Influence of CMV threshold on median GFR loss one year post-transplantation



A systematic exploration of the influence of CMV viral load threshold choice on GFR one year post-transplantation was performed. Patients with CMV peak viral load over the threshold were compared with the patients with no viral reactivation (BKV, CMV and EBV below DL, N = 208). All thresholds between 0 and 20,000 copies·mL⁻¹, with steps of 500 copies·mL⁻¹, were evaluated. Significance was evaluated through the Mann-Whitney test. The height of the points indicates the median difference in GFR one year post-transplantation between the CMV sub-group and the non-reactivating sub-group. Non-significant differences were plotted as red crosses, significant differences ($p < 0.05$) as black points whose size indicate the p value. As it can be observed, for all thresholds there was a negative effect of CMV on GFR one year post-transplantation, with increasing GFR loss for higher thresholds. GFR loss was significant for all thresholds between 6000 and 20,000 copies·mL⁻¹.

7.2.3 Figure S3

Exploration of viral load thresholds for BKV and CMV and their influence on GFR one year post-transplantation.



A systematic exploration was performed on the influence of viral load threshold choice on GFR one year post-transplantation for patients with BKV-CMV combined reactivation. For this, two sub-groups are generated for the comparison of their GFR at the end of the study: one (combined reactivation) with the patients that had BKV and CMV viral loads over certain thresholds; the second group (non-reactivating) with the patients that did not show any detectable viral load (BKV, CMV and EBV below DL, N = 208). For the BKV and CMV thresholds, all combinations between 0 and 20,000 copies·mL⁻¹, with steps of 100 copies·mL⁻¹, were evaluated. Significance was evaluated through the Mann-Whitney test, the colour shows the P value for each combination. Shown is the space $BKV \leq 5000$ copies·mL⁻¹, where all significant differences were found. In all cases, the combined reactivation group had a lower median GFR than the non-reactivating group.

8. Sex-associated differences in cytomegalovirus prevention: Prophylactic strategy is associated with a strong kidney function impairment in female renal transplant patients

This chapter* refers to the manuscript published as:

Blazquez-Navarro A, Dang-Heine C, Wittenbrink N, Bauer C, Wolk K, Sabat R, Witzke O, Westhoff TH, Sawitzki B, Reinke P, Thomusch O, Hugo C, Babel N and Or-Guil M (2019). Sex-associated differences in cytomegalovirus prevention: Prophylactic strategy is associated with a strong kidney function impairment in female renal transplant patients. *bioRxiv* 726968. doi:10.1101/726968

* The chapter corresponds to the version of the manuscript available at submission of this dissertation (version 2). At the time point of the defense, an updated version of the manuscript was available. In this version, an improved method for the variable selection in multivariable regression was employed with the goal of increasing the specificity of the analysis; the results and discussion were modified accordingly. The updated version (version 3) is available at bioRxiv.

Sex-associated differences in cytomegalovirus prevention: Prophylactic strategy is associated with a strong kidney function impairment in female renal transplant patients

Arturo Blazquez-Navarro, MSc^{1,2}, Dr. Chantip Dang-Heine¹, Dr. Chris Bauer³, Dr. Nicole Wittenbrink^{1,2}, Dr. Kerstin Wolk^{1,4}, Dr. Robert Sabat^{4,5}, Prof. Oliver Witzke⁶, Prof. Timm H. Westhoff⁷, Prof. Birgit Sawitzki¹, Prof. Petra Reinke^{1,8}, Prof. Oliver Thomusch⁹, Prof. Christian Hugo¹⁰, Prof. Nina Babel^{1,7*}, Dr. Michal Or-Guil^{2*}

¹*Berlin-Brandenburg Center for Regenerative Therapies (BCRT): Berlin-Brandenburg Centrum für Regenerative Therapien, Charité-Universitätsmedizin Berlin, Augustenburger Platz 1, 13353 Berlin, Germany.*

²*Systems Immunology Lab, Department of Biology, Humboldt-Universität zu Berlin: Philippstr. 13, 10115 Berlin, Germany.*

³*MicroDiscovery GmbH: Marienburger Str. 1, 10405 Berlin Germany.*

⁴*Psoriasis Research and Treatment Center, Institute of Medical Immunology/Department of Dermatology and Allergy, Charité-Universitätsmedizin Berlin: Charitéplatz 1, 10117 Berlin, Germany.*

⁵*Interdisciplinary Group of Molecular Immunopathology, Institute of Medical Immunology/Department of Dermatology and Allergy, Charité-Universitätsmedizin Berlin: Charitéplatz 1, 10117 Berlin, Germany.*

⁶*Department of Infectious Diseases, West German Centre of Infectious Diseases, University Hospital Essen, University Duisburg-Essen, Hufelandstraße 55, 45147 Essen, Germany.*

⁷*Universitätsklinikum der Ruhr-Universität Bochum, Medizinische Klinik I: Hölkeskampring 40, 44625 Herne, Germany.*

⁸*Berlin Center for Advanced Therapies (BeCAT), Charité-Universitätsmedizin Berlin, Augustenburger Platz 1, 13353 Berlin, Germany.*

⁹*Klinik für Allgemein- und Viszeralchirurgie, Universitätsklinikum Freiburg: Hugstetter Straße 55, 79106 Freiburg, Germany.*

¹⁰*Universitätsklinikum Carl Gustav Carus, Medizinische Klinik III - Bereich Nephrologie: Fetscherstraße 74, 01307 Dresden, Germany.*

*These authors contributed equally

Authorship

NB, NW, CH, OT, CB, KW, RS, OW, THW, BS, PR, and MO contributed to the study design, sample collection, and/or sample management. CDH carried out experiments. ABN, NB, and MO performed data interpretation. ABN, NB and MO drafted the manuscript. All authors have contributed to the manuscript and approved the final version of the manuscript for submission.

Funding sources

This work was funded by the German Federal Ministry of Education and Research (BMBF) 01ZX1312. The funder had no role in data collection, data analysis, data interpretation, writing of the manuscript, or manuscript submission.

Corresponding authors contact information

Prof. Nina Babel: Berlin-Brandenburg Centrum für Regenerative Therapien, Charité-Universitätsmedizin Berlin, Augustenburger Platz 1, 13353 Berlin, Germany. nina.babel@charite.de
 Michal Or-Guil: Systems Immunology Lab, Department of Biology, Humboldt-Universität zu Berlin: Philippstr. 13, 10115 Berlin, Germany. m.orguil@biologie.hu-berlin.de

Running title CMV prophylaxis is associated with lower eGFR in female patients

Keywords: cytomegalovirus, renal function, acute rejection, prophylaxis, pre-emptive, valganciclovir

Abbreviations

ATG, Antithymocyte globulin; CMV, Cytomegalovirus; 95% CI, 95% Confidence interval; D⁻R⁻, Seronegative donor and seronegative recipient; D⁺R⁻, Seropositive donor and seronegative recipient; D⁺R⁺, Seropositive donor and seropositive recipient; EBV, Epstein-Barr virus; eGFR, Estimated glomerular filtration rate; eGFR-1y, Estimated glomerular filtration rate one year after transplantation; IQR, Interquartile range; MMF, mycophenolate mofetil; OR, Odds ratio; qPCR, Quantitative polymerase chain reaction; R⁺, Seropositive Recipient.

Conflict of interest statement

OW has received research grants for clinical studies, speaker's fees, honoraria and travel expenses from Amgen, Astellas, Bristol-Myers Squibb, Chiesi, Janssen-Cilag, MSD, Novartis, Roche, Pfizer, and Sanofi. OW is supported by an unrestricted grant of the Rudolf-Ackermann-Stiftung (Stiftung für Klinische Infektiologie). All other authors have no conflicts of interest to disclose

Abstract

Cytomegalovirus (CMV) syndrome or disease, a serious health hazard after renal transplantation, can be prevented using the antiviral drug (val)ganciclovir. (Val)ganciclovir is typically administered following a prophylactic or a pre-emptive strategy. The prophylactic strategy entails early universal administration, the pre-emptive strategy early treatment in case of infection. However, it is not clear which strategy is superior with respect to transplantation outcome and viral clearance. We have retrospectively analysed 540 patients from the multicentre Harmony study: 308 were treated according to a prophylactic, 232 according to a pre-emptive strategy. As expected, we observed an association of prophylactic strategy with lower incidence of CMV syndrome, delayed onset and lower viral loads compared to the pre-emptive strategy. However, the prophylactic strategy was associated with higher incidence of acute rejection ($P=0.002$) and – for female patients – a strong impairment of glomerular filtration rate (eGFR) one year post-transplant ($P<0.001$, median difference: $18.5 \text{ mL} \cdot \text{min}^{-1} \cdot 1.73 \text{ m}^{-2}$). Additionally, the prophylactic strategy was associated with increased incidence of severe BK virus reactivation. Our results suggest for the first time that the prophylactic strategy might lead to inferior transplantation outcomes, providing evidence for a strong association with sex.

ClinicalTrials.gov number: NCT00724022

1. Introduction

Cytomegalovirus (CMV) is a herpes virus often reported as the most important viral pathogen after kidney transplantation.¹⁻³ It is a major cause of morbidity and mortality, being associated with retinitis, pneumonitis, colitis, encephalitis, allograft damage and allograft loss, among others.¹⁻⁴ CMV syndrome or disease may occur as a consequence of reactivation of latent infections or through primary infection, acquired from the donor or from the environment.² The major risk factor for CMV syndrome or disease is the pre-transplantation serostatus: CMV seronegative transplant recipients with a seropositive donor (D⁺R⁻) have the highest risk, while seropositive recipients (R⁺) have an intermediate risk and seronegative recipients with seronegative donors (D⁻R⁻) have the lowest risk.² Moreover, the use of immunosuppressive drugs like rabbit antithymocyte globulin (ATG) can additionally increase the incidence of CMV (re)activations.⁵

The standards in prevention and treatment of CMV (re)activation are based on ganciclovir or its oral prodrug valganciclovir.^{6,7} Two prevention strategies are routinely employed in the clinic: prophylactic and pre-emptive.^{2,6,7} The prophylactic strategy is based on the universal administration of (val)ganciclovir in case of patients with a CMV risk constellation, usually during 3-6 months after transplantation.^{6,7} In the pre-emptive strategy, patients are regularly monitored for CMV through quantitative polymerase chain reaction or pp65 antigenemia test; (val)ganciclovir is only administered after a positive test, ideally before any symptoms of CMV syndrome or disease manifest.^{6,7} The pre-emptive strategy thus leads to a reduction of unnecessary treatments, which is advantageous with respect to the appearance of side effects and resistances against antiviral drugs.^{6,7}

While the KDIGO guideline of 2009 preferred prophylaxis as the standard of prevention, the more recent reference CMV management guideline recommends both strategies for the prevention of CMV disease in patients with both high or intermediate CMV mismatch-based risk constellation.^{6,7} However, the differences in outcome with regard to other criteria, including renal function and other viral (re)activations is largely unclear. In addition to antiviral

therapy, CMV-specific T cell immunity has been shown to control CMV viral reactivations, determining the outcome of disease.^{8–10} Interestingly, there is evidence of sex differences in both ganciclovir pharmacokinetics and the anti-CMV immune response.^{11–14} Thus, female patients have been shown to have a faster ganciclovir clearance, and distinct anti-CMV immunological profiles e.g. higher number of secreting anti-CMV T cells.^{11–15} In spite of this, there are to our knowledge still no studies on the influence of sex on the clinical outcomes of CMV prevention strategies. In this work, we provide evidence that prophylaxis might be associated with inferior transplantation outcomes – including a strong reduction of renal function in female patients – at the end of the first year post-transplant.

2. Materials and Methods

2.1. Patient population

As part of the systems medicine project e:KID, we conducted a sub-study within the randomized, multi-centre, investigator-initiated Harmony trial (NCT 00724022)^{16,17} to determine the impact of CMV prevention strategy on transplant outcome. For this, CMV, Epstein-Barr virus (EBV) and BK virus (BKV) viral loads, white blood cell count and creatinine were measured at predetermined eight study visits.¹⁷ This viral monitoring was non-interventional and centrally performed and was independent from the internal, interventional viral monitoring (see section 2.3). The study was carried out in compliance with the Declaration of Helsinki and Good Clinical Practice.

2.2. Patient medication

According to study design, patients were treated with a quadruple (arm A) or triple (arms B and C) immunosuppressive therapy.¹⁶ Patients in arm A received an induction therapy with basiliximab and maintenance therapy consisting of tacrolimus (Advagraf®, Astellas), mycophenolate mofetil (MMF) and corticosteroids. Patients in arm B received the same treatment as in arm A, but corticosteroids were withdrawn at day 8. Patients in arm C received the same treatment as in arm B, except induction was achieved with ATG, instead

of basiliximab.

2.3. Patient monitoring

Patients were monitored for graft function along eight visits, scheduled at day 0 (pre-transplantation), 2nd week, 1st month, 2nd month, 3rd month, 6th month, 9th month, and 12th month. To assess graft function, glomerular filtration rate was calculated using the CKD-EPI formula, measured in $\text{mL} \cdot \text{min}^{-1} \cdot 1.73 \text{ m}^{-2}$.¹⁸ Serious adverse events were defined following the Good Clinical Practice guidelines. Suspected episodes of acute rejection had to be confirmed through biopsy; histologic characteristics were described according to the Banff criteria of 2005.¹⁹ Regarding the outcome assessment, acute rejection was analysed including and excluding borderline rejections. Routine surveillance biopsies were allowed but not mandatory.

2.4. Clinical monitoring and management of clinical complications

Viral (re)activations were monitored and managed at local centres as described previously.¹⁷ CMV in particular was monitored for all patients, independently of the prevention strategy. Monitoring was performed independently from the above described CMV viral load measurements and was based on three different methods: serum PCR viral load measurements; test for pp65 antigenemia and symptom monitoring according to the internal centre standards. Diagnosis of CMV syndrome was likewise based on the methods, where a qPCR over 1000 copies·mL⁻¹ was defined as positive. Patients with CMV syndrome were treated based on internal centre standards. Suggested treatment was (val)ganciclovir treatment according to local standards with/or without reduction of tacrolimus and MMF dose. No data on the time point of CMV syndrome diagnostic were available for this study; no data on CMV disease were available.

2.5. Screening of CMV, EBV and BKV viraemia

In parallel to the clinical monitoring performed at each centre, peripheral blood samples from

the eight visits were centrally monitored for CMV, EBV and BKV by TaqMan qPCR, as described previously.¹⁷ The centralized viral load assessment was non-interventional.

2.6. Definition of CMV prevention strategy groups and characterization of antiviral treatments

Patients were stratified into two prevention strategy groups based on the (val)ganciclovir treatments during the first 14 days. All patients that started a (val)ganciclovir treatment during the first 14 days were assigned into the prophylactic strategy group; the rest of the sub-cohort was classified in the pre-emptive strategy group. The 14 day threshold was chosen to allow comparability with our previous prospective study on the topic (VIPP), in which recruiting took place during the first two post-transplant weeks.^{20,21} CMV syndrome was treated equally for both strategy groups, as explained above. Antiviral treatments with no data on the end time point were disregarded for the calculation of the treatment duration but considered for the calculation of median dose. Accordingly, reported MMF dose and tacrolimus trough correspond to the 14 day threshold.

2.7. Viraemia-based patient classification

To assess the efficacy of prevention strategies regarding viral (re)activations, patients were classified based on their peak viral load values for CMV, EBV and BKV, as previously published.¹⁷ Briefly, the classifications are defined as follows: “detectable viral load” corresponds to patients with at least one viral load measurement over detection limit (250 copies·mL⁻¹)¹⁷, “elevated viral load” to patients with at least one viral load measurement over 2000 copies·mL⁻¹, “high viral load” to patients with at least one viral load measurement over 10000 copies·mL⁻¹. These groups can overlap with each other.

2.8. Analytical approach

The association between transplantation outcomes and prevention strategy was analyzed using the following approach: First, crude single-parameter associations between prevention strategy and the outcome were assessed; whenever possible, the associations were also

calculated stratified for the risk constellations of the outcome at hand. Second, to assess independence from confounders of potential associations, multi-parameter backwards elimination regression analysis was performed. Third, the difference of single-parameter strategy-outcome associations between sexes were assessed. Lastly, if there was a significant difference between the sexes and a significant association with the outcome was observed for only one sex, the association was tested in that sub-group employing multi-parameter backwards elimination regression analysis.

2.9. Statistical analysis

For descriptive statistics, categorical variables are summarised as numbers and frequencies; quantitative variables are reported as median and interquartile range (IQR). Differences between the groups were calculated using Pearson's chi-square test with continuity correction (or two-tailed Fisher's exact test, when stated); odds ratios (OR) and 95% confidence intervals (95% CI) are provided. In all cases, odds ratio over 1 denote a higher prevalence of the adverse event in the pre-emptive strategy group. Differences in quantitative variables between groups are analysed using the two-tailed Mann-Whitney test. Kaplan-Meier curves for time to occurrence of the first CMV (re)activation were calculated using the R survival package (version 2.43-3); strategy groups were compared using the log-rank test. Correlations are reported employing Spearman's rho and P value).

To control for the influence of confounders in the analysis of prevention strategies, multi-parameter regression was employed. Regression models incorporated as independent variables the prevention strategies and all potential confounding factors, and as dependent variable the outcome variable of interest. For categorical binary outcomes, logistic regression was employed, for continuous outcomes linear regression was used. For the peak viral load outcomes, the decimal logarithm was used. After logarithmisation, viral loads below detection level were set to zero. We considered as potential confounders all measured demographic factors (see Table 1 and Table S1) and centre effects. For the analysis of the eGFR one year after transplantation (eGFR-1y), CMV, BKV and EBV peak viral loads and acute rejection

were additionally included as potential confounders, as these events precede or are simultaneous to eGFR-1y and might hence have an influence on it. To exclude unimportant factors, backward elimination was performed, employing Akaike's information criterion. Factors in the final regression model were therefore considered to be independently associated with the dependent variable, regardless of the corresponding P value. Resulting linear regression models were tested for homoscedasticity of their residuals employing the studentized Breusch-Pagan test; multicollinearity was assessed for all models calculating the generalized variance-inflation factors. If homoscedasticity cannot be assumed ($P < 0.050$), robust standard errors are reported. For multicollinearity, a threshold of 5 for the generalized variance-inflation factors was employed to exclude a factor.

The analysis of the interactions of sex effects with the effect of strategy group on outcomes was assessed with a single-parameter ANOVA type 3 for continuous variables and a single-parameter analysis of deviance type 3 of a logistic model for categorical variables. In all cases, a P value below 0.050 was considered significant. P values were not corrected for multiple testing, as this study was of exploratory nature and we prioritized the minimization of type II errors.^{22–24} Analyses were performed using R (Version 3.3.2).

3. Results

3.1. Definition of study sub-cohorts

To assess the effects of CMV prevention strategy on transplantation outcome, we retrospectively analysed the cohort of an existent study (N=540 patients) with a female ratio of 35.9% (N=194).^{16,17} Patients were grouped into two sub-cohorts, based on whether they started an antiviral therapy during the first two post-transplant weeks (prophylactic strategy group, N=308) or not (pre-emptive strategy group, N=232) (see 2.6). As described previously, viral load (CMV, EBV and BKV), graft function and other clinical markers were collected along eight visits during the first post-transplant year; a total of 3715 blood samples were analysed.¹⁷

In this work, we have evaluated the effects of prevention strategy on eGFR, incidence of acute rejection, incidence of CMV complications, and incidence of BKV and EBV (re)activations following the analytical approach detailed in section 2.8. After an assessment of the baseline characteristics of the sub-cohorts, we describe in detail the most important findings in the next sections.

3.2. Study sub-cohorts characteristics

To assess differences between the two prevention strategy sub-cohorts regarding demographics or treatment procedures, we performed comparative statistics (see Table 1, for cause of end-stage kidney disease see Table S1). As shown in Table 1, significant ($P < 0.050$) differences were found for MMF daily dose, CMV mismatch-based risk and therapy arm; the difference was highly significant ($P < 0.001$) for the latter two factors.

Variable		Prophylactic strategy group (N=308)	Pre-emptive strategy group (N=232)	P value
Female sex		104 (33.8%)	90 (38.8%)	0.265
Caucasian race		304 (98.7%)	231 (99.6%)	0.397 ^a
Recipient age (years)		55 [46-64]	57 [44-64]	0.988
Body mass index ($\text{kg}\cdot\text{m}^{-2}$)		26.3 [23.5-29.7]	25.4 [22.8-28.4]	0.059
CMV mismatch-based risk	High (D'R)	119 (39.1%)	27 (12.1%)	<0.001
	Medium (R')	137 (45.1%)	129 (57.8%)	
	Low (D'R)	48 (15.8%)	67 (30.0%)	
EBV mismatch-based risk	High (D'R)	13 (5.1%)	11 (6.2%)	0.583 ^a
	Medium (R')	239 (93.4%)	161 (91.0%)	
	Low (D'R)	4 (1.6%)	5 (2.8%)	

Donor age (years)	55 [48-65]	55 [46-65]	0.931
No previous transplantations	298 (96.8%)	216 (94.7%)	0.346
Living donor	31 (10.1%)	35 (15.4%)	0.088
Donors with expanded criteria	136 (44.2%)	99 (42.7%)	0.798
Cold ischaemia time (min)	626 [427-844]	600 [414-840]	0.505
Number of HLA A, B and DR mismatches	3 [2-4]	3 [1-4]	0.457
No panel-reactive antibodies before transplantation	23 (7.6%)	17 (7.7%)	1.000
White blood cell count (cells·L ⁻¹)	7.2 [5.7-8.9]	7.1 [6.0-8.5]	0.676
Therapy arm	A (basiliximab+steroids)	93 (30.2%)	<0.001
	B (basiliximab)	92 (29.9%)	
	C (ATG)	123 (39.9%)	
Low MMF daily dose (< 2000 mg·day ⁻¹)	37 (12%)	45 (19.4%)	0.025
Tacrolimus trough level (ng·mL ⁻¹)	9.9 [7.4-12.5]	9.2 [7-12]	0.145

Table 1 – Differences in patient baseline characteristics between strategy groups. Data are given as

number (percentage) or median [interquartile range]. Donors with expanded criteria are defined as follows: age over 60 years or age over 50 years and at least two of the following factors: cerebrovascular accident as the cause of death, hypertension or a serum creatinine level over 1.5 mg·dL⁻¹. P value is calculated based on Pearson's chi-square test or Fisher's exact test for binary variables (marked with ^a) and based on Mann-Whitney test for continuous variables. Data on the cause of end-stage kidney disease are summarized in Table S1.

59 patients (25.4%) of the pre-emptive strategy group were treated with (val)ganciclovir after the second post-transplantation week. In total, 367 patients (68.0%) received (val)ganciclovir during the first post-transplant year, independently of their prevention strategy group; use of antivirals in both groups is shown in Table 2.

Variable	Prophylactic strategy group (N=308)	Pre-emptive strategy group treated with (val)ganciclovir

		(N=59)
Median time under (val)ganciclovir (days)	118 [87-182]	92 [46-155]
Valganciclovir average daily dose (mg·day ⁻¹)	277 [165-450]	450 [205-454]
Ganciclovir usage	34 (11.0%)	8 (13.6%)
Intravenous ganciclovir usage	31 (10.1%)	7 (11.9%)

Table 2 – Antiviral treatment details for the two strategy groups. Data are given as number (percentage) or median [interquartile range].

3.3. Prophylactic strategy group was associated with a serious impairment of graft function in female patients

Patients in the prophylactic strategy group had, in general, a poorer transplantation course than those in the pre-emptive strategy group, as confirmed by their significantly higher incidence of total serious adverse events (64.6% vs. 54.3%, $P=0.020$, OR: 0.65 [0.45-0.94]). For the main outcome, renal function, single-parameter analysis likewise revealed a significant difference between the prevention groups. Thus, eGFR-1y was lower in the prophylactic strategy group compared to the pre-emptive group (45.6 [33.5-58.3] vs. 50.3 [38.1-64.5] mL·min⁻¹·1.73m⁻², $P=0.011$). Of note, a significant difference in eGFR was detected for all visits from the third post-transplant month on (Figure S4).

Multi-parameter analysis could not confirm an independent association of prophylactic strategy with decreased eGFR-1y (Table S2 A). However, we observed that this association is subject to a strong interaction with sex ($P=0.003$, see Table 3): The significant impairment of eGFR-1y in the prophylactic group was only observed for female patients, with a difference of 18.5 mL·min⁻¹·1.73m⁻² (38.4 [28.8-53.6] vs. 56.8 [41.3-67.9] mL·min⁻¹·1.73m⁻², $P<0.001$). Among male patients, the prophylactic strategy group had a slightly higher median eGFR-1y (48.5 [36.3-61.5] vs. 47.2 [37.2-59.6] mL·min⁻¹·1.73m⁻², $P=1.000$). This significant

difference in eGFR for females can be observed already one month after transplantation (Figure 1). Importantly, the multi-parameter analysis confirmed that prevention strategy was independently associated with eGFR-1y in female patients (Table S2 B).

Outcomes		Effect size of prevention strategies in male patients (N=346)	Effect size of prevention strategies in female patients (N=194)	P value
Serious adverse event		0.76 [0.48-1.19]	0.49 [0.26-0.91]	0.237
eGFR-1y		-1.3 [-4.8-4.7]	18.5 [8.2-20.7]	0.003
Acute rejection		0.35 [0.13-0.81]	0.39 [0.12-1.12]	0.847
CMV	Detectable viral load	1.48 [0.80-2.73]	1.28 [0.57-2.85]	0.756
	Elevated viral load	1.77 [0.71-4.5]	1.01 [0.30-3.35]	0.416
	High viral load	1.24 [0.34-4.42]	0.77 [0.06-6.85]	0.654
	Syndrome	0.57 [0.31-0.99]	0.47 [0.19-1.07]	0.683
BKV	Detectable viral load	0.75 [0.48-1.18]	0.82 [0.45-1.51]	0.807
	Elevated viral load	0.64 [0.36-1.13]	0.71 [0.34-1.48]	0.809
	High viral load	0.49 [0.21-1.05]	0.71 [0.22-2.13]	0.545
EBV	Detectable viral load	0.68 [0.38-1.19]	2.26 [1.00-5.25]	0.009
	Elevated viral load	1.27 [0.54-2.97]	4.27 [0.79-43.19]	0.154
	High viral load	1.15 [0.22-5.46]	1.16 [0.01-91.65]	0.998

Table 3 – Differences in effect size of prevention strategy between sexes with respect to outcomes. The P value refers to the P value of the interaction term, as assessed by a single-parameter ANOVA type 3 for continuous variables or a single-parameter analysis of deviance type 3 of a logistic model for categorical variables. The effect sizes are given with 95% confidence intervals as OR (categorical variables) or as difference of medians (continuous variables). An OR over 1 indicates a higher incidence of the outcome in the prophylactic strategy group, compared to the pre-emptive; a positive difference of medians indicates a lower value of the median outcome in the prophylactic strategy group compared to the pre-emptive. For the definition of (re)activation severity degrees see Methods (2.7).

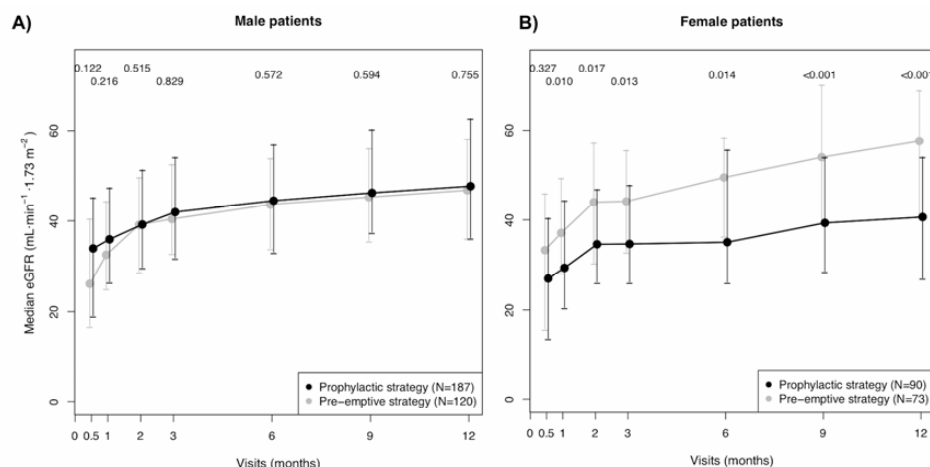


Figure 1. Graft function dynamics of the prevention strategy groups stratified for sex. To exclude the role of donor type in eGFR dynamics, only patients with a deceased donor are shown (for the eGFR dynamics of patients with living donors, see Figure S5). Median eGFR ($\text{mL} \cdot \text{min}^{-1} \cdot 1.73 \text{ m}^{-2}$) of the prevention strategy groups is plotted for each protocol visit. The bars indicate the interquartile range. The numbers indicate the p value of the difference in eGFR between the prevention strategy groups, as calculated using the Mann-Whitney test. Day 0 is not shown, as it is pre-transplantation.

We further investigated the nature of the difference in eGFR between prevention strategies in female patients, examining the associations of dose and beginning of therapy with eGFR-1y. We did not observe any negative effect of high doses: We compared the female patients in the pre-emptive strategy group that received a valganciclovir treatment, with those in the prophylactic strategy group, as the first group had a significantly higher daily dose than the second ($P=0.041$). Thus, we observed that these patients had a significantly higher eGFR-1y than those in the prophylactic group ($38.4 [28.8-53.6]$ vs. $57.7 [40.1-66.6]$ $\text{mL} \cdot \text{min}^{-1} \cdot 1.73 \text{ m}^{-2}$, $P=0.005$), in spite of the higher valganciclovir dose. On the other hand, we observed a significant effect of therapy timing in eGFR-1y, with a positive correlation between day of treatment beginning and eGFR-1y ($\rho=0.27$, $P=0.015$) among female patients who received (val)ganciclovir.

Based on the encountered strong interaction of sex and prevention strategy for renal function, we decided to evaluate systematically the sex effects for all transplantation outcomes. While no differences between sexes with respect to transplantation outcomes

were observed (Table 4), further interactions of sex with prevention strategy were observed with respect to (Table 3), as described in detail below.

Outcomes		Male patients (N=346)	Female patients (N=194)	P value
Serious adverse event		204 (59.0%)	121 (62.4%)	0.493
eGFR-1y		48.2 [36-5-61.4]	46.8 [33.3-58.8]	0.341
Acute rejection		38 (11.0%)	22 (11.3%)	1.000
CMV	Detectable viral load	57 (16.5%)	35 (18.0%)	0.730
	Elevated viral load	24 (6.9%)	15 (7.7%)	0.866
	High viral load	13 (3.8%)	5 (2.6%)	0.629
	Syndrome	78 (22.5%)	35 (18.0%)	0.261
BKV	Detectable viral load	173 (50.0%)	87 (44.8%)	0.289
	Elevated viral load	76 (22.0%)	45 (23.2%)	0.825
	High viral load	41 (11.8%)	18 (9.3%)	0.438
EBV	Detectable viral load	74 (21.4%)	35 (18.0%)	0.414
	Elevated viral load	28 (8.1%)	9 (4.6%)	0.178
	High viral load	9 (2.6%)	2 (1.0%)	0.343 ^a

Table 4 – Differences in outcomes between sexes. Data are given as number (percentage) or median [interquartile range]. P value is calculated based on Pearson's chi-square test or Fisher's exact test for binary variables (marked with ^a) and on Mann-Whitney test for continuous variables. For the definition of (re)activation severity degrees see Methods (2.7). As it can be observed, there were no significant differences between sexes with respect to the measured outcomes.

3.4. Prophylactic strategy was associated with higher incidence of acute rejection independently of sex

Regarding the important complication acute rejection, a significantly higher incidence was found in the prophylactic strategy group (14.9% vs. 6.0%, P=0.002, OR: 0.37 [0.18-0.70]).

The observed association between prevention strategy and incidence of acute rejection was confirmed to be independent from potential confounders by multi-parameter analysis (Table

S2 C). As shown in Table 3, there were no significant differences between sexes for this association.

3.5. The prophylactic strategy was associated with lower incidence of CMV (re)activation and syndrome than the pre-emptive strategy

We further tested the effectivity of the strategies in the prevention of CMV complications. The single-parameter analysis showed a higher incidence of CMV viral load in the pre-emptive strategy group (19.8% vs. 14.9%, $P=0.167$); for CMV syndrome a significantly higher incidence was found in the prophylactic strategy group (see Table S3 A). The latter was not unexpected, as most patients with high CMV risk were in the prophylactic strategy group. Stratifying for CMV risk, a clear trend for lower incidence of CMV (re)activation was observed in the prophylactic strategy group; but not for CMV syndrome (Table S3 B). However, the results of the multi-parameter regression show that prophylactic strategy was independently associated with both lower peak CMV viral load and CMV syndrome incidence (Table S2 D-E). No significant sex association were observed for these outcomes (Table 3 and Table S3 D-E).

Interestingly, CMV incidence showed significantly different temporal patterns in the two strategy groups (Figure 2): While in the pre-emptive strategy group 86.7% of all CMV load events occurred in the first 100 days post-transplant, in the prophylactic strategy group it was only 56.1% (Figure 2A). Moreover, a higher prevalence of detectable CMV viral load was observed in the prophylactic strategy group for all study visits after the third month (Figure

2B).

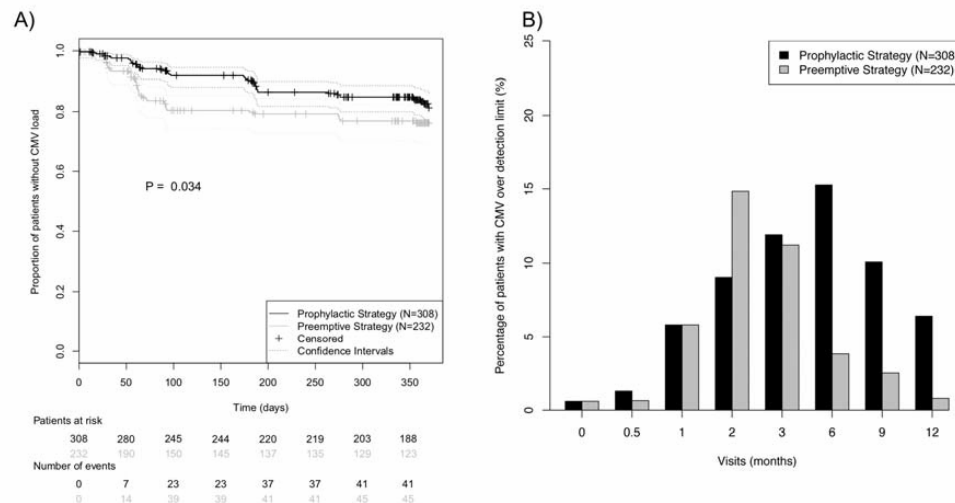


Figure 2. Incidence of CMV (re)activation in the prevention strategy groups during the first post-transplant year. (A) Kaplan-Meier curves for absence of CMV (re)activation during the first post-transplant year. CMV (re)activation was defined as viral load over detection limit. Prevention strategy groups were compared using the log-rank test. (B) Prevalence of CMV viral load over detection limit for each of the eight protocol visits.

3.6. The prophylactic strategy was associated with lower incidence of EBV (re)activation among women and higher incidence of BKV (re)activation

Regarding the effects of prevention strategy for other viruses, no effect of prevention strategy was found for EBV when considering both sexes, neither through (stratified) single-parameter analysis (Table S3 A and S3 C), nor through multi-parameter analysis (Table S2F). However, there was a significant interaction of sex and prevention strategy for EBV (re)activation ($P=0.009$, Table 3). Thus, there was an association of prophylactic strategy with reduced incidence of EBV (re)activation only for female patients ($P=0.049$, OR: 2.26 [1.00-5.25], see Table S3 D). An analysis stratified for viral risk constellations (Table S3 F) showed an even stronger association for female patients treated with ATG ($P=0.005$, OR: 5.65 [1.56-22.86]). Similarly, the multi-parameter analysis showed that prophylactic strategy was independently associated with decreased peak EBV load in female patients (Table S2 G).

On the other hand, we found a higher incidence of severe BKV (re)activation in patients of the prophylactic strategy group ($P=0.056$, OR: 0.55 [0.29-1.01]), see Table S3 A. The multi-parameter analysis confirmed that prophylactic strategy was independently associated with increased peak BKV load (Table S2 H). No significant sex-associated effect was observed for BKV (re)activation (Table 3 and Table S3 D-E), even though male sex was independently associated with increased peak BKV load in the multi-parameter analysis (Table S2 H).

4. Discussion

The goal of our study was to evaluate the clinical efficacy and sex-associated differences of two common CMV prevention strategies in a large cohort of kidney transplant patients from the multi-centre Harmony study.

The main finding of the study is the first evidence of superiority of the pre-emptive strategy with respect to acute rejection incidence and – for female patients – graft function.^{20,21,25–31}

While we have already reported a negative effect of prophylaxis on rejection within the VIPP study – albeit only for the D^R⁺ subgroup – this study is the first to report a significant association in the entire cohort.^{20,21} The observed association of prevention strategy with eGFR in female patients is especially relevant, as eGFR-1y is an accepted marker for long term transplantation outcomes.³²

Our results highlight the importance of sex-associated effects in transplantation. In recent years, sex differences have emerged as an essential factor in clinical studies.³³ In transplantation, several complications are associated with sex, including acute rejection, graft loss and viral (re)activations.^{11,13,34,35} However, the underlying reasons for these sex differences are not well understood; possible causes include the hormonal regulation of the immune system, the effects of pregnancy, and differences in the metabolism of drugs routinely employed in transplantation.¹¹ For example, there is tentative evidence of sex-related differences in the pharmacokinetics of (val)ganciclovir.^{11,12} Thus, ganciclovir clearance has been observed to be 24% faster in female transplantation patients, suggesting higher activity of the organic anion transporter 1.^{11,12} Furthermore, it has been shown

repeatedly that women and men have different anti-CMV immunological profiles, with an impact in the graft function and even the phenotype of the immune system as a whole.^{13–15} Notably, in a recent publication, Lindemann *et al.* have observed an association of high number of IL-21 secreting anti-CMV T cells with female sex and lower eGFR in a clinical transplantation context.¹³

Our analyses may provide some evidence on the nature of the observed association of eGFR-1y with prevention strategies in female patients. Although the impaired graft function in the female prophylactic strategy group can be partly explained through the higher incidence of BKV severe (re)activation and rejection, the results of the multi-parameter analysis showed an independent association of prevention strategy with graft function, regardless these adverse events.^{17,36,37} Therefore, our results do not support the hypothesis that these adverse events are the main cause for the difference in eGFR-1y between sub-cohorts. Regarding possible nephrotoxic effects of the antiviral drug, we did not find any association of higher valganciclovir doses with lower eGFR – rather, the opposite association was observed – in contrast to Heldenbrand *et al.*³⁸ The absence of a negative dose-dependent effect suggests that the observed difference was not a consequence of nephrotoxicity of valganciclovir. On the other hand, the time of beginning with the (val)ganciclovir therapy was determinant for the eGFR-1y: the later patients began the therapy, the higher the renal function.

Albeit being highly speculative, we hypothesize that the observed results may be (at least in part) caused by an immunological mechanism. As we previously demonstrated, an increased number of CMV-specific T-cells upon CMV (re)activation is associated with reduced alloreactivity and improved graft function in renal transplantation patients.³⁹ Similarly, in liver transplantation, primary CMV infection has been found to be associated with donor-specific CD8⁺ T-cell hyporesponsiveness and increased V δ 1/V δ 2 γ δ T-cell ratio – a surrogate marker for operational tolerance.⁴⁰ Accordingly, the higher rate of asymptomatic CMV (re)activation found in the pre-emptive strategy group could potentially lead to regulatory γ δ T-cell-based graft protection and explain the better graft function and lower incidence of

acute rejection; an early administration of (val)ganciclovir would therefore hinder the development of this protective immune response. Our hypothesis is compatible with the observed differences between male and female recipients, as sex-associated differences in the anti-CMV immunity have been shown by Lindemann *et al.* to correlate with graft function.¹³ Even though this effect cannot explain our observations, it demonstrates how sex and anti-CMV immunity can potentially interact and affect eGFR.¹³ Therefore, further research, including systems medicine approaches, is needed to better understand the effects of CMV prevention strategies from an immune, virological and pharmacokinetic point of view – with emphasis on sex-associated differences – and their effects on transplantation outcome.^{41,42}

Of interest, the prophylactic strategy group showed a higher incidence of late-onset CMV (from month six on); such increases of viral (re)activation incidence after the end of prophylaxis have been observed before.^{27,28} Regarding BKV, the observed association of prophylaxis with increased incidence of severe (re)activation is in line with two recent studies.^{43,44} On the other hand, an association of EBV with prevention strategy was observed only for female patients.⁴⁵ This is relevant, as there is currently no consensus in the literature on this topic. While a number of publications have observed an effect against EBV or post-transplant lymphoproliferative disease (the main EBV-associated complication), a meta-study with 2366 participants saw no effect of prophylaxis for this disease.^{46–50}

This study is based on the prospective Harmony study, a trial designed with the goal of identifying which immunosuppressive drug combination is superior with respect to acute rejections and secondary to a number of other outcome variables, including graft function and viral (re)activations.¹⁶ A potential shortcoming of the present study consists therefore in the fact that prevention strategy groups were not randomized, and no power calculation was performed with respect to this question. Therefore, even though we have controlled for all measured demographic factors in the analyses, we cannot completely exclude bias in unmeasured factors as the cause of the observed differences. A further limitation is related to the criteria employed for choosing prevention strategy for each patient: As the decision to

adopt a prophylactic or a pre-emptive strategy was taken by each individual physician or centre, it is difficult to ascertain the causes for the individual decisions, potentially introducing bias in the use of prevention strategies. On the other hand, our study does have some advantages: We have analysed a larger (N=540) and more heterogeneous cohort (patients with all CMV mismatch-based risk constellations) than most studies on the matter, thereby achieving higher statistical power.^{20,21,25–29} Moreover, our study design is closer to clinical reality, with similar valganciclovir doses and prophylaxis duration to those routinely employed in the clinic.⁵¹ Based on the limitations and advantages of the study, we deem our results as evidence that further research is needed to determine the effects of prevention strategies on transplantation outcome, especially the hypothetical interactions with sex.

In summary, our study provides the first evidence in the literature suggesting that the pre-emptive approach might be associated with improved graft function – especially in female patients. Even though the prophylactic strategy was associated with reduced prevalence of CMV (re)activation and syndrome, it was associated with higher incidence of acute rejection and, for female patients, with a strong impairment of the renal function. The effects of prevention strategy on graft function and acute rejection were shown in the multi-parameter analysis as independent from potential bias in the cohort. Further randomized controlled studies are needed to confirm these observations.

References

1. Elfadawy, N. *et al.* CMV Viremia is associated with a decreased incidence of BKV reactivation after kidney and kidney-pancreas transplantation. *Transplantation* **96**, 1097–1103 (2013).
2. Fehr, T., Cippà, P. E. & Mueller, N. J. Cytomegalovirus post kidney transplantation: Prophylaxis versus pre-emptive therapy? *Transpl. Int.* **28**, 1351–1356 (2015).
3. Le Page, A. K., Mackie, F. E., McTaggart, S. J. & Kennedy, S. E. Cytomegalovirus & Epstein Barr Virus serostatus as a predictor of the long-term outcome of kidney transplantation. *Nephrology (Carlton)*. **18**, 813–9 (2013).
4. Egli, A. *et al.* Cytomegalovirus and polyomavirus BK posttransplant. *Nephrol. Dial. Transplant.* **22**, viii72–viii82 (2007).
5. Malvezzi, P., Jouve, T. & Rostaing, L. Induction by anti-thymocyte globulins in kidney transplantation: a review of the literature and current usage. *J. Nephropathol.* **4**, 110–115 (2015).
6. Kotton, C. N. *et al.* *The Third International Consensus Guidelines on the Management of Cytomegalovirus in Solid-organ Transplantation.* *Transplantation* **102**, (2018).
7. Special Issue: KDIGO Clinical Practice Guideline for the Care of Kidney Transplant Recipients. *Am. J. Transplant.* **9**, S1–S157 (2009).
8. Egli, A. *et al.* Cytomegalovirus-specific T-cell responses and viral replication in kidney transplant recipients. *J. Transl. Med.* **6**, 29 (2008).
9. Bunde, T. *et al.* Protection from cytomegalovirus after transplantation is correlated with immediate early 1–specific CD8 T cells. *J. Exp. Med.* **201**, 1031–1036 (2005).
10. Sester, M. *et al.* Levels of virus-specific CD4 T cells correlate with cytomegalovirus control and predict virus-induced disease after renal transplantation. *Transplantation* **71**, 1287–1294 (2001).

11. Momper, J. D., Misel, M. L. & McKay, D. B. Sex differences in transplantation. *Transplant. Rev.* **31**, 145–150 (2017).
12. Perrottet, N. *et al.* Population pharmacokinetics of ganciclovir in solid-organ transplant recipients receiving oral valganciclovir. *Antimicrob. Agents Chemother.* **53**, 3017–3023 (2009).
13. Lindemann, M. *et al.* The Cytomegalovirus-Specific IL-21 ELISpot Correlates with Allograft Function of Kidney Transplant Recipients. *Int. J. Mol. Sci.* **19**, 3945 (2018).
14. Villacres, M. C., Longmate, J., Auge, C. & Diamond, D. J. Predominant type 1 CMV-specific memory T-helper response in humans: Evidence for gender differences in cytokine secretion. *Hum. Immunol.* **65**, 476–485 (2004).
15. Di Benedetto, S. *et al.* Impact of age, sex and CMV-infection on peripheral T cell phenotypes: results from the Berlin BASE-II Study. *Biogerontology* **16**, 631–643 (2015).
16. Thomusch, O. *et al.* Rabbit-ATG or basiliximab induction for rapid steroid withdrawal after renal transplantation (Harmony): an open-label, multicentre, randomised controlled trial. *Lancet* **388**, 3006–3016 (2016).
17. Blazquez-Navarro, A. *et al.* BKV, CMV, and EBV Interactions and their Effect on Graft Function One Year Post-Renal Transplantation: Results from a Large Multi-Centre Study. *EBioMedicine* **34**, 113–121 (2018).
18. Levey, A. S. *et al.* A new equation to estimate glomerular filtration rate. *Ann. Intern. Med.* **150**, 604–612 (2009).
19. Solez, K. *et al.* Banff '05 meeting report: Differential diagnosis of chronic allograft injury and elimination of chronic allograft nephropathy ('CAN'). *Am. J. Transplant.* **7**, 518–526 (2007).
20. Witzke, O. *et al.* Valganciclovir prophylaxis versus preemptive therapy in cytomegalovirus-positive renal allograft recipients: Long-term results after 7 years of a

- randomized clinical trial. *Transplantation* **102**, 876–882 (2018).
21. Witzke, O. *et al.* Valganciclovir Prophylaxis Versus Preemptive Therapy in Cytomegalovirus-Positive Renal Allograft Recipients: 1-Year Results of a Randomized Clinical Trial. *Transplantation* **93**, 61–68 (2012).
22. *Developing a Protocol for Observational Comparative Effectiveness Research A User's Guide*. (Agency for Healthcare Research and Quality, 2013).
23. Bender, R. & Lange, S. Adjusting for multiple testing - when and how? *J. Clin. Epidemiol.* **54**, 343–349 (2001).
24. Li, G. *et al.* An introduction to multiplicity issues in clinical trials: the what, why, when and how. *Int. J. Epidemiol.* 746–755 (2017). doi:10.1093/ije/dyw320
25. Kliem, V. *et al.* Improvement in long-term renal graft survival due to CMV prophylaxis with oral ganciclovir: Results of a randomized clinical trial. *Am. J. Transplant.* **8**, 975–983 (2008).
26. Spinner, M. L. *et al.* Impact of Prophylactic Versus Preemptive Valganciclovir on Long-term Renal Allograft Outcomes. *Transplantation* **90**, 412–418 (2010).
27. Florescu, D. F., Qiu, F., Schmidt, C. M. & Kalil, A. C. A direct and indirect comparison meta-analysis on the efficacy of cytomegalovirus preventive strategies in solid organ transplant. *Clin. Infect. Dis.* **58**, 785–803 (2014).
28. Khoury, J. A. *et al.* Prophylactic versus preemptive oral valganciclovir for the management of cytomegalovirus infection in adult renal transplant recipients. *Am. J. Transplant.* **6**, 2134–2143 (2006).
29. Van Der Beek, M. T. *et al.* Preemptive versus sequential prophylactic-preemptive treatment regimens for cytomegalovirus in renal transplantation: Comparison of treatment failure and antiviral resistance. *Transplantation* **89**, 320–326 (2010).
30. Small, L. N., Lau, J. & Snyderman, D. R. Preventing Post–Organ Transplantation Cytomegalovirus Disease with Ganciclovir: A Meta-Analysis Comparing Prophylactic

and Preemptive Therapies. *Clin. Infect. Dis.* **43**, 869–80 (2005).

31. Meije, Y. *et al.* Prevention strategies for cytomegalovirus disease and long-term outcomes in the high-risk transplant patient (D+/R-): Experience from the RESITRA-REIPI cohort. *Transpl. Infect. Dis.* **16**, 387–396 (2014).
32. Kasiske, B. L., Israni, A. K., Snyder, J. J. & Skeans, M. A. The relationship between kidney function and long-term graft survival after kidney transplant. *Am. J. Kidney Dis.* **57**, 466–475 (2011).
33. Rásky, ě. *et al.* Sex and gender matters: A sex-specific analysis of original articles published in the Wiener klinische Wochenschrift between 2013 and 2015. *Wien. Klin. Wochenschr.* **129**, 781–785 (2017).
34. Meier-Kriesche, H. U. *et al.* Gender differences in the risk for chronic renal allograft failure. *Transplantation* **71**, 429–432 (2001).
35. Hirsch, H. H. *et al.* Polyomavirus BK replication in de novo kidney transplant patients receiving tacrolimus or cyclosporine: A prospective, randomized, multicenter study. *Am. J. Transplant.* **13**, 136–145 (2013).
36. Salvadori, M. *et al.* Estimated one-year glomerular filtration rate is the best predictor of long-term graft function following renal transplant. *Transplantation* **81**, 202–206 (2006).
37. Schwarz, A. *et al.* Factors influencing viral clearing and renal function during polyomavirus BK-associated nephropathy after renal transplantation. *Transplantation* **94**, 396–402 (2012).
38. Heldenbrand, S. *et al.* Multicenter evaluation of efficacy and safety of low-dose versus high-dose valganciclovir for prevention of cytomegalovirus disease in donor and recipient positive (D+/R+) renal transplant recipients. *Transpl. Infect. Dis.* **18**, 904–912 (2016).
39. Nickel, P. *et al.* High levels of CMV-IE-1-specific memory T cells are associated with

- less alloimmunity and improved renal allograft function. *Transpl. Immunol.* **20**, 238–242 (2009).
40. Shi, X. L. *et al.* CMV Primary Infection Is Associated with Donor-Specific T Cell Hyporesponsiveness and Fewer Late Acute Rejections after Liver Transplantation. *Am. J. Transplant.* **15**, 2431–2442 (2015).
 41. Blazquez-Navarro, A. *et al.* Differential T cell response against BK virus regulatory and structural antigens: A viral dynamics modelling approach. *PLOS Comput. Biol.* **14**, e1005998 (2018).
 42. Maier, M., Takano, T. & Sapir-Pichhadze, R. Changing paradigms in the management of rejection in kidney transplantation: Evolving from protocol-based care to the era of P4 medicine. *Can. J. Kidney Heal. Dis.* **4**, 1–12 (2017).
 43. Reischig, T. *et al.* Less renal allograft fibrosis with valganciclovir prophylaxis for cytomegalovirus compared to high-dose valacyclovir: A parallel group, open-label, randomized controlled trial 11 Medical and Health Sciences 1103 Clinical Sciences. *BMC Infect. Dis.* **18**, 1–9 (2018).
 44. Reischig, T. *et al.* Randomized trial of valganciclovir versus valacyclovir prophylaxis for prevention of cytomegalovirus in renal transplantation. *Clin. J. Am. Soc. Nephrol.* **10**, 294–304 (2015).
 45. Végso, G., Hajdu, M. & Sebestyén, A. Lymphoproliferative disorders after solid organ transplantation-classification, incidence, risk factors, early detection and treatment options. *Pathol. Oncol. Res.* **17**, 443–454 (2011).
 46. Cameron, B. M., Kennedy, S. E., Rawlinson, W. D. & Mackie, F. E. The efficacy of valganciclovir for prevention of infections with cytomegalovirus and Epstein-Barr virus after kidney transplant in children. *Pediatr. Transplant.* **21**, 1–11 (2017).
 47. Höcker, B. *et al.* (Val-)ganciclovir prophylaxis reduces Epstein-Barr virus primary infection in pediatric renal transplantation. *Transpl. Int.* **25**, 723–731 (2012).

48. Verghese, P. S., Schmeling, D. O., Knight, J. A., Matas, A. J. & Balfour, H. H.
Valganciclovir administration to kidney donors to reduce the burden of
cytomegalovirus and epstein-barr virus transmission during transplantation.
Transplantation **99**, 1186–1191 (2015).
49. Funch, D. P., Walker, A. M., Schneider, G., Ziyadeh, N. J. & Pescovitz, M. D.
Ganciclovir and acyclovir reduce the risk of post-transplant lymphoproliferative
disorder in renal transplant recipients. *Am. J. Transplant.* **5**, 2894–2900 (2005).
50. Aldabbagh, M. A. *et al.* The Role of Antiviral Prophylaxis for the Prevention of Epstein-
Barr Virus-Associated Posttransplant Lymphoproliferative Disease in Solid Organ
Transplant Recipients: A Systematic Review. *Am. J. Transplant.* 770–781 (2016).
doi:10.1111/ajt.14020
51. Rissling, O. *et al.* High frequency of valganciclovir underdosing for cytomegalovirus
prophylaxis after renal transplantation. *Clin. Kidney J.* **11**, 564–573 (2018).

Description of Supporting Information

Table S1. Differences in cause of end-stage kidney disease between strategy groups.

Table S2. Detailed results of the multi-parameter analyses.

Table S3. Results of the single-parameter analyses for virus-related complications. The detailed results of single-parameter associations of prevention strategy, including stratified analysis for risk constellation and sex, are reported. Following complications were analysed: CMV (re)activation and syndrome, EBV (re)activation and BKV (re)activation

Figure S4. Graft function dynamics of the prevention strategy groups. Median eGFR ($\text{mL} \cdot \text{min}^{-1} \cdot 1.73 \text{ m}^{-2}$) of the prevention strategy groups is plotted for each protocol visit. The bars indicate the interquartile range. The numbers indicate the P value of the difference in eGFR between the prevention strategy groups, as calculated using the Mann-Whitney test. Day 0 is not shown, as it is pre-transplantation.

Figure S5. Graft function dynamics of the prevention strategy groups stratified according to sex, for patients with living donor. Median eGFR ($\text{mL} \cdot \text{min}^{-1} \cdot 1.73 \text{ m}^{-2}$) of the prevention strategy groups is plotted for each protocol visit. The bars indicate the interquartile range. The numbers indicate the p value of the difference in eGFR between the prevention strategy groups, as calculated using the Mann-Whitney test. Day 0 is not shown, as it is pre-transplantation. For the eGFR dynamics of patients with deceased donors, see Figure 1.

8.2 Supplementary materials

8.2.1 Table S1

Differences in cause of end-stage kidney disease between strategy groups.

Cause of end-stage kidney disease	Prophylactic strategy group (N=308)	Pre-emptive strategy group (N=232)	P Value
Hypertension or large vessel disease	111 (36.0%)	87 (37.8%)	0.738
Glomerulonephritis	79 (25.6%)	69 (30.0%)	0.308
Polycystic kidney disease (adult type, dominant)	64 (20.8%)	38 (16.5%)	0.256
Diabetes	32 (10.4%)	23 (10.0%)	0.997
Interstitial nephritis or pyelonephritis	20 (6.5%)	19 (8.3%)	0.539
Secondary glomerulonephritis or vasculitis	7 (2.3%)	4 (1.7%)	0.765 ^a
Other hereditary or congenital diseases	11 (3.6%)	8 (3.5%)	1.000
Neoplasms or tumours	4 (1.3%)	0 (0.0%)	0.139 ^a
Other	109 (35.4%)	72 (31.3%)	0.368
Undefined cause	27 (9.3%)	24 (11.0%)	0.621

Data are given in number (percentage). P value is calculated based on Pearson's chi-square test or Fisher's exact test (marked with a). Causes of end-stage kidney disease are not mutually exclusive.

8.2.2 Table S2

Detailed results of the multi-parameter analyses

8.2.2.1 Table S2A

Results of the multivariate analysis for eGFR-1

Explanatory variables	Estimate	Standard error	P value
(Intercept)	110.2396	7.6568	<0.001
Recipient age (years)	-0.2233	0.0964	0.021
Donor age (years)	-0.4487	0.0718	<0.001
Body mass index (kg·m ⁻²)	-0.9153	0.2174	<0.001
Cause of end-stage renal disease: Diabetes	6.8268	3.8602	0.078
White blood cell count (cells·L ⁻¹)	-0.0062	0.0023	0.007
Tacrolimus trough level (ng·mL ⁻¹)	0.5159	0.2412	0.033
Acute rejection	-6.9392	3.3713	0.041
Peak BKV viral load	-0.8511	0.5140	0.099
Centre effects	-	-	0.003

eGFR-1y was estimated by backwards elimination linear regression, employing all demographic factors (Table 1 and Table S1), CMV, BKV and EBV peak viral loads, acute rejection, and centre effects as independent variables. As it can be observed, prevention strategy was not an explanatory variable for eGFR-1y. Peak viral loads are employed in logarithmic scale (with a value of 0 for viral load below

detection limit). The multivariate analysis employs Akaike's selection criterion for feature selection, so that some explanatory variables can have p values over 0.050. The P value for centre effects refers to the minimum P value of any transplantation centre.

Antithymocyte globulin (ATG), BK virus (BKV), Cytomegalovirus (CMV), Epstein-Barr virus (EBV), Estimated glomerular filtration rate one year after transplantation (eGFR-1y)

8.2.2.2 Table S2B

Results of the multivariate analysis for eGFR-1y in female patients.

Explanatory variables	Estimate	Standard error	P value
(Intercept)	79.9233	13.3498	<0.001
Prophylactic strategy	-13.1533	3.1425	<0.001
Number of HLA A, B and DR mismatches	-3.6832	1.0715	0.001
Donor age (years)	-0.4428	0.1057	<0.001
Body mass index (kg·m ⁻²)	-0.4533	0.2391	0.063
Cause of end-stage renal disease: Glomerulonephritis	12.1778	3.7273	0.002
Cause of end-stage renal disease: Polycystic kidney disease (adult type, dominant)	6.1548	3.6943	0.101
Cause of end-stage renal disease: Other hereditary or congenital diseases	11.1914	6.1685	0.075
Cause of end-stage renal disease: Other	15.6094	3.2340	<0.001
Cause of end-stage renal disease: Undefined cause	-10.1062	5.7397	0.084
No previous transplantations	15.9178	8.6471	0.071
Living donor	12.1540	4.1758	0.005
Donors with expanded criteria	13.0148	4.2287	0.003
No panel-reactive antibodies before transplantation	-11.6819	3.8825	0.004
Low MMF daily dose (< 2000 mg·day ⁻¹)	-0.0060	0.0036	0.107
Centre effects	-	-	0.034

eGFR-1y was estimated by backwards elimination linear regression, employing all demographic factors (Table 1 and Table S1), CMV, BKV and EBV peak viral loads, acute rejection, and centre effects as independent variables. As it can be observed, prevention strategy was an explanatory variable for eGFR-1y in female patients. Peak viral loads are employed in logarithmic scale (with a value of 0 for viral load below detection limit). The multivariate analysis employs Akaike's selection criterion for feature selection, so that some explanatory variables can have p values over 0.050. The P value for centre effects refers to the minimum P value of any transplantation centre.

BK virus (BKV), Cytomegalovirus (CMV), Epstein-Barr virus (EBV), Estimated glomerular filtration rate one year after transplantation (eGFR-1y)

8.2.2.3 Table S2C

Results of the multivariate analysis for acute rejection

Explanatory variables	Estimate	Standard error	P value
(Intercept)	-4.4311	0.6013	<0.001
Prophylactic strategy	0.6058	0.3746	0.106
Number of HLA A, B and DR mismatches	0.4217	0.1126	<0.001
Cause of end-stage renal disease: Polycystic kidney disease (adult type, dominant)	1.1537	0.4486	0.010

Cause of end-stage renal disease: Interstitial nephritis or pyelonephritis	1.1407	0.5709	0.046
Cause of end-stage renal disease: Other	1.0108	0.4028	0.012

Acute rejection was estimated by backwards elimination logistic regression, employing all demographic factors (Table 1 and Table S1) and centre effects as independent variables. As it can be observed, prevention strategy was an explanatory variable for acute rejection. The multivariate analysis employs Akaike's selection criterion for feature selection, so that some explanatory variables can have p values over 0.050. Centre effects were not an explanatory variable.

8.2.2.4 Table S2D

Results of the multivariate analysis for CMV peak viral load

Explanatory variables	Estimate	Standard error	P value
(Intercept)	1.3397	0.2663	<0.001
Prophylactic strategy	-0.7617	0.1866	<0.001
Cause of end-stage renal disease: Other hereditary or congenital diseases	1.3151	0.6411	0.041
CMV mismatch-based risk: Medium (R ⁺)	-0.3411	0.2170	0.117
CMV mismatch-based risk: Low (D ⁻ R ⁻)	-1.2122	0.2216	<0.001
White blood cell count at transplantation (cells/L)	0.0003	0.0104	0.973
Therapy arm: arm B (basiliximab)	0.1139	0.1867	0.542
Therapy arm: arm C (ATG)	0.4730	0.2002	0.019

Peak viral load in logarithmic scale (with a value of 0 for viral load below detection limit) was estimated by backwards elimination linear regression, employing all demographic factors (Table 1 and Table S1) and centre effects as independent variables. As it can be observed, prevention strategy was an explanatory variable for CMV peak viral load. The multivariate analysis employs Akaike's selection criterion for feature selection, so that some explanatory variables can have p values over 0.050. Centre effects were not an explanatory variable.

Cytomegalovirus (CMV), Seronegative donor and seronegative recipient (D⁻R⁻), Seropositive donor and seronegative recipient (D⁺R⁻), Mycophenolate mofetil (MMF), Seropositive Recipient (R⁺)

8.2.2.5 Table S2E

Results of the multivariate analysis for CMV syndrome

Explanatory variables	Estimate	Standard error	P value
(Intercept)	0.2976	0.8122	0.714
Prophylactic strategy	-0.8545	0.4769	0.073
Donor age (years)	0.0322	0.0130	0.013
Cause of end-stage renal disease: Polycystic kidney disease (adult type, dominant)	-0.7911	0.4894	0.106
Cause of end-stage renal disease: Diabetes	1.4590	0.6467	0.024
Cause of end-stage renal disease: Undefined cause	-1.6710	0.7451	0.025
CMV mismatch-based risk: Medium (R ⁺)	-0.9432	0.4523	0.037
CMV mismatch-based risk: Low (D ⁻ R ⁻)	-4.9270	1.2280	<0.001
Living donor	-2.7670	0.8390	0.001
White blood cell count at transplantation (cells/L)	0.0024	0.0100	0.810
Centre effects	-	-	<0.001

CMV syndrome was estimated by backwards elimination logistic regression, employing all demographic factors (Table 1 and Table S1) and centre effects as independent variables. As it can be observed, prevention strategy was an explanatory variable for CMV syndrome. The multivariate analysis employs Akaike's selection criterion for feature selection, so that some explanatory variables can have p values over 0.050. The P value for centre effects refers to the minimum P value of any transplantation centre.

Cytomegalovirus (CMV), Seronegative donor and seronegative recipient (D⁻R⁻), Seropositive donor and seronegative recipient (D⁺R⁻), Epstein-Barr virus (EBV), Seropositive Recipient (R⁺)

8.2.2.6 Table S2F

Results of the multivariate analysis for EBV peak viral load

Explanatory variables	Estimate	Standard error	P value
(Intercept)	1.1734	0.3800	0.002
Number of HLA A, B and DR mismatches	0.0956	0.0504	0.059
Cause of end-stage renal disease: Hypertension	0.3177	0.1741	0.069
Cause of end-stage renal disease: Polycystic kidney disease (adult type, dominant)	-0.5856	0.2140	0.007
Cause of end-stage renal disease: Diabetes	-0.5938	0.2920	0.043
Cause of end-stage renal disease: Neoplasms or tumours	2.6790	0.9231	0.004
Cause of end-stage renal disease: Other	-0.2552	0.1758	0.148
Cause of end-stage renal disease: Undefined cause	-0.4536	0.2667	0.090
Donors with expanded criteria	0.3159	0.1722	0.068
No panel-reactive antibodies before transplantation	-0.6180	0.2861	0.032
Low MMF daily dose (< 2000 mg·day ⁻¹)	-0.0003	0.0002	0.077

Peak viral load in logarithmic scale (with a value of 0 for viral load below detection limit) was estimated by backwards elimination linear regression, employing all demographic factors (Table 1 and Table S1) and centre effects as independent variables. As it can be observed, prevention strategy was not an explanatory variable for EBV peak viral load. The multivariate analysis employs Akaike's selection criterion for feature selection, so that some explanatory variables can have p values over 0.050. The P value for centre effects refers to the minimum P value of any transplantation centre.

Epstein-Barr virus (EBV), Seronegative donor and seronegative recipient (D⁻R⁻), Seropositive donor and seronegative recipient (D⁺R⁻), Mycophenolate mofetil (MMF), Seropositive Recipient (R⁺)

8.2.2.7 Table S2G

Results of the multivariate analysis for EBV peak viral load in female patients

Explanatory variables	Estimate	Standard error	P value
(Intercept)	3.9382	1.5158	0.012
Prophylactic strategy	-0.4585	0.3007	0.132
Body mass index (kg·m ⁻²)	-0.0365	0.0236	0.128

Cause of end-stage renal disease: Hypertension	0.6433	0.3184	0.048
Cause of end-stage renal disease: Polycystic kidney disease (adult type, dominant)	-0.8790	0.2901	0.004
Cause of end-stage renal disease: Undefined cause	-0.8497	0.5349	0.117
EBV mismatch-based risk: Medium (R ⁺)	0.6816	0.9875	0.493
EBV mismatch-based risk: Low (D ⁻ R ⁻)	-1.5917	1.5922	0.321
No previous transplantations	-1.4546	0.8374	0.087
No panel-reactive antibodies before transplantation	-0.7155	0.3862	0.069
Low MMF daily dose (< 2000 mg·day ⁻¹)	-0.0006	0.0003	0.077
Centre effects	-	-	<0.001

Peak viral load in logarithmic scale (with a value of 0 for viral load below detection limit) was estimated by backwards elimination linear regression, employing all demographic factors (Table 1 and Table S1) and centre effects as independent variables. As it can be observed, prevention strategy was an explanatory variable for EBV peak viral load in female patients. The multivariate analysis employs Akaike's selection criterion for feature selection, so that some explanatory variables can have p values over 0.050. The P value for centre effects refers to the minimum P value of any transplantation centre.

Epstein-Barr virus (EBV), Seronegative donor and seronegative recipient (D⁻R⁻), Seropositive donor and seronegative recipient (D⁺R⁻), Mycophenolate mofetil (MMF), Seropositive Recipient (R⁺)

8.2.2.8 Table S2H

Results of the multivariate analysis for BKV peak viral load

Explanatory variables	Estimate	Standard error	P value
(Intercept)	1.3949	0.2858	<0.001
Prophylactic strategy	0.4350	0.2351	0.065
Number of HLA A, B and DR mismatches	-0.1121	0.0702	0.112
Male sex	0.3888	0.2434	0.111
Cause of end-stage renal disease: Glomerulonephritis	0.8651	0.4604	0.061
Cause of end-stage renal disease: Other	0.5334	0.2538	0.037

Peak viral load in logarithmic scale (with a value of 0 for viral load below detection limit) was estimated by backwards elimination linear regression, employing all demographic factors (Table 1 and Table S1) and centre effects as independent variables. As it can be observed, prevention strategy was an explanatory variable for BKV peak viral load. The multivariate analysis employs Akaike's selection criterion for feature selection, so that some explanatory variables can have p values over 0.050. Centre effects were not an explanatory variable.

BK virus (BKV)

8.2.3 Table S3

Results of the single-parameter analyses for virus-related complications

8.2.3.1 Table S3A

Differences in viral events between strategy groups

Viral Event	Severity	Prophylactic strategy group (N=308)	Pre-emptive strategy group (N=232)	P value	OR [95% CI]
CMV (re)activation	Detectable viral load	46 (14.9%)	46 (19.8%)	0.167	1.41 [0.87-2.27]
	Elevated viral load	19 (6.2%)	20 (8.6%)	0.357	1.43 [0.71-2.92]
	High viral load	10 (3.2%)	8 (3.4%)	1.000	1.06 [0.36-3.05]
CMV syndrome	All	78 (25.3%)	35 (15.1%)	0.005	0.52 [0.33-0.83]
	Mild	39 (50.0%)	24 (68.6%)	0.204	-
	Moderate	31 (39.7%)	9 (25.7%)		
	Severe	8 (10.3%)	2 (5.7%)		
EBV (re)activation	Detectable viral load	62 (20.1%)	47 (20.3%)	1.000	1.01 [0.64-1.57]
	Elevated viral load	17 (5.5%)	20 (8.6%)	0.215	1.61 [0.78-3.37]
	High viral load	6 (1.9%)	5 (2.2%)	1.000 ^a	1.11 [0.26-4.42]
BKV (re)activation	Detectable viral load	157 (51.0%)	103 (44.4%)	0.153	0.77 [0.54-1.10]
	Elevated viral load	78 (25.3%)	43 (18.5%)	0.077	0.67 [0.43-1.04]
	High viral load	41 (13.3%)	18 (7.8%)	0.056	0.55 [0.29-1.01]

Data are given in number (percentage). P value is calculated based on Pearson's chi-square test or Fisher's exact test (marked with ^a). Odds ratio and confidence intervals are given only for viral events that were significantly different between the strategy groups. For the definition of (re)activation severity degrees see Methods (2.7). With respect to severity of CMV syndrome, the percentage refers to the total number of CMV syndromes.

BK virus (BKV), Cytomegalovirus (CMV), 95% Confidence interval (95% CI), Epstein-Barr virus (EBV), Odds ratio (OR).

8.2.3.2 Table S3B

Differences in cytomegalovirus complications between strategy groups stratified for CMV risk constellation

CMV risk constellation	CMV event	Severity	Prophylactic strategy group (N=308)	Pre-emptive strategy group (N=232)	P value	OR [95% CI]
D+R- (N=146)	(re)activation	Detectable	31 (26.1%)	9 (33.3%)	0.598	1.42 [0.51-3.75]
		Elevated	13 (10.9%)	6 (22.2%)	0.123 ^a	2.31 [0.65-7.48]

		High	6 (5.0%)	3 (11.1%)	0.368 ^a	2.34 [0.35-11.9]
	Syndrome	All	43 (36.1%)	8 (29.6%)	0.677	0.75 [0.26-1.97]
		Mild	14 (32.6%)	6 (75.0%)	0.062 ^a	-
		Moderate	22 (51.2%)	1 (12.5%)		
		Severe	7 (16.3%)	1 (12.5%)		
R ⁺ (N=266)	(re)activation	Detectable	12 (8.8%)	35 (27.1%)	<0.001	3.86 [1.84-8.63]
		Elevated	5 (3.6%)	13 (10.1%)	0.066	2.95 [0.95-10.88]
		High	3 (2.2%)	5 (3.9%)	0.490 ^a	1.8 [0.34-11.81]
	Syndrome	All	30 (21.9%)	27 (20.9%)	0.966	0.94 [0.5-1.77]
		Mild	23 (76.7%)	18 (66.7%)	0.460 ^a	-
		Moderate	7 (23.3%)	8 (29.6%)		
		Severe	0 (0.0%)	1 (3.7%)		
D ⁻ R ⁻ (N=115)	(re)activation	Detectable	2 (4.2%)	1 (1.5%)	0.570 ^a	0.35 [0.01-6.94]
		Elevated	0 (0.0%)	1 (1.5%)	1.000 ^a	-
		High	0 (0.0%)	0 (0.0%)	-	-
	Syndrome	All	3 (6.2%)	0 (0.0%)	0.070	0 [0-1.7]
		Mild	2 (66.7%)	0 (0.0%)	1.000 ^a	-
		Moderate	0 (0.0%)	0 (0.0%)		
		Severe	1 (33.3%)	0 (0.0%)		
Arm C (N=176)	(re)activation	Detectable	21 (17.1%)	9 (17%)	1.000	0.99 [0.37-2.49]
		Elevated	10 (8.1%)	5 (9.4%)	0.774 ^a	1.18 [0.3-4.02]
		High	5 (4.1%)	2 (3.8%)	1.000 ^a	0.93 [0.09-5.88]
	Syndrome	All	29 (23.6%)	8 (15.1%)	0.287	0.58 [0.21-1.43]
		Mild	14 (48.3%)	4 (50.0%)	0.878 ^a	-
		Moderate	10 (34.5%)	2 (25.0%)		
		Severe	5 (17.2%)	2 (25.0%)		

Data are given in number (percentage). P value is calculated based on Pearson's chi-square test or Fisher's exact test (marked with ^a). Odds ratio and confidence intervals are given only for viral events that were significantly different between the strategy groups. For the definition of (re)activation severity degrees see Methods (2.7). With respect to severity of CMV syndrome, the percentage refers to the total number of CMV syndromes.

95% Confidence interval (95% CI), Cytomegalovirus (CMV), Seronegative donor and seronegative recipient (D⁻R⁻), Seropositive donor and seronegative recipient (D⁺R⁻), Odds ratio (OR), Seropositive Recipient (R⁺).

8.2.3.3 Table S3C

Differences in EBV (re)activations between strategy groups stratified for EBV risk constellation

EBV risk constellation	Severity of (re)activation	Prophylactic strategy group (N=308)	Pre-emptive strategy group (N=232)	P value	OR [95% CI]
D ⁺ R ⁻ (N=24)	Detectable	3 (23.1%)	3 (27.3%)	1.000 ^a	1.24 [0.13-12]
	Elevated	2 (15.4%)	3 (27.3%)	0.630 ^a	2.00 [0.18-29.33]
	High	1 (7.7%)	1 (9.1%)	1.000 ^a	1.19 [0.01-101.86]
R ⁺ (N=400)	Detectable	49 (20.5%)	32 (19.9%)	0.979	0.96 [0.56-1.63]
	Elevated	12 (5.0%)	14 (8.7%)	0.209	1.80 [0.75-4.39]
	High	5 (2.1%)	3 (1.9%)	1.000 ^a	0.89 [0.14-4.64]
D ⁻ R ⁻ (N=9)	Detectable	1 (25.0%)	1 (20.0%)	1.000 ^a	0.77 [0.01-78.24]
	Elevated	0 (0.0%)	0 (0.0%)	-	-
	High	0 (0.0%)	0 (0.0%)	-	-
Arm C (N=176)	Detectable	28 (22.8%)	18 (34%)	0.173	1.74 [0.80-3.73]
	Elevated	8 (6.5%)	6 (11.3%)	0.362 ^a	1.83 [0.49-6.39]
	High	2 (1.6%)	3 (5.7%)	0.162 ^a	3.60 [0.40-44.31]

Data are given in number (percentage). P value is calculated based on Pearson's chi-square test or Fisher's exact test (marked with ^a). Odds ratio and confidence intervals are given only for viral events that were significantly different between the strategy groups. For the definition of (re)activation severity degrees, see Methods (2.7).

95% Confidence interval (95% CI), Seronegative donor and seronegative recipient (D⁻R⁻), Seropositive donor and seronegative recipient (D⁺R⁻), Epstein-Barr virus (EBV), Odds ratio (OR), Seropositive Recipient (R⁺).

8.2.3.4 Table S3D

Differences in viral events between strategy groups stratified by sex

Sex	Viral Event	Severity	Prophylactic strategy group	Pre-emptive strategy group	P value	OR [95% CI]
Male (N=346)	CMV (re)activation	Detectable viral load	29 (14.2%)	28 (19.7%)	0.226	1.48 [0.80-2.73]
		Elevated viral load	11 (5.4%)	13 (9.2%)	0.254	1.77 [0.71-4.50]
		High viral load	7 (3.4%)	6 (4.2%)	0.925	1.24 [0.34-4.42]
	CMV syndrome	All	54 (26.5%)	24 (16.9%)	0.049	0.57 [0.31-0.99]
		Mild	29 (53.7%)	18 (75%)	0.213 ^a	-
		Moderate	19 (35.2%)	4 (16.7%)		

		Severe	6 (11.1%)	2 (8.3%)		
	EBV (re)activation	Detectable viral load	49 (24.0%)	25 (17.6%)	0.194	0.68 [0.38-1.19]
		Elevated viral load	15 (7.4%)	13 (9.2%)	0.686	1.27 [0.54-2.97]
		High viral load	5 (2.5%)	4 (2.8%)	1.000 ^a	1.15 [0.22-5.46]
	BKV (re)activation	Detectable viral load	108 (52.9%)	65 (45.8%)	0.229	0.75 [0.48-1.18]
		Elevated viral load	51 (25.0%)	25 (17.6%)	0.133	0.64 [0.36-1.13]
		High viral load	30 (14.7%)	11 (7.7%)	0.072	0.49 [0.21-1.05]
Female (N=194)	CMV (re)activation	Detectable viral load	17 (16.3%)	18 (20.0%)	0.636	1.28 [0.57-2.85]
		Elevated viral load	8 (7.7%)	7 (7.8%)	1.000	1.01 [0.30-3.35]
		High viral load	3 (2.9%)	2 (2.2%)	1.000 ^a	0.77 [0.06-6.85]
	CMV syndrome	All	24 (23.1%)	11 (12.2%)	0.076	0.47 [0.19-1.07]
		Mild	10 (41.7%)	6 (54.5%)	0.741 ^a	-
		Moderate	12 (50.0%)	5 (45.5%)		
		Severe	2 (8.3%)	0 (0.0%)		
	EBV (re)activation	Detectable viral load	13 (12.5%)	22 (24.4%)	0.049	2.26 [1.00-5.25]
		Elevated viral load	2 (1.9%)	7 (7.8%)	0.084 ^a	4.27 [0.79-43.19]
		High viral load	1 (1.0%)	1 (1.1%)	1.000 ^a	1.16 [0.01-91.65]
	BKV (re)activation	Detectable viral load	49 (47.1%)	38 (42.2%)	0.590	0.82 [0.45-1.51]
		Elevated viral load	27 (26.0%)	18 (20.0%)	0.418	0.71 [0.34-1.48]
		High viral load	11 (10.6%)	7 (7.8%)	0.673	0.71 [0.22-2.13]

Data are given in number (percentage). P value is calculated based on Pearson's chi-square test or Fisher's exact test (marked with ^a). Odds ratio and confidence intervals are given only for viral events that were significantly different between the strategy groups. For the definition of (re)activation severity degrees see Methods (2.7). With respect to severity of CMV syndrome, the percentage refers to the total number of CMV syndromes.

BK virus (BKV), Cytomegalovirus (CMV), 95% Confidence interval (95% CI), Epstein-Barr virus (EBV), Odds ratio (OR).

8.2.3.5 Table S3E

Differences in cytomegalovirus complications between strategy groups stratified for CMV risk constellation and sex

Sex	CMV risk constellation	CMV event	Severity	Prophylactic strategy group	Pre-emptive strategy group	P value	OR [95% CI]
Male (N=346)	D ⁺ R ⁻ (N=102)	(re)activation	Detectable	18 (21.7%)	7 (36.8%)	0.235 ^a	2.09 [0.60-6.82]
			Elevated	7 (8.4%)	6 (31.6%)	0.014 ^a	4.9 [1.17-20.34]
			High	3 (3.6%)	3 (15.8%)	0.077 ^a	4.89 [0.60-39.93]
		Syndrome	All	27 (32.5%)	6 (31.6%)	1.000	0.96 [0.27-3.07]
			Mild	8 (29.6%)	5 (83.3%)	0.028 ^a	-
			Moderate	14 (51.9%)	0 (0.0%)		
			Severe	5 (18.5%)	1 (16.7%)		
	R ⁺ (N=156)	(re)activation	Detectable	8 (9.8%)	20 (27.0%)	0.009	3.4 [1.31-9.63]
			Elevated	3 (3.7%)	6 (8.1%)	0.310 ^a	2.31 [0.47-14.82]
			High	3 (3.7%)	3 (4.1%)	1.000 ^a	1.11 [0.14-8.57]
		Syndrome	All	22 (26.8%)	18 (24.3%)	0.862	0.88 [0.40-1.92]
			Mild	19 (86.4%)	13 (72.2%)	0.423 ^a	-
			Moderate	3 (13.6%)	4 (22.2%)		
			Severe	0 (0.0%)	1 (5.6%)		
	D ⁺ R ⁻ (N=80)	(re)activation	Detectable	2 (5.6%)	1 (2.3%)	0.585 ^a	0.40 [0.01-7.98]
			Elevated	0 (0.0%)	1 (2.3%)	1.000 ^a	Inf [0.02-Inf]
			High	0 (0.0%)	0 (0.0%)	-	-
		Syndrome	All	3 (8.3%)	0 (0.0%)	0.087 ^a	0.00 [0.00-1.94]
			Mild	2 (66.7%)	0	1.000 ^a	-
			Moderate	0 (0.0%)	0		
			Severe	1 (33.3%)	0		
	Arm C (N=111)	(re)activation	Detectable	12 (14.6%)	5 (17.2%)	0.768 ^a	1.21 [0.30-4.20]
			Elevated	6 (7.3%)	3 (10.3%)	0.695 ^a	1.46 [0.22-7.42]
			High	4 (4.9%)	2 (6.9%)	0.651 ^a	1.44 [0.12-10.71]
		Syndrome	All	18 (22.0%)	6 (20.7%)	1.000	0.93 [0.27-2.84]
			Mild	9 (50.0%)	4 (66.7%)	0.467 ^a	-
			Moderate	5 (27.8%)	0 (0.0%)		

			Severe	4 (22.2%)	2 (33.3%)		
Female (N=194)	D ⁺ R ⁻ (N=44)	(re)activation	Detectable	13 (36.1%)	2 (25.0%)	0.695 ^a	0.60 [0.05-4.01]
			Elevated	6 (16.7%)	0 (0.0%)	0.573 ^a	0.00 [0.00-3.97]
			High	3 (8.3%)	0 (0.0%)	1.000 ^a	0.00 [0.00-11.54]
		Syndrome	All	16 (44.4%)	2 (25.0%)	0.439 ^a	0.42 [0.04-2.81]
			Mild	6 (37.5%)	1 (50.0%)	1.000 ^a	-
			Moderate	8 (50.0%)	1 (50.0%)		
			Severe	2 (12.5%)	0 (0.0%)		
	R ⁺ (N=110)	(re)activation	Detectable	4 (7.3%)	15 (27.3%)	0.012	4.72 [1.36-21.05]
			Elevated	2 (3.6%)	7 (12.7%)	0.161 ^a	3.82 [0.68-39.51]
			High	0 (0.0%)	2 (3.6%)	0.495 ^a	Inf [0.19-Inf]
		Syndrome	All	8 (14.5%)	9 (16.4%)	1.000	1.15 [0.36-3.75]
			Mild	4 (50%)	5 (55.6%)	1.000 ^a	-
			Moderate	4 (50%)	4 (44.4%)		
			Severe	0 (0.0%)	0 (0.0%)		
	D ⁻ R ⁻ (N=35)	(re)activation	Detectable	0 (0.0%)	0 (0.0%)	-	-
			Elevated	0 (0.0%)	0 (0.0%)	-	-
			High	0 (0.0%)	0 (0.0%)	-	-
		Syndrome	All	0 (0.0%)	0 (0.0%)	-	-
	Arm C (N=65)	(re)activation	Detectable	9 (22.0%)	4 (16.7%)	0.753 ^a	0.71 [0.14-3.00]
			Elevated	4 (9.8%)	2 (8.3%)	1.000 ^a	0.84 [0.07-6.45]
			High	1 (2.4%)	0 (0.0%)	1.000 ^a	0.00 [0.00-66.56]
		Syndrome	All	11 (26.8%)	2 (8.3%)	0.109 ^a	0.25 [0.02-1.34]
			Mild	5 (45.5%)	0 (0.0%)	0.551 ^a	-
			Moderate	5 (45.5%)	2 (100.0%)		
			Severe	1 (9.1%)	0 (0.0%)		

Data are given in number (percentage). P value is calculated based on Pearson's chi-square test or Fisher's exact test (marked with ^a). Odds ratio and confidence intervals are given only for viral events that were significantly different between the strategy groups. For the definition of (re)activation severity degrees see Methods (2.7). With respect to severity of CMV syndrome, the percentage refers to the total number of CMV syndromes.

95% Confidence interval (95% CI), Cytomegalovirus (CMV), Seronegative donor and seronegative recipient (D⁻R⁻), Seropositive donor and seronegative recipient (D⁺R⁻), Infinity (Inf), Odds ratio (OR), Seropositive Recipient (R⁺).

8.2.3.6 Table S3F

Differences in EBV (re)activations between strategy groups stratified for EBV risk constellation and sex

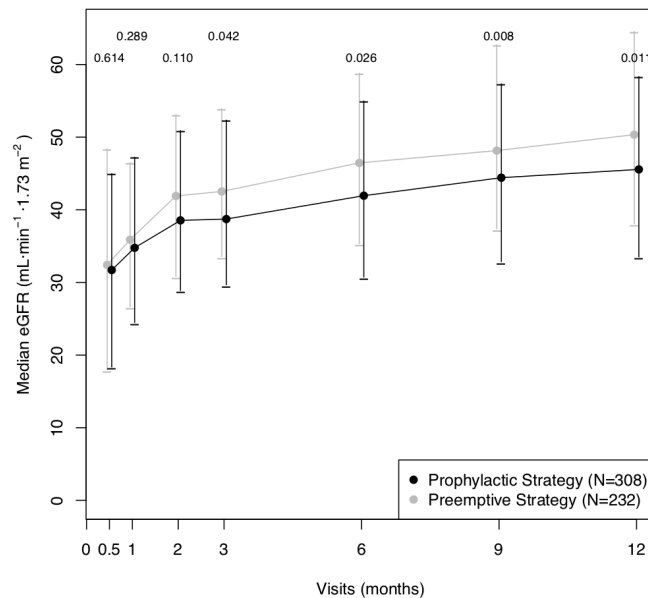
Sex	EBV risk constellation	Severity of (re)activation	Prophylactic strategy group	Pre-emptive strategy group	P value	OR [95% CI]
Male (N=346)	D ⁺ R ⁻ (N=19)	Detectable	3 (27.3%)	2 (25.0%)	1.000 ^a	0.89 [0.06-10.71]
		Elevated	2 (18.2%)	2 (25.0%)	1.000 ^a	1.47 [0.08-25.7]
		High	1 (9.1%)	1 (12.5%)	1.000 ^a	1.40 [0.02-123.06]
	R ⁺ (N=256)	Detectable	37 (23.6%)	18 (18.2%)	0.387	0.72 [0.36-1.41]
		Elevated	10 (6.4%)	10 (10.1%)	0.398	1.65 [0.59-4.61]
		High	4 (2.5%)	3 (3.0%)	1.000 ^a	1.19 [0.17-7.23]
	D ⁻ R ⁻ (N=5)	Detectable	1 (33.3%)	0 (0.0%)	1.000 ^a	0.00 [0.00-58.45]
		Elevated	0 (0.0%)	0 (0.0%)	-	-
		High	0 (0.0%)	0 (0.0%)	-	-
	Arm C (N=111)	Detectable	22 (26.8%)	6 (20.7%)	0.685	0.71 [0.21-2.13]
		Elevated	7 (8.5%)	3 (10.3%)	0.719 ^a	1.23 [0.19-5.92]
		High	2 (2.4%)	2 (6.9%)	0.279 ^a	2.93 [0.20-42.22]
Female (N=194)	D ⁺ R ⁻ (N=5)	Detectable	0 (0.0%)	1 (33.3%)	1.000 ^a	Inf [0.02-Inf]
		Elevated	0 (0.0%)	1 (33.3%)	1.000 ^a	Inf [0.02-Inf]
		High	0 (0.0%)	0 (0.0%)	1.000 ^a	Inf [0-Inf]
	R ⁺ (N=144)	Detectable	12 (14.6%)	14 (22.6%)	0.313	1.69 [0.66-4.4]
		Elevated	2 (2.4%)	4 (6.5%)	0.403 ^a	2.74 [0.38-31.24]
		High	1 (1.2%)	0 (0.0%)	1.000 ^a	0.00 [0.00-51.54]
	D ⁻ R ⁻ (N=4)	Detectable	0 (0.0%)	1 (33.3%)	1.000 ^a	Inf [0.01-Inf]
		Elevated	0 (0.0%)	0 (0.0%)	-	-
		High	0 (0.0%)	0 (0.0%)	-	-
	Arm C (N=65)	Detectable	6 (14.6%)	12 (50.0%)	0.005	5.65 [1.56-22.86]
		Elevated	1 (2.4%)	3 (12.5%)	0.138 ^a	5.56 [0.42-306.72]
		High	0 (0.0%)	1 (4.2%)	0.369 ^a	Inf [0.04-Inf]

Data are given in number (percentage). P value is calculated based on Pearson's chi-square test or Fisher's exact test (marked with ^a). Odds ratio and confidence intervals are given only for viral events that were significantly different between the strategy groups. For the definition of (re)activation severity degrees see Methods (2.7).

95% Confidence interval (95% CI), Seronegative donor and seronegative recipient (D^-R^-), Seropositive donor and seronegative recipient (D^+R^-), Epstein-Barr virus (EBV), Infinity (Inf), Odds ratio (OR), Seropositive Recipient (R^+).

8.2.4 Figure S4

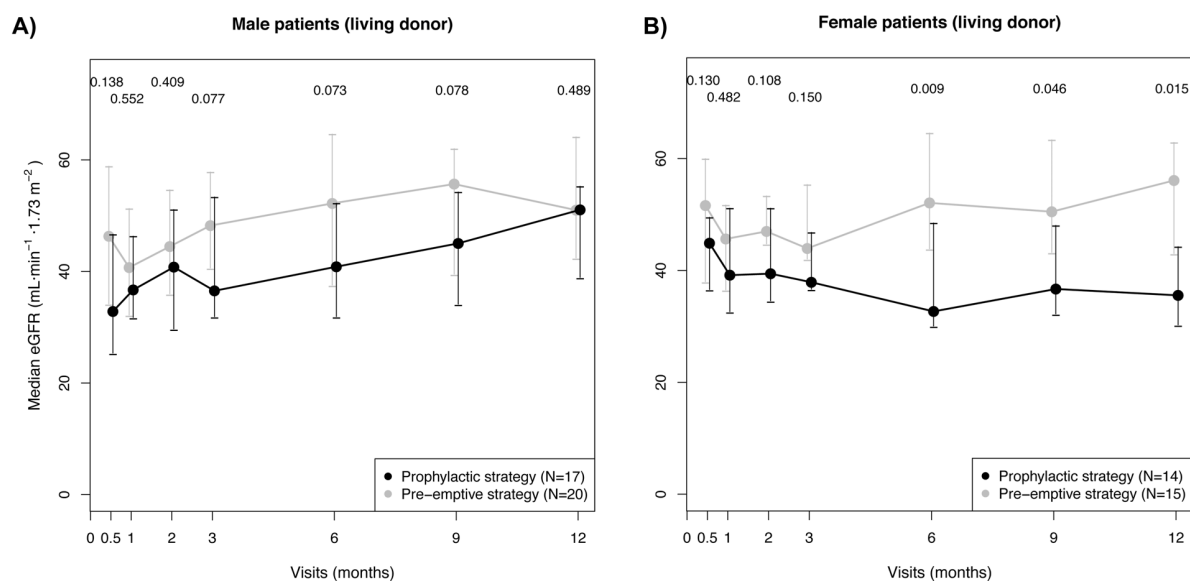
Graft function dynamics of the prevention strategy groups



Median eGFR ($\text{mL} \cdot \text{min}^{-1} \cdot 1.73 \text{ m}^{-2}$) of the prevention strategy groups is plotted for each protocol visit. The bars indicate the interquartile range. The numbers indicate the P value of the difference in eGFR between the prevention strategy groups, as calculated using the Mann-Whitney test. Day 0 is not shown, as it is pre-transplantation.

8.2.5 Figure S5

Graft function dynamics of the prevention strategy groups stratified according to sex, for patients with living donor



Median eGFR ($\text{mL} \cdot \text{min}^{-1} \cdot 1.73 \text{ m}^{-2}$) of the prevention strategy groups is plotted for each protocol visit. The bars indicate the interquartile range. The numbers indicate the p value of the difference in eGFR between the prevention strategy groups, as calculated using the Mann-Whitney test. Day 0 is not shown, as it is pre-transplantation. For the eGFR dynamics of patients with deceased donors, see Figure 1.

9. A novel approach reveals that HLA class 1 single antigen bead-signatures provide a means of high-accuracy pre-transplant risk assessment of acute cellular rejection

This chapter refers to the manuscript published as:

Wittenbrink N, Herrmann S, Blazquez-Navarro A, Bauer C, Lindberg E, Wolk K, Sabat R, Reinke P, Sawitzki B, Thomusch O, Hugo C, Babel N, Seitz H and Or-Guil M (2019). A novel approach reveals that HLA class 1 single antigen bead-signatures provide a means of high-accuracy pre-transplant risk assessment of acute cellular rejection. *BMC Immunology*. 20(11). doi:10.1186/s12865-019-0291-2

RESEARCH ARTICLE

Open Access

A novel approach reveals that HLA class 1 single antigen bead-signatures provide a means of high-accuracy pre-transplant risk assessment of acute cellular rejection in renal transplantation



Nicole Wittenbrink¹, Sabrina Herrmann², Arturo Blazquez-Navarro^{1,3}, Chris Bauer⁴, Eric Lindberg⁴, Kerstin Wolk^{3,5}, Robert Sabat^{5,6}, Petra Reinke^{3,7,8}, Birgit Sawitzki^{3,9}, Oliver Thomusch¹⁰, Christian Hugo¹¹, Nina Babel^{3,12}, Harald Seitz² and Michal Or-Guil^{1*}

Abstract

Background: Acute cellular rejection (ACR) is associated with complications after kidney transplantation, such as graft dysfunction and graft loss. Early risk assessment is therefore critical for the improvement of transplantation outcomes. In this work, we retrospectively analyzed a pre-transplant HLA antigen bead assay data set that was acquired by the eKID consortium as part of a systems medicine approach.

Results: The data set included single antigen bead (SAB) reactivity profiles of 52 low-risk graft recipients (negative complement dependent cytotoxicity crossmatch, PRA < 30%) who showed detectable pre-transplant anti-HLA 1 antibodies. To assess whether the reactivity profiles provide a means for ACR risk assessment, we established a novel approach which differs from standard approaches in two aspects: the use of quantitative continuous data and the use of a multiparameter classification method. Remarkably, it achieved significant prediction of the 38 graft recipients who experienced ACR with a balanced accuracy of 82.7% (sensitivity = 76.5%, specificity = 88.9%).

Conclusions: The resultant classifier achieved one of the highest prediction accuracies in the literature for pre-transplant risk assessment of ACR. Importantly, it can facilitate risk assessment in non-sensitized patients who lack donor-specific antibodies. As the classifier is based on continuous data and includes weak signals, our results emphasize that not only strong but also weak binding interactions of antibodies and HLA 1 antigens contain predictive information.

Trial registration: ClinicalTrials.gov [NCT00724022](https://clinicaltrials.gov/ct2/show/study/NCT00724022). Retrospectively registered July 2008.

Keywords: Renal transplantation, Acute cellular rejection, Pre-transplantation risk assessment, Anti-HLA-1 antibodies, Single HLA antigen bead assay, Immune signatures, Machine learning

* Correspondence: m.orguil@biologie.hu-berlin.de

¹Systems Immunology Lab, Department of Biology, Humboldt University Berlin, Berlin, Germany

Full list of author information is available at the end of the article



© The Author(s). 2019 **Open Access** This article is distributed under the terms of the Creative Commons Attribution 4.0 International License (<http://creativecommons.org/licenses/by/4.0/>), which permits unrestricted use, distribution, and reproduction in any medium, provided you give appropriate credit to the original author(s) and the source, provide a link to the Creative Commons license, and indicate if changes were made. The Creative Commons Public Domain Dedication waiver (<http://creativecommons.org/publicdomain/zero/1.0/>) applies to the data made available in this article, unless otherwise stated.

Background

The efficacy of immunosuppressive therapy in kidney transplantation has steadily increased over the last decade. As a consequence, the incidence of acute rejection (AR) episodes has decreased and short-term graft survival rates have improved [1, 2]. However, long-term transplant outcomes are still poor and episodes of AR are known to significantly exacerbate long-term outcomes [2, 3]. AR is associated with long-term complications, such as graft dysfunction and reduced graft survival and AR prevention continues to be a main focus in the design of new therapeutic strategies for renal transplantation [4–7]. The most common form of AR is acute cellular rejection (ACR) [8]. ACR is a T cell cytotoxic immune response against the graft, leading to inflammatory cell infiltration with tubulitis and, eventually, damage of the donor tissue [9, 10]. The positive outcome of ACR if treated early, as well as its potentially irreversible damage, render it particularly relevant for prevention research [10, 11]. Regarding non-invasive diagnostics, a number of studies have obtained good results using tissue, blood or urine markers [11–18]. For early risk assessment, the large majority of models are donor-dependent, as they either employ measurements from the early post-transplantation period or utilize donor-derived data (e.g. from crossmatch tests) [19–30]. The most common approach for pre-transplant risk assessment relies on the characterization of HLA antibodies in recipient serum samples by solid phase single HLA antigen bead (SAB) assay [24–29, 31]. The assay facilitates detection and identification of anti-HLA antibody specificities and provides a method for monitoring the development of donor-specific antibodies (DSA). The detection of DSA through SAB assays is a well-established method for antibody-mediated rejection (ABMR) pre-transplantation risk assessment, but not for ACR [24–30, 32].

Approaches for risk assessment of ACR do not employ DSA for the prediction – as both patients with or without DSA experience episodes of ACR – but other risk markers, such as soluble CD30 levels or panel of reactive T cells [23, 33–35]. However, the inspection of SAB serum antibody reactivity profiles (irrespective of DSA status) may provide a means to an ACR risk assessment tool for two reasons: (1) serum antibody binding profiles against antigen/protein libraries are generally powerful in discriminating between different health or disease conditions [36–39], and (2) antibody-mediated mechanisms have been shown to be involved in the T cell-mediated initiation, perpetuation, and progression of graft injury [40, 41].

In this work, as part of an exploratory study, we present a classifier achieving high-accuracy pre-transplant risk assessment of ACR. Remarkably, this classifier is based on continuous non-thresholded HLA 1 SAB data and does not rely on donor-specific HLA typing.

Results

Characteristics of the graft recipients included in the study

Pre-transplant HLA assay data were retrospectively analyzed as part of a systems medicine approach towards early risk assessment of ACR [42, 43]. The investigated study group comprised all kidney transplant recipients enrolled in the Harmony trial ($N = 615$) who experienced at least one ACR or borderline ACR event in the first year ($N = 77$) and all transplant recipients who experienced no serious adverse events ($N = 80$). Median time to the first ACR event was 20.5 days (range = 4–373 days) (Additional file 1: Figure S1). Demographics and clinical characteristics of the study groups are summarized in Additional file 4: Table S1.

Pre-transplantation HLA-1 and HLA-2 MAB data were available for $N = 63$ recipients of the ACR group and $N = 54$ recipients of the control group (for demographic and clinical characteristics, see Additional file 5: Table S2). Additionally, HLA-1 SAB data was measured for all those patients who tested positive for HLA-1 MAB screening (21 ACR + 13 control) and a random subset of patients who tested negative (13 ACR + 5 control). In total, pre-transplantation HLA-1 SAB data were available for $N = 34$ recipients of the ACR group and $N = 18$ of the control group. Due to the higher sensitivity of SAB assay compared to MAB, the former assay was considered a better candidate for ACR risk assessment.

Demographic and clinical characteristics of the SAB ACR ($N = 34$) and the SAB control group ($N = 18$) were compared and are summarized in Table 1. The majority of patients was male, received their first kidney transplant and had a deceased donor. There were no significant differences between the study groups for the above mentioned characteristics as well as immunosuppressive therapy. However, the mean age of patients in the ACR group (54.9 ± 11.0) was significantly higher than for the control group (51.6 ± 11.6 ; $p = 0.04$; Mann-Whitney U test) as was the body mass index (27.7 ± 5.4 vs. 24.2 ± 4.2 ; $p = 0.01$; Mann-Whitney U test). With respect to HLA mismatches, a significant difference was found for HLA-DR ($p = 0.03$; Pearson's chi-squared test), with an elevated frequency of patients with two mismatches in the ACR group (32.4% vs. 11.1%). No significant differences were found for HLA-A or HLA-B. There were no significant differences regarding PRA between the groups. There was a near-significant difference in cold ischemia time with longer times being observed for the ACR group (739 ± 295 vs. 637 ± 302 ; $P = 0.06$; Mann-Whitney U test).

Conventional HLA SAB data analysis does not permit pre-transplant risk assessment of ACR

To assess whether HLA-1 SAB reactivity profiles provide a means for ACR risk assessment, we initially applied

Table 1 Characteristics and medication details for the subset of patients included in the HLA class 1 SAB data set^a

	ACR	Control	<i>p</i> -value
Number of kidney transplant recipients	34	18	–
Age at time of transplantation (years)	57.9 ± 11.0	51.6 ± 11.6	0.04
Body mass index at time of transplantation (kg/m ²)	27.7 ± 5.4	24.2 ± 4.2	0.01
Gender			
Female	17 (50.0%)	7 (38.9%)	ns ^b
Male	17 (50.0%)	11 (61.1%)	
Type of donor			
Living	7 (20.6%)	4 (22.2%)	ns ^c
Deceased	27 (79.4%)	14 (77.8%)	
Re-transplantation	3 (8.8%)	0 (0.0%)	ns ^c
HLA-A Mismatches ^d			
0	11 (32.4%)	9 (50.0%)	ns ^c
1	18 (52.9%)	8 (44.4%)	
2	5 (14.7%)	1 (5.6%)	
HLA-B Mismatches ^d			
0	3 (8.8%)	4 (22.2%)	ns ^c
1	18 (52.9%)	11 (61.1%)	
2	13 (38.2%)	3 (16.7%)	
HLA-DR Mismatches			
0	3 (8.8%)	7 (38.9%)	0.03 ^c
1	20 (58.8%)	9 (50.0%)	
2	11 (32.4%)	2 (11.1%)	
PRA = 0%	31 (91.2%)	16 (88.9%)	ns ^c
Therapeutic Arm			
A	12 (35.3%)	6 (33.3%)	ns ^c
B	10 (29.4%)	3 (16.7%)	
C	12 (35.3%)	9 (50.0%)	
Cold ischemia time: only deceased donors (min)	739 ± 295	637 ± 302	ns

^aData are given as mean ± standard deviation for quantitative variables and as number (frequency) for categorical variables. *P* values for quantitative variables were calculated by Mann-Whitney U test, for categorical variables either chi-squared ^(b) or Fisher's exact test ^(c) were employed. ^(d) According to Fisher's exact test, there is also no statistically significant differences between the ACR and Control groups when HLA-A and HLA-B mismatches are combined into one group

the conventional data analysis approach used in HLA-diagnostics to our data set. Central to this approach is the conversion of the quantitative SAB assay read-out data into qualitative binary data (1 = presence of antibody-antigen reactivity, 0 = absence of reactivity) based on a mean fluorescence intensity (MFI) threshold. We performed all analyses for a fixed threshold of 1000 MFI and an individually adjusted threshold in the range 253–1068 MFI (Additional file 2: Figure S2). In both cases, there were no statistically significant differences between the SAB ACR and the SAB control group in any of the individual reactivities (Additional file 6: Table S3 and Additional file 7: Table S4). That is, there are no individual HLA-1 antibody reactivities that allow for risk assessment of ACR.

To assess whether there is a combination of reactivities that allows for risk assessment of ACR, we extended the conventional approach by applying a support vector machine-based multiparameter classification method to the binarized data (for details, see Material and Methods). The resulting multiparameter classifiers did not achieve significant classification performance ($p > 0.1$, Table 2). Taken together, our results indicate that the conventional HLA SAB data analysis approach does not permit pre-transplant risk assessment of ACR.

A novel approach built on multiparameter classification and quantitative data input allows for high accuracy pre-transplant prediction of ACR

In spite of the widespread use of HLA SAB assays, the interpretation of results obtained following the conventional

Table 2 Multiparameter pre-transplant prediction of ACR

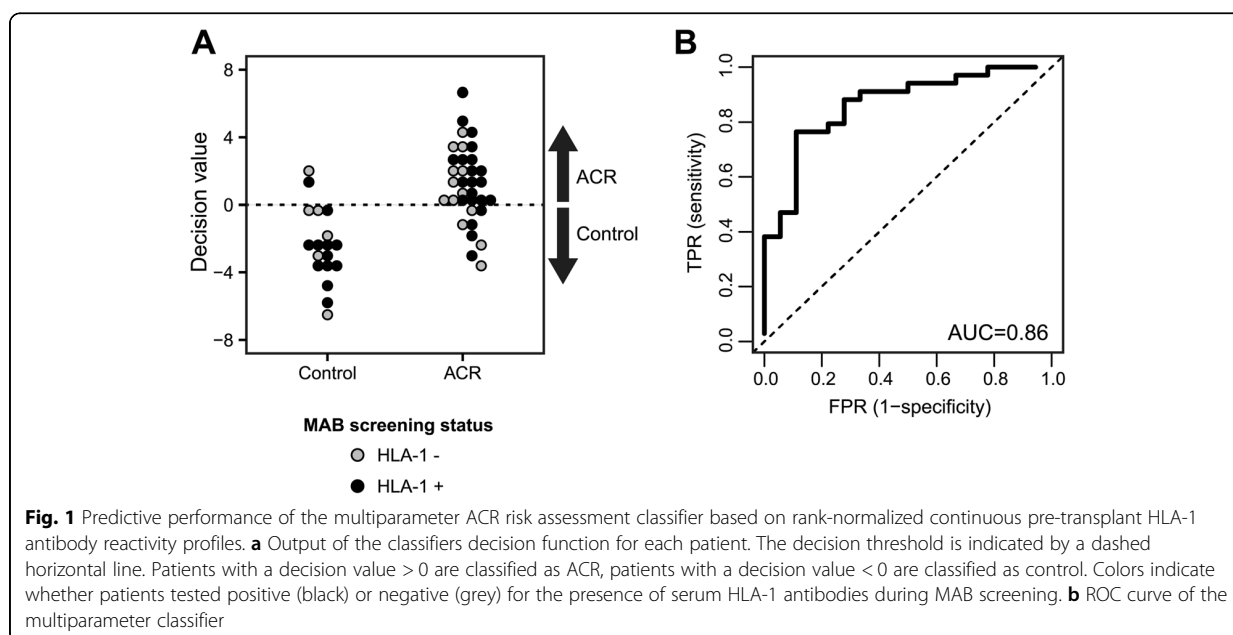
Data set	Data analysis approach	MFI-threshold	BACC [%]	Sens. [%]	Spec. [%]	p-value
HLA-1 SAB	Conventional, binary data input [0, 1]	1000	62.1	35.3	88.9	ns ($p > 0.1$)
	Conventional binary data input [0, 1]	Individually adjusted [253–1068]	70.9	52.9	88.9	ns ($p > 0.1$)
	Novel, continuous data input	–	82.7	76.5	88.9	0.002
MAB	Novel, continuous data input	–	63.9	55.6	72.2	0.040

data analysis approach remains controversial [44]. A strict MFI threshold consistently identifying clinically relevant antibody-antigen reactivities is challenging to define [45]. Since it is likely that the choice of MFI threshold compromises classification efforts, we applied a novel approach to the HLA-1 SAB data set that does not rely on MFI thresholding. Key to this novel approach is the rank-normalization of the continuous SAB assay read-out data. Remarkably, a support-vector machine-based multiparameter classifier built on these data achieved highly significant prediction performance with a balanced accuracy of 82.7% (Sens. = 76.5%, Spec. = 88.9%, $p = 0.002$, Fig. 1a and Table 2). Receiver operating characteristic (ROC) analysis further emphasizes that the prediction performance was better than a random guess (area under the curve [AUC] = 0.86) and illustrates the trade-off between the probability of correctly predicting ACR (true positive rate, sensitivity) and the probability of incorrectly predicting ACR (false positive rate, specificity) (Fig. 1b). Importantly, we found that prediction performance was independent of a patient's MAB screening test result, as patients who tested positive or negative for HLA-1 antibodies are predicted equally well (Fig. 1a). Moreover, the performance of the continuous data classifier was not due

to age, BMI or HLA-DR mismatch frequency as confounding factors; significant classification was not achieved when HLA class 1 SAB continuous data were grouped according to either of those factors (≤ 50 y vs. > 50 y, ≤ 25 BMI vs. > 25 BMI, or no-mismatch vs. 1–2 mismatches). In addition, median-centered bead MFIs did not show any association with age or BMI (mean Spearman correlation coefficient $r = 0.019 \pm 0.129$ and $r = 0.009 \pm 0.133$, respectively). Taken together, our results show that continuous, rank-normalized HLA-1 SAB reactivity profiles provide a means of high-accuracy risk assessment of pre-transplant ACR.

Diagnostics based on HLA antibody detection assays may generally benefit from the novel approach

The fact that continuous HLA-1 SAB reactivity data outperformed MFI-thresholded binary data in terms of pre-transplant prediction of ACR (Table 2) led us to the conjecture that the conventional approach entails a loss of information that may compromise HLA-diagnostics classification efforts in general. To substantiate this claim, we performed additional analyses on the MAB screening data (63 ACR + 54 controls). Conventional MFI-threshold based data analysis revealed no statistical



differences between the two study group as to the prevalence of HLA class I and/or HLA class II antibodies (Fig. 2). A multiparameter classifier based on the continuous rank-normalized data, however, achieved statistically significant prediction of the patients who experience ACR ($p = 0.04$, Table 2 and Additional file 3: Figure S3). Even though the accuracy of the classifier was low and not sufficient for routine risk assessment (BACC = 63.9%, Sens. = 55.6%, Spec. = 72.2%), the fact that it was significant emphasizes that the use of continuous non-thresholded antigen bead assay data favorably affects classification performance.

Discussion

The current study shows that pre-transplant HLA class I SAB signatures predict the risk of acute cellular rejection (ACR) with high accuracy. Importantly, it demonstrates that HLA antibody signatures contain information on cell-mediated events to come.

In contrast to the vast majority of existing pre-transplant risk assessment models [24–29, 31], our model does not rely on DSA reactivity data. The key advantages of this approach are that i) it facilitates risk assessment for non-sensitized patients lacking DSA and ii) it can be carried out independently of donor assignment.

HLA SAB data usually feed into prediction models in the form of binary data derived from MFI thresholding – the focus lying on strong binding interactions. Strikingly, our study emphasizes that such an approach entails a loss of information and ultimately results in loss of or suboptimal prediction performance. The fact that

continuous HLA reactivity data outperform thresholded binary data (Table 2) indicates that weak binding interactions hold high-value information for risk assessment of ACR. This is further emphasized by our finding that our risk assessment tool performs equally well for patients who tested positive or negative for the presence of HLA-I antibodies during MAB screening. There is indeed sufficient evidence in the literature to show that weak binding events are of great importance to biological systems, e.g. protein-peptide interactions [46], virus-cell interactions [47], cell adhesion, and cell-cell interactions [48–51]. Our data suggest that HLA SAB based diagnostics will profit from inclusion of weak interactions by feeding prediction models with non-thresholded continuous data. A further advantage of prediction models based on non-thresholded MFI data is that they are not affected by the prevailing uncertainties regarding the right choice of the threshold MFI level and by the yet missing internationally agreed standards [44, 52].

But why is the pre-transplant signature of serum antibodies against HLA-I SAB predictive for the risk of T cell mediated rejection? There is evidence in the literature for an association between anti-HLA serum antibodies and ACR. Crosslinking of HLA-I antigens expressed on the surface of donor cells by HLA class I antibodies has been shown to trigger the classical complement pathway through binding of C1q. The subsequent release of the complement peptides C3a and C5a then leads to enhanced allo-T cell responses and leucocyte recruitment [53]. That is, pre-transplant HLA class I antibodies may be involved in the initiation and

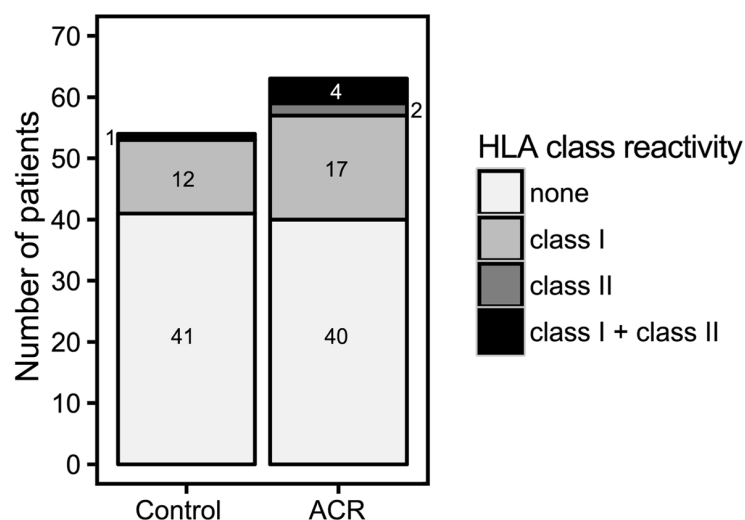


Fig. 2 Conventional MFI-thresholded binary MAB screening data do not allow for pre-transplant risk assessment of ACR. Illustrated are the results of the MAB screening data of the cohort (117 graft recipients, 63 ACR + 54 controls; for demographics and clinical characteristics, see Additional file 5: Table S2). Analyses were carried out on MFI-thresholded binary HLA MAB screening data (conventional approach); according to Fisher's exact test, differences with respect to the prevalence of HLA antibodies are not significant ($p > 0.05$)

perpetuation of ACR by boosting adaptive T cell activities after graft transfer. HLA class 1 antibodies have also been shown to be directly involved in mechanisms that cause severe graft injury such as endothelial cell activation or NK cell related FcγR-dependent processes [53]. However, these mechanisms usually result in histological manifestations strongly associated with ABMR [53]. Since our study cohort did not show such manifestations, these processes are unlikely to be relevant to the predictive value of our pre-transplant HLA 1 antibody signatures.

The HLA MAB and SAB data used in this study are part of a large multi-parameter database set up by the e:KID consortium that seeks to establish a systems medicine approach to personalized immunosuppressive treatment at an early stage after kidney transplantation (<http://www.sys-med.de/en/consortia/ekid/>). e:KID recorded a total of 478 parameters including, among others, gene expression, cytokine profile, epigenetics, metabolomics and viral load data as well as common clinical variables such as renal function or acute phase proteins. Evaluation of clinical parameters failed to identify any markers or combinations thereof which are predictive of ACR [4]. Additionally, no other single parameter or multiparameter set, other than HLA class 1 SAB signatures, achieved high accuracy pre-transplant prediction performance. This emphasizes the vast potential of serum antibodies in diagnostics in general, and, in particular, for diseases where the antigens are unknown.

The comparison of predictive performances between our classifier and classifiers in the literature underlines its relevance to pre-kidney transplant risk assessment (Additional file 8: Table S5). Its accuracy of 82.7% is i) one of the highest among all donor-independent risk assessment models [19, 22, 27, 34, 54], ii) comparable to any AR models [19–24, 26–30, 34, 35, 54, 55] and iii) comparable to any SAB data based models for ABMR [24, 26–30]. Furthermore, our classifier is based on SAB, an established diagnostics laboratory tool, thereby facilitating its further use for ACR risk assessment.

Conclusions

Our study establishes a novel tool for pre-transplant risk assessment of acute cellular rejection. Once externally validated, patients classified as high risk by our model will benefit from its implementation through modified immunosuppression as well as closer monitoring leading to earlier detection of rejection onset and initiation of treatment. Consequently, the prognosis and survival rate of the graft will improve.

Methods

Study aim

The aim of this study is to determine whether SAB serum antibody reactivity profiles of renal transplantation

recipients can be used for the prediction of ACR during the first post-transplantation year. For this goal, pre-transplant HLA assay data were retrospectively analyzed as part of a systems medicine approach.

Patient population and monitoring

Six hundred fifteen adult kidney transplant recipients were enrolled in the randomized, multicenter diagnostic trial Harmony (EudraCT-Nr. 2007–006516-31) [4]. Patients were treated with a quadruple (arm A) or triple (arms B and C) immunosuppressive therapy as described before [4]. The immunosuppressive therapy included induction with either monoclonal IL-2R antibody basiliximab (arms A and B) (Simulect®, Novartis) or rabbit ATG (arm C) (Thymoglobulin®, Sanofi). Maintenance immunosuppression consisted of tacrolimus (Advagraf®, Astellas) and mycophenolate mofetil (MMF) with (arm A) or without steroids (arms B and C) [4]. All transplantations were of low immunological risk, with recipient PRA scores ≤30% and no detectable DSA prior to transplantation (complement-dependent cytotoxicity cross-match) [4]. Further inclusion and exclusion criteria can be found in Thomusch et al. [4]. Suspected episodes of acute rejection were confirmed through biopsy according to the Banff criteria of 2005 [56]. For the e:KID project, which aims at early risk assessment of ACR by following a systems medicine approach [42, 43], 157 recipients were retrospectively monitored for the presence of HLA antibodies in blood serum on day 0 (pre-transplantation). All patients who experienced ACR (borderline or Banff class 1 or higher) in the first year were assigned to the ACR group ($N = 77$). The control group included all patients who neither experienced a rejection episode nor other serious adverse events ($N = 80$).

HLA antibody detection by Luminex multiplex bead assay

Screening for HLA class 1 and class 2 antibodies was performed using a MAB assay (LABScreen® Mixed Kit, One Lambda, Canoga Park, CA, USA). All sera that tested positive and a random subset of negative sera were subject to SAB assays to identify antibody specificities (LABScreen Single Antigen HLA Class I kit and/or LABScreen Single Antigen HLA Class II kit, One Lambda). Both MAB and SAB were performed according to the manufacturer's instructions. Briefly, following heat-inactivation at 56 °C for 30 min and clearance from debris (0.22 μm filter), 20 μl of undiluted serum was added to 3 μl of the LABScreen bead mix and incubated for 30 min in the dark at room temperature. After a washing step in 1x LABScreen wash buffer, the bead mix was incubated with 100 μl of a 1:100 dilution of the PE-conjugated goat anti-human IgG detection antibody for 30 min in the dark at room temperature. After a final washing step in 1x LABScreen wash buffer, data

acquisition was performed using a FLEXMAP3D Analyser in combination with xPONENT software version 4.1 (Luminex Corporation, Texas, USA).

Conventional HLA data processing and analysis

Key to the conventional method for HLA data processing is the binarization of the continuous xPONENT median fluorescence intensity (MFI) raw data by means of a MFI threshold (1 = presence of reactivity, 0 = absence of reactivity). For generation of binary data, raw MFI data were normalized to an in-house negative control serum (MAB) or the One Lambda negative serum OLINS (SAB). In case of MAB data, a bead was considered positive if its normalized background ratio exceeded 3. For binarization of SAB data, we used both a fixed threshold of 1000 MFI and an individually adjusted MFI threshold. In case of the latter, a bead was considered positive when its baseline normalized MFI exceeded 30% of the MFI of the bead showing the highest strength in reaction. Single parameter prediction performance of binarized HLA class I SAB data was assessed using Fisher's exact test. In the case of binarized HLA class reactivity screening data (MAB), study groups were compared using Fisher's exact test.

Experimental design and statistical rationale: novel strategy for HLA data processing and analysis

In this work we applied a novel approach to the HLA data sets that does not rely on MFI- thresholding. Key to it is the use of non-thresholded unprocessed continuous data, that is unprocessed raw MFI data given out by the FLEXMAP3D Analyser in combination with the xPONENT software. In contrast to the conventional approach, reactivity may take any value and is not limited to a binary set of values (reactivity/no reactivity). For downstream analyses these raw data are rank-transformed; they are not processed in any other way or form. To assess the predictive potential of the rank-normalized data, we performed multiparameter classification using an non-public R implementation of the Potential Support Vector Machine (P-SVM) algorithm [57]. An equivalent public release that can be run via command line or MatLab interface is provided under: <https://ml.jku.at/software/psvm/>. To assess the predictive performance of the classifier, we followed a leave-one-out cross-validation approach. The latter provides a well-established solution to assess a classifier's predictive performance for high-dimensional, low sample size data sets as ours [58]. To rate predictive performance, we used the statistical measures sensitivity (Sens.), specificity (Spec.) and balanced accuracy (BACC). To assess the statistical significance of the predictive performance, we used random class label-permutation testing. The significance level was set at $p < 0.05$. Training of the P-SVM classifier was performed using the function *psvm()*,

providing the matrix of training data, the class labels of the training data, the cost parameter C , the regularization parameter ϵ and the parameter *epsitol* as arguments. In case of classification of SAB data, we performed grid search for the hyperparameter space $\epsilon = \{0.25, 0.5, 0.75, 1\}$ and $C = \{1, 6\}$; the hyperparameter space for MAB data-based classification was $\epsilon = \{8, 9, 10, 11\}$ and $C = \{1, 6\}$. The parameter *epsitol* was set to 0.05 for all analyses. To predict the class labels of test data, we called the function *predict()* with the arguments *object* and *x* set to the trained classifier and the test data that is to be predicted, respectively. True classification and *p*-value estimation were always carried out for the same grid of hyperparameters. To further specify the performance of classifiers, receiver operating characteristic (ROC) curve analysis was performed. The numerical scores (decision values) that form the basis of P-SVM class identity label assignment were extracted by setting the argument *decision.values* of the *predict()* function to TRUE. After sorting the decision values in increasing order they were used as decision boundaries. For each boundary, both sensitivity and specificity were estimated. AUC was calculated based on Mann-Whitney U statistics [59].

Statistical analyses

To assess whether the two study groups (control/ACR) differed in any of the baseline population characteristics, Mann-Whitney U test (metric variables), Pearson's chi-squared or Fisher's exact test (categorical variables) were applied. A *p*-value < 0.05 was considered statistically significant. Variables are described with mean \pm standard deviation or median [interquartile range (IQR)].

Additional files

Additional file 1: Figure S1. Cumulative frequency of ACR through the first post-transplantation year. Frequency of patients in the ACR group who experienced at least one ACR event at different time points post-transplantation. At week 2 and month 3, 34% and 79% of patients in the ACR group had experienced an ACR event. (PDF 126 kb)

Additional file 2: Figure S2. Distribution of MFI cutoffs for generation of binary HLA class I SAB data. Illustrated are the MFI cutoff values of the 52 pre-transplant serum samples (control group = 18; ACR group, *Rej* = 34) of the binary HLA class I SAB data (1: presence of reactivity = above the MFI cutoff). (PDF 53 kb)

Additional file 3: Figure S3. Predictive performance of multiparameter ACR classification based on rank-normalized continuous pre-transplant MAB screening data. (A) Output of the classifiers decision function for each patient. The decision threshold is indicated by a dashed horizontal line. Patients with a decision value > 0 are classified as ACR, patients with a decision value < 0 are classified as control. Colors indicate whether patients tested positive (black) or negative (grey) for the presence of serum HLA-1 antibodies during MAB screening. (B) ROC curve of the multiparameter classifier. (PDF 211 kb)

Additional file 4: Table S1. Baseline characteristics and medication details for the Harmony patient ACR-control sub-cohort. Baseline characteristics and medication details for the Harmony patient ACR-control sub-cohort.^a (DOCX 18 kb)

Additional file 5: Table S2. Baseline characteristics and medication details for the patients with HLA MAB data.^a (DOCX 20 kb)

Additional file 6: Table S3. Single parameter pre-transplant prediction of ACR based on binarized HLA class 1 SAB data (fixed MFI threshold of 1000 MFI). (DOCX 18 kb)

Additional file 7: Table S4. Single parameter pre-transplant prediction of ACR based on binarized HLA class 1 SAB data (individually adjusted MFI threshold). (DOCX 18 kb)

Additional file 8: Table S5. Summary of existing AR prediction models. (DOCX 19 kb)

Abbreviations

ABMR: Acute antibody-mediated rejection; ACR: Acute cellular rejection; AR: Acute rejection; AUC: Area under the curve; BACC: Balanced accuracy; DSA: Donor-specific antibodies; IQR: Interquartile range; KTR: Kidney transplantation; MAB: Mixed HLA antigen bead; MFI: Median fluorescence intensity; post-Tx: Posttransplantation; PRA: Panel Reactive Antibodies; pre-Tx: Pretransplantation; P-SVM: Potential Support Vector Machine; ROC: Receiver operating characteristic; SAB: Single HLA antigen bead; Sens.: Sensitivity; Spec.: Specificity

Acknowledgements

The authors thank Dr. Nils Lachmann, Center for Tumor Medicine, H&L Laboratory, Charité University Medicine Berlin, for helpful advice and discussions. The authors also thank Ulrich Bodenhofer, now with QUOMATICA, Linz, Austria, and Sepp Hochreiter, Institute of Bioinformatics, Johannes Kepler University Linz, Austria, for insightful discussions. Part of this work was presented on the Kongress für Nephrologie 2018 – 10. Jahrestagung der Deutschen Gesellschaft für Nephrologie (DGfN), 27–30 September 2018 in Berlin (Germany).

Funding

This work was supported by the German Federal Ministry of Education and Research (BMBF) within the framework of the e:Med research and funding concept (01ZX1312). Funders had no role in study and collection of data, analysis, interpretation of data and writing of the manuscript.

Availability of data and materials

The datasets analysed during the current study are available from the corresponding author on reasonable request.

Authors' contributions

NW, EL, OT, KW, RS, CB, BS, PR, CH, HS, NB and MO contributed to sample collection and sample management. NW and MO contributed to study design. Data were generated by SH, data interpretation by NW, SH, CB, EL, ABN and MO and drafting of the manuscript by NW, ABN and MO. MO supervised the research and writing processes. All authors have contributed to the manuscript and approved the final version of the manuscript for submission.

Authors' information

The authors are part of the eKID consortium, an interdisciplinary group which has as its main aim the development and establishment a systems medicine approach to personalized immunosuppressive treatment at an early stage after kidney transplantation. The consortium's backgrounds areas include expertise in bioinformatics and machine learning (NW, ABN, CB, EL and MO), HLA antibody experimental analysis and immunology (NW, SH, KW, RS, BS, HS and MO), and the clinic of renal transplantation (PR, OT, CH and NB).

Ethics approval and consent to participate

The study was carried out in compliance with the Declaration of Helsinki and Good Clinical Practice. All participants provided written informed consent prior to inclusion into the study. The trial was approved by the Ethics Committee of the Universitätsklinikum Carl Gustav Carus Dresden. The trial is registered with ClinicalTrials.gov, number NCT00724022 (<https://clinicaltrials.gov/ct2/show/study/NCT00724022>). Date of registration was July 2008 (retrospectively registered), date of enrollment was June 2008.

Consent for publication

Not applicable.

Competing interests

The authors declare that they have no competing interests.

Publisher's Note

Springer Nature remains neutral with regard to jurisdictional claims in published maps and institutional affiliations.

Author details

¹Systems Immunology Lab, Department of Biology, Humboldt University Berlin, Berlin, Germany. ²Fraunhofer Institute for Cell Therapy and Immunology, Bioanalytics und Bioprocesses, Potsdam, Germany. ³Berlin-Brandenburg Center for Regenerative Therapies (BCRT), Berlin, Germany. ⁴MicroDiscovery GmbH, Berlin, Germany. ⁵Psoriasis Research and Treatment Center, Institute of Medical Immunology, Department of Dermatology and Allergy, Charité University Medicine Berlin, Berlin, Germany. ⁶Interdisciplinary Group of Molecular Immunopathology, Institute of Medical Immunology, Department of Dermatology and Allergy, Charité University Medicine Berlin, Berlin, Germany. ⁷Department of Nephrology and Internal Intensive Care, Charité University Medicine Berlin, Campus Virchow Clinic, Berlin, Germany. ⁸Berlin Center for Advanced Therapies (BeCAT), Charité University Medicine Berlin, Campus Virchow Clinic, Berlin, Germany. ⁹Molecular Immune Modulation, Institute for Medical Immunology, Charité University Medicine Berlin, Campus Virchow Clinic, Berlin, Germany. ¹⁰Klinik für Allgemein- und Viszeralchirurgie, Universitätsklinikum Freiburg, Freiburg, Germany. ¹¹University Hospital Carl Gustav Carus, Dresden University of Technology, Dresden, Germany. ¹²Medical Clinic I, Marien Hospital Herne, Ruhr University Bochum, Herne, Germany.

Received: 14 November 2018 Accepted: 8 April 2019

Published online: 27 April 2019

References

- Djamali A, Kaufman DB, Ellis TM, Zhong W, Matas A, Samaniego M. Diagnosis and management of antibody-mediated rejection: current status and novel approaches. *Am J Transplant.* 2014;14(2):255–71.
- Meier-Kriesche HU, Schold JD, Srinivas TR, Kaplan B. Lack of improvement in renal allograft survival despite a marked decrease in acute rejection rates over the Most recent era. *Am J Transplant.* 2004;4(3):378–83.
- Meier-Kriesche HU, Schold JD, Kaplan B. Long-term renal allograft survival: have we made significant progress or is it time to rethink our analytic and therapeutic strategies? *Am J Transplant.* 2004;4(8):1289–95.
- Thomusch O, Wiesener M, Opgenoorth M, Pascher A, Woitas RP, Witzke O, et al. Rabbit-ATG or basiliximab induction for rapid steroid withdrawal after renal transplantation (harmony): an open-label, multicentre, randomised controlled trial. *Lancet.* 2016;388:3006–16.
- Ciancio G, Burke GW, Gaynor JJ, Carreno MR, Cirocco RE, Mathew JM, et al. A randomized trial of three renal transplant induction antibodies: early comparison of tacrolimus, mycophenolate Mofetil, and steroid dosing, and newer immune-Monitoring1. *Transplantation.* 2005;80(4):457–65.
- Ekberg H, Tedesco-Silva H, Demirbas A, Vitko S, Nashan B, Gürkan A, et al. Reduced exposure to Calcineurin inhibitors in renal transplantation. *N Engl J Med.* 2007;357(25):2562–75.
- El-Zoghby ZM, Stegall MD, Lager DJ, Kremers WK, Amer H, Gloor JM, et al. Identifying specific causes of kidney allograft loss. *Am J Transplant.* 2009; 9(3):527–35.
- Roberts DM, Jiang SH, Chadban SJ. The treatment of acute antibody-mediated rejection in kidney transplant recipients—a systematic review. *Transp J.* 2012;94(8):775–83.
- Magil AB. Monocytes/macrophages in renal allograft rejection. *Transplant Rev.* 2009;23(4):199–208.
- Becker LE, Morath C, Suesal C. Immune mechanisms of acute and chronic rejection. *Clin Biochem.* 2016;49(4–5):320–3.
- Suthanthiran M, Schwartz JE, Ding R, Abecassis M, Dadhania D, Samstein B, Knechtle SJ, et al. Urinary-cell mRNA profile and acute cellular rejection in kidney allografts. *N Engl J Med.* 2013;369:20–31.
- Afaneh C, Muthukumar T, Lubetzky M, Ding R, Snopkowski C, Sharma VK, et al. Urinary cell levels of mRNA for OX40, OX40L, PD-1, PD-L1, or

- PD-L2 and acute rejection of human renal allografts. *Transplantation*. 2010;90(12):1381–7.
13. Hricik DE, Nickerson P, Formica RN, Poggio ED, Rush D, Newell KA, et al. Multicenter validation of urinary CXCL9 as a risk-stratifying biomarker for kidney transplant injury. *Am J Transplant*. 2013;13(10):2634–44.
 14. Roedder S, Sigdel T, Salomonis N, Hsieh S, Dai H, Bestard O, et al. The kSORT assay to detect renal transplant patients at high risk for acute rejection: results of the multicenter AART study. *PLoS Med*. 2014;11(11):e1001759.
 15. Wang JN, Zhou Y, Zhu TY, Wang X, Guo YL. Prediction of acute cellular renal allograft rejection by urinary metabolomics using MALDI-FTMS. *J Proteome Res*. 2008;7(8):3597–601.
 16. Reeve J, Einecke G, Mengel M, Sis B, Kayser N, Kaplan B, et al. Diagnosing rejection in renal transplants: a comparison of molecular- and histopathology-based approaches. *Am J Transplant*. 2009;9(8):1802–10.
 17. Desvaux D, Schwarzwinger M, Pastural M, Baron C, Abtahi M, Berrehar F, et al. Molecular diagnosis of renal-allograft rejection: correlation with histopathologic evaluation and antirejection-therapy resistance. *Transplantation*. 2004;78(5):647–53.
 18. Ting YT, Coates PT, Marti H-P, Dunn AC, Parker RM, Pickering JW, et al. Urinary soluble HLA-DR is a potential biomarker for acute renal transplant rejection. *Transplantation*. 2010;89(9):1071–8.
 19. Poggio ED, Augustine JJ, Clemente M, Danzig JM, Volokh N, Zand MS, et al. Pretransplant cellular Alloimmunity as assessed by a panel of reactive T cells assay correlates with acute renal graft rejection. *Transplantation*. 2007;83(7):847–52.
 20. Simon T, Opelz G, Wiesel M, Pelz S, Ott RC, Süsal C. Serial peripheral blood Interleukin-18 and perforin gene expression measurements for prediction of acute kidney graft rejection. *Am J Transplant*. 2003;3(1121–1127):1589–95.
 21. Hauser IA. Prediction of acute renal allograft rejection by urinary Monokine induced by IFN- (MIG). *J Am Soc Nephrol*. 2005;16(6):1849–58.
 22. Mancebo E, Castro MJ, Allende LM, Talayero P, Brunet M, Millán O, et al. High proportion of CD95+ and CD38+ in cultured CD8+ T cells predicts acute rejection and infection, respectively, in kidney recipients. *Transpl Immunol*. 2016;34:33–41.
 23. Dong W, Shunliang Y, Weizhen W, Qinghua W, Zhangxin Z, Jianming T, et al. Prediction of acute renal allograft rejection in early post-transplantation period by soluble CD30. *Transpl Immunol*. 2006;16(1):41–5.
 24. Malheiro J, Tafulo S, Dias L, Martins LS, Fonseca I, Beirão I, et al. Analysis of preformed donor-specific anti-HLA antibodies characteristics for prediction of antibody-mediated rejection in kidney transplantation. *Transpl Immunol*. 2015;32(2):66–71.
 25. Vlad G, Ho EK, Vasilescu ER, Colovai AI, Stokes MB, Markowitz GS, et al. Relevance of different antibody detection methods for the prediction of antibody-mediated rejection and deceased-donor kidney allograft survival. *Hum Immunol*. 2009;70(8):589–94.
 26. Riethmüller S, Ferrari-Lacraz S, Müller MK, Raptis DA, Hadaia K, Rüsi B, et al. Donor-specific antibody levels and three generations of crossmatches to predict antibody-mediated rejection in kidney transplantation. *Transp J*. 2010;90(2):160–7.
 27. Lefaucheur C, Loupy A, Hill GS, Andrade J, Nochy D, Antoine C, et al. Preexisting donor-specific HLA antibodies predict outcome in kidney transplantation. *J Am Soc Nephrol*. 2010;21(8):1398–406.
 28. Song EY, Lee YJ, Hyun J, Kim YS, Ahn C, Ha J, et al. Clinical relevance of pretransplant HLA class II donor-specific antibodies in renal transplantation patients with negative T-cell cytotoxicity crossmatches. *Ann Lab Med*. 2012;32(2):139–44.
 29. Salvadé I, Aubert V, Venetz JP, Golshayan D, Saouli AC, Matter M, et al. Clinically-relevant threshold of preformed donor-specific anti-HLA antibodies in kidney transplantation. *Hum Immunol*. 2016;77(6):483–9.
 30. Shaikhina T, Lowe D, Daga S, Briggs D, Higgins R, Khovanova N. Decision tree and random forest models for outcome prediction in antibody incompatible kidney transplantation. *Biomedical Signal Processing Control*. 2017; In press. DOI: <https://doi.org/10.1016/j.bspc.2017.01.012>.
 31. Ho EK, Vasilescu ER, Colovai AI, Stokes MB, Hallar M, Markowitz GS, et al. Sensitivity, specificity and clinical relevance of different cross-matching assays in deceased-donor renal transplantation. *Transpl Immunol*. 2008;20(1–2):61–7.
 32. Kannabhiran D, Lee J, Schwartz JE, Friedlander R, Aull M, Muthukumar T, et al. Characteristics of circulating donor human leukocyte antigen-specific immunoglobulin G antibodies predictive of acute antibody-mediated rejection and kidney allograft failure. *Transplantation*. 2015;99(6):1156–64.
 33. Poggio ED, Clemente M, Hricik DE, Heeger PS. Panel of reactive T cells as a measurement of primed cellular Alloimmunity in kidney transplant candidates. *J Am Soc Nephrol*. 2006;17:564–72.
 34. Vondran FWR, Timrott K, Kollrich S, Steinhoff AK, Kaltenborn A, Schrem H, et al. Pre-transplant immune state defined by serum markers and alloreactivity predicts acute rejection after living donor kidney transplantation. *Clin Transpl*. 2014;28(9):968–79.
 35. Nafar M, Farrokhi F, Vaezi M, Entezari AE, Pour-Reza-Gholi F, Firoozan A, et al. Pre-transplant and post-transplant soluble CD30 for prediction and diagnosis of acute kidney allograft rejection. *Int Urol Nephrol*. 2009;41(3):687–93.
 36. Hughes AK, Cichacz Z, Scheck A, Coons SW, Johnston SA, Stafford P. Immunosignaturing can detect products from molecular markers in brain cancer. *PLoS One*. 2012;7(7):e40201.
 37. Restrepo L, Stafford P, Johnston SA. Feasibility of an early Alzheimer's disease immunosignature diagnostic test. *J Neuroimmunol*. 2013 Jan;254(1–2):154–60.
 38. Stafford P, Cichacz Z, Woodbury NW, Johnston SA. Immunosignature for diagnosis of cancer. *Proc Natl Acad Sci U S A*. 2014 Jul;111(30):E3072–80.
 39. Legutki JB, Johnston SA. Immunosignatures can predict vaccine efficacy. *Proc Natl Acad Sci U S A*. 2013;110(46):18614–9.
 40. Cascalho MI, Chen BJ, Kain M, Platt JL. The paradoxical functions of B cells and antibodies in transplantation. *J Immunol*. 2013;190(3):875–9.
 41. Randhawa P. T-cell-mediated rejection of the kidney in the era of donor-specific antibodies: diagnostic challenges and clinical significance. *Curr Opin Organ Transplant*. 2015;20(3):325–32.
 42. Blazquez-Navarro A, Schachtner T, Stervbo U, Sefrin A, Stein M, Westhoff TH, et al. Differential T cell response against BK virus regulatory and structural antigens: a viral dynamics modelling approach. *PLoS Comput Biol*. 2018;14(5):1–20.
 43. Blazquez-Navarro A, Dang-Heine C, Wittenbrink N, Bauer C, Wolk K, Sabat R, et al. BKV, CMV, and EBV interactions and their effect on graft function one year post-renal transplantation: results from a large multi-Centre study. *EBioMedicine*. 2018;34:113–21.
 44. Sullivan HC, Liwski RS, Bray RA, Gebel HM. The road to HLA antibody evaluation: do not rely on MFI. *Am J Transplant*. 2017;XX:1–7.
 45. Konvalinka A, Tinckam K. Utility of HLA antibody testing in kidney transplantation. *J Am Soc Nephrol*. 2015;26(7):1489–502.
 46. Fairchild PJ, Wraith DC. Lowering the tone: mechanisms of immunodominance among epitopes with low affinity for MHC. *Immunol Today*. 1996;17(2):80–5.
 47. Haywood AM. Virus receptors: binding, adhesion strengthening, and changes in viral structure. *J Virol*. 1994;68(1):1–5.
 48. Hakomori S. Structure and function of Sphingoglycolipids in transmembrane Signalling and cell-cell interactions. *Biochem Soc Trans*. 1993;21(3):583–95.
 49. van der Merwe PA, Brown MH, Davis SJ, Barclay AN. Affinity and kinetic analysis of the interaction of the cell adhesion molecules rat CD2 and CD48. *EMBO J*. 1993;12(13):4945–54.
 50. Reilly PL, Woska JR, Jeanfavre DD, McNally E, Rothlein R, Bormann BJ. The native structure of intercellular adhesion molecule-1 (ICAM-1) is a dimer. Correlation with binding to LFA-1. *J Immunol*. 1995;155(2):529–32.
 51. Hage DS. Weak affinity chromatography. In: *Affinity chromatography methods and protocols*; 2000. p. 7–23.
 52. Szatmary P, Jones J, Hammad A, Middleton D. Impact of sensitivity of human leucocyte antigen antibody detection by Luminex technology on graft loss at 1 year. *Clin Kidney J*. 2013;6(3):283–6.
 53. Thomas KA, Valenzuela NM, Reed EF. The perfect storm: HLA antibodies, complement, FcγRs and endothelium in transplant rejection. *Trends Mol Med*. 2015;21(5):319–29.
 54. Pike R, Thomas N, Workman S, Ambrose L, Guzman D, Sivakumaran S, et al. PD1-expressing T cell subsets modify the rejection risk in renal transplant patients. *Front Immunol*. 2016;7:126.
 55. Zhang Q, Liu YF, Su ZX, Shi LP, Chen YH. Serum fractalkine and interferon-gamma inducible protein-10 concentrations are early detection markers for acute renal allograft rejection. *Transplant Proc*. 2014;46(5):1420–5.
 56. Solez K, Colvin RB, Racusen LC, Sis B, Halloran PF, Birk PE, et al. Banff '05 meeting report: differential diagnosis of chronic allograft injury and

- elimination of chronic allograft nephropathy ('CAN'). *Am J Transplant*. 2007; 7(3):518–26.
57. Hochreiter S, Obermayer K. Support vector machines for dyadic data. *Neural Comput*. 2006 Jun;18(6):1472–510.
58. Molinaro AM, Simon R, Pfeiffer RM. Prediction error estimation: a comparison of resampling methods. *Bioinformatics*. 2005;21(15):3301–7.
59. Mason SJ, Graham NE. Areas beneath the relative operating characteristics (ROC) and relative operating levels (ROL) curves: statistical significance and interpretation. *Q J R Meteorol Soc*. 2002;128(584):2145–66.

Ready to submit your research? Choose BMC and benefit from:

- fast, convenient online submission
- thorough peer review by experienced researchers in your field
- rapid publication on acceptance
- support for research data, including large and complex data types
- gold Open Access which fosters wider collaboration and increased citations
- maximum visibility for your research: over 100M website views per year

At BMC, research is always in progress.

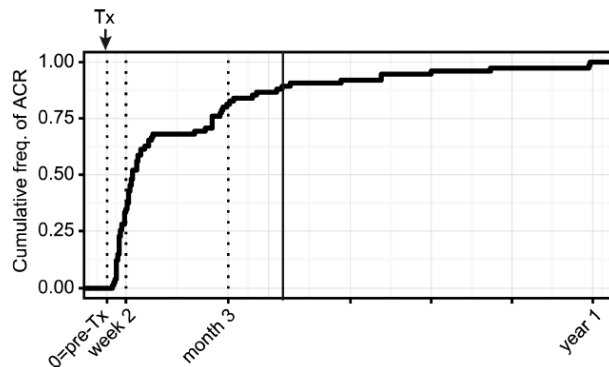
Learn more biomedcentral.com/submissions



9.2 Supplementary materials

9.2.1 Figure S1

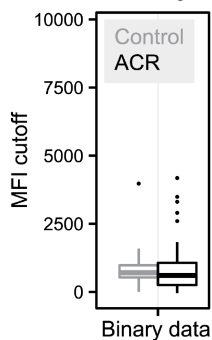
Cumulative frequency of ACR through the first post-transplantation year



Frequency of patients in the ACR group who experienced at least one ACR event at different time points post-transplantation. At week 2 and month 3, 34% and 79% of patients in the ACR group had experienced an ACR event.

9.2.2 Figure S2

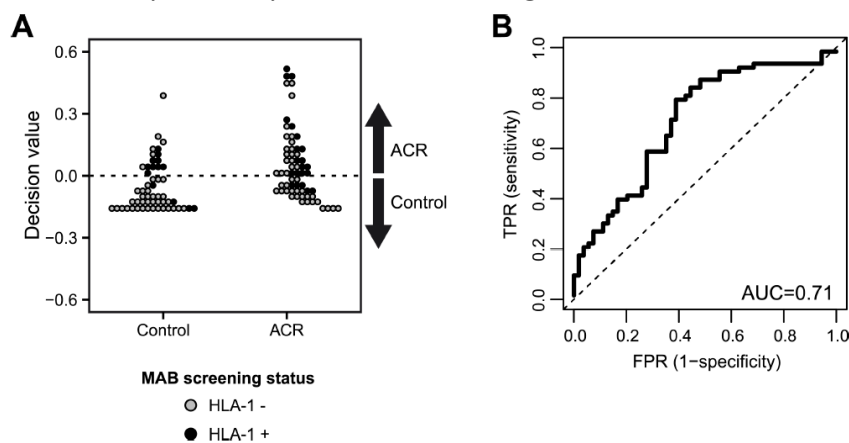
Distribution of MFI cutoffs for generation of binary HLA class 1 SAB data



Illustrated are the MFI cutoff values of the 52 pre-transplant serum samples (control group = 18; ACR group, Rej = 34) of the binary HLA class 1 SAB data (1: presence of reactivity = above the MFI cutoff).

9.2.3 Figure S3

Predictive performance of multiparameter ACR classification based on rank-normalized continuous pre-transplant MAB screening data.



(A) Output of the classifiers decision function for each patient. The decision threshold is indicated by a dashed horizontal line. Patients with a decision value > 0 are classified as ACR, patients with a decision value < 0 are classified as control. Colors indicate whether patients tested positive (black) or negative (grey) for the presence of serum HLA-1 antibodies during MAB screening. (B) ROC curve of the multiparameter classifier.

9.2.4 Table S1

Study population characteristics and medication details of the Harmony cohort^a

		ACR	Control	p-value
Number of kidney transplant recipients		77	80	-
Age at time of transplantation (years)		54.9 ± 12.1	49.5 ± 12.6	0.005
Body mass index at time of transplantation (kg/m ²)		27.0 ± 5.3	25.6 ± 4.6	0.09
Gender	Female	31 (40.3%)	29 (36.2%)	ns ^b
	Male	46 (59.7%)	51 (63.8%)	
Type of donor	Living	10 (13.0%)	19 (23.8%)	0.13 ^b
	Deceased	67 (87.0%)	61 (76.2%)	
Re-transplantation		5 (6.5%)	1 (1.3%)	0.11 ^c
HLA-A Mismatches	0	25 (32.5%)	33 (41.3%)	0.18 ^b
	1	38 (49.4%)	40 (50.0%)	
	2	14 (18.2%)	7 (8.7%)	
HLA-B Mismatches	0	13 (16.9%)	24 (30.0%)	0.09 ^b
	1	39 (50.6%)	39 (48.7%)	
	2	25 (32.5%)	17 (21.3%)	
HLA-DR Mismatches	0	16 (20.8%)	28 (35.0%)	0.03 ^b
	1	39 (50.6%)	41 (51.2%)	
	2	22 (28.6%)	11 (13.8%)	
PRA = 0%		70 (90.9%)	75 (93.4%)	ns ^c
Therapeutic Arm	A	25 (32.5%)	33 (41.3%)	ns ^b
	B	29 (37.7%)	21 (26.2%)	
	C	23 (29.9%)	26 (32.5%)	
Cold ischemia time: only deceased donors (min)		704 ± 290	718 ± 275	0.06

^aData are given as mean±standard deviation for quantitative variables and as number (frequency) for categorical variables. P values for quantitative variables were calculated by Mann-Whitney U test, for categorical variables either chi-squared (b) or Fisher's exact test (c) were employed.

ACR: acute cellular rejection; ns: non-significant; PRA: panel reactive antibody.

9.2.5 Table S2

Study population characteristics and medication details of the patients with HLA MAB data^a

		ACR	Control	p-value
Number of kidney transplant recipients		63	54	-
Age at time of transplantation (years)		55.8 ± 11.3	49.7 ± 12.6	0.007

Body mass index at time of transplantation (kg/m ²)		26.8 ± 5.3	25.1 ± 4.4	0.09
Gender	Female	26 (41.3%)	16 (29.6%)	ns ^b
	Male	37 (58.7%)	38 (70.4%)	
Type of donor	Living	8 (12.7%)	12 (22.2%)	ns ^b
	Deceased	55 (87.3%)	42 (77.8%)	
Re-transplantation		4 (6.3%)	0 (0.0%)	0.12 ^c
HLA-A Mismatches	0	20 (31.7%)	20 (37.0%)	ns ^b
	1	30 (47.6%)	29 (53.7%)	
	2	13 (20.6%)	5 (9.3%)	
HLA-B Mismatches	0	9 (14.3%)	12 (22.2%)	ns ^b
	1	34 (54.0%)	29 (53.7%)	
	2	20 (31.7%)	13 (24.1%)	
HLA-DR Mismatches	0	10 (15.9%)	20 (37.0%)	0.009 ^b
	1	35 (55.6%)	28 (51.9%)	
	2	18 (28.6%)	6 (11.1%)	
PRA = 0%		59 (93.7%)	51 (94.4%)	ns ^c
Therapeutic Arm	A	22 (34.9%)	20 (37.0%)	ns ^b
	B	21 (33.3%)	17 (31.5%)	
	C	20 (31.7%)	17 (31.5%)	
Cold ischemia time: only deceased donors (min)		710 ± 292	729 ± 293	0.10

^aData are given as mean±standard deviation for quantitative variables and as number (frequency) for categorical variables. P values for quantitative variables were calculated by Mann-Whitney U test, for categorical variables either chi-squared (b) or Fisher's exact test (c) were employed.

ACR: acute cellular rejection; ns: non-significant; PRA: panel reactive antibody.

9.2.6 Table S3

Single parameter pre-transplant prediction of ACR based on binarized HLA class 1 single antigen bead (SAB) data (fixed MFI threshold of 1000 MFI).

Serotype	Fisher's exact test p-value*		
A1	1.000	A36	1.000
A11	0.272	A43	1.000
A2	0.470	A66	0.287
A23	1.000	A68	0.648
A24	0.602	A69	1.000
A25	0.602	A74	NA
A26	0.272	A80	0.425
A29	1.000	B13	0.682
A3	0.346	B18	0.285
A30	1.000	B27	0.543
A31	0.346	B35	1.000
A32	1.000	B37	1.000
A33	0.272	B38	0.543
A34	0.648	B39	1.000
		B41	1.000

B42	1.000
B44	1.000
B45	1.000
B46	0.602
B47	1.000
B48	0.150
B49	0.543
B50	0.538
B51	0.399
B52	0.081
B53	1.000
B54	NA
B55	0.538
B56	1.000
B57	0.300
B58	0.698
B59	0.285
B60	0.543
B61	0.543
B62	1.000
B63	0.285
B64	NA
B65	NA
B67	0.538
B7 B	0.648

B71	1.000
B72	0.543
B73	1.000
B75	0.648
B76	0.327
B77	0.543
B78	1.000
B8 B	0.648
B81	0.648
B82	0.285
Cw1	0.115
Cw10	0.538
Cw12	0.346
Cw14	1.000
Cw15	0.648
Cw16	NA
Cw17	0.139
Cw18	1.000
Cw2	0.114
Cw4	1.000
Cw5	1.000
Cw6	1.000
Cw7	NA
Cw8	NA
Cw9	0.538

*P-values are not corrected for multiple testing.

ACR: acute cellular rejection; SAB: single antigen bead screening; NA: not applicable.

9.2.7 Table S4

Single parameter pre-transplant prediction of ACR based on binarized HLA class 1 single antigen bead (SAB) data (individually adjusted MFI threshold).

Serotype	Fisher's exact test p-value*
A1	1.000
A11	0.602
A2	1.000
A23	1.000
A24	1.000
A25	1.000
A26	0.272
A29	1.000
A3	1.000
A30	NA
A31	0.346
A32	1.000

A33	1.000
A34	0.399
A36	NA
A43	1.000
A66	1.000
A68	0.399
A69	0.399
A74	1.000
A80	0.272
B13	0.236
B18	0.543
B27	0.543
B35	0.648

B37	0.538
B38	0.538
B39	0.538
B41	0.538
B42	1.000
B44	1.000
B45	1.000
B46	1.000
B47	1.000
B48	0.081
B49	0.285
B50	0.538
B51	0.648
B52	0.150
B53	0.648
B54	1.000
B55	0.543
B56	0.538
B57	0.425
B58	1.000
B59	0.543
B60	0.285
B61	0.543
B62	0.543
B63	0.285
B64	1.000
B65	1.000
B67	0.538
B7 B	0.285
B71	0.543
B72	0.285
B73	NA
B75	0.150
B76	1.000
B77	0.285
B78	0.543
B8 B	0.538
B81	0.285
B82	1.000
Cw1	NA
Cw10	1.000
Cw12	0.346
Cw14	NA
Cw15	0.538
Cw16	NA
Cw17	0.081
Cw18	NA

Cw2	0.272
Cw4	1.000
Cw5	0.538
Cw6	1.000
Cw7	NA
Cw8	NA
Cw9	1.000

*P-values are not corrected for multiple testing.

ACR: acute cellular rejection; SAB: single antigen bead screening; NA: not applicable.

9.2.8 Table S5

Summary of existing AR prediction models

Manuscript	PMID	Sens. [%]	Spec. [%]	BACC* [%]	Marker	Pre-Tx	Donor-ind	Cohort
Song <i>et al.</i> 2012	22389881	100	87	93.5	HLA-2 DSA SAB	Yes	No	5 ABMR (2 Mixed ABMR+ACR) vs. 22 No ABMR (4 ACR)
Hauser <i>et al.</i> 2005	15857922	93.3	89	91.15	Urinary CXCL9	No	-	15 AR (14 ACR, 1 ABMR) vs. 54 No AR
Dong <i>et al.</i> 2006	16701175	87.1	91.8	89.45	sCD30	No	-	49 AR vs. 182 No AR
Lefaucheur <i>et al.</i> 2010	20634297	90.6	85.4	88	HLA DSA SAB	Yes	No	32 ABMR vs. 370 No ABMR (18 ACR)
Simon <i>et al.</i> 2003	15239627	82	90	86	Expression levels of Perforin and Granzyme B	No	-	17 AR vs. 50 No AR
Shaikhina <i>et al.</i> 2017	-	81.8	88.9	85.35	DSA HLA + IgG4 Levels + HLA Mismatches + Others	Yes	No	46 ABMR vs. 34 No ABMR
This work Wittenbrink <i>et al.</i> 2019	31029086	76.5	88.9	82.7	Quantitative HLA-1 SAB	Yes	Yes	34 ACR vs. 18 No AR
Riethmüller <i>et al.</i> 2010	20658760	75	90	82.5	HLA-1 DSA SAB	Yes	No	8 ABMR (Includes Chronic and Hyperacute; 5 Mixed) vs. 29 No ABMR (10 ACR)
Poggio <i>et al.</i> 2007	17460554	86	78	82	Elispot Panel of Reactive Cells	Yes	Yes	7 ACR (1 Mixed ABMR+ACR) vs. 23 No AR
Salvadé <i>et al.</i> 2016	27085791	70	93	81.5	HLA DSA SAB	Yes	No	10 ABMR vs. 14 No ABMR (2 ACR)
Mancebo <i>et al.</i> 2016	26773856	87.5	73.4	80.45	Proportion of CD95+ CD8+ T Cells	Yes	Yes	14 AR (2 ABMR) vs. 65 No AR
Pike <i>et al.</i> 2016	27148254	78	82.35**	80.17	PD1 Expression T cells	Yes	Yes	9 AR (1 ABMR) vs. 17 No AR
Malheiro <i>et al.</i> 2015	25661873	85.7	73.1	79.4	HLA DSA SAB	Yes	No	14 ABMR (5 Mixed ABMR+ACR) vs.

								26 No ABMR (2 ABMR)
Zhang <i>et al.</i> 2014	24935307	80	76.4	78.2	Fractalkine and IP10	No	-	15 ACR vs. 35 No AR
Vondran <i>et al.</i> 2014	24931031	75	69.2	72.1	sCD25, sCD30 and sCD44	Yes	Yes	7 ACR vs. 18 No AR (5 Borderline)
Nafar <i>et al.</i> 2009	19142743	70	71.7	70.85	sCD30	No	-	23 AR vs. 180 No AR

*Calculated by the authors of this study as the average of specificity and sensitivity.

** Not shown in the publication; calculated by the authors of this study.

ABMR: antibody-mediated rejection; ACR: acute cellular rejection; AR: acute rejection; BACC: balanced accuracy; Donor-ind: donor-independent marker; DSA: donor-specific antibodies; SAB: single antigen bead screening; Sens: sensitivity; Spec: specificity; NA: not applicable; PMID: PubMed Identifier; Pre-Tx: pre-transplantation marker.

10. Differential T cell response against BK virus regulatory and structural antigens: A viral dynamics modelling approach

This chapter refers to the manuscript published as:

Blazquez-Navarro A, Schachtner T, Stervbo U, Sefrin A, Stein M, Westhoff TH, Reinke P, Klipp E, Babel N, Neumann AU and Or-Guil M (2018). Differential T cell response against BK virus regulatory and structural antigens: A viral dynamics modelling approach. *PLOS Computational Biology*. 14(5):1-20. doi:10.1371/journal.pcbi.1005998

RESEARCH ARTICLE

Differential T cell response against BK virus regulatory and structural antigens: A viral dynamics modelling approach

Arturo Blazquez-Navarro^{1,2}, Thomas Schachtner^{1,3}, Ulrik Stervbo^{1,4}, Anett Sefrin³, Maik Stein¹, Timm H. Westhoff⁴, Petra Reinke^{1,3}, Edda Klipp⁵, Nina Babel^{1,4}, Avidan U. Neumann^{1,6,7}*, Michal Or-Guil²

1 Berlin-Brandenburg Center for Regenerative Therapies (BCRT), Charité-Universitätsmedizin, Berlin, Germany, **2** Systems Immunology Lab, Department of Biology, Humboldt-Universität zu Berlin, Berlin, Germany, **3** Department of Nephrology and Internal Intensive Care, Charité-Universitätsmedizin, Berlin, Germany, **4** Medical Clinic I, Marien Hospital Herne, Ruhr University Bochum, Herne, Germany, **5** Theoretical Biophysics Group, Department of Biology, Humboldt-Universität zu Berlin, Berlin, Germany, **6** Institute of Environmental Medicine, UNIKA-T, Helmholtz Zentrum München, Augsburg, Germany, **7** Institute of Computational Biology, Helmholtz Zentrum München, Munich, Germany

* These authors contributed equally to this work.

* auneumann@gmail.com



OPEN ACCESS

Citation: Blazquez-Navarro A, Schachtner T, Stervbo U, Sefrin A, Stein M, Westhoff TH, et al. (2018) Differential T cell response against BK virus regulatory and structural antigens: A viral dynamics modelling approach. *PLoS Comput Biol* 14(5): e1005998. <https://doi.org/10.1371/journal.pcbi.1005998>

Editor: Becca Asquith, Imperial College London, UNITED KINGDOM

Received: March 15, 2017

Accepted: January 24, 2018

Published: May 10, 2018

Copyright: © 2018 Blazquez-Navarro et al. This is an open access article distributed under the terms of the [Creative Commons Attribution License](https://creativecommons.org/licenses/by/4.0/), which permits unrestricted use, distribution, and reproduction in any medium, provided the original author and source are credited.

Data Availability Statement: All relevant data contained within this manuscript is available on Open Science Framework (<https://osf.io/vy9s7/>).

Funding: This work was supported by the German Federal Ministry of Education and Research (BMBF) within the framework of the e:Med research and funding concept (01ZX1312A, D, F, G), <https://www.bmbf.de/>. The funders had no role in study design, data collection and analysis,

Abstract

BK virus (BKV) associated nephropathy affects 1–10% of kidney transplant recipients, leading to graft failure in about 50% of cases. Immune responses against different BKV antigens have been shown to have a prognostic value for disease development. Data currently suggest that the structural antigens and regulatory antigens of BKV might each trigger a different mode of action of the immune response. To study the influence of different modes of action of the cellular immune response on BKV clearance dynamics, we have analysed the kinetics of BKV plasma load and anti-BKV T cell response (Elispot) in six patients with BKV associated nephropathy using ODE modelling. The results show that only a small number of hypotheses on the mode of action are compatible with the empirical data. The hypothesis with the highest empirical support is that structural antigens trigger blocking of virus production from infected cells, whereas regulatory antigens trigger an acceleration of death of infected cells. These differential modes of action could be important for our understanding of BKV resolution, as according to the hypothesis, only regulatory antigens would trigger a fast and continuous clearance of the viral load. Other hypotheses showed a lower degree of empirical support, but could potentially explain the clearing mechanisms of individual patients. Our results highlight the heterogeneity of the dynamics, including the delay between immune response against structural versus regulatory antigens, and its relevance for BKV clearance. Our modelling approach is the first that studies the process of BKV clearance by bringing together viral and immune kinetics and can provide a framework for personalised hypotheses generation on the interrelations between cellular immunity and viral dynamics.

decision to publish, or preparation of the manuscript.

Competing interests: The authors have declared that no competing interests exist.

Author summary

BK virus (BKV) is the cause of a kidney disease affecting 1–10% of kidney transplant recipients, which leads to transplantation failure in about 50% of the cases. This disease is not well understood, but there are indications that markers of the immune response against BKV can be used to predict the outcome. Since the immune response can act through different modes of action, we have studied the dynamics between immune response and virus to determine which modes of action play an important role in the fight against BKV. We have analysed immune and viral kinetics in six kidney transplantation patients and developed a mathematical model to integrate the data and better understand the interactions between virus and immune response to different BKV antigens. Our results allow for discarding the majority of action modes hypotheses. The most supported hypothesis is: structural proteins trigger the blocking of virus production by infected cells, whereas non-structural proteins trigger the acceleration of infected cells death. This difference could be central for disease outcome, as under this hypothesis only the latter would trigger a fast and continuous BKV clearance.

Introduction

In the last years, BK virus-associated nephropathy (BKVN) has become the most challenging infectious cause of renal graft dysfunction in kidney transplant, leading to graft failure in over 50% of cases [1,2]. The rise in BKVN incidence has been attributed, at least to some degree, to the increased potency of immunosuppressive drugs [3,4]. Given the absence of specific antiviral treatments, BKVN is handled by changing the immunosuppressive regimes of the patients, enabling the development of a specific antiviral immune response [3–5]. Diagnosis of BKVN is performed through renal biopsy [3,6–8] as progression of the illness occurs without clinical signs, except for an increase in serum creatinine concentrations [1]. In the absence of medical intervention, BKVN can cause extensive fibrosis and tubular atrophy in the allograft, leading to transplant loss [1,3,7]. This progression is accompanied by a high BK virus (BKV) plasma load. Therefore, screening of plasma BKV viral load is currently recommended for the monitoring of BKVN [8,9].

BKV is a non-enveloped virus with an icosahedral capsid and a small circular double-stranded DNA genome (~5kb), which encodes for the early regulatory proteins: small tumor antigen (st) and large tumor antigen (LT) (here collectively referred to as sLT antigens), the late structural viral proteins 1–3 (VP1, VP2 and VP3) (here referred to as VP antigens) and the agnoprotein [3,10]. Latent BKV infection is very common among the healthy population, with a prevalence above 80% [3,11–13].

In spite of a high frequency of self-limited BKV reactivation in kidney transplant recipients [12,14,15], only 1–10% [2] of transplant recipients do actually develop BKVN. To determine the factors leading to BKVN, much emphasis has been placed on the immune reaction against BKV antigens. sLT and VP antigens (but not the agnoprotein) have been demonstrated to elicit a T cell response, as we previously showed in our studies [16–18]. Our data suggest that cellular immune reaction has a prognostic value for BKVN evolution [16]. However, T cell response can act through a number of mechanisms—killing of infected cells, blocking virus production or infection, among others—which should have different impacts on viremia control. Although our data [16] suggest that VP and sLT antigens trigger substantially different immune responses, the experimental data alone do not allow to determine the relation between antigens, immune mechanisms and clearance. Sophisticated instruments, such as

mathematical models tailored for data analysis of this particular question, are required to formalise and analyse whether different antigens trigger different immune mechanisms and what these modes of action are.

The most widely used method for modelling viral dynamics is ordinary differential equations (ODE). It has, for instance, helped elucidate the dynamics of HIV-1, hepatitis and opportunistic viruses in transplant recipients [19]. It has also been used for the study of BKV, simulating the dynamics of viral production, predicting cytopathic effects of the virus and explaining the interactions between viral reactivation in tubular epithelial cells, urothelial cells, viremia and viruria [20,21]. However, to our knowledge, no model exists that incorporates the activation of the immune response with viral clearance dynamics.

Therefore, in this study we have retrospectively analysed the data of BKV plasma load kinetics and T cell responses against BKV antigens in six patients with biopsy-proven BKVN [16]. The objective of the analysis was to determine the dominant modes of action of the observed immune responses. For this, a tailor-made ODE model was generated, allowing for the formalisation of different hypotheses on the dominant modes of action of the immune response against BKVN.

To accomplish our goal, we pursued the following strategy: Firstly, we obtained a continuous curve that fits the time course of the T cell response data (Elispot) for each patient and antigen. Secondly, we designed an ODE model for the viral load clearance dynamics dependent on the T cell response curves. This model uses the former curves as input and simulates the dynamics of three variables: number of healthy cells, number of infected cells and BKV viral load. It incorporates three mechanisms of the immune system in viral clearance, allowing for the simulation of nine different hypotheses about dominant modes of action. Lastly, we evaluated all hypotheses for their capacity to reproduce the viral clearance data. Our results allowed for the discarding of most hypotheses and suggested that the anti-VP response induces the blocking of virus production while anti-sLT responses induces killing of infected cells. This difference in modes of action could be central for disease outcome, since only the sLT responses would trigger a fast and continuous BKV clearance under this hypothesis. These results could therefore have implications in the development of new immunotherapies against BKVN.

Results

Patient characteristics and clinical data

The study involved six renal transplant patients analysed in our previous study [16]. These six patients (called Patient A to F in the following) received renal transplants between 12/2004 and 05/2009 and developed severe BKV reactivation in follow-up. The patients were monitored for BKV viral load by quantitative polymerase chain reaction (qPCR). Cellular adaptive immune response against the BKV antigens (VP1, VP2, VP3, st and LT) was monitored by Interferon gamma (IFN- γ) Enzyme-Linked ImmunoSpot (Elispot), measured in spot forming units (SFU) per 10^6 peripheral blood mononuclear cells (PBMC). Elispot read-outs are known to accurately quantify antigen-specific T cell responses for BKV [22].

All patients had biopsy-proven BKVN and were initially treated with a tacrolimus-based immunosuppressive regimen. Tacrolimus is a calcineurin inhibitor. It inhibits T cell activation but does not have cell-depleting effects [23]. It is associated with significantly higher incidence of BKVN compared to cyclosporine A, a less potent calcineurin inhibitor [24]. Upon BKV reactivation and diagnosis of BKVN, tacrolimus was replaced by cyclosporine A. This immunosuppressant switch is a commonly used protocol against BKVN, as cyclosporine A is known to allow the onset of a T cell response against BKV [16,25]. Patients were monitored for BKV

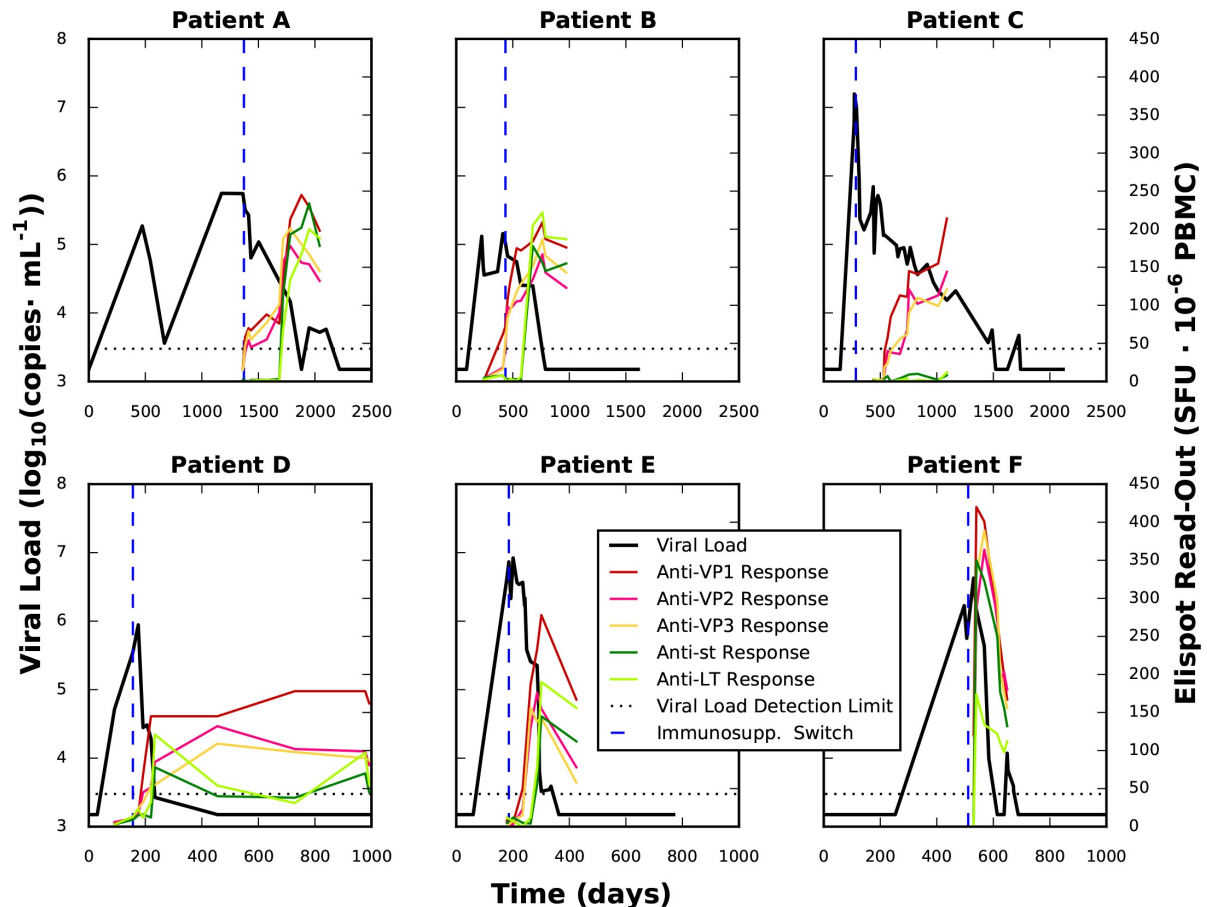


Fig 1. Viral load and immune response data of the patients. For each patient, the time course of viral load (black) and the Elispot read-out for each immunogenic BKV antigen (coloured) are plotted. The change of immunosuppressant therapy is marked as a dashed blue line. This change in immunosuppressant therapy is known to foster the development of an immune response against BKV. On the upper row the patients that had not cleared within 700 days after transplantation are shown, while those that achieved clearance in a shorter time appear in the lower row. Please note the difference of time scales between the rows.

<https://doi.org/10.1371/journal.pcbi.1005998.g001>

viral load during the complete evolution of the illness. The immune response was measured at the latest from the point of immunosuppressant switch until BKV clearance (Fig 1).

Description of viral load and Elispot experimental data

We observed a considerable diversity in the times needed to reach viremia clearance for each patient, ranging from 117 days after viremia onset for Patient F to 1744 days (~4 years) for Patient A. However, some common patterns could be observed. The immune response came generally in two waves, the first with an anti-VP immune response (red, pink and yellow lines in Fig 1) and the second, targeted against sLT antigens (light and dark green). Importantly, the immune response against VP was triggered for all but patient C within a relatively short span of time (< 70 days) after immunosuppressant switch. On the other hand, immune response against the sLT antigens was observed in only five patients. Again patient C did not show any

immune response against either sLT antigen. Based on the delay between the VP and the sLT immune responses, patients could be grouped in two categories: Patients D, E and F showed a short delay of approximately 30 days, while patients A and B showed a much longer delay of over 180 days.

The triggering of cellular immune responses against the BKV antigens occurred after the immunosuppressant switch. This immune response led to a progressive decrease of viral load until viral clearance was achieved. This decreasing phase took place for hundreds of days on most cases. In the five patients showing an anti-sLT immune response, the emergence of this response was tied to a substantially faster viral load decrease. This strongly suggests that the kind of immune response triggered by the sLT antigens is inherently different from the one triggered by VP antigens.

Fitting of a model of the immune response against BKV to obtain continuous curves describing the T cell response

With the goal of using the immune response data as an input for the viral load clearance dynamics model, we developed a simple curve based on one or more logistic functions to describe the experimentally observed T cell response. The use of logistic functions to describe T cell dynamics of antigen specific populations was chosen due to their simplicity and capacity to describe saturation-limited growth processes [26–28]. The model for one logistic function is

$$\frac{d}{dt} anti_a(t) = \begin{cases} 0, & \text{for } 0 \leq t \leq t_a \\ r_a \cdot anti_a(t) \cdot \left(1 - \frac{anti_a(t)}{max_{anti_a} \cdot (1 - dec_a \cdot t)} \right), & \text{for } t > t_a \end{cases} \quad (1)$$

$anti_a(t)$ is the T cell response for an antigen, where a represents the antigen that elicits the response. For the definition of parameters see Table 1. We chose the activation time t_a as a free parameter because the T cell response may start at different points in time for every antigen. As it is possible that an immune response presents multiple boosting episodes, we considered the possibility that at a second time point t_{a2} the parameters of the curve are replaced by a second set of parameters. We fitted this function to the BKV specific immune response against each of the five antigens (VP1, VP2, VP3, st and LT).

$t = 0$ was defined at a day for which there are both Elispot and viral load data and the viral load is maximum compared to all later measurements. This was defined as follows: Patient A, day 1363 after transplantation; B, day 412; C, day 538; D, day 175; E, day 235; and F, day 530. Simulations were performed until the time point viral load becomes undetectable or there are no further Elispot measurements. This time point was chosen because we aim to model only the clearance process. The objective function used for the fitting takes the form of vertical

Table 1. Immune function curve parameters.

Name	Meaning	Unit
t_a	Activation time of immune response	Days
r_a	Immune response growth rate	Days ⁻¹
max_{anti_a}	Maximum immune response	SFU · 10 ⁻⁶ PBMC
dec_a	Maximum response decay rate	Days ⁻¹

Definition of the parameters of the immune function curve (Eq 1)

<https://doi.org/10.1371/journal.pcbi.1005998.t001>

least-squares such that

$$f = \frac{\sum_{t=1}^N \sum_{a=1}^A (\log_{10}(\bar{y}(t, a)) - \log_{10}(y(t, a, p)))^2}{N} \quad (2)$$

where $\bar{y}(t, a)$ is the experimental value of the Elispot read-out at time t for antigen a . $y(t, a, p)$ is the calculated Elispot read-out for a given parameter set p . N is the total number of measurements and A is the number of screened antigens. The results of the parameter estimation are shown in S1 Table and Fig 2. As depicted in Fig 2, Eq 1 was sufficient to reproduce the immune response time courses of all six patients. For the immune response to the structural antigens of Patient A, a time point t_{a2} with a second parameter set was employed to achieve a minimum value for the objective function of $(4.16 \cdot 10^{-2})$, instead of the minimum achieved for only one parameter set $(2.24 \cdot 10^{-1})$ (see S1 Fig).

In order to study the differences in the mechanisms of the immune responses against structural (VP1, VP2, VP3) and regulatory (st, LT) antigens, the results of the fitting were summarised

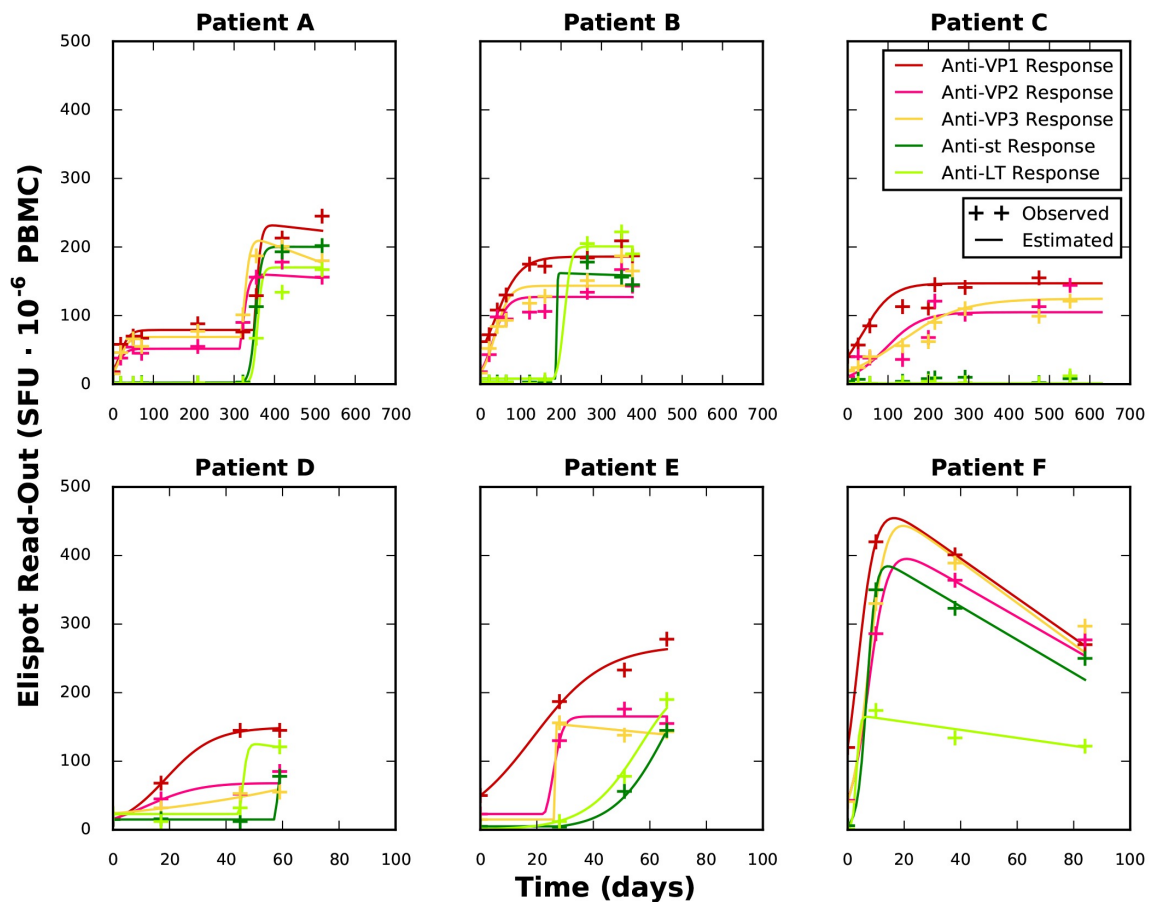


Fig 2. Fitting of immune response data. The calculated values for the immune response (lines) are plotted against the observed values (plus sign). Note the difference of time scales between the rows.

<https://doi.org/10.1371/journal.pcbi.1005998.g002>

in a VP function and a sLT function. These functions are employed in the model of BKV viral load clearance as an input, to model the influence of each immune response against BKV.

$$VP(t) = \max(anti_{VP1}(t), anti_{VP2}(t), anti_{VP3}(t)) - 1$$

$$sLT(t) = \max(anti_{sL}(t), anti_{LT}(t)) - 1 \quad (3)$$

The maximum value is taken under the assumption that the effects of the antigens are not additive, but that there is some degree of saturation. The functions are subtracted by one unit because 1 is the baseline value of the logistic curve $anti_a(t)$.

Model of BKV viral load clearance in dependence on immune response time course

The evolution of BKV viral load clearance was described using a modified version of a basic model of viral dynamics [29], such that

$$\frac{d}{dt}C(t) = g \cdot C(t) \cdot \left(1 - \frac{C(t) + I(t)}{max_c}\right) - d \cdot C(t) - \beta \cdot C(t) \cdot V(t) \cdot (1 - v(t))$$

$$\frac{d}{dt}I(t) = \beta \cdot C(t) \cdot V(t) \cdot (1 - v(t)) - d \cdot k \cdot I(t) \cdot (1 + m \cdot \mu(t))$$

$$\frac{d}{dt}V(t) = p \cdot I(t) \cdot (1 - \epsilon(t)) - c \cdot V(t) \quad (4)$$

This model contains three variables: number of healthy cells (C), number of infected cells (I) and BKV viral load in copies \cdot mL⁻¹ (V). Healthy cells proliferate at a rate proportional to g ; this rate is limited by max_c , which represents total number of cells (including both healthy and infected). Healthy cells die at a rate d and are infected in presence of virus at a rate β . Infected cells die at a rate $d \cdot k$, where k is virus-associated cytopathicity. Viruses are produced by the infected cells at a rate p and get cleared by the excretory system at a rate c . For a schematic representation of the model, see Fig 3. For a further definition of the parameters, see Table 2.

The three model variables (C , I and V) depend on the T cell response curves as defined in previous section. To study the mode of action of T cell responses, we consider that T cells can act via three mechanisms: (1) virus production blockage (described by function $\epsilon(t)$), (2) killing of the infected cells (described by function $\mu(t)$) and (3) infection blockage (described by function $v(t)$). $\epsilon(t)$, $\mu(t)$ and $v(t)$ take the form of the sum of Hill functions, a standard form for describing a saturating function, with a maximum value of 1, such that

$$\epsilon(t) = max_{\epsilon} \cdot \frac{VP(t)^{hill_{\epsilon}}}{\theta_{\epsilon}^{hill_{\epsilon}} + VP(t)^{hill_{\epsilon}}} + max_E \cdot \frac{sLT(t)^{hill_E}}{\theta_E^{hill_E} + sLT(t)^{hill_E}}$$

$$\mu(t) = max_{\mu} \cdot \frac{VP(t)^{hill_{\mu}}}{\theta_{\mu}^{hill_{\mu}} + VP(t)^{hill_{\mu}}} + max_M \cdot \frac{sLT(t)^{hill_M}}{\theta_M^{hill_M} + sLT(t)^{hill_M}}$$

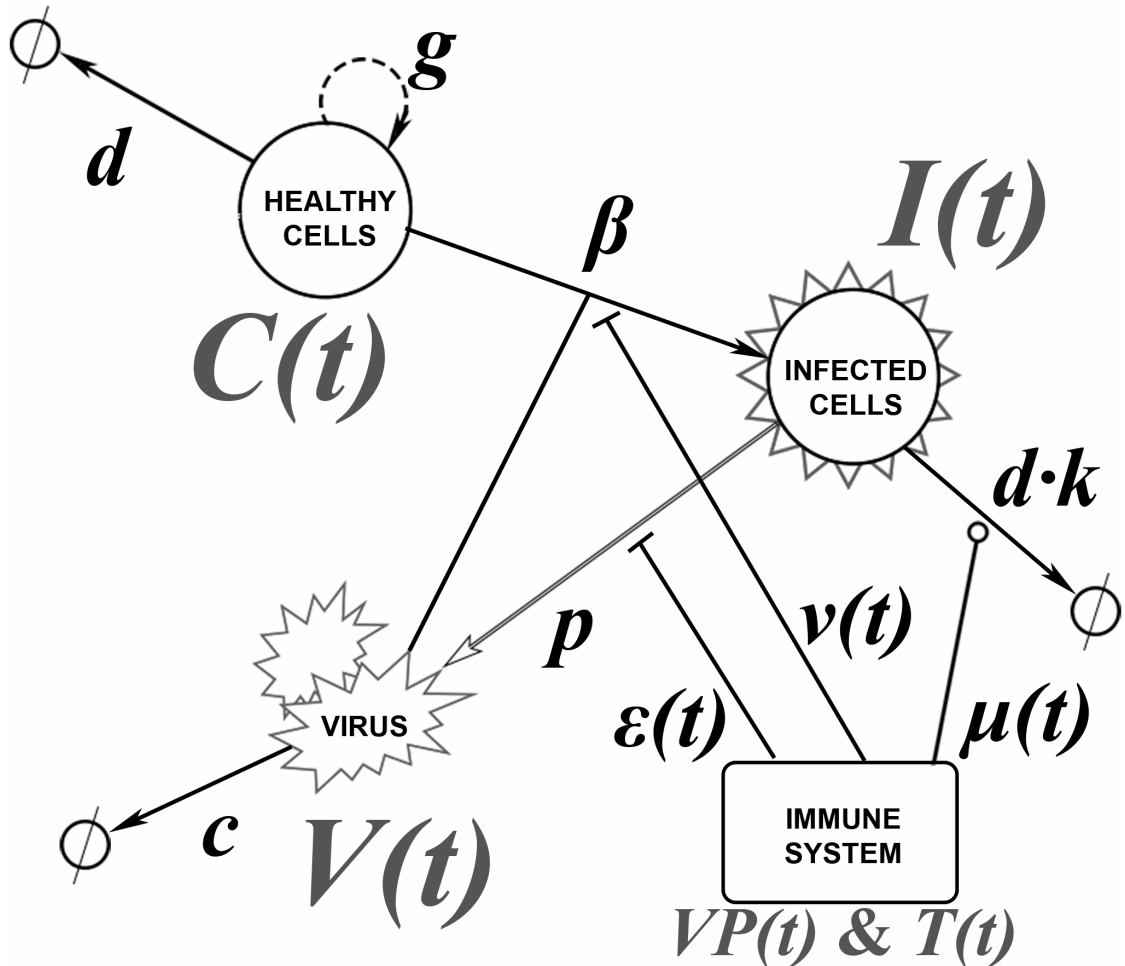


Fig 3. Schematic representation of the ODE model. Healthy cells produce other healthy cells (rate proportional to g) and die at rate d . The virus triggers the conversion of healthy cells into infected cells (rate β). Infected cells die at rate $d \cdot k$ and produce the virus at rate p , which is cleared at rate c . The immune system can intervene through three different mechanisms: blocking virus production ($\epsilon(t)$), enhancing infected cell death ($\mu(t)$) and blocking infection ($v(t)$).

<https://doi.org/10.1371/journal.pcbi.1005998.g003>

$$v(t) = \max_v \cdot \frac{VP(t)^{hill_v}}{\theta_v^{hill_v} + VP(t)^{hill_v}} + \max_N \cdot \frac{sLT(t)^{hill_N}}{\theta_N^{hill_N} + sLT(t)^{hill_N}}$$

$$\max_\epsilon + \max_E \leq 1$$

$$\max_\mu + \max_M \leq 1$$

$$\max_v + \max_N \leq 1 \quad (5)$$

Table 2. Viral load clearance model parameters.

Name	Meaning	Unit
g	Self-regeneration of healthy cells rate	Days ⁻¹
max_c	Maximum number of total cells	Cells
d	Cell death independent of viral cytotoxicity rate	Days ⁻¹
β	Cell infection rate	Copies ⁻¹ · mL · days ⁻¹
k	Viral cytopathicity factor	Unitless
p	Virus production rate	Copies · mL ⁻¹ · cells ⁻¹ · days ⁻¹
c	Virus clearing rate	Days ⁻¹
m	Maximum value of accelerated killing with $\mu(t)$	Unitless

Definition of the parameters of the viral load clearance model (Eq 4)

<https://doi.org/10.1371/journal.pcbi.1005998.t002>

where $\varepsilon(t)$, $\mu(t)$ and $v(t)$ depend on the $VP(t)$ and the $sLT(t)$ immune responses, as defined in Eq 3.

Hypotheses on immune modes of action on the BKV viral load clearance model

The objective of our work is to find the dominant modes of action responsible for viral load clearance. Therefore, we assume for the model that each one of the two immune responses ($VP(t)$ and $sLT(t)$) acts through only one mode of action, either $\varepsilon(t)$, $\mu(t)$ or $v(t)$ (Eq 5). As these are three modes of action and two antigen-specific responses, nine different hypotheses on the relationship between dominant modes of action and immune response are possible. These nine hypotheses are referenced here following this convention: For example, the hypothesis that anti-VP triggers a $\mu(t)$ response (accelerated killing) and anti-sLT triggers a $v(t)$ response (infection blockage) is named $VP\mu$ -sLT v hypothesis. For the definition and description of all nine hypotheses, see S2 Table.

Testing of hypotheses for dominant modes of action of the immune system in BKV clearance

To evaluate the feasibility of the hypotheses for dominant modes of action of the immune system, the model was fitted against the BKV clearance data for all nine hypotheses. The parameters c , g , d , β and p were estimated based on previous publications. Parameter k was estimated for each hypothesis based on one particular patient, while the remainder of the parameters were estimated individually for each patient and hypothesis.

The rate constant c for virus clearance was fixed to the value calculated by Funk *et al.* [30]. In the case of g , which is the maximum replication capacity for $C(t) + I(t) \ll max_c$, cell culture results show a maximum duplication rate of approximately one day for renal foetal kidney cells [31]. Therefore, for the sake of simplicity we assigned a value of 1 days⁻¹ for g . For the cell death rate of healthy cells d , a value of 0.01 days⁻¹ was used on a model of similar structure for Hepatitis C virus [32] and it was deemed to be reasonable estimation here. The value of the virus production rate p was calculated in the same model to be 100 copies · mL⁻¹ · cells⁻¹ · days⁻¹ [32]. Given that BKV is a less aggressive infection, we deemed it reasonable to assume a value of 15 copies · mL⁻¹ · cells⁻¹ · days⁻¹. This has the property that, for $I(t) = V(t)$ and no immune reaction, the viral load is in a steady state. Likewise, as the cell infection rate β for the Hepatitis C virus was estimated to be $3 \cdot 10^{-7}$ copies⁻¹ · mL · days⁻¹ [32], a value of $3 \cdot 10^{-8}$ copies⁻¹ · mL · days⁻¹ for BKV was assumed. Patient C had the slowest progression of viral

clearance, which suggests that immune cytotoxic effects were relatively low. Therefore, we estimated the viral cythopathic factor (k) for all patients using data obtained from Patient C. The model as defined by Eqs 3–5 was fitted for all nine hypotheses (S2 Table) with the objective function

$$f = \frac{\sum_{t=1}^N (\log_{10}(\bar{y}(t)) - \log_{10}(y(t, p)))^2}{N} \quad (6)$$

which takes the form of vertical least-squares. N is the total number of measurements, $\bar{y}(t)$ is the viral load at the time t , $y(t, p)$ is the simulated viral load for a parameter set p and time t . The initial conditions for all cases were

For $t = 0$:

$$\begin{aligned} C(0) &= \max_c - \frac{c}{p} \cdot V(0) \\ I(0) &= \frac{c}{p} \cdot V(0) \\ V(0) &= V(0) \end{aligned} \quad (7)$$

so that, at time $t = 0$ and no immune response, viral load is in steady state. $V(0)$ is defined as the observed viral load at $t = 0$. $t = 0$ was defined as above. The results obtained for the fittings, as well as the model selection criterion (see Materials and methods) for each hypothesis and patient, are shown in Table 3.

The results in Table 3 were interpreted to discard hypotheses based on the Δ BIC score and the value of the objective function. Accordingly, there is good empirical support to generally discard hypotheses VPv-sLTv and VPv-sLTc as probable mechanisms for viral clearance.

Table 3. Results of the model fitting for the hypotheses on dominant immune modes of action.

Patient	Measurement	VPc-sLTc	VPc-sLTμ	VPc-sLTv	VPμ-sLTc	VPμ-sLTμ	VPμ-sLTv	VPv-sLTc	VPv-sLTμ	VPv-sLTv
Number parameters		7	6	5	6	7	6	5	6	7
A	f	0.11957	0.03090	0.06613	0.05490	0.04409	0.06091	0.14584	0.05053	1.88160
	Δ BIC	11.4180	0.0000	3.3800	4.0233	4.4336	4.7510	8.9165	3.4425	30.7098
B	f	0.06843	0.01120	0.06046	0.03153	0.02190	0.02233	0.06159	0.01994	0.06227
	Δ BIC	14.6151	0.0000	9.8562	7.2449	6.6399	4.8297	9.9857	4.0387	13.9550
C	f	0.01280	0.01030	0.01230	0.01070	0.01070	0.01070	0.01050	0.01050	0.01020
	Δ BIC	5.6813	0.0000	2.48438	0.5334	3.1725	0.5334	0.2692	0.2692	2.5025
D	f	0.00005	0.00044	0.10923	0.01080	0.18563	0.15925	0.01870	0.13048	2.33900
	Δ BIC	0.0000	7.2157	27.9327	20.0636	32.8264	30.8273	20.8732	30.0301	42.9616
E	f	0.17314	0.05591	0.25664	0.05083	0.08718	0.11018	3.03501	0.28754	2.40041
	Δ BIC	11.8850	0.7632	10.8748	0.0000	6.3957	6.1895	30.6372	13.8637	32.9195
F	f	1.25703	0.15598	1.31113	0.24925	0.21315	0.12060	1.31455	0.12063	4.25438
	Δ BIC	10.7624	1.0289	8.1584	2.9039	3.6644	0.0000	8.1688	0.0008	15.6392
f_{SUM}		1.63101	0.26472	1.81587	0.40800	0.56264	0.48397	4.58619	0.61961	10.94786
Median Δ BIC		11.0902	0.3816	9.0073	3.4636	5.4146	4.7903	9.4511	3.7406	23.1745

The results for the objective function f (Eq 6) and Δ BIC (Eqs 8 and 9) are shown for each one of the hypotheses and patients. The sum of the objective functions over all patients is shown as f_{SUM} . In bold are highlighted: The lowest per patient values for f , as well as the scores of Δ BIC within the range of substantial empirical support (<2). The definitions of the hypotheses are shown in S2 Table. Detailed results of the model selection criteria are shown in S3 Table. S2 Fig shows the results of the fittings for each hypothesis, compared to the best-performing hypothesis.

<https://doi.org/10.1371/journal.pcbi.1005998.t003>

Table 4. Parameter for the viral load clearance model under hypothesis VPε-sLTμ.

Parameter	Type	Patients					
		A	B	C	D	E	F
g	Fixed value	1.00					
d	Fixed value	$1.00 \cdot 10^{-2}$					
p	Fixed value	15.00					
β	Fixed value	$3 \cdot 10^{-8}$					
c	Fixed value	15.00					
k	Fixed value	1.02					
max_c	Estimated value	$5.52 \cdot 10^5$	$6.91 \cdot 10^5$	$3.39 \cdot 10^5$	$1.91 \cdot 10^8$	$3.78 \cdot 10^6$	$1.17 \cdot 10^7$
	95% Confidence interval	$[5.52 \cdot 10^5, 7.07 \cdot 10^5]$	$[5.44 \cdot 10^5, 1.46 \cdot 10^6]$	$[2.86 \cdot 10^5, 3.62 \cdot 10^5]$	$[1.43 \cdot 10^8, 2.64 \cdot 10^8]$	$[3.69 \cdot 10^6, 1.43 \cdot 10^9]$	$[4.25 \cdot 10^6, 5.53 \cdot 10^7]$
m	Estimated value	48.3	4.27	-	15.8	25.9	24.9
	95% Confidence interval	[47.3, 55.9]	[4.21, 4.86]	-	[13.2, 18.5]	[16.4, 41.6]	[11.5, 86.5]
$hill_e$	Estimated value	$2.00 \cdot 10^{-1}$	$8.59 \cdot 10^{-1}$	$1.12 \cdot 10^2$	$8.93 \cdot 10^{-1}$	1.92	$1.82 \cdot 10^{-9}$
	95% Confidence interval	$[1.85 \cdot 10^{-1}, 2.07 \cdot 10^{-1}]$	$[8.44 \cdot 10^{-1}, 8.61 \cdot 10^{-1}]$	$[1.07 \cdot 10^2, 1.15 \cdot 10^2]$	$[7.96 \cdot 10^{-1}, 9.05 \cdot 10^{-1}]$	[1.00, 2.88]	$[1.80 \cdot 10^{-61}, 4.45 \cdot 10^{-1}]$
θ_e	Estimated value	$1.08 \cdot 10^2$	$1.16 \cdot 10^2$	$1.48 \cdot 10^2$	$3.15 \cdot 10^{-1}$	61.0	78.7
	95% Confidence interval	$[1.04 \cdot 10^2, 1.37 \cdot 10^2]$	$[48.2, 1.45 \cdot 10^2]$	$[1.36 \cdot 10^2, 1.70 \cdot 10^2]$	$[9.02 \cdot 10^{-2}, 3.76 \cdot 10^{-1}]$	[5.93, 89.4]	$[3.07 \cdot 10^{-4}, 1.68 \cdot 10^8]$
$hill_\mu$	Estimated value	$1.30 \cdot 10^2$	$1.34 \cdot 10^2$	-	98.6	$1.36 \cdot 10^2$	$1.13 \cdot 10^2$
	95% Confidence interval	$[1.29 \cdot 10^2, 1.30 \cdot 10^2]$	$[1.28 \cdot 10^2, 1.34 \cdot 10^2]$	-	[47.5, $1.49 \cdot 10^2$]	$[38.8, 1.74 \cdot 10^2]$	$[19.5, 1.49 \cdot 10^2]$
θ_μ	Estimated value	$2.04 \cdot 10^2$	$2.00 \cdot 10^2$	-	22.7	87.3	$2.10 \cdot 10^2$
	95% Confidence interval	$[2.03 \cdot 10^2, 2.04 \cdot 10^2]$	$[1.99 \cdot 10^2, 2.00 \cdot 10^2]$	-	[22.2, 29.2]	$[50.0, 1.19 \cdot 10^2]$	$[1.37, 3.28 \cdot 10^2]$
f	Obj. Function	$3.10 \cdot 10^{-2}$	$1.12 \cdot 10^{-2}$	$1.03 \cdot 10^{-2}$	$4.40 \cdot 10^{-3}$	$5.60 \cdot 10^{-2}$	$1.56 \cdot 10^{-1}$

Results of the fitting for the viral clearance model (Eqs 3–5) under hypothesis VPε-sLTμ (S2 Table) for all six patients. The last row indicates the value of the objective function (Eq 6).

<https://doi.org/10.1371/journal.pcbi.1005998.t004>

Hypotheses VPμ-sLTv, VPε-sLTv, VPε-sLTε, VPμ-sLTμ and VPv-sLTμ can only be considered as possible mechanisms for individual patients but not for the entire patient cohort. Hypothesis VPμ-sLTε cannot be discarded but does not show the highest degree of empirical support.

The hypothesis VPε-sLTμ has the lowest median ΔBIC and thus the highest empirical support. For five out of six patients, this hypothesis was within the range of substantial empirical support (ΔBIC < 2) [33], while no other hypothesis had comparable support for more than two patients. This hypothesis associates an anti-VP response with virus production blockage and an anti-sLT response with accelerated killing of infected cells. The hypothesis VPε-sLTμ is shown compared to the other alternative hypotheses in S2 Fig.

Results of the parameter estimation, confidence intervals and the objective function for the VPε-sLTμ hypothesis are shown in Table 4. The fitted model for each patient is shown on Fig 4.

In spite of the good results of the fitting, the estimated values of the parameters should be taken with caution. The results show heterogeneity between patients, especially max_c , $hill_e$ and θ_e , with a range of around 3 orders of magnitude. This could be partly caused by parameter uncertainty, as supported by the 95% confidence intervals, which for some parameters range over 2 orders of magnitude. However, the variation of parameters between patients is larger than the confidence intervals for each patient, confirming that the high variation is not solely a

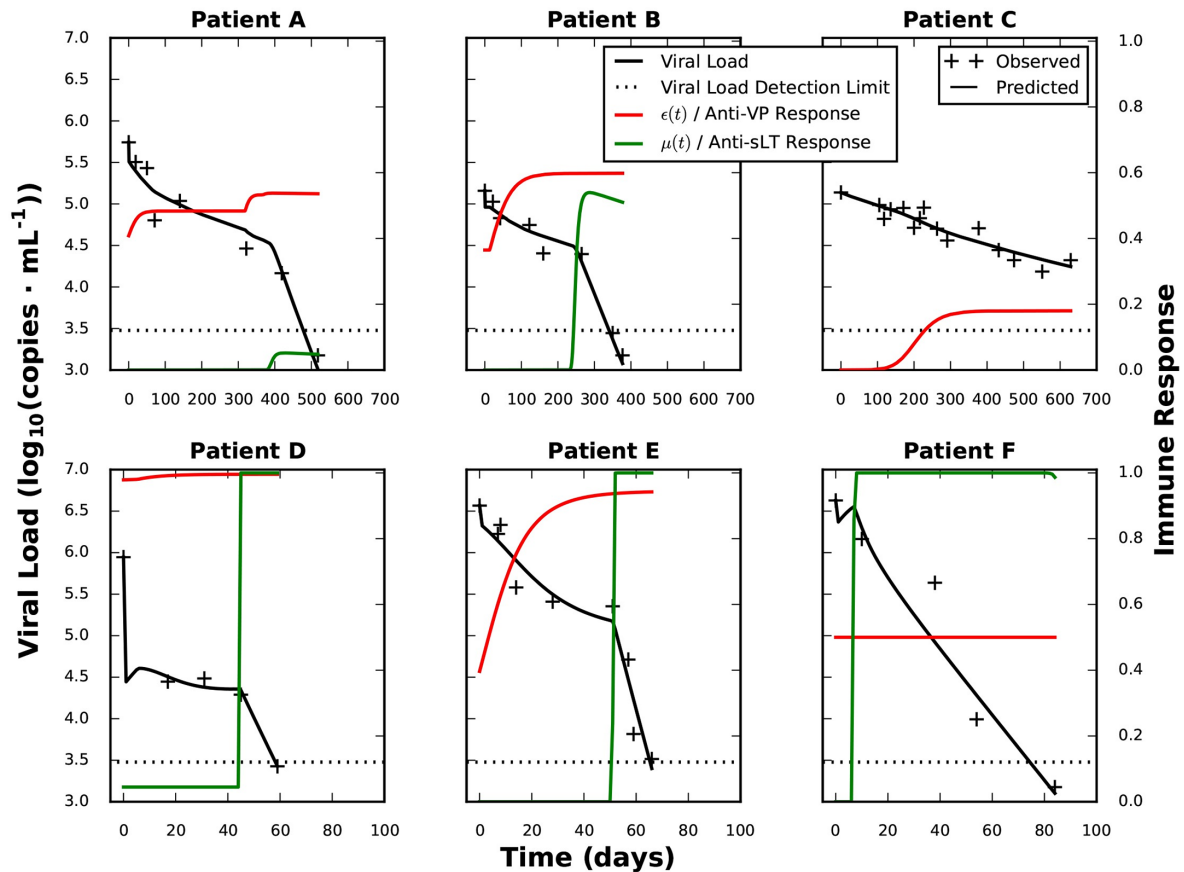


Fig 4. Modelled time course of BKV viral load clearance for hypothesis VPε-sLTμ. The results of the model (Eqs 3–5) under hypothesis VPε-sLTμ (S2 Table) using the parameters in Table 4 are plotted: viral load ($V(t)$) is shown as a black line, the immune responses virus production blockage ($\epsilon(t)$) and accelerated killing of infected cells ($\mu(t)$) are shown in green and red, respectively. Observed viral load values are shown as black plus signs. Please note the difference of time scales between the rows.

<https://doi.org/10.1371/journal.pcbi.1005998.g004>

product of parameter uncertainty. This is not surprising, as there is a very high degree of variation in the clearing time courses of the patients.

Note that the fitted parameters summarise complex biological processes, as opposed to reflecting fundamental mechanisms, rendering it difficult to interpret parameter variations. Nevertheless, fundamental biological variation between patients is conceivable. A clear case is patient F. This patient had a simultaneous activation of the anti-VP and anti-sLT immune response, and the extremely low estimate for $hill_{\epsilon}$ and very broad confidence intervals $hill_{\epsilon}$ and θ_{ϵ} , suggest that the anti-sLT immune response through the μ mode of action could have a saturating effect over the anti-VP immune response. In fact, assuming only an anti-sLT response for patient F led to an increase of f of less than 5% in comparison to the original VPε-sLTμ, with substantially lower BIC values (see S3 Table). This result supports the possibility of a saturating anti-sLT response for this patient.

Sensitivity analysis of the model

To analyse the impact of the chosen values for the fixed parameters g , d , p , β and k on the behaviour of the model, a sensitivity analysis was performed. The goal was to analyse whether the same quality of fitting and qualitative behaviour of the model can be achieved for different values of these parameters. The analysis was performed following the principle of one-factor-at-a-time. The value of a single parameter was modified over a span ranging from a factor 0.1 of the original value up to 10; for each new value of the parameter a fitting was performed to minimise the value of the objective function (Eq 6). The detailed results of the sensitivity analysis are shown in S4 Table, the results for the extreme values (factors 0.1. and 10) are plotted in S3 Fig.

Briefly, the results show that the model VPε-sLTμ can robustly simulate the viral clearance dynamics of the six patients and is not sensitive to variations of the fixed parameters: For the extreme values (factors 0.1 and 10), fittings with $f_{\text{SUM}} < 0.4$ were achieved in all cases. This is especially relevant when comparing the results with those for the mode of action hypotheses (Table 3), where the best alternative hypothesis had a $f_{\text{SUM}} = 0.40800$. Taken together, the results of the analysis reinforce the relevance of the hypothesis VPε-sLTμ, demonstrating that it is able to fit the viral dynamics better than the other hypotheses, even when modifying the fixed parameters across two orders of magnitude.

Discussion

In this work we have created the first model that provides evidence of the dominant modes of action involved in the clearance of BKV. It is the first model that covers the process of BKV clearance harmonising the viral and immune dynamics and formalising different modes of action of the immune system and their influence on the viral dynamics. It incorporates the influence of the adaptive immune system on the clearance of BKV reactivation in a patient-to-patient basis by considering multiple antigens and immune reactions against the same viral infection and highlighting certain patterns of the process of immunological re-arming against BKV after immunosuppressant switch. Our results show that immune modes of action can be captured by acquisition of time series of blood markers not directly related to mechanistic observations. Taken together, our work can be used as a tool for personalised hypothesis generation and evaluation of the modes of action through which the immune system successfully fights against BKVN.

Our model suggests that for VP-specific cellular immune response, the dominant mode of action is reducing the rate of virus production, while the mode of action triggered by sLT-anti-gen specific T cells is an increased death rate of infected cells. This remarkable feature would be central for BKV clearance: the VP-triggered immune response would cause an initial drop in the viral load, leading to a plateau, where reduction of the viral load is slower than $0.5 \log_{10}(\text{virus} \cdot \text{mL}^{-1})$ every 100 days. Only the acceleration of death of infected cells, triggered by the sLT antigens, would lead to a fast and continuous clearance of the viral load. It further suggests that in cases of simultaneous anti-VP and anti-sLT response, the latter response would play the central role in viral clearing.

This hypothesis, VPε-sLTμ, achieved substantial empirical support for five out of six patients, while none of the alternative hypotheses on dominant modes of action had substantial empirical support for more than two patients. Even though one alternative hypothesis could be used to fit the viral dynamics of the patients satisfactorily, the VPε-sLTμ hypothesis achieved the lowest total value for the objective function.

The suggested VP-triggered blockage of virus production can be linked mechanistically to the action of some cytokines, such as type I-interferons; while sLT-triggered accelerated

killing can be associated with cytotoxic cells. This qualitatively different role of both antigen groups is in agreement with biological evidence provided by a previous flow cytometry-based study on VP1- and LT-specific CD4⁺ and CD8⁺ T-cells in patients with BKV reactivation [34]. In this work, VP1 elicited a significantly higher response in CD4⁺ T-cells than in CD8⁺ T-cells. In the case of the LT antigen, even though there was no significant difference between the magnitude of the CD4⁺ and the CD8⁺ T-cell responses, CD8⁺ cells were significantly more likely to respond against LT than VP1. The agreement between the hypothesis with the highest empirical support and the cited study highlights, in our opinion, the capabilities of using our model as an instrument for hypothesis generation on the physiological background of BKV clearance.

Interestingly, our model highlights a feature of heterogeneity among patients, the delay between anti-VP and anti-sLT immune response, as central for BKV dynamics, linking it to the previously presented division of patients into two groups—with a first group (upper row in Fig 4) clearing the infection after over 300 days and a second group (lower row) clearing the infection in around 100 days after immunosuppressant switch—in terms of an increased clearance speed associated with anti-sLT immune response. Our model highlights the close relationship between viral clearance and this delay, underscoring that anti-sLT specific T cells are needed for clearance. A delay between VP and sLT responses has been observed in two previous studies [16,34]. However, in spite of having been observed repeatedly, there is to our knowledge at present no discussion in the literature on this striking factor. Possible causes could be related to the different ways of VP and sLT antigen presentation or to the effects of immunosuppression. Based on the results of our model, we would welcome more profound experimental and theoretical research on the reasons underlying the delay.

Moreover, our results suggest that heterogeneity is not confined to the delay between immune responses but is a central feature of the BKV clearing dynamics: For certain individual patients, hypotheses other than $VP\epsilon$ -sLT μ might be specifically suitable to explain their viral clearance dynamics. There is also a high degree of variation in the estimated values of the parameters between individuals for each hypothesis. A part of this variation may stem from physiological differences. For example, in the case of patient F, for whom particularly extreme values for some parameters were found, this can be linked to this patient being the only one with simultaneous activation of anti-VP and anti-sLT immune responses: Analyses suggested that the latter response could have a saturating effect, rendering the former irrelevant for the viral dynamics.

A relevant aspect of the model is that the dynamics of the immune response and their dependence on viral load were not explicitly modelled. The influence of the immune response on viral load is taken into account but the hypothetical contribution of BKV viral load to the building of an immune reaction is not addressed. This approach was chosen due to the high complexity and heterogeneity of the dynamics of immune reaction after immunosuppressant switch—especially the VP-sLT delay. Given that the mechanisms underlying this delay are currently unknown, we consider it to be highly unlikely that using currently available knowledge the immune response can be predicted from viral load.

The findings of our work on immune modes of action are especially relevant for future immunotherapeutic approaches against BKVN, since they suggest that the immune response against regulatory sLT antigens is central for BKV clearance. The use of T cells specific for BKV regulatory antigens is an interesting clinical approach, which has recently been shown to be technically possible [35]. In this study, the authors established a protocol for the ex-vivo generation of T cells specific for the antigens VP1 and LT, offering evidence of the specificity and safety of these cells [35].

Our BKV clearance modelling approach provides a framework for the hypothesis generation on the interrelations between cellular immunity and viral load at a personalised basis. Further research with the model could help us to improve therapeutic approaches in patients with BKVN, with the final aim of preventing kidney graft failure. The results of our model strongly suggest a general association between different target antigens and distinct mechanisms of the cellular immune system, linking structural VP antigens with the blockage of viral production and regulatory sLT antigens with cytotoxic effects. It further highlights the essential role of anti-sLT antigen response in clearance. These results should serve as a stimulus for further research on the differences between anti-VP and anti-sLT responses, particularly on their mechanisms, exploring possible physiological differences between patients in this respect. A suggested method could involve complementing the Elispot analysis with flow cytometry analysis of different cell populations reacting to each antigen (e.g. CD4⁺, CD8⁺, T helper 17, T regulatory) at all time points of the clearance process, with a special emphasis on the differences between the early- and late-stage responses. The knowledge gained through these experiments, as well as further implementations of our model, could open the door to the use of immunotherapy in the treatment, and perhaps prevention, of BKVN. Modelling approaches built upon our work could then be used in a personalised basis to tailor the therapy according to the characteristics of their viral and immune dynamics.

Materials and methods

Ethics statement

This study was approved by our local ethical review committee in compliance with the declaration of Helsinki. Informed consent was obtained from all patients (Ethic Committee Charité University Medicine, Berlin, Germany, 126/2001, 07/30/2001).

Monitoring of BKVN patients

Patients were monitored for serum BKV viral load from 4/2006 to 9/2012 and for BKV specific immune response against VP and sLT from 01/2008 to 07/2010 as described in our previous study [16]. Screening for viral load was performed monthly over the first six months after kidney transplantation, then every three months, and again monthly during active BKV reactivation, while screening for specific immune response with Elispot was performed monthly since approximately the change of immunosuppressive therapy, until BKV clearance (<3000 copies·mL⁻¹). A total of 167 viral load samples and 98 Elispot samples were collected. BKVN was confirmed by histological examination of the graft biopsy.

Screening of BKV viral load

BKV viral load was measured by qPCR as described previously [15]. Briefly, BKV viral load was measured with TaqMan Real Time PCR. DNA was isolated from serum using a QIAamp DNA Mini Kit (Qiagen Corp., Hilden, Germany) according to the instructions of the manufacturer. PCR was performed with the TaqMan platform (ABI). PCR amplifications were set up in a reaction volume of 25 μ L using primer and probe at final concentrations of 900 nM and 5 μ M, respectively, amplifying the VP1 region of BKV. A plasmid standard containing the VP1 coding region of respective virus was used to determine the copy number per millilitre. Thermal cycling was begun with an initial denaturation step at 95°C for 10 min that was followed by 40 cycles at 95°C for 15 s and 60°C for 1 min.

Screening of anti-BKV immune reaction

BKV-specific T cell immune response was determined by IFN- γ Elispot upon stimulation of PBMC with 5 different BKV proteins (VP1, VP2, VP3, st and LT) as described in our previous study [16]. Briefly, PBMC were isolated from 10–20 mL of heparinised blood using the standard Ficoll Hypaque density gradient centrifugation technique. For the Elispot assay, 96-well multiscreen filter plates (MAIPS 4510, Millipore, Billerica, MA, USA) were coated with 100 μ L of primary IFN- γ monoclonal antibody (mAb) at a concentration of 3 μ g/mL (IFNG M700A, Endogen, Woburn, MA, USA) and incubated overnight at 4°C. A standardised responder T-cell number of 2.5×10^5 PBMC per well was added in quadruple or at least triplicate wells with one of the five stimulating peptides (1 μ g/mL). Staphylococcus enterotoxin B (SEB; Sigma, Munich, Germany, 1 μ g/mL) was used as positive control and negative controls were run in parallel using responder cells plus medium alone. Probes were incubated for 24 hours at 37°C. The detection of IFN- γ took place after an overnight incubation at 4°C with 100 μ L (1 μ L/mL) biotinylated detection IFN- γ antibody (IFNG-M701-B Biotin, Endogen). After adding streptavidine (1 μ g/mL) for 2 hours at room temperature, spots were developed by adding 200 μ L visualization solution, AEC (3-amino-9-ethylcarbazole, Sigma) in acetate buffer supplemented with H₂O₂ 30% for 3–5 min. Resulting spots were counted using a computer-assisted Elispot reader (Immunospot, Cellular Technologies, Ltd., Cleveland, OH, USA). The number of SFU $\cdot 10^{-6}$ PBMC was calculated by adding spot counts from each well.

Parameter estimation of the mathematical models

The models were fitted using the function `fminsearch` of the mathematical open-access software Scilab, which employs the Nelder-Mead algorithm [36]. To ensure that the minimum of the objective function is reached, several replications (> 100) of the estimation were performed, using vastly different (> 2 orders of magnitude in some cases) starting parameter sets. The objective functions for the immune dynamics and the viral dynamics, which take the form of vertical least-squares, are defined in the Results section (Eqs 2 and 7).

To avoid overestimating the degrees of freedom of each hypothesis, parameters appearing only as the product of two free parameters are considered as only one free parameter. This is the case for model $VP_{\mu}\text{-}sLT_{\mu}$, where $m \cdot max_{\mu}$ and $m \cdot max_M$ are estimated as two parameters, instead of three parameters.

Model selection

Bayesian Information Criterion (BIC) differences were employed as the model selection criterion. Additionally, the Akaike's Information Criterion (AIC) was also calculated. The corrected Akaike's Information Criterion (AICc) was not used, as its value was not calculable for certain patient/hypotheses combinations. BIC and AIC were estimated for each patient i and hypothesis h under the assumption of independent, normally distributed errors

$$\begin{aligned} BIC_{ih} &= N_i \ln f_{ih} + K_{ih} \ln N_i \\ AIC_{ih} &= N_i \ln f_{ih} + 2K_{ih} \end{aligned} \quad (8)$$

where N_i is the total number of measurements per patient i , K_{ih} is the number of parameters for patient i and hypothesis h , and f_{ih} is the objective function for patient i and hypothesis h as

defined in Eq 6. [33] AIC and BIC differences were calculated as

$$\Delta BIC_{ih} = BIC_{ih} - \min(BIC_i)$$

$$\Delta AIC_{ih} = AIC_{ih} - \min(AIC_i) \quad (9)$$

where the function min denotes the lowest AIC or BIC achieved for a patient. A difference in the range [0, 2] for ΔBIC_{ih} is considered to give substantial empirical support for the hypothesis h in patient i [33].

Estimation of 95% confidence intervals

95% confidence intervals were estimated using bootstrapping, as described in Banks *et al.* [37]. Briefly, for each of the six patients the dynamics were simulated with the best-performing hypothesis (VPe-sLTμ) and the best-fitting parameter set (Table 4). Residuals for the viral load were calculated as the difference between predicted and observed viral load for each time point. The residuals of each patient (excluding the first residual, which is zero by definition) were randomly resampled with replacement 1000 times, constructing 1000 artificial data sets for each patient, each with the same number of measurements as the patient. These artificial data sets were subject to fitting using as initial parameter values those in Table 4. The obtained distribution of estimated parameters for each patient was employed to calculate the 95% confidence intervals: for a normal distribution of parameter values for a patient, the confidence intervals were calculated as the mean $\pm 1.96 \cdot$ standard deviation; for skewed distributions (absolute value of skewness or kurtosis higher than 2), the 95% confidence intervals were calculated directly from the 25th and 975th entries in the set of ordered parameter estimates.

Supporting information

S1 Table. Parameters for the immune function curve. Results of the fitting for the immune response model in Eq 1 for all six patients and five antigens.
(PDF)

S2 Table. Hypotheses on the dominant modes of action of the immune system as defined by the model. Description of the possible hypotheses on the dominant modes of action of the immune response against VP and sLT antigens, as defined by the model (Eqs 3–5).
(PDF)

S3 Table. Detailed results for the model comparison criteria of the fittings for the nine hypotheses. The results for patient F and hypothesis VPe-sLTμ are shown additionally under the special assumption of a saturating sLT response.
(PDF)

S4 Table. Results of the sensitivity analysis for the fixed parameters.
(PDF)

S1 Fig. Comparison of anti-VP responses fittings for patient A. Results of the fitting assuming only one activation event, compared to the fitting for two activation events.
(TIF)

S2 Fig. Comparison of the fittings of the hypotheses to the best-performing hypothesis. The hypotheses are shown in order of increasing f_{SUM}
(PDF)

S3 Fig. Plotting of the sensitivity analysis results for the extreme parameter values. Note that for k only $k = 10.7$ was plotted, as $k = 0.107$ is not biologically meaningful. (PDF)

Author Contributions

Conceptualization: Arturo Blazquez-Navarro, Ulrik Stervbo, Edda Klipp, Avidan U. Neumann, Michal Or-Guil.

Data curation: Arturo Blazquez-Navarro, Ulrik Stervbo, Avidan U. Neumann.

Formal analysis: Arturo Blazquez-Navarro.

Funding acquisition: Nina Babel, Avidan U. Neumann, Michal Or-Guil.

Investigation: Thomas Schachtner, Anett Sefrin, Maik Stein, Timm H. Westhoff, Petra Reinke, Nina Babel.

Methodology: Arturo Blazquez-Navarro, Avidan U. Neumann, Michal Or-Guil.

Project administration: Nina Babel, Avidan U. Neumann, Michal Or-Guil.

Resources: Petra Reinke, Nina Babel, Avidan U. Neumann, Michal Or-Guil.

Software: Arturo Blazquez-Navarro.

Supervision: Edda Klipp, Nina Babel, Avidan U. Neumann, Michal Or-Guil.

Validation: Arturo Blazquez-Navarro.

Visualization: Arturo Blazquez-Navarro, Avidan U. Neumann, Michal Or-Guil.

Writing – original draft: Arturo Blazquez-Navarro, Avidan U. Neumann, Michal Or-Guil.

Writing – review & editing: Thomas Schachtner, Ulrik Stervbo, Anett Sefrin, Maik Stein, Timm H. Westhoff, Petra Reinke, Edda Klipp, Nina Babel.

References

1. Ramos E, Drachenberg CB, Wali R, Hirsch HH. The decade of polyomavirus BK-associated nephropathy: state of affairs. *Transplantation*. 2009; 87: 621–630. <https://doi.org/10.1097/TP.0b013e318197c17d> PMID: 19295303
2. Comoli P, Binggeli S, Ginevri F, Hirsch HH. Polyomavirus-associated nephropathy: update on BK virus-specific immunity. *Transpl Infect Dis*. 2006; 8: 86–94. <https://doi.org/10.1111/j.1399-3062.2006.00167.x> PMID: 16734631
3. Hirsch HH, Steiger J. Polyomavirus BK. *Lancet Infect Dis*. 2003; 3: 611–623. PMID: 14522260
4. Hirsch HH. BK virus: opportunity makes a pathogen. *Clin Infect Dis*. 2005; 41: 354–360. <https://doi.org/10.1086/431488> PMID: 16007533
5. Rinaldo CH, Hirsch HH. Antivirals for the treatment of polyomavirus BK replication. *Expert Rev Anti Infect Ther*. 2007; 5: 105–115. <https://doi.org/10.1586/14787210.5.1.105> PMID: 17266458
6. Purighalla R, Shapiro R, McCauley J, Randhawa P. BK virus infection in a kidney allograft diagnosed by needle biopsy. *Am J Kidney Dis*. 1995; 26: 671–3. PMID: 7573026
7. Trofe J, Gordon J, Roy-Chaudhury P, Koralknik IJ, Atwood WJ, Alloway RR, et al. Polyomavirus nephropathy in kidney transplantation. *Prog Transplant*. 2004; 14: 130–140. PMID: 15264457
8. Nickeleit V, Singh HK, Mihatsch MJ. Polyomavirus nephropathy: morphology, pathophysiology, and clinical management. *Curr Opin Nephrol Hypertens*. 2003; 12: 599–605. PMID: 14564196
9. Bennett WM, Meyer L, Ridenour J, Batiuk TD. Surveillance and modification of immunosuppression minimizes BK virus nephropathy. *Am J Nephrol*. 2010; 32: 10–2. <https://doi.org/10.1159/000313888> PMID: 20484894
10. Babel N, Volk HD, Reinke P. BK polyomavirus infection and nephropathy: the virus—immune system interplay. *Nat Rev Nephrol*. 2011 May 24; 7(7): 399–406. <https://doi.org/10.1038/nrneph.2011.59>

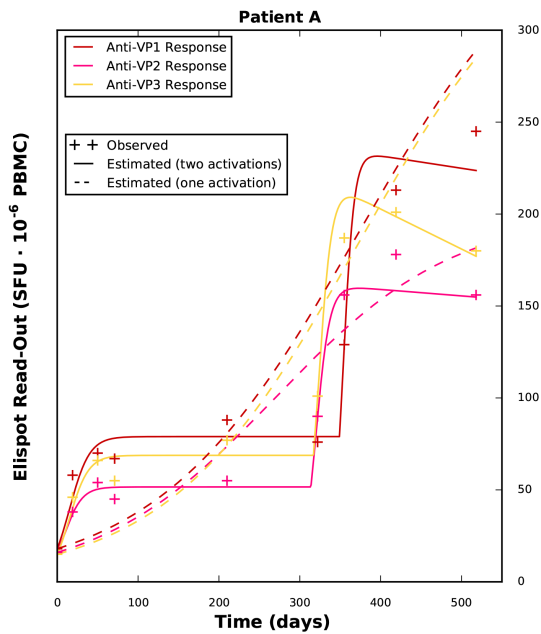
11. Egli A, Infanti L, Dumoulin A, Buser A, Samaridis J, Stebler C, et al. Prevalence of Polyomavirus BK and JC Infection and Replication in 400 Healthy Blood Donors. *J Infect Dis*. 2009; 199: 837–846. <https://doi.org/10.1086/597126> PMID: 19434930
12. Hirsch HH, Knowles W, Dickenmann M, Passweg J, Klimkait T, Mihatsch MJ, et al. Prospective study of polyomavirus type BK replication and nephropathy in renal-transplant recipients. *N Engl J Med*. 2002; 347.
13. Egli A, Binggeli S, Bodaghi S, Dumoulin A, Funk GA, Khanna N, et al. Cytomegalovirus and polyomavirus BK posttransplant. *Nephrol Dial Transplant*. 2007; 22: viii72–viii82. <https://doi.org/10.1093/ndt/gfm648> PMID: 17890268
14. Hirsch HH, Vincenti F, Friman S, Tuncer M, Citterio F, Wiecek A, et al. Polyomavirus BK replication in de novo kidney transplant patients receiving tacrolimus or cyclosporine: a prospective, randomized, multicenter study. *Am J Transplant*. 2013; 13: 136–145. <https://doi.org/10.1111/j.1600-6143.2012.04320.x> PMID: 23137180
15. Babel N, Fendt J, Karaivanov S, Bold G, Arnold S, Seifin A, et al. Sustained BK viremia as an early marker for the development of BKV-associated nephropathy: analysis of 4128 urine and serum samples. *Transplantation*. 2009; 88: 89–95. <https://doi.org/10.1097/TP.0b013e3181aa8f62> PMID: 19584686
16. Schachtner T, Müller K, Stein M, Diezemann C, Seifin A, Babel N, et al. BK virus-specific immunity kinetics: a predictor of recovery from polyomavirus BK-associated nephropathy. *Am J Transplant*. 2011; 11: 2443–52. <https://doi.org/10.1111/j.1600-6143.2011.03693.x> PMID: 21831150
17. Trydzenskaya H, Sattler A, Müller K, Schachtner T, Dang-Heine C, Friedrich P, et al. Novel approach for improved assessment of phenotypic and functional characteristics of BKV-specific T-cell immunity. *Transplantation*. 2011; 92: 1269–77. <https://doi.org/10.1097/TP.0b013e318234e0e5> PMID: 22124284
18. Mueller K, Schachtner T, Sattler A, Meier S, Friedrich P, Trydzenskaya H, et al. BK-VP3 as a New Target of Cellular Immunity in BK Virus Infection. *Transplantation*. 2011; 91: 100–107. <https://doi.org/10.1097/TP.0b013e3181fe1335> PMID: 21452414
19. Perelson AS. Modelling viral and immune system dynamics. *Nat Rev Immunol*. 2002 Jan; 2(1): 28–36.
20. Funk GA, Gosert R, Comoli P, Ginevri F, Hirsch HH. Polyomavirus BK replication dynamics in vivo and in silico to predict cytopathology and viral clearance in kidney transplants. *Am J Transplant*. 2008; 8: 2368–77. <https://doi.org/10.1111/j.1600-6143.2008.02402.x> PMID: 18925904
21. Funk GA, Steiger J, Hirsch HH. Rapid dynamics of polyomavirus type BK in renal transplant recipients. *J Infect Dis*. 2006; 193: 80–87. <https://doi.org/10.1086/498530> PMID: 16323135
22. Chakera A, Bennett S, Lawrence S, Morteau O, Mason PD, O'Callaghan CA, et al. Antigen-specific T cell responses to BK polyomavirus antigens identify functional anti-viral immunity and may help to guide immunosuppression following renal transplantation. *Clin Exp Immunol*. 2011; 165: 401–409. <https://doi.org/10.1111/j.1365-2249.2011.04429.x> PMID: 21671906
23. Wiseman AC. Immunosuppressive medications. *Clin J Am Soc Nephrol*. 2016; 11: 332–343. <https://doi.org/10.2215/CJN.08570814> PMID: 26170177
24. Renner FC, Dietrich H, Bulut N, Celik D, Freitag E, Gaertner N, et al. The risk of polyomavirus-associated graft nephropathy is increased by a combined suppression of cd8 and cd4 cell-dependent immune effects. *Transplant Proc*. Elsevier Inc.; 2013; 45: 1608–1610. <https://doi.org/10.1016/j.transproceed.2013.01.026> PMID: 23726630
25. Johnston O, Jaswal D, Gill JS, Doucette S, Fergusson DA, Knoll GA. Treatment of Polyomavirus Infection in Kidney Transplant Recipients: A Systematic Review. *Transplantation*. 2010; 89: 1057–1070. <https://doi.org/10.1097/TP.0b013e3181d0e15e> PMID: 20090569
26. Cappuccio A, Elishmereni M, Agur Z. Cancer immunotherapy by interleukin-21: Potential treatment strategies evaluated in a mathematical model. *Cancer Res*. 2006; 66: 7293–7300. <https://doi.org/10.1158/0008-5472.CAN-06-0241> PMID: 16849579
27. Perelson AS, Nelson PW. Mathematical Analysis of HIV-1 Dynamics in Vivo. *SIAM Rev*. 1999; 41: 3–44. <https://doi.org/10.1137/S0036144598335107>
28. Huang Y, Rosenkranz SL, Wu H. Modeling HIV dynamics and antiviral response with consideration of time-varying drug exposures, adherence and phenotypic sensitivity. *Math Biosci*. 2003; 184: 165–186. [https://doi.org/10.1016/S0025-5564\(03\)00058-0](https://doi.org/10.1016/S0025-5564(03)00058-0) PMID: 12832146
29. Wodarz D, Nowak MA. Mathematical models of HIV pathogenesis and treatment. *BioEssays*. 2002; 24: 1178–1187. <https://doi.org/10.1002/bies.10196> PMID: 12447982
30. Funk GA, Steiger J, Hirsch HH. Rapid dynamics of polyomavirus type BK in renal transplant recipients. *J Infect Dis*. 2006; 193: 80–87. <https://doi.org/10.1086/498530> PMID: 16323135

31. Kim S-S, Gwak S-J, Han J, Park MH, Song KW, Kim B-S. Regeneration of kidney tissue using in vitro cultured fetal kidney cells. *Exp Mol Med*. 2008; 40: 361–369. <https://doi.org/10.3858/emm.2008.40.4.361> PMID: 18779648
32. Neumann AU, Lam NP, Dahari H, Gretch DR, Wiley TE, Layden TJ, et al. Hepatitis C viral dynamics in vivo and the antiviral efficacy of interferon-therapy. *Science* (80-). 1998; 282: 103. <https://doi.org/10.1126/science.282.5386.103>
33. Burnham KP, Anderson DR. Model Selection and Multimodel Inference: A Practical Information-Theoretic Approach (2nd ed). *Ecological Modelling*. 2002. <https://doi.org/10.1016/j.ecolmodel.2003.11.004>
34. Binggeli S, Egli A, Schaub S, Binet I, Mayr M, Steiger J, et al. Polyomavirus BK-specific cellular immune response to VP1 and large T-antigen in kidney transplant recipients. *Am J Transplant*. 2007; 7: 1131–9. <https://doi.org/10.1111/j.1600-6143.2007.01754.x> PMID: 17359507
35. Lamarche C, Orio J, Georges-Tobar V, Pincez T, Goupil M, Dahmani A, et al. Clinical-scale Rapid Autologous BK-virus Specific T Cell Line generation from Kidney Transplant Recipients with Active Viremia for Adoptive Immunotherapy. *Transplantation*. 2017. <https://doi.org/10.1097/TP.0000000000001698> PMID: 28230645
36. Nelder JA, Mead R. A simplex method for function minimization. *Comput J*. 1965; 7: 308–313.
37. Banks HT, Baraldi R, Cross K, Flores K, McChesney C, Poag L, et al. Uncertainty quantification in modeling HIV viral mechanics. *Math Biosci Eng*. 2015; 12: 937–964. <https://doi.org/10.3934/mbe.2015.12.937> PMID: 26280189

10.2 Supplementary materials

10.2.1 Figure S1

Comparison of anti-VP responses fittings for patient A



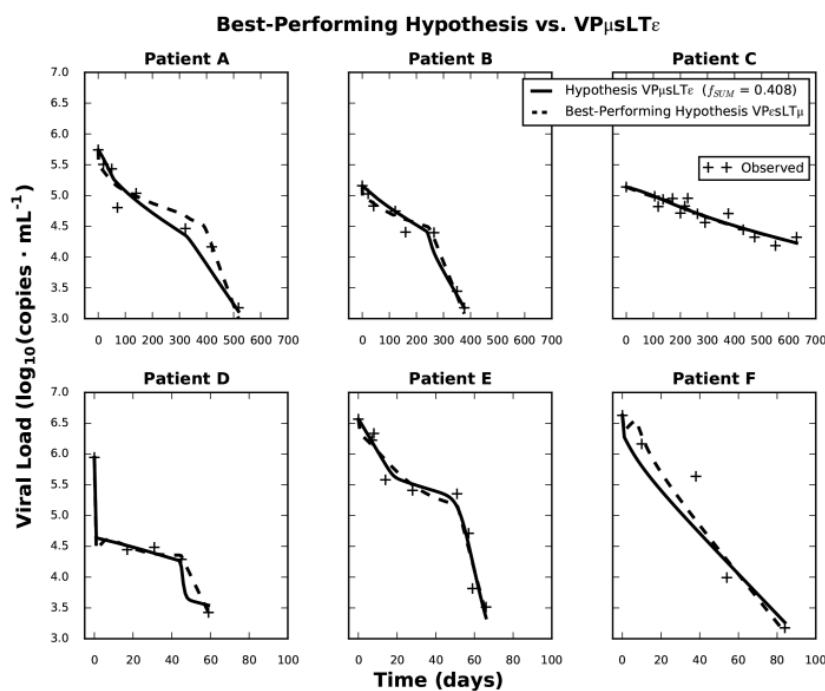
Results of the fitting assuming only one activation event, compared to the fitting for two activation events.

10.2.2 Figure S2

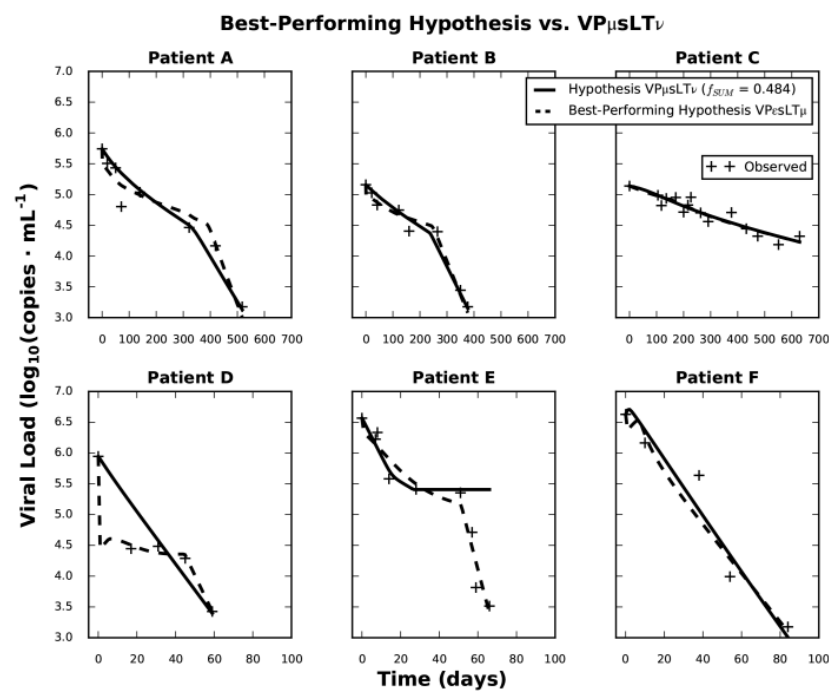
Comparison of the fittings of the hypotheses to the best-performing hypothesis

The hypotheses are shown in order of increasing f_{SUM}

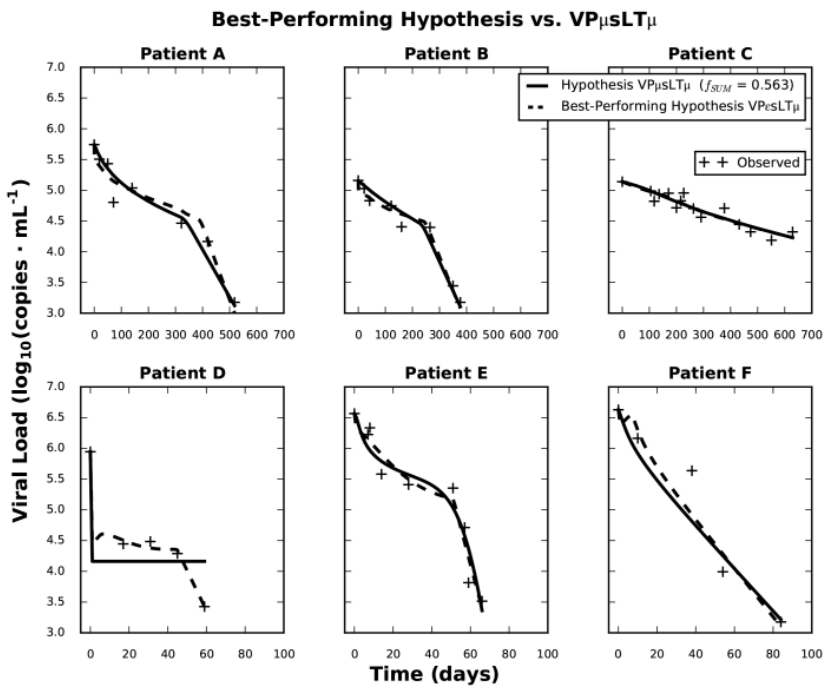
10.2.2.1 Figure S2A



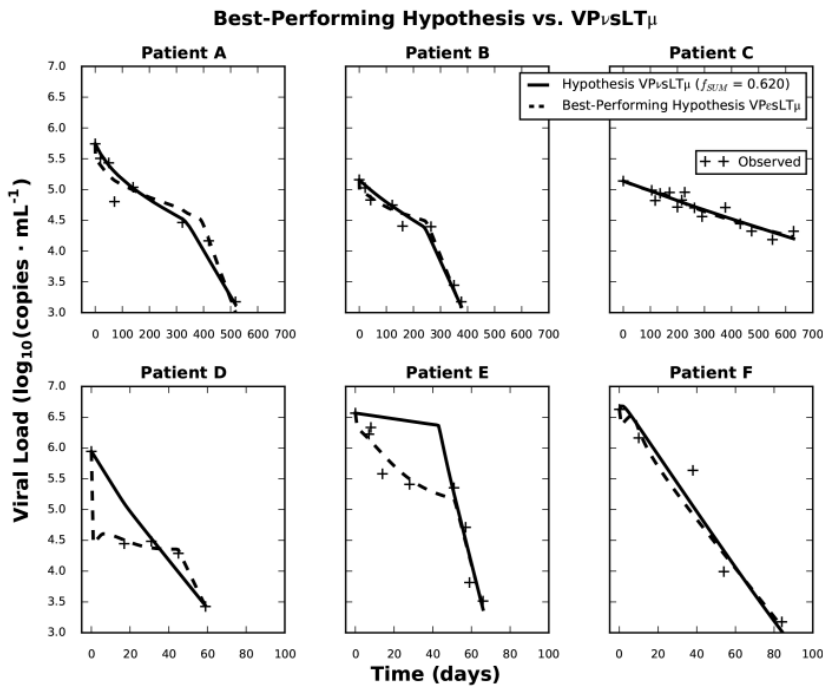
10.2.2.2 Figure S2B



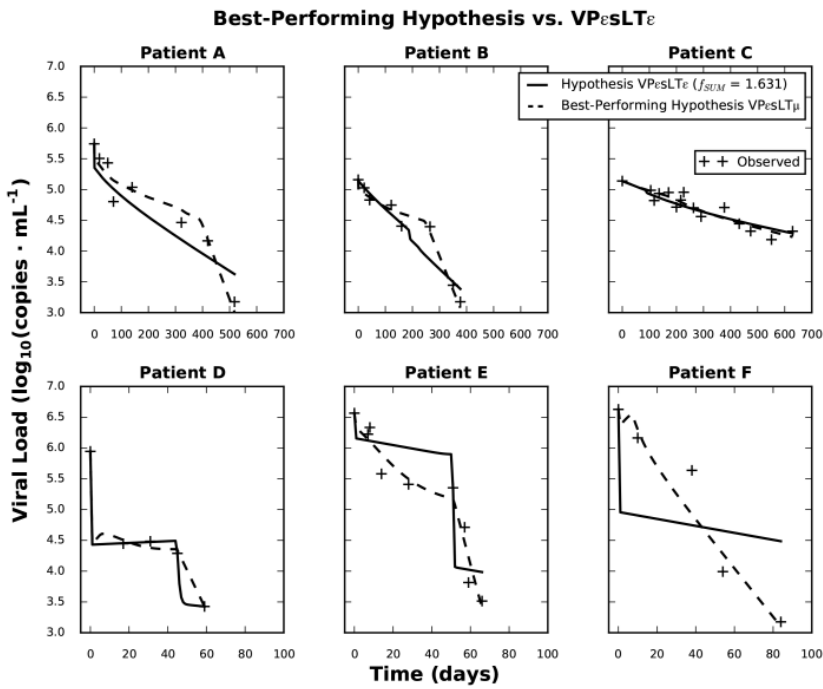
10.2.2.3 Figure S2C



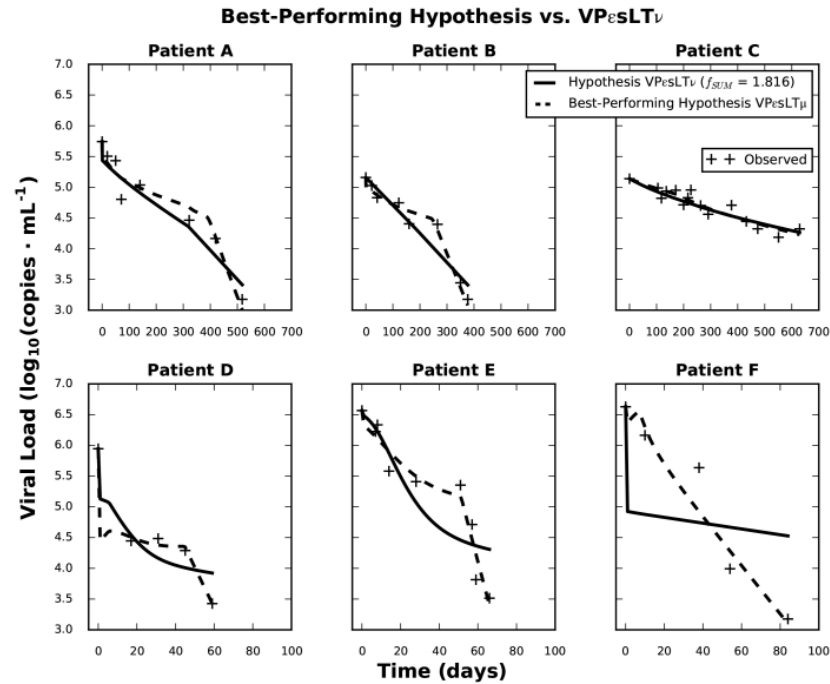
10.2.2.4 Figure S2D



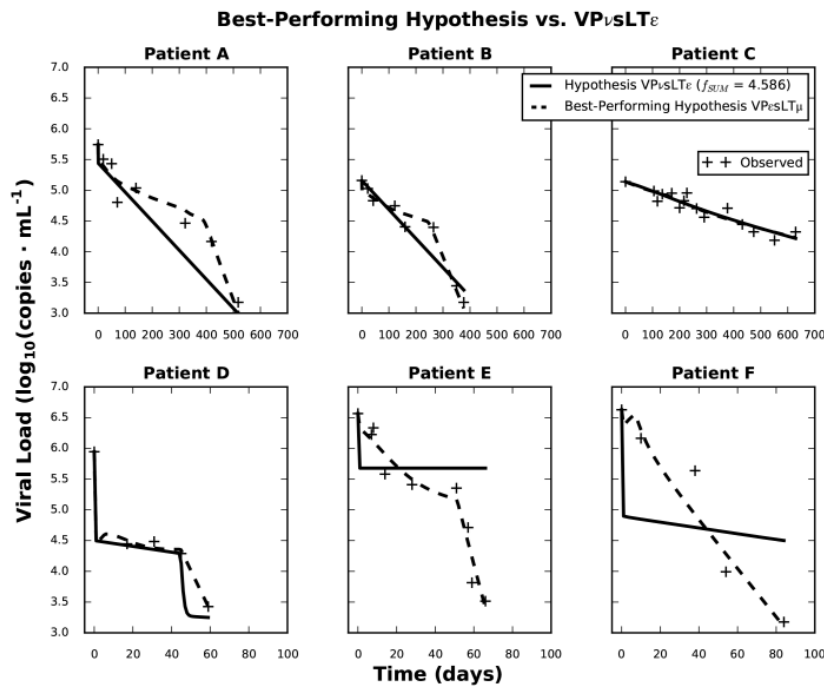
10.2.2.5 Figure S2E



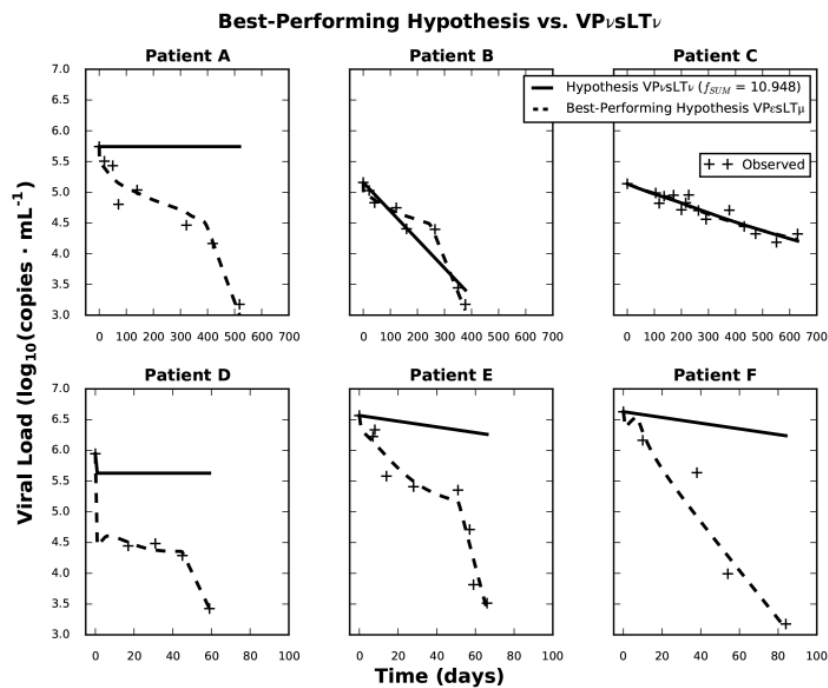
10.2.2.6 Figure S2F



10.2.2.7 Figure S2G



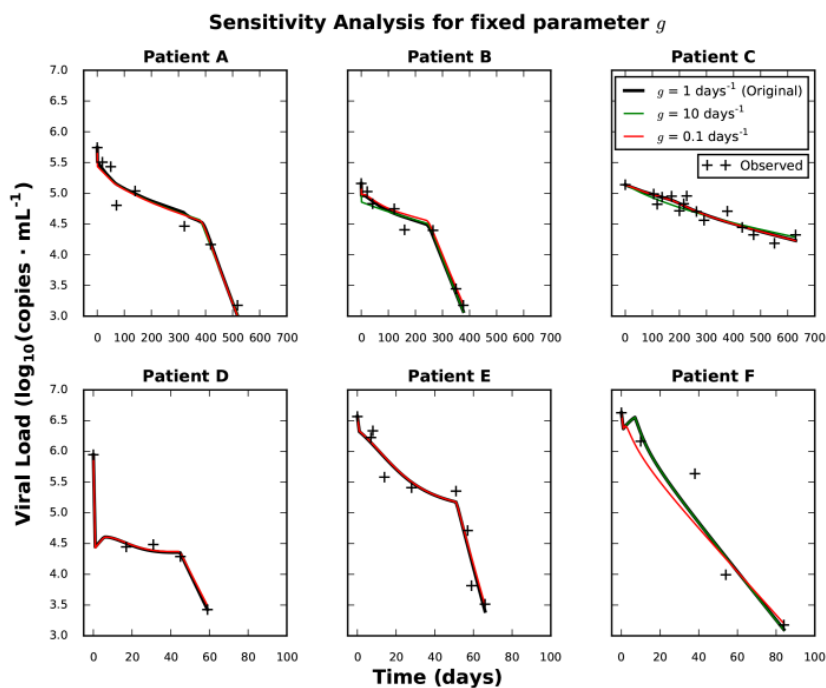
10.2.2.8 Figure S2H



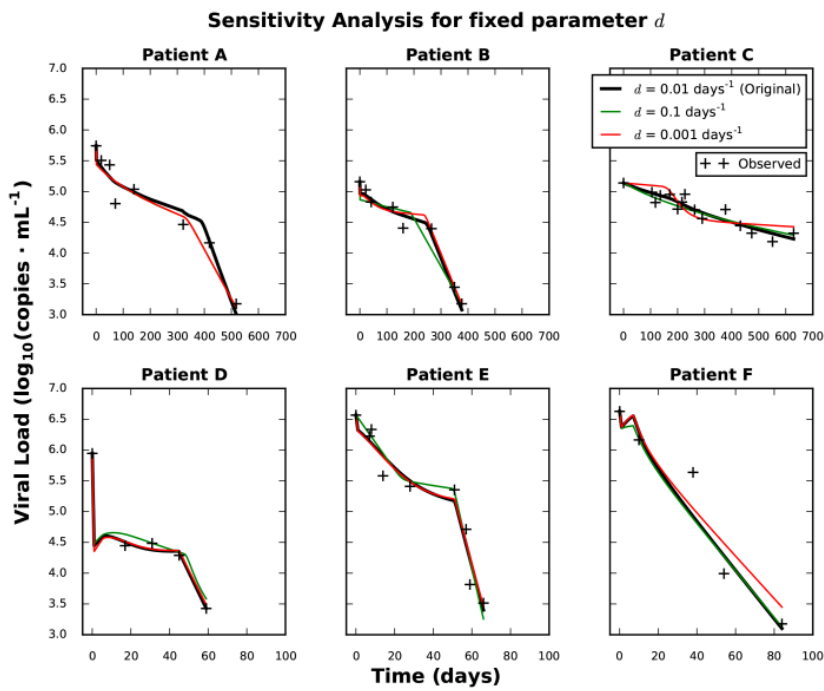
10.2.3 Figure S3

Plotting of the sensitivity analysis results for the extreme parameter values.

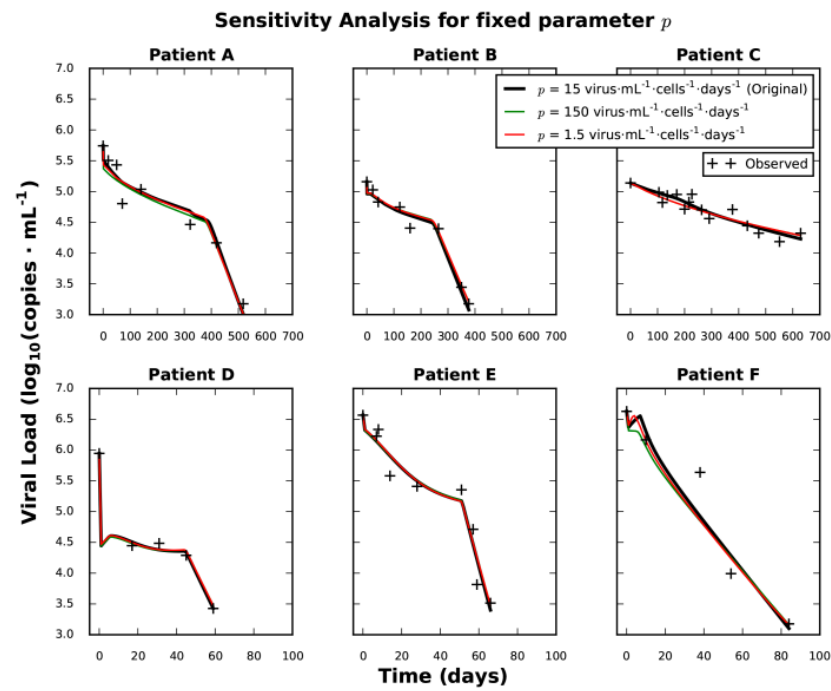
10.2.3.1 Figure S3A



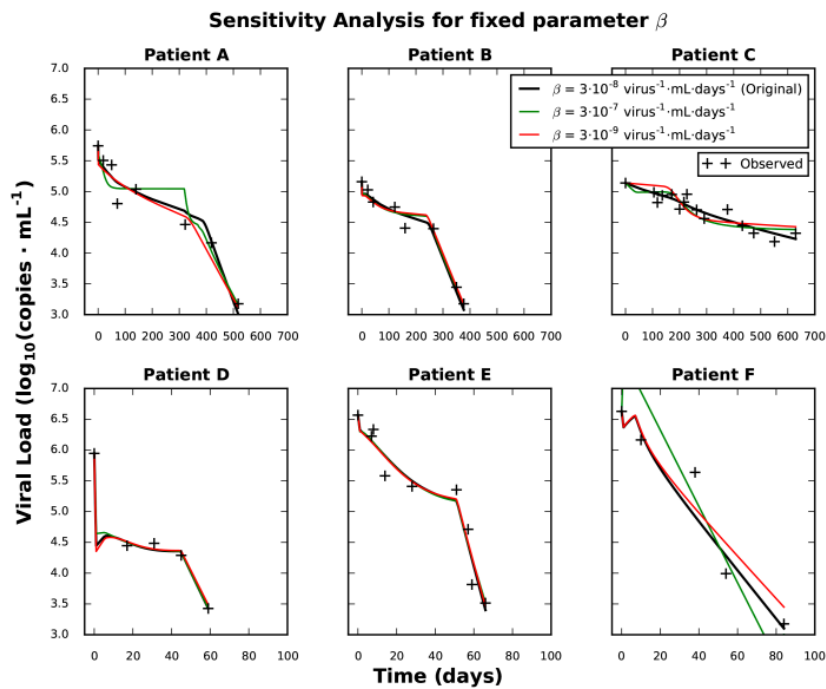
10.2.3.2 Figure S3B



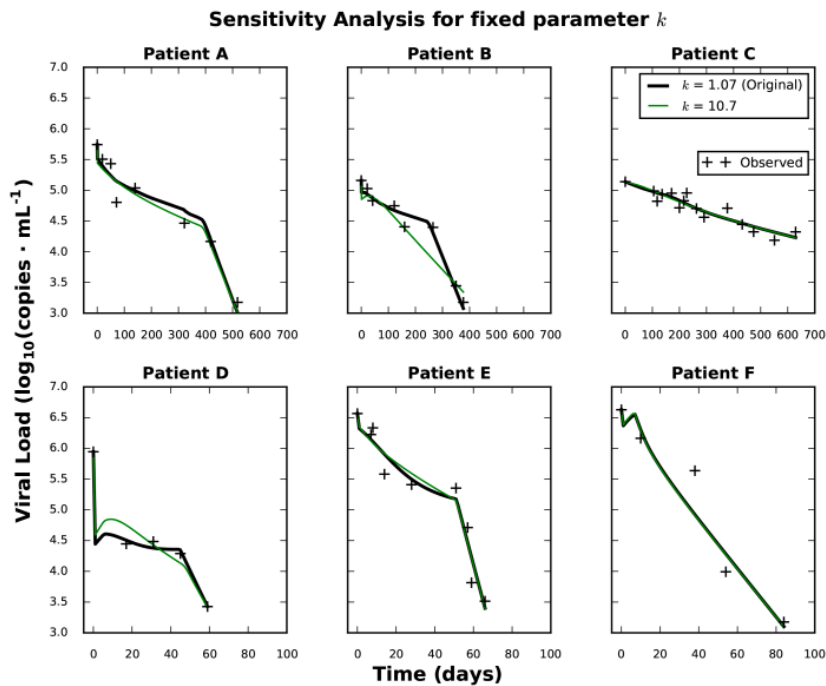
10.2.3.3 Figure S3C



10.2.3.4 Figure S3D



10.2.3.5 Figure S3E



Note that for k only $k = 10.7$ was plotted, as $k = 0.107$ is not biologically meaningful.

10.2.4 Table S1

Parameters for the immune function curve.

Antigens	Parameters	Patients					
		A ^a	B	C	D	E	F
VP1	t_{VP1}	0.00	13.4	0.00	$7.05 \cdot 10^{-1}$	0.00	0.00
		$3.49 \cdot 10^2$					
	r_{VP1}	$8.06 \cdot 10^{-2}$	$3.19 \cdot 10^{-2}$	$2.74 \cdot 10^{-2}$	$1.18 \cdot 10^{-1}$	$7.94 \cdot 10^{-2}$	$3.03 \cdot 10^{-1}$
		$1.48 \cdot 10^{-1}$					
	$max_{antiVP1}$	79.0	$1.86 \cdot 10^2$	$1.47 \cdot 10^2$	$1.50 \cdot 10^2$	$2.70 \cdot 10^2$	$5.02 \cdot 10^2$
		$2.58 \cdot 10^2$					
	dec_{VP1}	0.00	0.00	0.00	0.00	0.00	$5.76 \cdot 10^{-3}$
		$2.62 \cdot 10^{-4}$					
	t_{VP2}	0.00	0.00	0.00	$1.17 \cdot 10^{-1}$	22.7	0.00
		$3.14 \cdot 10^2$					
VP2	r_{VP2}	$9.05 \cdot 10^{-2}$	$5.73 \cdot 10^{-2}$	$2.28 \cdot 10^{-2}$	$1.01 \cdot 10^{-1}$	$5.89 \cdot 10^{-1}$	$2.89 \cdot 10^{-1}$
		$1.18 \cdot 10^{-1}$					
	$max_{antiVP2}$	51.6	$1.28 \cdot 10^2$	$1.05 \cdot 10^2$	71.4	$1.65 \cdot 10^2$	$4.44 \cdot 10^2$
		$1.73 \cdot 10^2$					
	dec_{VP2}	0.00	$1.15 \cdot 10^{-5}$	0.00	$8.69 \cdot 10^{-4}$	0.00	$5.32 \cdot 10^{-3}$
		$2.04 \cdot 10^{-4}$					
VP3	t_{VP3}	0.00	$2.71 \cdot 10^{-2}$	0.00	$4.38 \cdot 10^{-1}$	26.7	0.00
		$3.17 \cdot 10^2$					
	r_{VP3}	$8.48 \cdot 10^{-2}$	$5.69 \cdot 10^{-2}$	$1.31 \cdot 10^{-2}$	$1.55 \cdot 10^{-2}$	$1.27 \cdot 10^2$	$3.16 \cdot 10^{-1}$
		$1.21 \cdot 10^{-1}$					

VP3	$max_{antiVP3}$	68.8	$1.43 \cdot 10^2$	$1.25 \cdot 10^2$	$6.30 \cdot 10^4$	$1.65 \cdot 10^2$	$5.02 \cdot 10^2$
		$2.88 \cdot 10^2$					
	dec_{VP3}	0.00	$7.52 \cdot 10^{-10}$	0.00	$1.70 \cdot 10^{-6}$	$2.41 \cdot 10^{-3}$	$5.99 \cdot 10^{-3}$
		$7.56 \cdot 10^{-4}$					
st	t_{st}	$3.19 \cdot 10^2$	$1.85 \cdot 10^2$	-	57.0	28.0	0.00
	r_{st}	$1.34 \cdot 10^{-1}$	$8.36 \cdot 10^{-1}$	-	1.25	$1.06 \cdot 10^{-1}$	$6.16 \cdot 10^{-1}$
	max_{antist}	$2.01 \cdot 10^2$	$1.66 \cdot 10^2$	-	$1.29 \cdot 10^2$	$2.95 \cdot 10^2$	$4.19 \cdot 10^2$
	dec_{st}	$7.60 \cdot 10^{-6}$	$1.22 \cdot 10^{-4}$	-	$1.84 \cdot 10^{-5}$	0.00	$5.80 \cdot 10^{-3}$
LT	t_{LT}	$3.27 \cdot 10^2$	$1.81 \cdot 10^2$	-	44.6	1.13	0.00
	r_{LT}	$1.66 \cdot 10^{-1}$	$1.18 \cdot 10^{-1}$	-	1.17	$9.63 \cdot 10^{-2}$	1.66
	max_{antiLT}	$1.70 \cdot 10^2$	$2.02 \cdot 10^2$	-	$1.55 \cdot 10^2$	$4.30 \cdot 10^2$	$1.69 \cdot 10^2$
	dec_{LT}	$1.00 \cdot 10^{-6}$	$1.08 \cdot 10^{-5}$	-	$3.82 \cdot 10^{-3}$	$6.53 \cdot 10^{-3}$	$3.46 \cdot 10^{-3}$
f	Obj. Function	$4.16 \cdot 10^{-2}$	$3.99 \cdot 10^{-1}$	$8.21 \cdot 10^{-1}$	$3.84 \cdot 10^{-2}$	$8.30 \cdot 10^{-3}$	$3.70 \cdot 10^{-3}$

Results of the fitting for the immune response model in Eq. 1 for all six patients and five antigens. The last row indicates the achieved value of the objective function (Eq. 2).

^aFor Patient A, the response against the VP antigens was described using a second activation time t_{a2} with a second parameter set to achieve a better fit.

10.2.5 Table S2

Hypotheses on the dominant modes of action of the immune system as defined by the model.

Hypothesis	Definition	Description
VP ϵ -sLT ϵ	$max_{\mu} = max_M = max_u = max_N = 0$ $0 < max_{\epsilon} < 1$ $0 < max_E < 1$	Anti-VP response and anti-sLT response both trigger blockage of virus production
VP ϵ -sLT μ	$max_E = max_{\mu} = max_u = max_N = 0$ $max_{\epsilon} = 1$ $max_M = 1$	Anti-VP response triggers blockage of virus production Anti-sLT response triggers accelerated killing of infected cells
VP ϵ -sLT u	$max_E = max_{\mu} = max_M = max_u = 0$ $max_{\epsilon} = 1$ $max_N = 1$	Anti-VP response triggers blockage of virus production Anti-sLT response triggers blockage of cell infection

VP μ -sLT ϵ	$max_{\epsilon} = max_M = max_U = max_N = 0$ $max_{\mu} = 1$ $max_E = 1$	Anti-VP response triggers accelerated killing of infected cells Anti-sLT response triggers blockage of virus production
VP μ -sLT μ	$max_{\epsilon} = max_E = max_U = max_N = 0$ $0 < max_{\mu} < 1$ $0 < max_M < 1$	Anti-VP response and anti-sLT response both trigger accelerated killing of infected cells
VP μ -sLT U	$max_{\epsilon} = max_E = max_M = max_U = 0$ $max_{\mu} = 1$ $max_N = 1$	Anti-VP response triggers accelerated killing of infected cells Anti-sLT response triggers blockage of cell infection
VP U -sLT ϵ	$max_{\epsilon} = max_{\mu} = max_M = max_N = 0$ $max_U = 1$ $max_E = 1$	Anti-VP response triggers blockage of cell infection Anti-sLT response triggers blockage of virus production
VP U -sLT μ	$max_{\epsilon} = max_E = max_{\mu} = max_N = 0$ $max_U = 1$ $max_M = 1$	Anti-VP response triggers blockage of cell infection Anti-sLT response triggers accelerated killing of infected cells
VP U -sLT U	$max_{\epsilon} = max_E = max_M = max_{\mu} = 0$ $0 < max_U < 1$ $0 < max_N < 1$	Anti-VP and anti-sLT response both trigger blockage of cell infection

Description of the possible hypotheses on the dominant mechanisms of the immune response against VP and sLT antigens, as defined by the model (Eqs. 3-5).

10.2.6 Table S3

Detailed results for the model comparison criteria of the fittings for the nine hypotheses.

Patient	Measurement	VPe-sLTe	VPe-sLTp	VPe-sLTv	VPp-sLTe	VPp-sLTp	VPp-sLTv	VPe-sLTe	VPe-sLTp	VPe-sLTv	Number Measurements	VPe-sLTp-Saturated
No. of parameters		7	6	5	6	7	6	5	6	7		4
No. of parameters Patient C		4	3	3	4	4	4	3	3	4		
A	RSS	0.83700	0.21630	0.46290	0.38430	0.30860	0.42640	1.02090	0.35370	13.17120		
	f	0.11957	0.03090	0.06613	0.05490	0.04409	0.06091	0.14584	0.05053	1.88160		
	BIC	-1.24552	-12.66353	-9.28353	-8.64023	-8.22997	-7.91255	-3.74703	-9.22105	18.04623		
	ABIC	11.41801	0.00000	3.38000	4.02330	4.43357	4.75098	8.91650	3.44248	30.70976		
	AIC	-0.86689	-12.33899	-9.01308	-8.31569	-7.85134	-7.58801	-3.47658	-8.89651	18.42486	7	
B	AAIC	11.47210	0.00000	3.32591	4.02330	4.48766	4.75098	8.86241	3.44248	30.76385		
	RSS	0.47900	0.07840	0.42320	0.22070	0.15330	0.15630	0.43110	0.13960	0.43590		
	f	0.06843	0.01120	0.06046	0.03153	0.02190	0.02233	0.06159	0.01994	0.06227		
	BIC	-5.15238	-19.76743	-9.91119	-12.52257	-13.12751	-14.93776	-9.78173	-15.72873	-5.81240		
	ABIC	14.61505	0.00000	9.85624	7.24486	6.63992	4.82967	9.98570	4.03870	13.95503		
C	AIC	-4.77375	-19.44289	-9.64074	-12.19803	-12.74888	-14.61322	-9.51128	-15.40419	-5.43377	14	
	AAIC	14.66914	0.00000	9.80215	7.24486	6.69401	4.82967	9.93161	4.03870	14.00912		
	RSS	0.17920	0.14420	0.17220	0.14980	0.14980	0.14980	0.14700	0.14700	0.14280		
	f	0.01280	0.01030	0.01230	0.01070	0.01070	0.01070	0.01050	0.01050	0.01020		
	BIC	-50.46011	-56.14139	-53.65701	-55.60799	-52.96893	-55.60799	-55.87215	-55.87215	-53.63892		
D	ABIC	5.68128	0.00000	2.48438	0.53340	3.17246	0.53340	0.26924	0.26924	2.50247	4	
	AIC	-53.01634	-58.05856	-55.57418	-57.52516	-55.52516	-57.52516	-57.78932	-57.78932	-56.19515		
	AAIC	5.04222	0.00000	2.48438	0.53340	2.53340	0.53340	0.26924	0.26924	1.86341		
	RSS	0.00020	0.00174	0.43690	0.04320	0.74250	0.63700	0.07480	0.52190	9.35600		
	f	0.00005	0.00044	0.10923	0.01080	0.18563	0.15925	0.01870	0.13048	2.33900		
E	BIC	-29.85862	-22.64289	-1.92591	-9.79507	2.96795	0.96865	-8.98546	0.17147	13.10295	8	
	ABIC	0.00000	7.21573	27.93271	20.06355	32.82657	30.82727	20.87316	30.03009	42.96157		
	AIC	-25.56268	-18.96066	1.14262	-6.11284	7.26389	4.65088	-5.91693	3.85371	17.39889		
	AAIC	0.00000	6.60202	26.70530	19.44984	32.82657	30.21356	19.64575	29.41639	42.96157		
	RSS	1.38510	0.44730	2.05310	0.40660	0.69740	0.88140	24.28010	2.30030	19.20330		
F	f	0.17314	0.05591	0.25664	0.05083	0.08718	0.11018	3.03501	0.28754	2.40041	4	
	BIC	0.52674	-10.59509	-0.48352	-11.35829	-4.96261	-5.16883	19.27893	2.50543	21.56122		
	ABIC	11.88502	0.76320	10.87477	0.00000	6.39568	6.18945	30.63722	13.86372	32.91950		
	AIC	-0.02935	-11.07174	-0.88073	-11.83494	-5.51870	-5.64548	18.88172	2.02878	21.00512		
	AAIC	11.80558	0.76320	10.95421	0.00000	6.31623	6.18945	30.71666	13.86372	32.84006		
G	RSS	5.02810	0.62390	5.24450	0.99700	0.85260	0.48240	5.25820	0.48250	17.01750	4	0.65240
	f	1.25703	0.15598	1.31113	0.24925	0.21315	0.12060	1.31455	0.12063	4.25438		0.16310
	BIC	10.61905	0.88553	8.01501	2.76057	3.52102	-0.14334	8.02545	-0.14251	15.49585		-1.70839
	ABIC	10.76239	1.02887	8.15835	2.90391	3.66436	0.00000	8.16879	0.00083	15.63919		-1.56505
	AIC	14.91499	4.56776	11.08354	6.44280	7.81696	3.53890	11.09398	3.53973	19.79179		0.4643
H	AAIC	11.37610	1.02887	7.54465	2.90391	4.27807	0.00000	7.55508	0.00083	16.25290	4	-2.79246
	f_{sum}	1.63101	0.26472	1.81587	0.40800	0.56264	0.48397	4.58619	0.61961	10.94786		
	Median ABIC	11.09020	0.38160	9.00729	3.46360	5.41462	4.79033	9.45110	3.74059	23.17448		
	Median AAIC	11.42410	0.38160	8.67340	3.46360	5.40195	4.79033	9.39701	3.74059	23.50837		

The results for the residual sum of squares (RSS), the objective function f (Eq. 6), BIC, Δ BIC, AIC and Δ AIC (Eq. 8 and 9) are shown for each one of the hypotheses and patients; as well as for a special case of the VP ϵ -sLT μ for patient F, assuming a saturating anti-sLT response. The sum of the objective functions over all patients is shown as f_{SUM} . In bold are highlighted: The lowest per patient values for f , as well as the scores of Δ BIC and Δ AIC within the range of substantial empirical support (<2). The definitions of the hypotheses are shown in S2 Table.

10.2.7 Table S4

Results of the sensitivity analysis for the fixed parameters

The results for the sensitivity analysis of the fixed parameters (d , p , g , β , and k) are reproduced below. The results for the original values of the parameters are marked in red. The sensitivity analysis was on a one-factor-at-a-time principle, with the values shown on the first row of each table. f is the lowest value of the objective function (Eq. 6) achieved for each patient and value of the parameter, f_{SUM} indicates the sum of the objective functions for all six patients.

10.2.7.1 Table S4A

Value g	1.00 $\cdot 10^{-1}$	1.58 $\cdot 10^{-1}$	2.51 $\cdot 10^{-1}$	3.98 $\cdot 10^{-1}$	6.31 $\cdot 10^{-1}$	1.00	1.58	2.51	3.98	6.31	10.0
f_A	$3.12 \cdot 10^{-2}$	$3.40 \cdot 10^{-2}$	$3.40 \cdot 10^{-2}$	$2.99 \cdot 10^{-2}$	$3.40 \cdot 10^{-2}$	3.09 $\cdot 10^{-2}$	$3.00 \cdot 10^{-2}$	$3.12 \cdot 10^{-2}$	$3.22 \cdot 10^{-2}$	$3.40 \cdot 10^{-2}$	$3.19 \cdot 10^{-2}$
f_B	$1.64 \cdot 10^{-2}$	$1.56 \cdot 10^{-2}$	$1.64 \cdot 10^{-2}$	$1.64 \cdot 10^{-2}$	$1.64 \cdot 10^{-2}$	1.12 $\cdot 10^{-2}$	$1.12 \cdot 10^{-2}$	$1.64 \cdot 10^{-2}$	$1.64 \cdot 10^{-2}$	$1.64 \cdot 10^{-2}$	$1.58 \cdot 10^{-2}$
f_C	$1.03 \cdot 10^{-2}$	$1.27 \cdot 10^{-2}$	$1.27 \cdot 10^{-2}$	$1.27 \cdot 10^{-2}$	$1.27 \cdot 10^{-2}$	1.03 $\cdot 10^{-2}$	$1.27 \cdot 10^{-2}$	$1.27 \cdot 10^{-2}$	$1.27 \cdot 10^{-2}$	$1.27 \cdot 10^{-2}$	$1.27 \cdot 10^{-2}$
f_D	$5.40 \cdot 10^{-3}$	$5.40 \cdot 10^{-3}$	$5.40 \cdot 10^{-3}$	$5.40 \cdot 10^{-3}$	$5.40 \cdot 10^{-3}$	4.30 $\cdot 10^{-3}$	$4.30 \cdot 10^{-3}$	$5.40 \cdot 10^{-3}$	$5.40 \cdot 10^{-3}$	$5.40 \cdot 10^{-3}$	$5.40 \cdot 10^{-3}$
f_E	$5.77 \cdot 10^{-2}$	$5.77 \cdot 10^{-2}$	$5.77 \cdot 10^{-2}$	$5.77 \cdot 10^{-2}$	$5.77 \cdot 10^{-2}$	5.59 $\cdot 10^{-2}$	$5.59 \cdot 10^{-2}$	$5.77 \cdot 10^{-2}$	$5.77 \cdot 10^{-2}$	$5.77 \cdot 10^{-2}$	$5.77 \cdot 10^{-2}$
f_F	$2.04 \cdot 10^{-1}$	$1.75 \cdot 10^{-1}$	$2.12 \cdot 10^{-1}$	$2.12 \cdot 10^{-1}$	$1.84 \cdot 10^{-1}$	1.56 $\cdot 10^{-1}$	$1.56 \cdot 10^{-1}$	$2.12 \cdot 10^{-1}$	$1.75 \cdot 10^{-1}$	$2.12 \cdot 10^{-1}$	$1.56 \cdot 10^{-1}$
f_{SUM}	3.25 $\cdot 10^{-1}$	3.01 $\cdot 10^{-1}$	3.38 $\cdot 10^{-1}$	3.34 $\cdot 10^{-1}$	3.11 $\cdot 10^{-1}$	2.69 $\cdot 10^{-1}$	2.70 $\cdot 10^{-1}$	3.36 $\cdot 10^{-1}$	2.99 $\cdot 10^{-1}$	3.38 $\cdot 10^{-1}$	2.80 $\cdot 10^{-1}$

10.2.7.2 Table S4B

Value d	1.00 $\cdot 10^{-3}$	1.58 $\cdot 10^{-3}$	2.51 $\cdot 10^{-3}$	3.98 $\cdot 10^{-3}$	6.31 $\cdot 10^{-3}$	1.00 $\cdot 10^{-2}$	1.58 $\cdot 10^{-2}$	2.51 $\cdot 10^{-2}$	3.98 $\cdot 10^{-2}$	6.31 $\cdot 10^{-2}$	1.00 $\cdot 10^{-1}$
f_A	$4.21 \cdot 10^{-2}$	$6.16 \cdot 10^{-2}$	$4.16 \cdot 10^{-2}$	$5.76 \cdot 10^{-2}$	$4.30 \cdot 10^{-2}$	3.09 $\cdot 10^{-2}$	$2.93 \cdot 10^{-2}$	$4.29 \cdot 10^{-2}$	$4.19 \cdot 10^{-2}$	$3.55 \cdot 10^{-2}$	$4.17 \cdot 10^{-2}$
f_B	$1.60 \cdot 10^{-2}$	$1.31 \cdot 10^{-2}$	$1.22 \cdot 10^{-2}$	$1.58 \cdot 10^{-2}$	$1.47 \cdot 10^{-2}$	1.12 $\cdot 10^{-2}$	$1.16 \cdot 10^{-2}$	$2.92 \cdot 10^{-2}$	$2.64 \cdot 10^{-2}$	$3.85 \cdot 10^{-2}$	$3.84 \cdot 10^{-2}$
f_C	$2.55 \cdot 10^{-2}$	$2.12 \cdot 10^{-2}$	$1.57 \cdot 10^{-2}$	$3.46 \cdot 10^{-2}$	$1.27 \cdot 10^{-2}$	1.03 $\cdot 10^{-2}$	$1.11 \cdot 10^{-2}$	$1.27 \cdot 10^{-2}$	$1.28 \cdot 10^{-2}$	$1.29 \cdot 10^{-2}$	$1.30 \cdot 10^{-2}$
f_D	$5.50 \cdot 10^{-3}$	$5.70 \cdot 10^{-3}$	$5.90 \cdot 10^{-3}$	$6.20 \cdot 10^{-3}$	$5.50 \cdot 10^{-3}$	4.30 $\cdot 10^{-3}$	$4.70 \cdot 10^{-3}$	$5.60 \cdot 10^{-3}$	$9.00 \cdot 10^{-3}$	$7.40 \cdot 10^{-3}$	$1.54 \cdot 10^{-2}$
f_E	$5.52 \cdot 10^{-2}$	$5.58 \cdot 10^{-2}$	$5.61 \cdot 10^{-2}$	$5.69 \cdot 10^{-2}$	$5.67 \cdot 10^{-2}$	5.59 $\cdot 10^{-2}$	$5.86 \cdot 10^{-2}$	$6.02 \cdot 10^{-2}$	$6.07 \cdot 10^{-2}$	$6.48 \cdot 10^{-2}$	$5.42 \cdot 10^{-2}$
f_F	$2.03 \cdot 10^{-1}$	$1.98 \cdot 10^{-1}$	$1.65 \cdot 10^{-1}$	$1.99 \cdot 10^{-1}$	$2.00 \cdot 10^{-1}$	1.56 $\cdot 10^{-1}$	$1.56 \cdot 10^{-1}$	$2.01 \cdot 10^{-1}$	$1.97 \cdot 10^{-1}$	$2.15 \cdot 10^{-1}$	$1.64 \cdot 10^{-1}$
f_{SUM}	3.47 $\cdot 10^{-1}$	3.55 $\cdot 10^{-1}$	2.97 $\cdot 10^{-1}$	3.70 $\cdot 10^{-1}$	3.32 $\cdot 10^{-1}$	2.69 $\cdot 10^{-1}$	2.72 $\cdot 10^{-1}$	3.52 $\cdot 10^{-1}$	3.47 $\cdot 10^{-1}$	3.74 $\cdot 10^{-1}$	3.27 $\cdot 10^{-1}$

10.2.7.3 Table S4C

Value p	1.50	2.38	3.77	5.97	9.46	15.0	23.8	37.7	59.7	94.6	1.50 $\cdot 10^2$
f_A	$3.47 \cdot 10^{-2}$	$3.47 \cdot 10^{-2}$	$3.57 \cdot 10^{-2}$	$3.22 \cdot 10^{-2}$	$3.46 \cdot 10^{-2}$	3.09 $\cdot 10^{-2}$	$3.39 \cdot 10^{-2}$	$3.12 \cdot 10^{-2}$	$3.55 \cdot 10^{-2}$	$2.90 \cdot 10^{-2}$	$3.42 \cdot 10^{-2}$
f_B	$1.48 \cdot 10^{-2}$	$1.48 \cdot 10^{-2}$	$2.00 \cdot 10^{-2}$	$1.55 \cdot 10^{-2}$	$1.51 \cdot 10^{-2}$	1.12 $\cdot 10^{-2}$	$1.12 \cdot 10^{-2}$	$2.58 \cdot 10^{-2}$	$1.56 \cdot 10^{-2}$	$1.60 \cdot 10^{-2}$	$1.69 \cdot 10^{-2}$
f_C	$1.27 \cdot 10^{-2}$	$1.27 \cdot 10^{-2}$	$1.27 \cdot 10^{-2}$	$1.27 \cdot 10^{-2}$	$1.27 \cdot 10^{-2}$	1.03 $\cdot 10^{-2}$	$1.27 \cdot 10^{-2}$	$1.27 \cdot 10^{-2}$	$1.27 \cdot 10^{-2}$	$1.27 \cdot 10^{-2}$	$1.27 \cdot 10^{-2}$
f_D	$5.10 \cdot 10^{-3}$	$5.10 \cdot 10^{-3}$	$5.30 \cdot 10^{-3}$	$5.40 \cdot 10^{-3}$	$5.20 \cdot 10^{-3}$	4.40 $\cdot 10^{-3}$	$4.90 \cdot 10^{-3}$	$5.20 \cdot 10^{-3}$	$5.20 \cdot 10^{-3}$	$5.40 \cdot 10^{-3}$	$5.40 \cdot 10^{-3}$
f_E	$5.82 \cdot 10^{-2}$	$5.82 \cdot 10^{-2}$	$5.80 \cdot 10^{-2}$	$5.84 \cdot 10^{-2}$	$5.73 \cdot 10^{-2}$	5.59 $\cdot 10^{-2}$	$5.61 \cdot 10^{-2}$	$5.80 \cdot 10^{-2}$	$5.72 \cdot 10^{-2}$	$5.80 \cdot 10^{-2}$	$5.73 \cdot 10^{-2}$
f_F	$1.56 \cdot 10^{-1}$	$1.56 \cdot 10^{-1}$	$2.03 \cdot 10^{-1}$	$1.60 \cdot 10^{-1}$	$2.08 \cdot 10^{-1}$	1.56 $\cdot 10^{-1}$	$1.56 \cdot 10^{-1}$	$2.08 \cdot 10^{-1}$	$2.06 \cdot 10^{-1}$	$1.83 \cdot 10^{-1}$	$1.83 \cdot 10^{-1}$
f_{SUM}	3.47 $\cdot 10^{-2}$	3.47 $\cdot 10^{-2}$	3.57 $\cdot 10^{-2}$	3.22 $\cdot 10^{-2}$	3.46 $\cdot 10^{-2}$	3.09 $\cdot 10^{-2}$	3.39 $\cdot 10^{-2}$	3.12 $\cdot 10^{-2}$	3.55 $\cdot 10^{-2}$	2.90 $\cdot 10^{-2}$	3.42 $\cdot 10^{-2}$

10.2.7.4 Table S4D

Value β	$3.00 \cdot 10^{-9}$	$4.75 \cdot 10^{-9}$	$7.54 \cdot 10^{-9}$	$1.19 \cdot 10^{-8}$	$1.89 \cdot 10^{-8}$	$3.00 \cdot 10^{-8}$	$4.75 \cdot 10^{-8}$	$7.54 \cdot 10^{-8}$	$1.19 \cdot 10^{-7}$	$1.89 \cdot 10^{-7}$	$3.00 \cdot 10^{-7}$
f_A	$3.79 \cdot 10^{-2}$	$3.34 \cdot 10^{-2}$	$3.56 \cdot 10^{-2}$	$3.86 \cdot 10^{-2}$	$3.55 \cdot 10^{-2}$	$3.09 \cdot 10^{-2}$	$4.06 \cdot 10^{-2}$	$5.18 \cdot 10^{-2}$	$4.60 \cdot 10^{-2}$	$6.34 \cdot 10^{-2}$	$7.03 \cdot 10^{-2}$
f_B	$2.49 \cdot 10^{-2}$	$1.55 \cdot 10^{-2}$	$1.52 \cdot 10^{-2}$	$1.57 \cdot 10^{-2}$	$1.71 \cdot 10^{-2}$	$1.12 \cdot 10^{-2}$	$1.33 \cdot 10^{-2}$	$1.45 \cdot 10^{-2}$	$1.37 \cdot 10^{-2}$	$1.50 \cdot 10^{-2}$	$1.48 \cdot 10^{-2}$
f_C	$1.05 \cdot 10^{-2}$	$1.05 \cdot 10^{-2}$	$1.05 \cdot 10^{-2}$	$1.06 \cdot 10^{-2}$	$1.12 \cdot 10^{-2}$	$1.03 \cdot 10^{-2}$	$1.06 \cdot 10^{-2}$	$1.11 \cdot 10^{-2}$	$1.22 \cdot 10^{-2}$	$1.40 \cdot 10^{-2}$	$1.72 \cdot 10^{-2}$
f_D	$5.90 \cdot 10^{-3}$	$6.10 \cdot 10^{-3}$	$5.70 \cdot 10^{-3}$	$6.40 \cdot 10^{-3}$	$5.40 \cdot 10^{-3}$	$4.40 \cdot 10^{-3}$	$4.30 \cdot 10^{-3}$	$4.30 \cdot 10^{-3}$	$4.50 \cdot 10^{-3}$	$4.30 \cdot 10^{-3}$	$3.70 \cdot 10^{-3}$
f_E	$5.82 \cdot 10^{-2}$	$5.83 \cdot 10^{-2}$	$5.81 \cdot 10^{-2}$	$5.82 \cdot 10^{-2}$	$5.78 \cdot 10^{-2}$	$5.59 \cdot 10^{-2}$	$5.56 \cdot 10^{-2}$	$5.70 \cdot 10^{-2}$	$5.59 \cdot 10^{-2}$	$5.44 \cdot 10^{-2}$	$5.56 \cdot 10^{-2}$
f_F	$1.23 \cdot 10^{-1}$	$1.54 \cdot 10^{-1}$	$1.59 \cdot 10^{-1}$	$1.32 \cdot 10^{-1}$	$1.44 \cdot 10^{-1}$	$1.56 \cdot 10^{-1}$	$1.85 \cdot 10^{-1}$	$1.55 \cdot 10^{-1}$	$1.52 \cdot 10^{-1}$	$1.52 \cdot 10^{-1}$	$2.11 \cdot 10^{-1}$
f_{SUM}	$2.60 \cdot 10^{-1}$	$2.78 \cdot 10^{-1}$	$2.85 \cdot 10^{-1}$	$2.62 \cdot 10^{-1}$	$2.71 \cdot 10^{-1}$	$2.69 \cdot 10^{-1}$	$3.09 \cdot 10^{-1}$	$2.94 \cdot 10^{-1}$	$2.85 \cdot 10^{-1}$	$3.03 \cdot 10^{-1}$	$3.73 \cdot 10^{-1}$

10.2.7.5 Table S4E

Value k	$1.02 \cdot 10^{-1}$	$1.62 \cdot 10^{-1}$	$2.56 \cdot 10^{-1}$	$4.06 \cdot 10^{-1}$	$6.44 \cdot 10^{-1}$	1.02	1.62	2.56	4.06	6.44	10.2
f_A	$7.25 \cdot 10^{-2}$	$4.20 \cdot 10^{-2}$	$5.11 \cdot 10^{-2}$	$5.86 \cdot 10^{-2}$	$4.28 \cdot 10^{-2}$	$3.09 \cdot 10^{-2}$	$2.93 \cdot 10^{-2}$	$4.03 \cdot 10^{-2}$	$3.42 \cdot 10^{-2}$	$4.62 \cdot 10^{-2}$	$2.91 \cdot 10^{-2}$
f_B	$1.73 \cdot 10^{-2}$	$1.65 \cdot 10^{-2}$	$1.65 \cdot 10^{-2}$	$1.69 \cdot 10^{-2}$	$1.44 \cdot 10^{-2}$	$1.12 \cdot 10^{-2}$	$1.16 \cdot 10^{-2}$	$1.36 \cdot 10^{-2}$	$3.87 \cdot 10^{-2}$	$1.73 \cdot 10^{-2}$	$3.06 \cdot 10^{-2}$
f_C	$2.49 \cdot 10^{-2}$	$2.07 \cdot 10^{-2}$	$1.58 \cdot 10^{-2}$	$3.39 \cdot 10^{-2}$	$1.27 \cdot 10^{-2}$	$1.03 \cdot 10^{-2}$	$1.12 \cdot 10^{-2}$	$1.27 \cdot 10^{-2}$	$1.08 \cdot 10^{-2}$	$1.07 \cdot 10^{-2}$	$1.07 \cdot 10^{-2}$
f_D	$5.30 \cdot 10^{-3}$	$5.30 \cdot 10^{-3}$	$2.80 \cdot 10^{-3}$	$5.60 \cdot 10^{-3}$	$5.60 \cdot 10^{-3}$	$4.30 \cdot 10^{-3}$	$4.80 \cdot 10^{-3}$	$6.00 \cdot 10^{-3}$	$5.30 \cdot 10^{-3}$	$1.51 \cdot 10^{-2}$	$3.00 \cdot 10^{-2}$
f_E	$5.53 \cdot 10^{-2}$	$5.58 \cdot 10^{-2}$	$5.58 \cdot 10^{-2}$	$5.63 \cdot 10^{-2}$	$5.68 \cdot 10^{-2}$	$5.59 \cdot 10^{-2}$	$5.89 \cdot 10^{-2}$	$6.01 \cdot 10^{-2}$	$6.21 \cdot 10^{-2}$	$5.99 \cdot 10^{-2}$	$6.28 \cdot 10^{-2}$
f_F	$1.56 \cdot 10^{-1}$	$2.02 \cdot 10^{-1}$	$2.05 \cdot 10^{-1}$	$2.01 \cdot 10^{-1}$	$1.56 \cdot 10^{-1}$	$1.56 \cdot 10^{-1}$	$1.56 \cdot 10^{-1}$	$1.99 \cdot 10^{-1}$	$1.64 \cdot 10^{-1}$	$1.72 \cdot 10^{-1}$	$1.58 \cdot 10^{-1}$
f_{SUM}	$3.31 \cdot 10^{-1}$	$3.42 \cdot 10^{-1}$	$3.47 \cdot 10^{-1}$	$3.73 \cdot 10^{-1}$	$2.88 \cdot 10^{-1}$	$2.69 \cdot 10^{-1}$	$2.72 \cdot 10^{-1}$	$3.32 \cdot 10^{-1}$	$3.15 \cdot 10^{-1}$	$3.21 \cdot 10^{-1}$	$3.22 \cdot 10^{-1}$

11. Summary of the manuscripts in the context of personalized medicine

The work in this thesis was performed as part of a study on personalized medicine for renal transplantation, the e:KID study.^{*} The four manuscripts I present analyse the clinical evolution of patients after renal transplantation, with special emphasis on complications such as viral reactivations and acute rejections.^{130,211,213,237} Different analytical methods were applied in these works to achieve different goals: In the first manuscript (chapter 7) descriptive statistical analysis was applied to detect correlations suggestive for causal relationships between clinical outcome and viral reactivations.¹³⁰ In the second manuscript (chapter 8) we utilized a mixture of descriptive bivariate statistical analysis and diagnostic multivariate analysis to tentatively determine the influence of anti-viral prevention strategies on patient outcome in a non-randomised design.²¹³ In our third manuscript (chapter 9), machine learning methods were used for the predictive analysis of biomarkers of acute cellular rejection.¹³⁰ Lastly, in the fourth manuscript (chapter 10) we employed ordinary differential equation modelling for a diagnostic analysis of the immune modes of action against BK virus.²³⁷

Together, these four manuscripts show how different analytical methods can be employed to generate complementary knowledge on personalized factors associated with transplantation outcome and how this knowledge can be employed to improve medical interventions for the benefit of the patient.^{130,211,213,237} In this chapter, a summary of the background, methods and results of these four works is provided, with special emphasis on their contributions to personalized medicine.

11.1 Studying the prevalence, risk factors and consequences of combined viral reactivations: A thorough exploratory statistical analysis

The use of modern immunosuppressive drugs in renal transplantation has led in the last decades to a dramatic increase of short term graft survival, but also to the emergence of viral infections.^{19,20,239,240} Cytomegalovirus (CMV) and Epstein-Barr virus (EBV), together with BK virus (BKV), are major viral pathogens, increasing morbidity and mortality of the patients.²⁴¹ Due to their high prevalence, combined infections of two of these viruses (either simultaneously or subsequently) are expected to be a common event.^{242–244} Yet, it is unclear whether there is an association between the reactivations, and what the effects of such combined infections in transplantation outcome might be.^{242–244} Therefore, we decided to analyse the Harmony cohort for the prevalence, risk factors of viral reactivations and their association with transplantation outcome.²¹¹

A thorough exploratory (not hypothesis-based) analysis of the data was performed employing conventional bivariate statistics. These methods were chosen due to their simplicity, as they best suited the goals of the analysis – finding associations between variables. They allow moreover for a fast evaluation of a large number of comparisons, as we performed a systematic evaluation over a large range of thresholds for each of the viral reactivations.

Almost fifty thousand tests were performed for this publication. An example for an analysis requiring a large number of simple tests is the determination of the influence of immunosuppressant on viral reactivations. We compared the quantitative variable *immunosuppressant usage* for patients during viral reactivation with a cohort with no

^{*} For details on the e:KID study, see section 6.1.

reactivation. For patients with no reactivation, the time point of immunosuppressant usage was randomly selected, so that the final temporal distribution is similar to that of the viral reactivation group. This analysis was replicated a hundred times for each threshold and drug combination, in order to ensure the statistical significance of the results. An additional example of analyses requiring a high number of tests is the investigation of the influence of viral load thresholds on renal function (GFR). These were performed to ensure the robustness of our results on GFR, and account for 81% of the tests performed in this publication.

Note that no multiple testing correction was necessary in spite of the large number of tests (see sub-section 5.4.1.2). The great majority of the tests were either performed for different thresholds or with replications, so that their results are not independent from each other and a correction of the significance values would not be appropriate.⁸¹ Furthermore, as the study had an exploratory character, our goal was maximising the output based on the precautionary principle. A correction of these data would have led to a discarding of potentially relevant clinical effects.^{81,82}

A total of 540 patients were analysed for BKV, CMV and EBV reactivations after renal transplantation during the eight study visits. Reactivations were extremely common, in spite of the Harmony cohort having a low immunological risk: Almost half of the patients suffered BKV reactivation and around one fifth CMV and EBV. BKV and CMV were significantly associated with a lower GFR at the end of the study; for the first time this was observed for patients with combined BKV-CMV infections, already at low viral load levels. This is especially relevant, as CMV was significantly associated with both BKV and EBV, thereby suggesting possible interactions between the viruses. Moreover, long cold ischaemia times were shown for the first time in a large study to be associated with very high viral loads of CMV, which in turn are associated with reduced GFR.

This study is the most systematic analysis so far of viral reactivations in renal transplantation, due to the large number of samples obtained along the first post-transplantation year and the large number of associations tested. Our results reveal BKV as an emerging virus, demonstrating it is the most relevant viral reactivation from the epidemiological point of view. Moreover, our results have the potential of improving BKV and CMV management, appealing for a more frequent monitoring of these viruses and stricter intervention – especially for patients with a history of subclinical reactivations for one of the two viruses. These developments of personalized viral monitoring may eventually contribute to reverting the growing trend of viral reactivations after renal transplantation.

11.2 Improving prevention of cytomegalovirus complications: A hypothesis-based assessment of sex-treatment interactions on transplantation outcomes by means of multivariate statistics

Antiviral agents can be employed to prevent and treat cytomegalovirus (CMV) reactivations.^{245,246} Ganciclovir and its oral prodrug valganciclovir are routinely employed in the clinic after renal transplantation for this goal, following two main prevention strategies: prophylactic strategy, which comprises the universal administration of antiviral drugs (during the first 3-6 months after transplantation), and the pre-emptive strategy, in which patients are regularly monitored for CMV and antiviral drugs are employed only after a positive test.^{245–247} While current guidelines accept both strategies for patients with a high or intermediate risk constellation, it is unclear which therapy is superior with respect to transplantation outcomes.²⁴⁶ Importantly, in spite of increasing evidence of the relevance of sex differences

in anti-CMV immunity and prevention, there are still no studies analysing the interactions of sex with these prevention strategies in a clinical context.^{248–251} Because of this, we decided to analyse the Harmony cohort to determine which prevention strategy is associated with a better patient outcome regarding renal function (GFR), acute rejection and viral reactivations, and identify potential sex-associated differences in these outcomes.²¹³

Our study was designed following the schema of a non-randomized controlled trial, in which patients are assigned to one of the two prevention strategies. The assignment was based on the VIPP study, the most relevant study on the matter: Patients receiving (val)ganciclovir during the first two post-transplantation weeks were assigned to the prophylactic group, the rest were assigned to the pre-emptive group.^{32,33} Comparisons between the two groups were initially performed using standard bivariate statistical tests, both for the whole cohort and stratifying according to risk factors; sex-associated differences were assessed both independently from and in interaction with prevention strategy. These methods are sensitive to potential bias in the sub-cohorts, due to the non-randomized character of the study.⁹⁰ In fact, significant demographic differences between the sub-cohorts were observed, which constitute potential confounders.⁹⁰ Because of this, multivariate analysis techniques were employed to control for potential confounders. Multi-parameter regression with backward elimination was the method of choice, as it is a standard and recommended approach for controlling confounders (see sub-section 5.4.1.2).^{93,96} Furthermore, to avoid P value inflation issues, Akaike's information criterion was chosen as the basis for variable selection.^{93,96}

A total of 540 patients – 194 (35.9%) female – were analysed, of which 308 (57.0%) followed a prophylactic strategy and 232 (43.0%) a pre-emptive strategy. As expected, prophylactic strategy was associated with lower incidence of CMV syndrome and lower CMV viral loads. On the other hand, prophylaxis also was associated with higher acute rejection incidence, higher BK virus loads and lower GFR from the third post-transplantation month on, as confirmed by the multivariate analysis. There was a strong sex effect in the association of prevention strategy with GFR: while for male patients there was no difference between prevention strategies, female patients receiving prophylaxis suffered a severe impairment in the GFR. Furthermore, a significant female-specific association of prophylaxis with lower incidence of Epstein-Barr virus reactivations was observed.

This study provides the first evidence in the literature of a strong, clinically relevant sex effect in the outcomes of anti-CMV prevention strategies. Furthermore, it is the first study suggesting that the pre-emptive strategy might be superior for both male and female patients with respect to transplantation outcomes. While it is unclear what the explanation for this effect might be, our data suggest an effect of immunological nature where subclinical CMV reactivations and the immune reaction against them have a protective effect on the graft, as suggested by previous works.^{252,253} In spite of the difficulties associated with the interpretation of non-randomized analysis, our study has a number of advantages, including the closeness to clinical reality and the large number of participants.^{32,33,254} Therefore, our results support a broader use of the pre-emptive strategy, especially in female patients. This personalization of the prevention strategy would then lead to improved patient outcomes.

11.3 Predicting acute cellular rejection employing pre-transplant antibody profiles: Identification of markers for risk assessment using a machine learning tool

Acute cellular rejection (ACR) is a severe complication caused by a T cell cytotoxic immune response against the transplanted kidney, which is associated with graft dysfunction and

loss.^{255,256} Early treatment of ACR generally leads to a positive outcome; therefore much effort is dedicated to the development of non-invasive diagnostic and risk assessment methods.^{35,257} Most early risk assessment methods are donor-dependent, as they either incorporate data on the donor or employ samples taken during the early post-transplantation period.^{224,225,262,263,226–228,230,258–261} Until now, the characterization of anti-HLA antibodies in serum through single antigen bead assays has been employed as a means of detecting donor specific antibodies (DSA), which can cause antibody-mediated rejection.^{224–230} However, the potential of anti-HLA antibody profiles for the prediction of ACR has not been fully explored yet. Because of this, we analysed the antibody profile of a sub-group of 52 patients of the immunological low risk and DSA-free Harmony cohort, to determine whether these profiles can also be employed for the prediction of ACR.¹³⁰

Pre-transplantation anti-HLA 1 serum antibody profiles were analysed employing the method Potential Support Vector Machine (PSVM), an implementation of the support vector machine (see section 5.4.2.1).⁶² Due to the low number of patients with available data, a validation cohort could not be defined. Therefore, to avoid a bias in the prediction, the performance of the classifier was estimated employing leave-one-out cross validation, so that for each patient the predictor was optimized employing the rest of the cohort. Furthermore, a P value of the prediction was estimated employing a permutation test.

Our antibody-based ACR risk assessment tool predicts this condition with a balanced accuracy of 82.7% (sensitivity=76.5%, specificity=88.9%), one of the best performances in the literature of pre-transplant ACR risk assessment.^{227,258,263–265} Therefore, our results demonstrate that antibody profiles can be employed for the prediction of ACR. Interestingly, this prediction was not achieved with the conventional pre-processing of antibody profiles used in the clinic, which transforms the quantitative profiles into categorical (presence/absence) data. This highlights the potential hidden in the raw single antigen bead data, which is lost with the conventional pre-processing method.

As usual in association studies, the mechanism linking antibody profiles with ACR is not known. The prediction of our tool is based on a large number of features, thereby making its interpretation difficult.^{5,133,135} We hypothesize that the prediction is based on an immunosignature effect, as immunosignatures have already been shown to be useful in disease diagnosis.^{266–269} Further studies with a larger cohort are necessary to externally validate the predictor, as well as further investigate the mechanism of prediction.

As profiling of anti-HLA antibodies is a standard clinical procedure for the detection of anti-donor antigens, our tool can contribute to an improved risk assessment after transplantation.^{256,270} It allows for high-accuracy pre-transplantation prediction of ACR in a low-risk no-DSA cohort. Therefore, once validated, this tool could be employed in the clinic without additional cost, allowing for an improved and personalized prevention of ACR and thereby better long-term survival expectative.

11.4 Inferring mechanisms of T cell response against BK virus: A mathematical model of viral dynamics

Reactivations of BK virus (BKV) are a common adverse event after renal transplantation.²⁷¹ BKV is the cause of BK virus-associated nephropathy (BKVN), a major complication affecting 1-10% of kidney transplantation recipients.^{271,272} It leads to graft failure in over half of the cases and currently there are no specific treatments against it.^{18,272} BKVN is treated by

reducing or changing the immunosuppression, fostering an antiviral immune response; simultaneously, progression of the disease can be monitored through screening of plasma BKV load.^{240,273,274} Cellular immune response has been shown to have a prognostic value for BKVN outcome.²⁷⁵ Five BKV proteins can elicit such a response: the structural antigens VP1, VP2 and VP3 and the regulatory antigens st and LT.²⁷⁶ However, immune response does not equal immune response: There is evidence that responses against these two classes of antigens might play different roles in BKV immunity, as only immune responses against regulatory antigens seem to be associated with BKV clearance.²⁷⁵ Because of this, we decided to analyse data of six patients with BKVN that had been closely monitored after immunosuppression reduction, to better understand which modes of action of the cellular immune system play a dominant role in BKV clearance and what the implications of differing modes of action are.²³⁷

With this goal, we created an ordinary differential equation model of the BK virus life cycle and of the cellular immune response against it, based on a basic model of viral dynamics (see 5.4.3.2).¹⁸⁸ This method has been employed in the past to achieve insights in several viral infections, including BKV.^{70,164,165} The model allows for three different modes of action of the immune system: (i) blocking of BKV production by infected cells, (ii) killing of infected cells and (iii) blocking of new infection of cells. As the mathematical model describes three modes of action and there are two antigen classes, nine hypotheses on the dominant modes of action of each antigen type could be evaluated.

The aforementioned hypotheses were evaluated individually for the six BKVN patients.²⁷⁵ Viral load and immune cellular response against BKV were monitored frequently during BKVN.²⁷⁵ This frequent monitoring as well as the high degree of heterogeneity in their viral and immune dynamics made this small cohort ideal for the hypothesis testing using our model. The hypotheses were tested by individually fitting the model to the data of each patient and selecting the models with the higher empirical support, as assessed by the Bayesian information criterion (see sub-section 5.4.3.3).

The results allowed for the rejection of the majority of hypotheses. The hypothesis linking immune response against structural antigens with the (i) mode of action and regulatory antigens with the (ii) mode of action achieved the highest degree of empirical support, in spite of the high degree of heterogeneity in the time courses. This is in agreement with biological evidence provided by flow cytometry analysis of immune cells specific for each antigen type, therefore supporting the validity of our approach.²⁷⁷ Following this hypothesis, regulatory antigens, as drivers of a cytotoxic response, would lead to a fast and continuous clearing of viral load.

Interestingly, some hypotheses could also potentially explain the viral-immune dynamics of certain individual patients, opening the possibility that different modes of action are dominant for different patients. The results therefore highlight the individualised character of the immune response against BKV and the capacity of our model to detect different modes of action of the immune system. Our approach can therefore be employed for the determination of which modes of action are dominant for each BKVN patient, in order to accordingly tailor the immunotherapy for the patient. As the generation of T cells specific against VP1 (structural) and LT (regulatory) has been shown to be possible, a personalized adoptive immunotherapy based on specifically generated T cells might one day become real.²⁷⁸

12. Outlook: Personalized medicine and big data

The four manuscripts included in this doctoral thesis offer a broad perspective on the methodological possibilities for addressing research questions and obtaining new results out of a large database with clinical and biological data. Bi- and multivariate statistical methods for the assessment of the consequences of viral infections and therapeutic strategies on the patient outcome; machine learning has been used to identify prediction models for complications from the very first day and modelling approaches have been employed for the analysis of mechanisms of the immune system. Taken together, these four studies have the potential of contributing to an improvement in patient care, influencing the establishment of new therapeutic approaches and better defining the individual risk profiles of each patient for a personalized health care, based on immunological, virological and demographic criteria.

However, these four manuscripts have only scratched the surface of the data generated within the e:KID consortium. At the moment, at least three research sub-projects are ongoing: We have developed a biomarker-based prediction of 1-year renal transplant function (GFR), employing markers (e.g. metabolomics, expression and cytokine data) measured at the second week and the third month post-transplantation (publication pending); we are analysing the correlation networks of a cytokine central for GFR prediction to better understand its mechanistic role in the achievement of a high renal function; finally we are searching for biomarkers of viral reactivations during the first year post-transplantation. We expect these projects to improve individualized risk assessment for renal transplantation patients, as well as to contribute to a systemic understanding of the processes involved in a positive clinical outcome, which could in turn lead to new therapeutic approaches. Moreover, new data from newly performed measurements on the collected samples are still flowing into the database, and we expect to receive in short the first follow-up data on the patient cohort, so that the factors leading to a long-term positive outcome can also be investigated. Finally, a validation study has recently started and is currently recruiting patients, in order to obtain an independent validation of the biomarker signatures established in the first phase of the e:KID project.

All results of the e:KID consortium, both present and future, are only possible by addressing data management, analysis, and interpretation – i.e. the real problem in systems medicine is not obtaining the data, but *knowing what to do with them*. As shown in the chapter reporting on data management experience at e:KID, data management cannot be easily automatized, as its success relies highly on the biological and clinical knowledge of the data scientist. Not every method is adequate for each data analysis, but it has to be tailored for the research goals and the characteristics of the employed data. This is critical when attempting to upscale the methods for the research on personalized systems medicine based on big data approaches, as the number of data-related problems will increase in orders of magnitude. Nevertheless, we have also shown the high hidden potential of our dataset to answer a wide range of research questions, even with *just* a few hundreds of patients. I thus expect that big data approaches can achieve much more: With large, dedicated, expert teams of data scientists, we will be able to truly obtain high-throughput results in personalized medicine, thereby profoundly improving the lives of millions of patients.

13. References

1. Galas DJ, Hood L. Systems Biology and Emerging Technologies Will Catalyze the Transition from Reactive Medicine to Predictive, Personalized, Preventive and Participatory (P4) Medicine. *Interdiscip Bio Cent*. 2009;1(2):1-4.
2. Flores M, Glusman G, Brogaard K, Price ND, Hood L. P4 medicine: how systems medicine will transform the healthcare sector and society. *Per Med*. 2013;10(6):565-576.
3. Simonetta Pulciani, Di Lonardo A, Fagnani C, Taruscio D. P4 Medicine versus Hippocrates. *Ann Ist Super Sanità*. 2017;53(3):185-191.
4. Alyass A, Turcotte M, Meyre D. From big data analysis to personalized medicine for all: Challenges and opportunities. *BMC Med Genomics*. 2015;8:33.
5. Fröhlich H, Balling R, Beerenwinkel N, Kohlbacher O, Kumar S, Lengauer T, et al. From hype to reality: data science enabling personalized medicine. *BMC Med*. 2018;16:150.
6. Fernald GH, Capriotti E, Daneshjou R, Karczewski KJ, Altman RB. Bioinformatics challenges for personalized medicine. *Bioinformatics*. 2011;27(13):1741-1748.
7. Apweiler R, Beissbarth T, Berthold MR, Blüthgen N, Burmeister Y, Dammann O. Whither systems medicine ? *Exp Mol Med*. 2018;50:e453.
8. Di Paolo A, Sarkozy F, Ryll B, Siebert U. Personalized medicine in Europe: not yet personal enough? *BMC Health Serv Res*. 2017;17:289.
9. Wang R-S, Maron BA, Loscalzo J. Systems Medicine: Evolution of Systems Biology From Bench To Bedside. *Wiley Interdiscip Rev Syst Biol Med*. 2015;7(4):141-161.
10. Gietzelt M, Löffrich M, Karmen C, Knaup P, Ganzinger M. Models and Data Sources Used in Systems Medicine: A Systematic Literature Review. *Methods Inf Med*. 2016;55:107-113.
11. Benson M. Clinical implications of omics and systems medicine: Focus on predictive and individualized treatment. *J Intern Med*. 2016;279:229-240.
12. Bontha S V., Maluf DG, Mueller TF, Mas VR. Systems Biology in Kidney Transplantation: The Application of Multi-Omics to a Complex Model. *Am J Transplant*. 2017;17:11-21.
13. Stapleton CP, Conlon PJ, Phelan PJ. Using omics to explore complications of kidney transplantation. *Transpl Int*. 2018;31:251-262.
14. Abettan C. Between hype and hope: What is really at stake with personalized medicine? *Med Heal Care Philos*. 2016;19:423-430.
15. Maughan T. The Promise and the Hype of 'Personalised Medicine.' *New Bioeth*. 2017;23(1):13-20.
16. Maier M, Takano T, Sapir-Pichhadze R. Changing paradigms in the management of rejection in kidney transplantation: Evolving from protocol-based care to the era of P4 medicine. *Can J Kidney Heal Dis*. 2017;4:1-12.

17. Abecassis M, Bartlett ST, Collins AJ, Davis CL, Delmonico FL, Friedewald JJ, et al. Kidney transplantation as primary therapy for end-stage renal disease: A National Kidney Foundation/Kidney Disease Outcomes Quality Initiative (NKF/KDOQITM) conference. *Clin J Am Soc Nephrol*. 2008;3:471-480.
18. Ramos E, Drachenberg CB, Wali R, Hirsch HH. The decade of polyomavirus BK-associated nephropathy: state of affairs. *Transplantation*. 2009;87:621-630.
19. Hart A, Smith JM, Skeans MA, Gustafson SK, Wilk AR, Robinson A, et al. OPTN / SRTR 2016 Annual Data Report Kidney. *Am J Transplant*. 2018;(Suppl 1):18-113.
20. Wekerle T, Segev D, Lechler R, Oberbauer R. Strategies for long-term preservation of kidney graft function. *Lancet*. 2017;389:2152-2162.
21. Tantravahi J, Womer KL, Kaplan B. Why hasn't eliminating acute rejection improved graft survival? *Annu Rev Med*. 2007;58:369-385.
22. Guimarães-Souza NK, Dalboni MA, Câmara NC, Medina-Pestana J, Paheco-Silva A, Cendoroglo M. Infectious complications after deceased kidney donor transplantation. *Transplant Proc*. 2010;42:1137-1141.
23. Tufton N, Ahmad S, Rolfe C, Rajkariar R, Byrne C, Chowdhury TA. New-onset diabetes after renal transplantation. *Diabet Med*. 2014;31:1284-1292.
24. Petrara MR, Giunco S, Serraino D, Dolcetti R, De Rossi A. Post-transplant lymphoproliferative disorders: From epidemiology to pathogenesis-driven treatment. *Cancer Lett*. 2015;369:37-44.
25. Safa K, Magee CN, Azzi J. A critical review of biomarkers in kidney transplantation. *Curr Opin Nephrol Hypertens*. 2017;26:509-515.
26. Sawitzki B, Schlickeiser S, Reinke P, Volk H-D. Monitoring tolerance and rejection in organ transplant recipients. *Biomarkers*. 2011;16(sup1):S42-S50.
27. Lebranchu Y, Baan C, Biancone L, Legendre C, Morales JM, Naesens M, et al. Pretransplant identification of acute rejection risk following kidney transplantation. *Transpl Int*. 2013;27:129-138.
28. Roedder S, Vitalone M, Khatri P, Sarwal MM. Biomarkers in solid organ transplantation: Establishing personalized transplantation medicine. *Genome Med*. 2011;3:37.
29. Liyanage T, Ninomiya T, Jha V, Neal B, Patrice HM, Okpechi I, et al. Worldwide access to treatment for end-stage kidney disease: A systematic review. *Lancet*. 2015;385:1975-1982.
30. Zaza G, Granata S, Tomei P, Gassa AD, Lupo A. Personalization of the immunosuppressive treatment in renal transplant recipients: The great challenge in "omics" medicine. *Int J Mol Sci*. 2015;16:4281-4305.
31. Thomusch O, Wiesener M, Opgenoorth M, Pascher A, Woitas RP, Witzke O, et al. Rabbit-ATG or basiliximab induction for rapid steroid withdrawal after renal transplantation (Harmony): an open-label, multicentre, randomised controlled trial. *Lancet*. 2016;388:3006-3016.

32. Witzke O, Nitschke M, Bartels M, Wolters H, Wolf G, Reinke P, et al. Valganciclovir prophylaxis versus preemptive therapy in cytomegalovirus-positive renal allograft recipients: Long-term results after 7 years of a randomized clinical trial. *Transplantation*. 2018;102:876-882.
33. Witzke O, Hauser IA, Bartels M, Wolf G, Wolters H, Nitschke M. Valganciclovir Prophylaxis Versus Preemptive Therapy in Cytomegalovirus-Positive Renal Allograft Recipients: 1-Year Results of a Randomized Clinical Trial. *Transplantation*. 2012;93:61-68.
34. Asare A, Kanaparthi S, Lim N, Phippard D, Vincenti F, Friedewald J, et al. B Cell Receptor Genes Associated with Tolerance Identify a Cohort of Immunosuppressed Patients with Improved Renal Allograft Graft Function. *Am J Transpl*. 2017;18(10):2627-2639.
35. Suthanthiran M, Schwartz JE, Ding R, Abecassis, Michael Dadhania D, Samstein B, Knechtle SJ, et al. Urinary-Cell mRNA Profile and Acute Cellular Rejection in Kidney Allografts. *N Engl J Med*. 2013;369(1):20-31.
36. Lee AH, Shannon CP, Amenyogbe N, Bennike TB, Diray-Arce J, Idoko OT, et al. Dynamic molecular changes during the first week of human life follow a robust developmental trajectory. *Nat Commun*. 2019;10:1092.
37. Hasin Y, Seldin M, Lusis A. Multi-omics approaches to disease. *Genome Biol*. 2017;18:83.
38. Banas M, Neumann S, Eiglsperger J, Schiffer E, Putz FJ, Reichelt-Wurm S, et al. Identification of a urine metabolite constellation characteristic for kidney allograft rejection. *Metabolomics*. 2018;14:116.
39. Keeren K, Friedrich M, Gebuhr I, Philipp S, Sabat R, Sterry W, et al. Expression of Tolerance Associated Gene-1, a Mitochondrial Protein Inhibiting T Cell Activation, Can Be Used to Predict Response to Immune Modulating Therapies. *J Immunol*. 2009;183:4077-4087.
40. Matkar S, Gangawane A. An outline of data management in clinical research. *Int J Clin Trials*. 2017;4(1):1-6.
41. Krishnankutty B, Bellary S, Kumar NBR, Moodahadu LS. Data management in clinical research. *Indian J Pharmacol*. 2012;44(2):168-172.
42. Institute of Medicine (US). *Assuring Data Quality and Validity in Clinical Trials for Regulatory Decision Making*. (Davis JR, Nolan VP, Woodcock J ER, ed.). Washington; 1999.
43. Lu Z, Su J. Clinical data management: Current status, challenges, and future directions from industry perspectives. *Open Access J Clin Trials*. 2010;2:93-105.
44. Tenopir C, Allard S, Sinha P, Pollock D, Newman J, Dalton E, et al. Data Management Education from the Perspective of Science Educators. *Int J Digit Curation*. 2016;11(1):232-251.
45. Griffin PC, Khadake J, LeMay KS, Lewis SE, Orchard S, Pask A, et al. Best practice data life cycle approaches for the life sciences. *F1000Research*. 2017;6:1618.

46. Van Den Broeck J, Cunningham SA, Eeckels R, Herbst K. Data cleaning: Detecting, diagnosing, and editing data abnormalities. *PLoS Med*. 2005;2(10):e267.
47. Pomerantseva V, Ilicheva O. Clinical data collection, cleaning and verification in anticipation of database lock: Practices and recommendations. *Pharmaceut Med*. 2011;25(4):223-233.
48. Pomerantseva V. Coding & Designing a Clinical Database. *Appl Clin Trials*. 2012;21(3).
49. Bellary S, Krishnankutty B, Latha M. Basics of case report form designing in clinical research. *Perspect Clin Res*. 2014;5(4):159-166.
50. Lapatas V, Stefanidakis M, Jimenez RC, Via A, Schneider MV. Data integration in biological research: an overview. *J Biol Res*. 2015;22:9.
51. Sujansky W. Heterogeneous database integration in biomedicine. *J Biomed Inform*. 2001;34:285-298.
52. Hamid JS, Hu P, Roslin NM, Ling V, Greenwood CMT, Beyene J. Data Integration in Genetics and Genomics: Methods and Challenges. *Hum Genomics Proteomics*. 2009;2009:869093.
53. Lee K, Weiskopf N, Pathak J. A Framework for Data Quality Assessment in Clinical Research Datasets. *AMIA Annu Symp Proc*. 2017:1080-1089.
54. Kahn MG, Callahan TJ, Barnard J, Bauck AE, Brown J, Davidson BN, et al. A Harmonized Data Quality Assessment Terminology and Framework for the Secondary Use of Electronic Health Record Data. *eGEMs*. 2016;4(1):18.
55. Jakobsen JC, Gluud C, Wetterslev J, Winkel P. When and how should multiple imputation be used for handling missing data in randomised clinical trials - A practical guide with flowcharts. *BMC Med Res Methodol*. 2017;17:162.
56. Ibrahim J, Chu H, Chen M-H. Missing data in clinical studies: Issues and methods. *J Clin Oncol*. 2012;30(26):3297-3303.
57. Sterne JAC, White IR, Carlin JB, Spratt M, Royston P, Kenward MG, et al. Multiple imputation for missing data in epidemiological and clinical research: potential and pitfalls. *BMJ*. 2009;338:b2393.
58. Zhang Y, Alyass A, Vanniyasingam T, Sadeghirad B, Flórez ID, Pichika SC, et al. A systematic survey of the methods literature on the reporting quality and optimal methods of handling participants with missing outcome data for continuous outcomes in randomized controlled trials. *J Clin Epidemiol*. 2017;88:67-80.
59. Pohlabeln H, Reineke A, Schill W. Data Management in Epidemiology. In: *Handbook of Epidemiology*. Vol 101. ; 2009:402-403.
60. Jayalakshmi T, Santhakumaran A. Statistical Normalization and Back Propagation for Classification. *Int J Comput Theory Eng*. 2011;3(1):1793-8201.
61. Maadooliat M, Huang JZ, Hu J. Integrating Data Transformation in Principal Components Analysis. *J Comput Graph Stat*. 2015;24(1):84–103.

62. Hochreiter S, Obermayer K. Support vector machines for dyadic data. *Neural Comput.* 2006;18(6):1472-1510.
63. Kim TK. T test as a parametric statistic. *Korean J Anesthesiol.* 2015;68(6):540-546.
64. Peng CYJ, Lee KL, Ingersoll GM. An introduction to logistic regression analysis and reporting. *J Educ Res.* 2002;96(1):3-14.
65. Karvanen J. The Statistical Basis of Laboratory Data Normalization. *Drug Infwmtion J.* 2003;37:101-107.
66. Curran-Everett D. Explorations in statistics: the log transformation. *Adv Physiol Educ.* 2018;42:343-347.
67. Kahan BC. Accounting for centre-effects in multicentre trials with a binary outcome - When, why, and how? *BMC Med Res Methodol.* 2014;14:20.
68. Emmert-Streib F, Dehmer M. A Machine Learning Perspective on Personalized Medicine: An Automized, Comprehensive Knowledge Base with Ontology for Pattern Recognition. *Mach Learn Knowl Extr.* 2018;1:149-156.
69. El abouidi N, Benhlima L. Big Data Management for Healthcare Systems: Architecture, Requirements, and Implementation Naoual. *Adv Bioinformatics.* 2018;2018:4059018.
70. Perelson AS. Modelling viral and immune system dynamics. *Nat Rev Immunol.* 2002;2:28-36.
71. Ferreira JC, Patino CM. Types of outcomes in clinical research. *J Bras Pneumol.* 2017;43(1):5-5.
72. Wassertheil-Smoller S, Kim MY. Statistical analysis of clinical trials. *Semin Nucl Med.* 2010;40:357-363.
73. Thiese MS. Observational and interventional study design types; an overview. *Biochem Medica.* 2014;24(2):199-210.
74. Anglemeyer A, Horvath H, L B. Cochrane Database of Systematic Reviews Healthcare outcomes assessed with observational study designs compared with those assessed in randomized trials (Review). *Cochrane Database Syst Rev.* 2014;(4):MR000034.
75. Moyé L. What Can We Do About Exploratory Analyses in Clinical Trials? *Contemp Clin Trials.* 2015;45(0 0):302-310.
76. Lee J, Chuen ST, Kee SC. A practical guide for multivariate analysis of dichotomous outcomes. *Ann Acad Med Singapore.* 2009;38(8):714-719.
77. Zhang Z. Univariate description and bivariate statistical inference: the first step delving into data. *Ann Transl Med.* 2016;4(5):91.
78. Simpson SH. Creating a data analysis plan: What to consider when choosing statistics for a study. *Can J Hosp Pharm.* 2015;68(4):311-317.
79. Vargason T, Howsmon D, McGuinness D, Hahn J. On the Use of Multivariate Methods for Analysis of Data from Biological Networks. *Processes.* 2017;5:36.

80. Velentgas P, Dreyer NA, Nourjah P, Smith SR, Torchia MM, eds. *Developing a Protocol for Observational Comparative Effectiveness Research A User's Guide*. Rockville, MD: Agency for Healthcare Research and Quality; 2013.
81. Bender R, Lange S. Adjusting for multiple testing - when and how? *J Clin Epidemiol*. 2001;54:343-349.
82. Li G, Taljaard M, Van den Heuvel ER, Levine MA, Cook DJ, Wells GA, et al. An introduction to multiplicity issues in clinical trials: the what, why, when and how. *Int J Epidemiol*. 2017;746-755.
83. Deeks J, Dinnes J, D'Amico R, Sowden A, Sakarovich C, Song F, et al. Evaluating non-randomised intervention studies. *Health Technol Assess (Rockv)*. 2003;7(27).
84. Kang M, Ragan BG, Park JH. Issues in outcomes research: An overview of randomization techniques for clinical trials. *J Athl Train*. 2008;43(2):215-221.
85. Cartwright N. What are randomised controlled trials good for? *Philos Stud*. 2010;147:59-70.
86. Deaton A, Cartwright N. Understanding and misunderstanding randomized controlled trials. *Soc Sci Med*. 2018;210:2-21.
87. Kabisch M, Ruckes C, Seibert-Grafe M, Blettner M. Randomized Controlled Trials. *Dtsch Arztebl Int*. 2011;108(39):663-668.
88. Groenwold RHH, Hak E, Hoes AW. Quantitative assessment of unobserved confounding is mandatory in nonrandomized intervention studies. *J Clin Epidemiol*. 2009;62:22-28.
89. Vetter TR, Mascha EJ. Bias, Confounding, and Interaction: Lions and Tigers, and Bears, Oh My! *Anesth Analg*. 2017;125(3):1042-1048.
90. Skelly A, Dettori J, Brodt E. Assessing bias: the importance of considering confounding. *Evid Based Spine Care J*. 2012;3(1):9-12.
91. Braga LHP, Farrokhyar F, Bhandari M. Confounding: What is it and how do we deal with it? *Can J Surg*. 2012;55(2):132-138.
92. Heinze G, Wallisch C, Dunkler D. Variable selection – A review and recommendations for the practicing statistician. *Biometrical J*. 2018;60:431-449.
93. Heinze G, Dunkler D. Five myths about variable selection. *Transpl Int*. 2017;30:6-10.
94. Bursac Z, Gauss CH, Williams DK, Hosmer DW. Purposeful selection of variables in logistic regression. *Source Code Biol Med*. 2008;3:17.
95. Greenland S, Daniel R, Pearce N. Outcome modelling strategies in epidemiology: Traditional methods and basic alternatives. *Int J Epidemiol*. 2016:565-575.
96. Goodenough AE, Hart AG, Stafford R. Regression with empirical variable selection: Description of a new method and application to ecological datasets. *PLoS One*. 2012;7(3):e34338.
97. Mulder R, Singh AB, Hamilton A, Das P, Outhred T, Morris G, et al. The limitations of

- using randomised controlled trials as a basis for developing treatment guidelines. *Evid Based Ment Health*. 2018;21(1):4-6.
98. Schork N. Randomized clinical trials and personalized medicine. *Soc Sci Med*. 2018;210:71-73.
 99. Obermeyer Z, Emanuel EJ. Predicting the Future - Big Data, Machine Learning, and Clinical Medicine. *N Engl J Med*. 2016;375(13):1216-1219.
 100. Deo RC. Machine Learning in Medicine. *Circulation*. 2015;132(20):1920-1930.
 101. Breiman L. Statistical Modeling: The Two Cultures. *Stat Sci*. 2001;16(3):199-215.
 102. Baştanlar Y, Özuysal M. Introduction to Machine Learning. In: *MiRNomics: MicroRNA Biology and Computational Analysis*. ; 2014:105-128.
 103. Ojala M, Garriga GC. Permutation Tests for Studying Classifier Performance. *J of Machine Learn Res*. 2010;11:1833-1863.
 104. Wang L, Wang Y, Chang Q. Feature selection methods for big data bioinformatics: A survey from the search perspective. *Methods*. 2016;111:21-31.
 105. Hira ZM, Gillies DF. A Review of Feature Selection and Feature Extraction Methods Applied on Microarray Data. *Adv Bioinformatics*. 2015;2015:198363.
 106. Saeys Y, Inza I, Larrañaga P. A review of feature selection techniques in bioinformatics. *Bioinformatics*. 2007;23(19):2507-2517.
 107. Heikamp K, Bajorath J. Support vector machines for drug discovery. *Expert Opin Drug Discov*. 2014;9(1):93-104.
 108. Han H, Jiang X. Overcome Support Vector Machine Diagnosis Overfitting. *Cancer Inform*. 2014;13(S1):145-158.
 109. Tian Y, Shi Y, Liu X. Recent Advances on Support Vector Machines Research. *Technol Econ Dev Econ*. 2012;18(1):5-33.
 110. Mitchell JBO. Machine learning methods in chemoinformatics. *WIREs Comput Mol Sci*. 2014;4:468-481.
 111. Hsu CW, Lin CJ. A comparison of methods for multiclass support vector machines. *IEEE Trans Neural Networks*. 2002;13(2):415-425.
 112. Noble WS. What is a support vector machine? *Nat Biotechnol*. 2006;24(12):1565-1567.
 113. Lin KM, Lin CJ. A study of reduced support vector machines. *IEEE Trans Neural Networks*. 2003;14(6):1449-1459.
 114. Dybowski R, Gant V, eds. *Clinical Applications of Artificial Neural Networks*. Cambridge, United Kingdom: Cambridge University Press; 2001.
 115. Min S, Lee B, Yoon S. Deep learning in bioinformatics. *Brief Bioinform*. 2017;18(5):851-869.

116. Deng L, Yu D. *Deep Learning: Methods and Applications*. Vol 7.; 2013.
117. Li X, Liu L, Zhou J, Wang C. Heterogeneity Analysis and Diagnosis of Complex Diseases Based on Deep Learning Method. *Sci Rep*. 2018;8:6155.
118. Mamoshina P, Vieira A, Putin E, Zhavoronkov A. Applications of Deep Learning in Biomedicine. *Mol Pharm*. 2016;13:1445-1454.
119. Huang T, ed. *Computational Systems Biology: Methods and Protocols*. Humana Press; 2018.
120. Ali M, Aittokallio T. Machine learning and feature selection for drug response prediction in precision oncology applications. *Biophys Rev*. 2019;11:31-39.
121. Fabris F, Magalhães JP de, Freitas AA. A review of supervised machine learning applied to ageing research. *Biogerontology*. 2017;18:171-188.
122. Katako A, Shelton P, Goertzen AL, Levin D, Bybel B, Aljuaid M, et al. Machine learning identified an Alzheimer's disease-related FDG-PET pattern which is also expressed in Lewy body dementia and Parkinson's disease dementia. *Sci Rep*. 2018;8:13236.
123. Bisaso KR, Anguzu GT, Karungi SA, Kiragga A, Castelnuovo B. A survey of machine learning applications in HIV clinical research and care. *Comput Biol Med*. 2017;91:366-371.
124. González G, Washko GR, San José Estépar R. Deep learning for biomarker regression: application to osteoporosis and emphysema on chest CT scans. *Proc SPIE Int Soc Opt Eng*. 2018:10574.
125. Odish OFF, Johnsen K, van Someren P, Roos RAC, van Dijk JG. EEG may serve as a biomarker in Huntington's disease using machine learning automatic classification. *Sci Rep*. 2018;8:16090.
126. Ambale-Venkatesh B, Yang X, Wu CO, Liu K, Hundley WG, McClelland R, et al. Cardiovascular Event Prediction by Machine Learning: The Multi-Ethnic Study of Atherosclerosis. *Circ Res*. 2017;121:1092-1101.
127. Kavakiotis I, Tsave O, Salifoglou A, Maglaveras N, Vlahavas I, Chouvarda I. Machine Learning and Data Mining Methods in Diabetes Research. *Comput Struct Biotechnol J*. 2017;15:104-116.
128. Baron D, Giral M, Brouard S. Reconsidering the detection of tolerance to individualize immunosuppression minimization and to improve long-term kidney graft outcomes. *Transpl Int*. 2015;28:938-959.
129. Salvadori M, Tsalouchos A. Biomarkers in renal transplantation: An updated review. *World J Transplant*. 2017;7(3):161-178.
130. Wittenbrink N, Herrmann S, Blazquez-Navarro A, Bauer C, Lindberg E, Reinke P, et al. A novel approach reveals that HLA class 1 single antigen bead-signatures provide a means of high-accuracy pre-transplant risk assessment of acute cellular rejection. *BMC Immunol*. 2019;20:11.

131. Saigi-Morgui N, Quteineh L, Bochud P-Y, Crettol S, Kutalik Z, Mueller NJ, et al. Genetic and clinic predictors of new onset diabetes mellitus after transplantation. *Pharmacogenomics J*. 2019;19:53-64.
132. Chen JH, Asch SM. Machine Learning and Prediction in Medicine — Beyond the Peak of Inflated Expectations. *N Engl J Med*. 2017;376(26):2507-2509.
133. Towards trustable machine learning. *Nat Biomed Eng*. 2018;2:709-710.
134. Zou J, Schiebinger L. Design AI so that it's fair. *Nature*. 2018;559:324-326.
135. Watson DS, Krutzinna J, Bruce IN, Griffiths CEM, McInnes IB, Barnes MR, et al. Clinical applications of machine learning algorithms: Beyond the black box. *BMJ*. 2019;364:l886.
136. Djordjevic M, Rodic A, Graovac S. From biophysics to 'omics and systems biology. *Eur Biophys J*. 2019.
137. Price WN. Big data and black-box medical algorithms. *Sci Transl Med*. 2018;10:eaao5333.
138. Han L, Luo S, Yu J, Pan L, Chen S. Rule extraction from support vector machines using ensemble learning approach: an application for diagnosis of diabetes. *IEEE J Biomed Heal Inf*. 2015;19(2):728-734.
139. Doshi-Velez F, Kim B. Towards A Rigorous Science of Interpretable Machine Learning. *arXiv*. 2017.
140. O'Malley MA, Dupré J. Fundamental issues in systems biology. *BioEssays*. 2005;27(12):1270-1276.
141. Lindner JM, Cornacchione V, Sathe A, Be C, Srinivas H, Riquet E, et al. Human Memory B Cells Harbor Diverse Cross-Neutralizing Antibodies against BK and JC Polyomaviruses. *Immunity*. 2019.
142. Ingalls B. *Mathematical Modeling in Systems Biology: An Introduction.*; 2013.
143. Edda Klipp, Rolfe Herwig, Axel Kowald, Christoph Wierling HL. *Systems Biology in Practice. Concepts, Implementation and Application*. Weinheim: WILEY-VCH Verlag GmbH & Co. KGaA; 2005.
144. Mc Auley MT, Martinez Guimera A, Hodgson D, McDonald N, Mooney KM, Morgan AE, et al. Modelling the molecular mechanisms of aging. *Biosci Rep*. 2017;37:BSR20160177.
145. Bocharov G, Meyerhans A, Bessonov N, Trofimchuk S, Volpert V. Modelling the dynamics of virus infection and immune response in space and time G. *Int J Parallel, Emergent Distrib Syst*. 2016;00(00):1-15.
146. Barbosa Bonin CR, Cortes Fernandes G, Weber dos Santos R, Lobosco M. Mathematical modeling based on ordinary differential equations: A promising approach to vaccinology. *Hum Vaccines Immunother*. 2017;13(2):484-489.
147. Cedersund G. Conclusions via unique predictions obtained despite unidentifiability -

- new definitions and a general method. *FEBS J.* 2012;279:3513-3527.
148. Antia R, Ganusov V V, Ahmed R. The role of models in understanding CD8+ T-cell memory. *Nat Rev Immunol.* 2005;5(2):101-111.
 149. Voropaeva OF, Bayadilov T V., Leontiev S V., Senotrusova SD, Tsгоеv CA, Shokin YI. Mathematical modeling of degenerative diseases. *AIP Conf Proc.* 2018;2027:030075.
 150. Lythe G, Molina-París C. Some deterministic and stochastic mathematical models of naïve T-cell homeostasis. *Immunol Rev.* 2018;285:206-217.
 151. Le D, Miller JD, Ganusov V V. Mathematical modeling provides kinetic details of the human immune response to vaccination. *Front Cell Infect Microbiol.* 2014;4(January):177.
 152. Enderling H, Chaplain MA. Mathematical Modeling of Tumor Growth and Treatment. *Curr Pharm Des.* 2014;20:000-000.
 153. Gebremichael Y, Lu J, Shankaran H, Helmlinger G, Mettetal J, Hallow KM. Multiscale Mathematical Model of Drug-Induced Proximal Tubule Injury: Linking Urinary Biomarkers to Epithelial Cell Injury and Renal Dysfunction. *Toxicol Sci.* 2018;162(1):200-211.
 154. Canini L, Perelson AS. Viral kinetic modeling: State of the art. *J Pharmacokinet Pharmacodyn.* 2014;41(5):431-443.
 155. Klipp E, Liebermeister W, Wierling C, Kowald A, Lehrach H, Herwig R. *Systems Biology: A Textbook.* Weinheim: WILEY-VCH Verlag GmbH & Co. KGaA; 2009.
 156. Perelson AS, Ribeiro RM. Introduction to modeling viral infections and immunity. *Immunol Rev.* 2018;285:5-8.
 157. Zhang X, Cao J, Carroll RJ. On the selection of ordinary differential equation models with application to predator-prey dynamical models. *Biometrics.* 2015;71:131-138.
 158. Moles CG, Mendes P, Banga JR. Parameter estimation in biochemical pathways: A comparison of global optimization methods. *Genome Res.* 2003;13:2467-2474.
 159. Huynh GT, Rong L. Modeling the dynamics of virus shedding into the saliva of Epstein-Barr virus positive individuals. *J Theor Biol.* 2012;310:105-114.
 160. Kalemira M, Mincheva D, Grove J, Illingworth CJR. Building a mechanistic mathematical model of hepatitis C virus entry. *PLoS Comput Biol.* 2019;15(3):e1006905.
 161. Banerjee S, Guedj J, Ribeiro RM, Moses M, Perelson AS. Estimating biologically relevant parameters under uncertainty for experimental within-host murine West Nile virus infection. *J R Soc Interface.* 2016;13:20160130.
 162. Wodarz D, Rodriguez-Brenes I. Early Stochastic Dynamics in Human Cytomegalovirus Infection. *J Virol.* 2017;91:e00949-17.
 163. Rose J, Emery VC, Kumar D, Asberg A, Hartmann A, Jardine AG, et al. Novel decay dynamics revealed for virus-mediated drug activation in cytomegalovirus infection.

PLoS Pathog. 2017;13(4):e1006299.

164. Funk GA, Steiger J, Hirsch HH. Rapid dynamics of polyomavirus type BK in renal transplant recipients. *J Infect Dis.* 2006;193:80-87.
165. Funk GA, Gosert R, Comoli P, Ginevri F, Hirsch HH. Polyomavirus BK replication dynamics in vivo and in silico to predict cytopathology and viral clearance in kidney transplants. *Am J Transplant.* 2008;8:2368-2377.
166. Goyal A, Ribeiro RM, Perelson AS. The role of infected cell proliferation in the clearance of acute HBV infection in humans. *Viruses.* 2017;9:350.
167. Wu H, Miao H, Xue H, Topham DJ, Zand M. Quantifying Immune Response to Influenza Virus Infection via Multivariate Nonlinear ODE Models with Partially Observed State Variables and Time-Varying Parameters. *Stat Biosci.* 2015;7(1):147-166.
168. Regoes RR, Yates A, Antia R. Mathematical models of cytotoxic T-lymphocyte killing. *Immunol Cell Biol.* 2007;85:274-279.
169. Huang Y, Rosenkranz SL, Wu H. Modeling HIV dynamics and antiviral response with consideration of time-varying drug exposures, adherence and phenotypic sensitivity. *Math Biosci.* 2003;184:165-186.
170. Burg D, Rong L, Neumann AU, Dahari H. Mathematical modeling of viral kinetics under immune control during primary HIV-1 infection. *J Theor Biol.* 2009;259:751-759.
171. Banks HT, Hu S, Link K, Rosenberg ES, Mitsuma S, Rosario L. Modelling immune response to BK virus infection and donor kidney in renal transplant recipients. *Inverse Probl Sci Eng.* 2016;24(1):127-152.
172. Smith AM. Validated models of immune response to virus infection. *Curr Opin Syst Biol.* 2018;12:46-52.
173. Wei X, Ghosh SK, Taylor ME, Johnson VA, Emini EA, Deutsch P, et al. Viral dynamics in human immunodeficiency virus type 1 infection. *Nature.* 1995;373:117-122.
174. Ho D, Neumann A, Perelson A, Chen W, Leonard J, Markowitz M. Rapid Turnover of Plasma Virions and CD4 Lymphocytes in HIV-1 Infection. *Nature.* 1995;373:123-126.
175. Hill AL, Rosenbloom DIS, Nowak MA, Siliciano RF. Insight into treatment of HIV infection from viral dynamics models. *Immunol Rev.* 2018;285:9-25.
176. Siliciano JD, Kajdas J, Finzi D, Quinn TC, Chadwick K, Margolick JB, et al. Long-term follow-up studies confirm the stability of the latent reservoir for HIV-1 in resting CD4 + T cells. *Nat Med.* 2003;9(6):727-728.
177. Palmer S, Maldarelli F, Wiegand A, Bernstein B, Hanna GJ, Brun SC, et al. Low-level viremia persists for at least 7 years in patients on suppressive antiretroviral therapy. *Proc Natl Acad Sci.* 2008;105(10):3879-3884.
178. Smith AM. Host-pathogen kinetics during influenza infection and coinfection: insights from predictive modeling. *Immunol Rev.* 2018;285:97-112.

179. Manchanda H, Seidel N, Krumbholz A, Sauerbrei A, Schmidtke M, Guthke R. Within-host influenza dynamics: A small-scale mathematical modeling approach. *BioSystems*. 2014;118:51-59.
180. Price I, Mochan-Keef ED, Swigon D, Ermentrout GB, Lukens S, Toapanta FR, et al. The inflammatory response to influenza A virus (H1N1): an experimental and mathematical study. *J Theor Biol*. 2015;374:83-93.
181. Holder BP, Simon P, Liao LE, Abed Y, Bouhy X, Beauchemin CAA, et al. Assessing the in vitro fitness of an oseltamivir-resistant seasonal A/H1N1 influenza strain using a mathematical model. *PLoS One*. 2011;6(3).
182. Shrestha S, Foxman B, Dawid S, Aiello AE, Davis BM, Berus J, et al. Time and dose-dependent risk of pneumococcal pneumonia following influenza: A model for within-host interaction between influenza and *Streptococcus pneumoniae*. *J R Soc Interface*. 2013;10:20130233.
183. Smith AM, Adler FR, Ribeiro RM, Gutenkunst RN, McAuley JL, McCullers JA, et al. Kinetics of Coinfection with Influenza A Virus and *Streptococcus pneumoniae*. *PLoS Pathog*. 2013;9(3):e1003238.
184. Smith AM, Smith AP. A Critical, Nonlinear Threshold Dictates Bacterial Invasion and Initial Kinetics during Influenza. *Sci Rep*. 2016;6:38703.
185. Califano D, Furuya Y, Metzger DW. Effects of Influenza on Alveolar Macrophage Viability Are Dependent on Mouse Genetic Strain. *J Immunol*. 2018;201(1):134-144.
186. Ghoneim HE, Thomas PG, McCullers JA. Depletion of alveolar macrophages during influenza infection facilitates bacterial super-infections. *J Immunol*. 2013;191(3):1250-1259.
187. Brunetto MR, Colombatto P, Bonino F. Bio-mathematical models of viral dynamics to tailor antiviral therapy in chronic viral hepatitis. *World J Gastroenterol*. 2009;15(5):531-537.
188. Wodarz D, Nowak MA. Mathematical models of HIV pathogenesis and treatment. *BioEssays*. 2002;24:1178-1187.
189. Korobeinikov A. Global properties of basic virus dynamics models. *Bull Math Biol*. 2004;66:879-883.
190. J M, H A, J J, R A, R A, R A. What controls the acute viral infection following Yellow Fever vaccination? *Bull Math Biol*. 2018;80(1):46-63.
191. Schmid B, Rinas M, Ruggieri A, Acosta EG, Bartenschlager M, Reuter A, et al. Live Cell Analysis and Mathematical Modeling Identify Determinants of Attenuation of Dengue Virus 2'-O-Methylation Mutant. *PLoS Pathog*. 2015;11(12):e1005345.
192. Miao H, Xia X, Perelson AS, Wu H. On Identifiability of Nonlinear ODE Models and Applications in Viral Dynamics. *SIAM Rev*. 2011;53(1):3-39.
193. Raue A, Kreutz C, Maiwald T, Bachmann J, Schilling M, Klingmüller U, et al. Structural and practical identifiability analysis of partially observed dynamical models by

- exploiting the profile likelihood. *Bioinformatics*. 2009;25(15):1923-1929.
194. Muñoz-Tamayo R, Puillet L, Daniel JB, Sauvant D, Martin O, Taghipoor M, et al. To be or not to be an identifiable model. Is this a relevant question in animal science modelling? *Animal*. 2018;12(4):701-712.
 195. Schaber J, Klipp E. Model-based inference of biochemical parameters and dynamic properties of microbial signal transduction networks. *Curr Opin Biotechnol*. 2011;22:109-116.
 196. Denis-Vidal L, Joly-Blanchard G. An easy to check criterion for (Un)identifiability of uncontrolled systems and its applications. *IEEE Trans Automat Contr*. 2000;45(4):768-771.
 197. Audoly S, Bellu G, D'angiò L, Saccomani MP, Cobelli C. Global identifiability of nonlinear models of biological systems. *IEEE Trans Biomed Eng*. 2001;48(1):55-65.
 198. Kreutz C, Raue A, Timmer J. Likelihood based observability analysis and confidence intervals for predictions of dynamic models. *BMC Syst Biol*. 2012;6:120.
 199. Zi Z. Sensitivity analysis approaches applied to systems biology models. *IET Syst Biol*. 2011;5(6):336-346.
 200. Joshi M, Seidel-Morgenstern A, Kremling A. Exploiting the bootstrap method for quantifying parameter confidence intervals in dynamical systems. *Metab Eng*. 2006;8:447-455.
 201. Banks HT, Baraldi R, Cross K, Flores K, McChesney C, Poag L, et al. Uncertainty quantification in modeling HIV viral mechanics. *Math Biosci Eng*. 2015;12(5):937-964.
 202. Zarnitsyna VI, Lavine J, Ellebedy A, Ahmed R, Antia R. Multi-epitope Models Explain How Pre-existing Antibodies Affect the Generation of Broadly Protective Responses to Influenza. *PLoS Pathog*. 2016;12(6):e1005692.
 203. Miao H, Dykes C, Demeter LM, Wu H. Differential Equation Modeling of HIV Viral Fitness Experiments: Model Identification, Model Selection, and Multimodel Inference. *Biometrics*. 2009;65(1):292-300.
 204. Burnham KP, Anderson DR. *Model Selection and Multimodel Inference: A Practical Information-Theoretic Approach*. 2nd ed. New York: Springer-Verlag; 2002.
 205. Timmer J, Müller TG, Swameye I, Sandra O, Klingmüller U. Modeling the Nonlinear Dynamics of Cellular Signal Transduction. *Int J Bifurc Chaos*. 2004;14(6):2069-2079.
 206. Abdullah A, Deris S, Mohamad MS, Anwar S. An Improved Swarm Optimization for Parameter Estimation and Biological Model Selection. *PLoS One*. 2013;8(4):e61258.
 207. Crawford K, Hasan HM, Warne L, Linger H. From traditional knowledge management in hierarchical organizations to a network centric paradigm for a changing world. *Emerg Complex Organ*. 2009;11(1):1-18.
 208. Horiguchi H, Yasunaga H, Hashimoto H, Ohe K. A user-friendly tool to transform large scale administrative data into wide table format using a mapreduce program with a pig

- latin based script. *BMC Med Inform Decis Mak.* 2012;12:151.
209. Emwas A-H, Saccenti E, Gao X, T McKay R, Martins dos Santos VAP, Roy R, et al. Recommended strategies for spectral processing and post-processing of 1D ¹H-NMR data of biofluids with a particular focus on urine. *Metabolomics.* 2018;14:31.
 210. Derveaux S, Vandesompele J, Hellemans J. How to do successful gene expression analysis using real-time PCR. *Methods.* 2010;50:227-230.
 211. Blazquez-Navarro A, Dang-Heine C, Wittenbrink N, Bauer C, Wolk K, Sabat R, et al. BKV, CMV, and EBV Interactions and their Effect on Graft Function One Year Post-Renal Transplantation: Results from a Large Multi-Centre Study. *EBioMedicine.* 2018;34:113-121.
 212. Helgesson CF. From Dirty Data To Credible Scientific Evidence: Some Practices Used To Clean Data In Large Randomised Clinical Trials. In: *Medical Proofs, Social Experiments: Clinical Trials in Shifting Contexts.* ; 2010:49-181.
 213. Blazquez-Navarro A, Dang-Heine C, Bauer C, Wittenbrink N, Wolk K, Sabat R, et al. Sex-associated differences in cytomegalovirus prevention: Prophylactic strategy is associated with a strong kidney function impairment in female renal transplant patients. *bioRxiv.* 2019:726968.
 214. Egli A, Infanti L, Dumoulin A, Buser A, Samaridis J, Stebler C, et al. Prevalence of Polyomavirus BK and JC Infection and Replication in 400 Healthy Blood Donors. *J Infect Dis.* 2009;199:837-846.
 215. Griffiths P, Baraniak I, Reeves M. The pathogenesis of human cytomegalovirus. *J Pathol.* 2015;235:288-297.
 216. Ng S-B, Khoury JD. Epstein-Barr virus in lymphoproliferative processes: an update for the diagnostic pathologist. *Adv Anat Pathol.* 2009;16(1):40-55.
 217. Womer KL, Huang Y, Herren H, Dibadj K, Peng R, Murawski M, et al. Dendritic cell deficiency associated with development of BK viremia and nephropathy in renal transplant recipients. *Transplantation.* 2010;89:115-123.
 218. Landry A, Docherty P, Ouellette S, Cartier LJ. Causes and outcomes of markedly elevated C-reactive protein levels. *Can Fam Physician.* 2017;63:e316-e323.
 219. van Ree RM, Oterdoom LH, de Vries APJ, Gansevoort RT, van der Heide Jaap JJH, van Son WJ, et al. Elevated levels of C-reactive protein independently predict accelerated deterioration of graft function in renal transplant recipients. *Nephrol Dial Transplant.* 2007;22:246-253.
 220. Kellum JA, Lameire N, Aspelin P, Barsoum RS, Burdmann E a, Goldstein SL, et al. KDIGO Clinical Practice Guideline for Acute Kidney Injury. *Kidney Int Suppl.* 2012;2(1):1-138.
 221. Yabu JM, Winkelmayer WC. Posttransplantation anemia: Mechanisms and management. *Clin J Am Soc Nephrol.* 2011;6:1794-1801.
 222. Fakhry SM, Fata P. How low is too low? Cardiac risks with anemia. *Crit Care.* 2004;8(SUPPL. 2):S11-S14.

223. Vaux DL, Fidler F, Cumming G. Replicates and repeats-what is the difference and is it significant? *EMBO Rep.* 2012;13(4):291-296.
224. Malheiro J, Tafulo S, Dias L, Martins LS, Fonseca I, Beirão I, et al. Analysis of preformed donor-specific anti-HLA antibodies characteristics for prediction of antibody-mediated rejection in kidney transplantation. *Transpl Immunol.* 2015;32:66-71.
225. Vlad G, Ho EK, Vasilescu ER, Colovai AI, Stokes MB, Markowitz GS, et al. Relevance of different antibody detection methods for the prediction of antibody-mediated rejection and deceased-donor kidney allograft survival. *Hum Immunol.* 2009;70:589-594.
226. Riethmüller S, Ferrari-Lacraz S, Müller MK, Raptis DA, Hadaya K, Rüsi B, et al. Donor-Specific Antibody Levels and Three Generations of Crossmatches to Predict Antibody-Mediated Rejection in Kidney Transplantation. *Transplant J.* 2010;90(2):160-167.
227. Lefaucheur C, Loupy A, Hill GS, Andrade J, Nochy D, Antoine C, et al. Preexisting donor-specific HLA antibodies predict outcome in kidney transplantation. *J Am Soc Nephrol.* 2010;21(8):1398-1406.
228. Song EY, Lee Y-J, Hyun J, Kim YS, Ahn C, Ha J, et al. Clinical relevance of pretransplant HLA Class II Donor-specific antibodies in renal transplantation patients with negative T-cell cytotoxicity crossmatches. *Ann Lab Med.* 2012;32:139-144.
229. Ho EK, Vasilescu ER, Colovai AI, Stokes MB, Hallar M, Markowitz GS, et al. Sensitivity, specificity and clinical relevance of different cross-matching assays in deceased-donor renal transplantation. *Transpl Immunol.* 2008;20:61-67.
230. Salvadé I, Aubert V, Venetz JP, Golshayan D, Saouli AC, Matter M, et al. Clinically-relevant threshold of preformed donor-specific anti-HLA antibodies in kidney transplantation. *Hum Immunol.* 2016;77:483-489.
231. Sullivan HC, Liwski RS, Bray RA, Gebel HM. The Road to HLA antibody evaluation: Do not rely on MFI. *Am J Transplant.* 2017;17:1455-1461.
232. Levey AS, Stevens LA, Schmid CH, Zhang YL, Castro AF, Feldman HI, et al. A new equation to estimate glomerular filtration rate. *Ann Intern Med.* 2009;150(9):604-612.
233. Lenihan CR, O'Kelly P, Mohan P, Little D, Walshe JJ, Kieran NE, et al. MDRD-estimated GFR at one year post-renal transplant is a predictor of long-term graft function. *Ren Fail.* 2008;30(4):345-352.
234. Levey AS, Coresh J, Greene T, Stevens LA, Zhang Y (Lucy), Hendriksen S, et al. Using Standardized Serum Creatinine Values in the Modification of Diet in Renal Disease Study Equation for Estimating Glomerular. *Ann Intern Med.* 2006;(145):247-254.
235. Cockcroft DW, Gault MH. Prediction of creatinine clearance from serum creatinine. *Nephron.* 1976;16:31-41.
236. Michels WM, Grootendorst DC, Verduijn M, Elliott EG, Dekker FW, Krediet RT. Performance of the Cockcroft-Gault, MDRD, and new CKD-EPI formulas in relation to GFR, age, and body size. *Clin J Am Soc Nephrol.* 2010;5:1003-1009.

237. Blazquez-Navarro A, Schachtner T, Stervbo U, Sefrin A, Stein M, Westhoff TH, et al. Differential T cell response against BK virus regulatory and structural antigens: A viral dynamics modelling approach. *PLOS Comput Biol*. 2018;14(5):e1005998.
238. Lyon L, Brenner A. Bridging the Data Talent Gap: Positioning the iSchool as an Agent for Change. *Int J Digit Curation*. 2015;10(1):111-122.
239. Masutani K. Viral infections directly involved in kidney allograft function. *Nephrology*. 2018;23(Suppl. 2):31-37.
240. Hirsch HH. BK virus: opportunity makes a pathogen. *Clin Infect Dis*. 2005;41:354-360.
241. Smith TF, Espy MJ, Mandrekar J, Jones MF, Cockerill FR, Patel R. Quantitative real-time polymerase chain reaction for evaluating DNAemia due to cytomegalovirus, Epstein-Barr virus, and BK virus in solid-organ transplant recipients. *Clin Infect Dis*. 2007;45:1056-1061.
242. Meyer T, Scholz D, Warnecke G, Kunz M, Arndt R, Reischl U, et al. Importance of simultaneous active cytomegalovirus and Epstein-Barr virus infection in renal transplantation. *Clin Diagn Virol*. 1996;6:79-91.
243. Elfadawy N, Flechner SM, Liu X, Schold J, Srinivas TR, Poggio E, et al. CMV Viremia is associated with a decreased incidence of BKV reactivation after kidney and kidney-pancreas transplantation. *Transplantation*. 2013;96(12):1097-1103.
244. Park SB, Kwak JH, Lee KT, Hwang E a, Han SY, Kim HT, et al. Polyoma virus-associated nephropathy and concurrent cytomegalovirus infection in the kidney transplant recipients. *Transplant Proc*. 2006;38:2059-2061.
245. Special Issue: KDIGO Clinical Practice Guideline for the Care of Kidney Transplant Recipients. *Am J Transplant*. 2009;9(Suppl 3):S1-S157.
246. Kotton CN, Kumar D, Caliendo AM, Huprikar S, Chou S, Danziger-Isakov L, et al. *The Third International Consensus Guidelines on the Management of Cytomegalovirus in Solid-Organ Transplantation*. Vol 102.; 2018.
247. Fehr T, Cippà PE, Mueller NJ. Cytomegalovirus post kidney transplantation: Prophylaxis versus pre-emptive therapy? *Transpl Int*. 2015;28:1351-1356.
248. Momper JD, Misel ML, McKay DB. Sex differences in transplantation. *Transplant Rev*. 2017;31(3):145-150.
249. Perrottet N, Csajka C, Pascual M, Manuel O, Lamothe F, Meylan P, et al. Population pharmacokinetics of ganciclovir in solid-organ transplant recipients receiving oral valganciclovir. *Antimicrob Agents Chemother*. 2009;53(7):3017-3023.
250. Lindemann M, Korth J, Sun M, Xu S, Struve C, Werner K, et al. The Cytomegalovirus-Specific IL-21 ELISpot Correlates with Allograft Function of Kidney Transplant Recipients. *Int J Mol Sci*. 2018;19(12):3945.
251. Villacres MC, Longmate J, Auge C, Diamond DJ. Predominant type 1 CMV-specific memory T-helper response in humans: Evidence for gender differences in cytokine secretion. *Hum Immunol*. 2004;65(5):476-485.

252. Nickel P, Bold G, Presber F, Biti D, Babel N, Kreutzer S, et al. High levels of CMV-IE-1-specific memory T cells are associated with less alloimmunity and improved renal allograft function. *Transpl Immunol*. 2009;20:238-242.
253. Shi XL, De Mare-Bredemeijer ELD, Tapirdamaz Ö, Hansen BE, Van Gent R, Van Campenhout MJH, et al. CMV Primary Infection Is Associated with Donor-Specific T Cell Hyporesponsiveness and Fewer Late Acute Rejections after Liver Transplantation. *Am J Transplant*. 2015;15:2431-2442.
254. Rissling O, Naik M, Brakemeier S, Schmidt D, Staeck O, Hohberger A, et al. High frequency of valganciclovir underdosing for cytomegalovirus prophylaxis after renal transplantation. *Clin Kidney J*. 2018;11(4):564-573.
255. Ingulli E. Mechanism of cellular rejection in transplantation. *Pediatr Nephrol*. 2010;25:61-74.
256. Becker LE, Morath C, Suesal C. Immune mechanisms of acute and chronic rejection. *Clin Biochem*. 2016;49:320-323.
257. Becker BN, Becker YT, Levenson GE, Simmons WD, Sollinger HW, Pirsch JD. Reassessing the impact of cytomegalovirus infection in kidney and kidney-pancreas transplantation. *Am J Kidney Dis*. 2002;39(5):1088-1095.
258. Poggio ED, Augustine JJ, Clemente M, Danzig JM, Volokh N, Zand MS, et al. Pretransplant Cellular Alloimmunity as Assessed by a Panel of Reactive T Cells Assay Correlates With Acute Renal Graft Rejection. *Transplantation*. 2007;83:847-852.
259. Simon T, Opelz G, Wiesel M, Ott RC, Süsal C. Serial Peripheral Blood Perforin and Granzyme B Gene Expression Measurements for Prediction of Acute Rejection in Kidney Graft Recipients. *Am J Transplant*. 2003;3:1121–1127.
260. Dong W, Shunliang Y, Weizhen W, Qinghua W, Zhangxin Z, Jianming T, et al. Prediction of acute renal allograft rejection in early post-transplantation period by soluble CD30. *Transpl Immunol*. 2006;16:41-45.
261. Shaikhina T, Lowe D, Daga S, Briggs D, Higgins R, Khovanova N. Decision tree and random forest models for outcome prediction in antibody incompatible kidney transplantation. *Biomed Signal Process Control*. 2017.
262. Hauser IA, Spiegler S, Kiss E, Gauer S, Sichler O, Scheuermann EH, et al. Prediction of Acute Renal Allograft Rejection by Urinary Monokine Induced by IFN- γ (MIG). *J Am Soc Nephrol*. 2005;16:1849-1858.
263. Mancebo E, Castro MJ, Allende LM, Talayero P, Brunet M, Millán O, et al. High proportion of CD95+ and CD38+ in cultured CD8+ T cells predicts acute rejection and infection, respectively, in kidney recipients. *Transpl Immunol*. 2016;34:33-41.
264. Pike R, Thomas N, Workman S, Ambrose L, Guzman D, Sivakumaran S, et al. PD1-expressing T cell subsets modify the rejection risk in renal transplant patients. *Front Immunol*. 2016;7:126.
265. Vondran FWR, Timrott K, Kollrich S, Steinhoff AK, Kaltenborn A, Schrem H, et al. Pre-

- transplant immune state defined by serum markers and alloreactivity predicts acute rejection after living donor kidney transplantation. *Clin Transplant*. 2014;28:968-979.
266. Hughes AK, Cichacz Z, Scheck A, Coons SW, Johnston SA, Stafford P. Immunosignaturing Can Detect Products from Molecular Markers in Brain Cancer. *PLoS One*. 2012;7(7):e40201.
 267. Restrepo L, Stafford P, Johnston SA. Feasibility of an early Alzheimer's disease immunosignature diagnostic test. *J Neuroimmunol*. 2013;254(1-2):154-160.
 268. Stafford P, Cichacz Z, Woodbury NW, Johnston SA. Immunosignature system for diagnosis of cancer. *Proc Natl Acad Sci U S A*. 2014;111(30):E3072-3080.
 269. Legutki JB, Johnston SA. Immunosignatures can predict vaccine efficacy. *Proc Natl Acad Sci U S A*. 2013;110(46):18614-18619.
 270. Dunn TB, Noreen H, Gillingham K, Maurer D, Ozturk OG, Pruett TL, et al. Revisiting traditional risk factors for rejection and graft loss after kidney transplantation. *Am J Transplant*. 2011;11:2132-2143.
 271. Babel N, Volk H-D, Reinke P. BK polyomavirus infection and nephropathy : the virus – immune system interplay. *Nat Rev Nephrol*. 2011;7:399-406.
 272. Comoli P, Binggeli S, Ginevri F, Hirsch HH. Polyomavirus-associated nephropathy: update on BK virus-specific immunity. *Transpl Infect Dis*. 2006;8:86-94.
 273. Rinaldo CH, Hirsch HH. Antivirals for the treatment of polyomavirus BK replication. *Expert Rev Anti Infect Ther*. 2007;5(1):105-115.
 274. Bennett WM, Meyer L, Ridenour J, Batiuk TD. Surveillance and modification of immunosuppression minimizes BK virus nephropathy. *Am J Nephrol*. 2010;32:10-12.
 275. Schachtner T, Müller K, Stein M, Diezemann C, Sefrin A, Babel N, et al. BK virus-specific immunity kinetics: a predictor of recovery from polyomavirus BK-associated nephropathy. *Am J Transplant*. 2011;11:2443-2452.
 276. Mueller K, Schachtner T, Sattler A, Meier S, Friedrich P, Trydzenskaya H, et al. BK-VP3 as a New Target of Cellular Immunity in BK Virus Infection. *Transplantation*. 2011;91:100-107.
 277. Binggeli S, Egli A, Schaub S, Binet I, Mayr M, Steiger J, et al. Polyomavirus BK-specific cellular immune response to VP1 and large T-antigen in kidney transplant recipients. *Am J Transplant*. 2007;7:1131-1139.
 278. Lamarche C, Orio J, Georges-Tobar V, Pincez T, Goupil M, Dahmani A, et al. Clinical-scale Rapid Autologous BK-virus Specific T Cell Line generation from Kidney Transplant Recipients with Active Viremia for Adoptive Immunotherapy. *Transplantation*. 2017;101(11):2713-2721.

14. Selbstständigkeitserklärung

Hiermit erkläre ich, die Dissertation selbstständig und nur unter Verwendung der angegebenen Hilfen und Hilfsmittel angefertigt zu haben.

Ich habe mich anderwärts nicht um einen Doktorgrad beworben und besitze keinen entsprechenden Doktorgrad.

Ich erkläre, dass ich die Dissertation oder Teile davon nicht bereits bei einer anderen wissenschaftlichen Einrichtung eingereicht habe und dass sie dort weder angenommen noch abgelehnt wurde.

Ich erkläre die Kenntnisnahme der dem Verfahren zugrunde liegenden Promotionsordnung der Lebenswissenschaftlichen Fakultät der Humboldt-Universität zu Berlin vom 5. März 2015.

Weiterhin erkläre ich, dass keine Zusammenarbeit mit gewerblichen Promotionsbearbeiterinnen/Promotionsberatern stattgefunden hat und dass die Grundsätze der Humboldt-Universität zu Berlin zur Sicherung guter wissenschaftlicher Praxis eingehalten wurden.

08.08.2019

Arturo Blázquez Navarro